MASS TRANSFER BETWEEN ORGANIC AND
AQUEOUS PHASES: INVESTIGATIONS USING A
CONTINUOUSLY STIRRED FLOW CELL

By

EDWARD HEYSE

A DISSERTATION PRESENTED TO THE GRADUATE SCHOOL
OF THE UNIVERSITY OF FLORIDA IN PARTIAL FULFILLMENT
OF THE REQUIREMENTS FOR THE DEGREE OF
DOCTOR OF PHILOSOPHY

UNIVERSITY OF FLORIDA

1994

This dissertation is dedicated to

my wife, Jeanna,

and our children, Sarah and Lucas.

## ACKNOWLEDGMENTS

I am grateful for the opportunity to have attended the University of Florida. That I was able to achieve my goals here was due in no small part to the help of all the faculty, staff, and students that I had the good fortune to meet and work with over the past three years.

I wish to thank my advisor, Dr. Joe Delfino, and cochairman, Dr. Suresh Rao. I appreciate the time and effort they invested in me. Dr. Delfino carefully guided my progress through the Ph.D. program and this dissertation preparation. Dr. Rao graciously offered the use of his laboratory and provided the scientific inspiration for my research. It has been a privilege to be mentored these two scientists, and I am proud to be the latest graduate in the Delfino-Rao tradition.

I would like to thank my committee members, Dr. Kirk Hatfield, Dr. Tom Stauffer, and Dr. Paul Chadik for their assistance during my Ph.D. program. In particular, I appreciate Dr. Hatfield's assistance with computer programming, and Dr. Stauffer's help in securing research funding.

Three fellow students provided assistance that was especially helpful. Dr. Denie Augustijn introduced me to the two-site mass transfer model and was available for several enlightening discussions on mass transfer. Dongping Dai taught me laboratory techniques and analysis and graciously supplied me with the Eustis column

# TABLE OF CONTENTS

LIST OF TABLES

## LIST OF FIGURES

Abstract of Dissertation Presented to the Graduate School
of the University of Florida in Partial Fulfillment of the
Requirements of the Degree of Doctor of Philosophy

MASS TRANSFER BETWEEN ORGANIC AND
AQUEOUS PHASES: INVESTIGATIONS USING A
CONTINUOUSLY STIRRED FLOW CELL

By

Edward Heyse

December 1994

Chairman: Joseph J. Delfino
Cochairman: P.S.C. Rao
Major Department: Environmental Engineering Sciences

Contaminant partitioning between organic and aqueous phases in porous media includes nonaqueous phase liquid (NAPL) dissolution and sorption by soil organic matter. Mass transport in the aqueous phase is governed by advection, but partitioning is a diffusion-controlled process. Since diffusion is usually slower than advective transport, dissolution and sorption are often subject to mass transfer (rate) limitations. Mass transfer is often modeled using a first-order, two-site model. Deficiencies of the two-site model include model parameters that are dependent on pore water velocity and an inability to predict slow, long-term desorption (tailing).

This study focused on three questions:

1.      What phase controls mass transfer?

2.  Why are first-order mass transfer model coefficients dependent on pore water velocity?

3.  Are two sorption sites adequate to describe mass transfer?

This study involved the development of: (1) a continuously stirred flow cell to investigate sorption mass transfer and (2) multisite mass transfer models. The stir cell features a flow reversal valve to maintain soil in suspension. Correlation between mass transfer parameters derived from stir cell experiments, column experiments and a predictive equation demonstrate that mass transfer is not controlled by extraparticulate diffusion; diffusion in the organic phase or in intraparticle micropores must control mass transfer.

The multisite models have sorption sites arranged either in parallel (MSP model) or in series (MSS model). The MSP and MSS models are defined by frequency distributions of first-order mass transfer rate coefficients and diffusion path lengths, respectively. Models parameters were fit to data from a series of stir cell experiments conducted at different hydraulic residence times. The MSP model resulted in the best fits (lowest sum of squares of error), but only the MSS provided velocity-independent parameters. Therefore velocity dependence of mass transfer rate coefficients results from modeling a diffusion process with a first-order model. The stochastic nature and the computational simplicity of MSP model make it attractive for further development as an alternative to the conventional two-site model.

# CHAPTER 1
## INTRODUCTION

### Objectives

Transport of solutes in porous media is influenced by partitioning between organic and aqueous phases. The organic phases of interest to this study are: (1) nonaqueous phase liquids (NAPLs), where the partitioning process is referred to as dissolution, and (2) soil organic matter, where the partitioning process is referred to as sorption. Mass transfer refers to the processes that govern this partitioning and the rates at which the interphase transport occurs.

This study was conducted to investigate the following questions concerning mass transfer:

1.   In what phase is mass transfer limited?

2.   Why are mass transfer rate coefficients a function of pore water velocity?

3.   Is the two-site sorption mass transfer model adequate?

Mass transfer involves diffusion: (1) in the organic phase, (2) across the interfacial boundary, and (3) through immobile water. If transport in one domain is significantly slower than in the others, the slowest segment will govern the overall mass transfer rate. Several researchers have suggested that diffusion in soil organic

matter (Brusseau and Rao, 1989b) or in large ganglia of multicomponent NAPLs (Conrad et al., 1992) is the rate limiting step. Determination of the rate limiting step would aid in the development of methods to predict mass transfer rate coefficients. One objective of this study was to determine if intraorganic phase diffusion is the rate limiting step.

Several researchers have noted a correlation between first-order mass transfer rate coefficients and pore water velocity (Miller et al., 1990; Borden and Kao, 1992; Brusseau, 1992b; Guarnaccia et al., 1992; Powers et al., 1992; Augustijn, 1993; Kookana et al., 1993). The velocity dependence may be caused by: (1) increased shear forces at the interfacial boundary decreasing the diffusion path length in extra-aggregate immobile water, (2) an artifact of describing mass transfer relative to advective transport, and/or (3) an artifact of describing a diffusion-controlled process with a first-order model. Another objective of this study was to explain the velocity dependence of mass transfer rate coefficients.

The two-site model has been used to describe mass transfer for soil organic matter sorption (Brusseau and Rao, 1989a) and for dissolution of multicomponent NAPLs (Borden and Kao, 1992; Augustijn, 1993). Besides the velocity dependence of the model parameters noted above, the two-site model often fails to predict the long-term slow desorption known as tailing. Modeling mass transfer with only one or two compartments results in describing sorption sites by averaged coefficients. In reality, sorption sites are located at many and varied diffusion path distances from the interfacial boundary. Modeling the mass transfer of real systems may be better

accomplished by using multisite models where sorption sites are defined by distributions of mass transfer rate coefficients or diffusion path lengths. An objective of this study is to further develop multisite sorption models by expanding the "continuum of compartments" approach of Connaughton et al. (1993) as an alternative to, and improvement of, the conventional two-site model.

## Scope

This study is composed of two major components: (1) development of a continuously stirred flow cell for conducting experiments designed to estimate mass transfer parameters, and (2) development of multisite mass transfer models. A series of experiments was conducted using the stir cell, and data were fit using the multisite models to achieve the objectives of this study.

The stir cell approach has several advantages for investigating both mass transfer limited by organic phase diffusion and velocity dependence of mass transfer model parameters. The stir cell creates high turbulence at the soil/solvent boundary; mass transfer limitations in extra-aggregate water are insignificant and the potential for organic phase diffusion limitations is maximized. Further, these turbulent conditions at the interface are independent of the flow rate through the cell. Any dependence of mass transfer parameters on hydraulic residence time (velocity) must therefore be artifacts of the model and not due to a changing diffusion domain outside the soil particles. The stir cell has additional advantages. The hydrodynamics are different (and simpler) than flow in porous media, and therefore

can provide a method of estimating mass transfer parameters independent of column studies. Because the cell experiences flow, the boundary conditions (i.e., influent concentration, flow rate) can be changed and the system response can provide information about mass transfer which cannot be obtained in batch systems.

Two multisite models were developed and tested in an attempt to overcome deficiencies of the two-site model. The multisite models have two advantages over the two-site model: (1) all sites are defined by finite mass transfer rates instead of by equilibrium conditions (a measure that is relative to advective transport), and (2) since many sites are used, the averaged mass transfer rate coefficient can change with time. Since sites are defined by a frequency distribution of either first-order mass transfer rates or diffusion path lengths, the multisite models retain the desirable attribute of the two-site model, i.e., needing only one or two fitting parameters.

Four series of experiments were conducted to test both the stir cell and multisite models and ultimately to achieve the objectives of the study. The characteristics and goals of these experiments are summarized in Table 1-1.

The first set of experiments was conducted to determine if the stir cell provided estimates of mass transfer parameters similar to parameters estimated from column experiments. If estimates of mass transfer rates were slower in column studies, it would be evidence that diffusion in extra-aggregate immobile water controls mass transfer in columns. Similar estimates of mass transfer rates is evidence that extra-aggregate (possibly intraorganic phase diffusion) controls mass transfer in columns and in the stir cell. The experiments involved estimating two-site

Table 1-1. Summary of experiments.

| Set | Characteristics | Purpose |
|-----|-----------------|---------|
| 1 | Varying Partition Coefficient | Test Stir Cell; Compare with other methods |
| 2 | Varying Hydraulic Residence Time | Test Multisite Models; Velocity dependence of model parameters |
| 3 | Nylon Balls | Test Multisite Models; Predict known distribution of sorption sites |
| 4 | Paraffin Beads | Test Multisite Models; Compare sorption and desorption techniques |

model mass transfer parameters from stir cell experiments conducted with a variety of soils, solvents, and solutes (varying partition coefficient). The mass transfer parameter estimates obtained from stir cell experiments were compared to estimates obtained from column studies and from a published parameter estimation correlation.

The second set of experiments was conducted to investigate the velocity dependence of mass transfer model parameters. The soil, solute and solvent used in each experiment was the same, but the hydraulic residence time was changed. The breakthrough curves were used to fit parameters for the two site model and both multisite models. The objective was to determine if "velocity" dependence of parameters was, in fact, an artifact of the two-site model, and if the multisite models would produce velocity-independent parameters.

The third set of experiments involved sorption by nylon balls. The distribution of sorption sites along the diffusion path is known (i.e., spherical). The purpose of these experiments was to determine if the distribution could be predicted from breakthrough curve data.

The final set of experiments represented initial development of techniques for the use of paraffin as a surrogate for soil organic matter or coal tar pitch (residual contamination found at abandoned manufactured-gas plants). A solute can be dissolved in molten paraffin to achieve a known, uniform distribution of solute in paraffin beads. Desorption experiments can be performed on these beads without first conducting a sorption experiment. Sorption and desorption experiments were then conducted and compared.

### Dissertation Organization

This dissertation is organized into three major chapters. A detailed review of mass transfer between organic and aqueous phases in porous media is presented as Chapter 2. The purpose of the review was to identify the physical and chemical processes that govern mass transfer. A key feature of the review is that the composition of various organic phases is considered as a continuum, ranging from the simple case of single component NAPLs, through multicomponent NAPLs (petroleum hydrocarbons and coal tars), to the most complex case, soil organic matter. The comparison of dissolution and sorption/desorption processes was conducted both to clarify the circumstances wherein individual mass transfer

processes are important, and to use, where possible, information concerning one organic phase to predict behavior in another organic phase.

The stir cell design and testing is detailed in Chapter 3. The results of experiment set 1 are presented in Chapter 3, which purpose was to prove that the stir cell design could be used to estimate mass transfer model parameters, and to compare those stir cell-derived model estimates with column-derived estimates. Then we could determine if extra-aggregate immobile water influenced mass transfer rates.

The multisite models are introduced in Chapter 4. The results of experiment sets 2 through 4 are presented and discussed therein. The purpose of Chapter 4 is to determine if the multisite models can overcome the deficiencies of the two-site model (velocity-dependent parameters and failure to simulate tailing).

Conclusions derived from all experiments discussed in Chapters 3 and 4 are summarized in Chapter 5. The dissertation also includes a number of appendices. Sorption isotherms are presented in Appendix A. Stir cell blank and tracer experiments which determine sorption by stir cell wall surfaces are presented in Appendix B. Data sets for all stir cell experiments are presented in Appendix C. Computer programs used to manipulate data and fit mass transfer rate coefficients to breakthrough curve data are presented in Appendix D.

CHAPTER 2
REVIEW OF MASS TRANSFER BETWEEN ORGANIC
AND AQUEOUS PHASES IN POROUS MEDIA

Introduction

Objective

Processes involved in the partitioning of hydrophobic organic chemicals between organic and aqueous phases in porous media are reviewed in this chapter. Of particular interest to this study are comparisons of the partitioning process and rates of dissolution from multicomponent nonaqueous phase liquid (NAPL) ganglia, and sorption/desorption of NAPL constituents by soil organic matter. Both processes are governed by partitioning based on the affinity hydrophobic molecules have for each other, and both processes may be limited by mass transfer constraints. A conceptual difference between the processes is the direction of mass transfer. An organic NAPL is the source of the contaminants, and the overall direction of mass transfer is from the NAPL to the aqueous phase. Soil organic matter is not the original source of organic contaminants, and systems involving the sorption process must be concerned with mass transfer in both directions (sorption and desorption). This difference is, in fact, simply one of different initial conditions.

Phase Partitioning in Porous Media

Partitioning, or the dissolution of a component from one fluid phase to another, is an important process for the fate and transport of hydrophobic organic chemicals in porous media. Partitioning occurs between liquid and vapor phases (water and soil gas or organic phases and soil gas) and between liquid phases (water and organic phases). Organic phases of interest include NAPLs and soil organic matter. Although soil organic matter is not a liquid, its polymer-like structure allows sorption to be described as a partitioning process (Chiou et al., 1983).

Hydrophobic organic chemicals of interest in this review include chlorinated compounds such as trichloroethene and polychlorinated biphenyls as well as nonpolar hydrocarbon compounds found in petroleum products. These chemicals typically enter the subsurface as a NAPL. Augustijn (1993) detailed the distribution and fate of NAPLs in porous media. The release and transport of organic chemicals in NAPL-contaminated soils is controlled by three major partitioning processes: dissolution, volatilization, and sorption. The fate of organic chemicals may also be controlled by degradation, but as this involves processes other than partitioning, it will not be addressed in this study.

Augustijn (1993) distinguished five different zones in porous media which the three partitioning processes may occur (Figure 2-1). Zone I is the region in which the NAPL is a free moving liquid; Zones II and III represent the regions containing residual NAPL in the saturated and unsaturated zone, respectively; Zone IV represents the contaminant plume in the saturated zone; and Zone V represents the
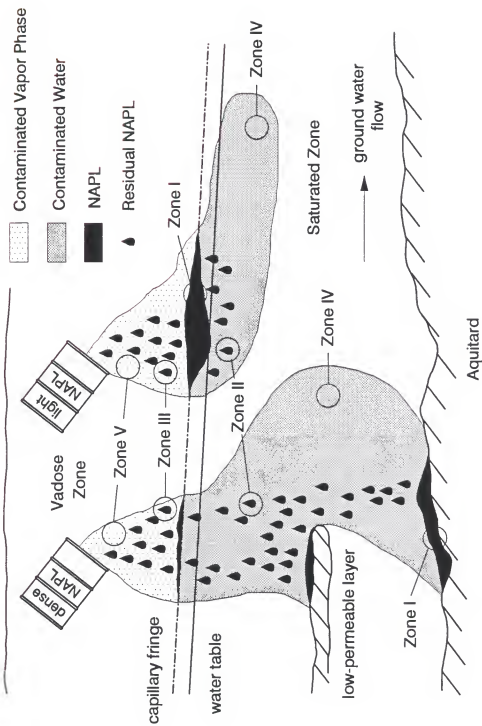
Figure 2-1. Schematic overview of soils contaminated with NAPLs (Augustijn, 1993, copyright by D.C.M. Augustijn, reprinted with permission).

contaminated vapor phase in the vadose zone. Augustijn (1993) referred to Zones I through III as the "source" and "near-field region" of the contaminated site, whereas Zones IV and V are referred to as "far-field regions." Dissolution is the primary process controlling the release of organic contaminants at the source; sorption is the dominant process in the far-field; and volatilization is only important in the vadose zone. Figure 2-2 shows schematics of the distribution of phases in each of these zones, which will be discussed individually.

Zone I. Augustijn (1993) defined this zone as the region in which free-moving NAPL has accumulated due to a reduced permeability for the NAPL, such as the water table or a clay layer. In this zone, the volumetric NAPL content exceeds the residual saturation, but will almost never occupy all pore spaces. The solute concentration in the air and water phases present in this zone are most likely in equilibrium with the NAPL and sorbed phases. It is, however, the contact between this region and the flowing groundwater that determines the mass transfer rate of organic contaminants from NAPL to water. This contact area is often very limited compared to the total volume of the NAPL pool, and is usually considered as a planar area (Johnson and Pankow, 1992).

Zone II. In this zone, the NAPL is trapped as ganglia by capillary forces in the saturated zone. This zone includes residual saturation of both DNAPL, resulting from migration below the water table, and LNAPL, entrapped in the capillary fringe by the rising and falling of the water table. Augustijn (1993) reported that dissolution of NAPL constituents is the primary process of interest in this zone;

Source/Near-Field Region

Zone I — Free Moving NAPL

Zone II — Residual NAPL in Saturated Zone

Zone III — Residual NAPL in Vadose Zone

Far-Field Region

Zone IV — Contaminated Ground Water

Zone V — Contaminated Vapor Phase

■ NAPL  ▨ Water  □ Vapor Phase  ▨ Sand Grains
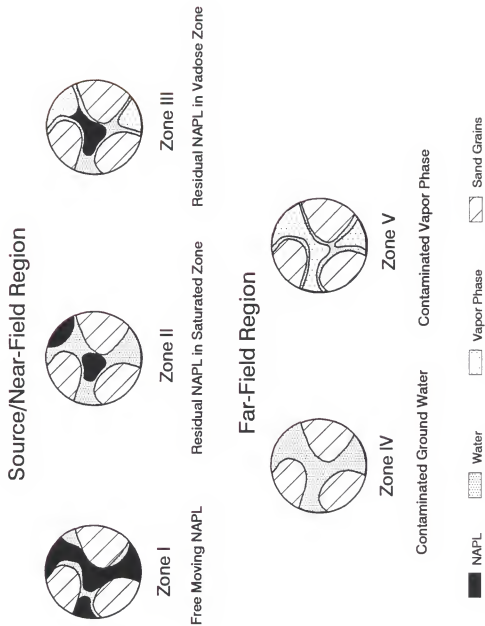
Figure 2-2. Schematic representation of the phase distribution of five different regions of a contaminated soil (Augustijn, 1993, copyright by D.C.M. Augustijn, reprinted with permission).

NAPL is generally present much greater quantities than soil organic matter so that the sorption process is overwhelmed. Interfacial contact area between the water and NAPL is greater than that experienced in Zone I. Most researchers have found that equilibrium conditions are established quickly in this zone (Van der Waarden et al., 1971; Fried et al., 1979; Hunt et al., 1988b; Anderson et al., 1992a; Guarnaccia et al., 1992). Mass transfer limitations can be important if the water/NAPL contact is limited, such as in cases of high pore water velocity or large ganglia size (Powers et al., 1991).

Zone III. Augustijn (1993) designated the regions in the vadose zone that contain residual NAPL as Zone III. Air is the least preferential wetting fluid for mineral surfaces; hence, the most likely sequence of phase distributions in Zone III is mineral/water/NAPL/air. Since the NAPL is a discontinuous phase at residual saturation, both NAPL and water may contact the air phase.

The unsaturated zone is a very dynamic component of the subsurface hydrology. During wetting and drying cycles, the air and water content can vary considerably, changing contact areas between the different phases almost continuously. If the NAPL contains volatile components, volatilization is an important process. Advantage has been taken of the volatilization process both for contaminant detection through soil gas analysis and contaminant removal using venting technology. Dissolution of the residual NAPL components will be important when water percolates through the vadose zone. Sorption and desorption will determine the rate at which the NAPL constituents move down once they are

dissolved. Water infiltration at the surface causes periodic inputs of contaminants into the saturated zone.

Zone IV. Augustijn (1993) describes Zone IV as the contaminant plume in the saturated zone, originating from the NAPL phases present in other zones described previously. The size and shape of the plume depend on the time that the NAPL has resided in the soil, the groundwater flow rate, heterogeneity of the vadose and aquifer zones, and sorption. Sorption is the primary process that controls the relative rate at which the contaminants are being transported. Different chemicals experience different affinities for the solid phase, which lead to chromatographic separation of the chemicals in the contaminant plume.

Zone V. The contaminated vadose zone free of NAPL is indicated by Zone V (Augustijn, 1993). Since the phase distribution in the vadose zone changes frequently, vapor phase transport may be important for volatile organic compounds during periods when air is present as a continuous phase. Transport of organic vapors is controlled by diffusion, advection due to density differences (Falta et al., 1989; Mendoza and Frind, 1990), or advection due to pressure gradients caused, for example, by infiltrating water. In these cases, the vapor phase acts as a medium in which contaminants are slowly being transported from NAPL contaminated regions to the atmosphere, groundwater, or other regions of the unsaturated zone. Sorption of organic vapors increase with decreasing water content. At low water content, sorption of organic vapors at the air/water interface (Pennell et al., 1992) and onto

mineral surfaces becomes more important (Rhue et al., 1989; Pennell et al., 1992),
affecting the rate of transport through the vapor phase.

Distributions of Organic Phases in Porous Media

Studying NAPL dissolution and soil organic matter sorption requires
consideration of both equilibrium conditions and rates of mass transfer. Equilibrium
conditions are exclusively dependent on chemistry (the composition of the NAPL and
aqueous phases), whereas mass transfer is dependent on both chemistry and physics
(the composition and distribution of the organic phases and water flow dynamics in
the porous media). Partitioning depends on mole fractions and activity coefficients
in each phase. For a multicomponent NAPL and soil organic matter, the mole
fraction of each component will influence the concentration found in the aqueous
phase in contact with the organic phase. Mass transfer ultimately depends on the
interfacial contact area between the organic and aqueous phases, and the rate that
chemicals can be transported to and from that interface. The occurrence and
distribution of organic phases in porous media are therefore critical to understanding
mass transfer. Common types of distributions of organic phases in porous media are:
(1) free particles or ganglia in the larger pore spaces, (2) surface coatings on mineral
surfaces, and (3) coating or filling micropores of porous soil particles. These
distributions are illustrated in Figure 2-3.

Distributions of NAPL in porous media. Behavior of the bulk phase of
NAPLs in porous media is described by a number of authors (e.g., Schwille, 1981;
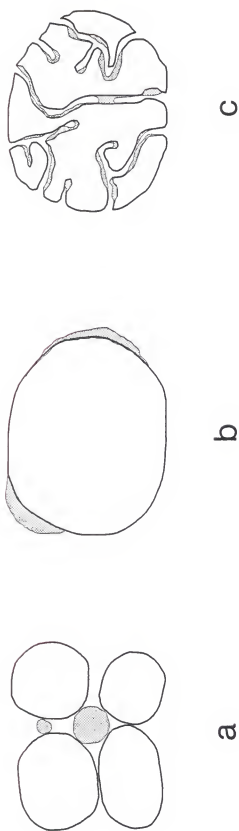
Figure 2-3. Distributions of organic phases in soils: a) as ganglia or particulates, b) as surface coatings, c) in micropores of porous soil particles (Augustijn, 1993, copyright by D.C.M. Augustijn, reprinted with permission).

Mackay et al., 1985; Mercer and Cohen, 1990; Conrad et al., 1992; Augustijn, 1993). Several NAPL properties have an important influence on their behavior in porous media. Density determines whether a NAPL will float (light NAPL or LNAPL) or sink (dense NAPL or DNAPL) in water. Viscosity influences both NAPL migration as a bulk fluid and diffusive transport of component molecules within the NAPL. Hydrophobicity of the NAPL components is perhaps the most important property as it influences not only solubility and tendency to be sorbed by soil organic matter, but also influences interfacial tension and therefore capillary forces.

Capillary forces play a dominant role in the migration and distribution of NAPLs in porous media. The capillary force is proportional to the interfacial tension and the strength of fluid wetting to the solid surface and inversely proportional to the pore size. In "clean" porous media (e.g., glass beads or sand) that have been previously saturated with water, organic NAPLs generally behave as a nonwetting phase with respect to water or as an intermediate phase between water (wetting phase) and air (nonwetting phase). To move in porous media, NAPL, like all fluids, requires a certain entry pressure to overcome capillary forces. The NAPL will preferentially flow into the most permeable portions of the media. As NAPL bulk fluid moves through porous media, the tailing end of the NAPL will not have the necessary entry pressure to move through a pore throat. Discontinuous "blobs" or "ganglia" of NAPL will become entrapped in the media as the tailing fluid breaks off from the bulk fluid (Schwille, 1981; Mackay et al., 1985; Mercer and Cohen, 1990; Conrad et al., 1992). The resulting distribution of discontinuous ganglia of entrapped

NAPL (Figure 2-3a) is known as residual saturation. The NAPL bulk fluid will continue to migrate until it is: (1) totally distributed as residual saturation, (2) meets a stratum with a higher entry pressure than the bulk fluid can overcome, or (3) in the case of NAPLs less dense than water, encounters water saturated media. Pump-and-treat systems may be able to recover some of the continuous phase NAPL, but some immobile entrapped residual saturation of NAPL will always be left behind to act as a source of aqueous phase contamination.

Residual saturation is expressed as the fraction of pore spaces occupied by the NAPL and depends on several factors, such as the media's pore-size distribution, wetability, fluid viscosity and density ratios, interfacial surface tension, gravity and buoyancy forces, and hydraulic gradients (Mercer and Cohen, 1990). The residual saturation can vary widely; Mercer and Cohen (1990) tabulated literature values of residual saturation for various NAPLs and soil types. Conrad et al. (1992) observed that the majority of NAPL is stored in complex multipore ganglia.

For "clean" soils, water is the wetting fluid, i.e., water preferentially covers the mineral surfaces. Soil organic matter, however, prefers contact with the organic liquid due to hydrophobic forces. Therefore, for soils high in organic matter, the solid matrix may have a preference for wetting by NAPL (Mercer and Cohen, 1990). Also, if a dry soil is exposed to an organic NAPL, the NAPL will become the wetting fluid (Figure 2-3b or 2-3c). Subsequent saturation with water may not displace the NAPL as the wetting fluid. In these cases, the distribution of residual NAPL in subsurface systems may be different from the distributions observed for experimental

media in which the solid surfaces are preferably wetted by water, and the mass transfer of organic contaminants from NAPL to water can be affected.

Comparison to sorption processes. Sorption processes were reviewed in detail by Brusseau and Rao (1989a) and Weber et al. (1991). Both reviews detail how sorption of organic chemicals by soil organic matter is often a process limited by mass transfer. Theories used to explain mass transfer limitations involve diffusive transport, through either immobile water or organic matter. Immobile water has been visualized at the microscale as thin films (Weber et al., 1991) and as water in micropores (Ball and Roberts, 1991) and at the macroscale as water in less permeable zones of heterogeneous media.

Dissolution of NAPLs differs from the process of desorption of organic compounds from soil organic matter in two important geometrical aspects. First, natural organic material is more likely to be located on the surface of soil particles (Figures 2-3b and 2-3c), and desorption mass transfer is more likely to limited by diffusion through immobile water. For example, the retarded intra-aggregate particle diffusion (RIPD) model developed by Ball and Roberts (1991) visualizes soil organic matter coating the walls of intra-aggregate micropores (Figure 2-3c). In contrast, NAPLs may be located in the largest pore spaces (Figure 2-3a) and are more likely to be at least partially in contact with mobile water. Second, in sorption systems the mass of organic material and its surface area are unlikely to change with time, allowing these parameters to be treated as constants in mass transfer considerations. For NAPL systems, the volume fraction occupied by NAPL may significantly decrease

as it dissolves. This can affect the kinetics of dissolution because interfacial surface area decreases (slowing dissolution), but the fraction of surface area contacting mobile water may increase (speeding up dissolution). Also, the ratio of water to NAPL volume fractions will increase, complicating attempts to model the process.

Further, dissolution of NAPLs differs from the process of desorption from soil organic matter in the constituent makeup of the sorbent. In sorption systems, even when present in high concentrations the sorbate is assumed to constitute an insignificant fraction of the total mass of sorbent (infinite dilution). Partitioning and mass transfer rate coefficients are assumed independent of the amount of constituent sorbed. For multicomponent NAPL dissolution systems, a given constituent may make up a significant fraction of the NAPL. As that constituent dissolves, the average molecular weight, density and viscosity of the remaining NAPL will change, causing partitioning and mass transfer rate coefficients to be time-dependent variables.

The distinction between dissolution and desorption is not always clear. Hydrophobic NAPLs in the subsurface will affiliate with soil organic material so that, in time, the two can become indistinguishable. If the NAPL is incorporated into the soil organic matter that adheres to the soil mineral surfaces (Figures 2-3b and 2-3c), the organic mixture becomes, in effect, a wetting phase. NAPL located on solid surfaces instead of in the large pore spaces results in the NAPL/water interface being less likely to be in contact with mobile water and mass transfer being more prone to be rate limited by diffusion through immobile water. Similarly, if a NAPL

contains a large fraction of "insoluble" components (e.g., alkanes in petroleum fuels, pitch in coal tar), these components can behave similarly to soil organic matter in sorption systems. The large fraction of insoluble components attenuate the changes in volume, molecular weight, density, and viscosity of the NAPL during the dissolution process.

Aged NAPL-contaminated soils containing a significant fraction of insoluble components would therefore be expected to behave more like a sorption system than those experimental systems employing "clean" media such as glass beads or sandy aquifers and single component NAPLs. Study of sorption is therefore helpful in the study of dissolution of organic immiscible NAPLs, and the empirical approaches to sorption systems becomes useful as NAPL dissolution systems become more complex.

## Partitioning Equilibria

### Raoult's Law Approach

Thermodynamic basis of Raoult's law. The thermodynamic principles governing partitioning between aqueous and NAPL phases were presented in detail by Burris and MacIntyre (1985). They are identical to the thermodynamic principles of partitioning between aqueous and sorbent phases as described by Weber et al. (1990). The equation development for a NAPL/water system is presented in Table 2-1. Notation for these and following equations are defined in the Glossary.

Thermodynamic equilibrium is achieved when the chemical potential in both the aqueous and NAPL phases are equal. Equilibrium of a component $i$ between

Table 2-1. Development of Raoult's law.

| Single Component NAPL | Multicomponent NAPL |
|---|---|
| $\mu_{i(w)}^0 = \mu_{i(n)}^0$   (2-1a) | $\mu_{i(w)} = \mu_{i(n)}$   (2-1b) |
| $\mu_{i(w)}^0 = \mu_i^* + R_g \tau \ln(\gamma_{i(w)}^0 X_{i(w)}^0)$   (2-2a) | $\mu_{i(w)} = \mu_i^* + R_g \tau \ln(\gamma_{i(w)} X_{i(w)})$   (2-2b) |
| $\mu_{i(n)}^0 = \mu_i^* + R_g \tau \ln(\gamma_{i(n)}^0 X_{i(n)}^0)$   (2-3a) | $\mu_{i(n)} = \mu_i^* + R_g \tau \ln(\gamma_{i(n)} X_{i(n)})$   (2-3b) |
| $X_{i(w)}^0 = \dfrac{\gamma_{i(n)}^0 X_{i(n)}^0}{\gamma_{i(w)}^0}$   (2-4a) | $X_{i(w)} = \dfrac{X_{i(n)}\, \gamma_{i(n)}\, \gamma_{i(w)}^0}{X_{i(n)}^0\, \gamma_{i(n)}^0\, \gamma_{i(w)}} X_{i(w)}^0$   (2-4b) |
| $X_{i(w)}^0 = (\gamma_{i(w)}^0)^{-1}$   (2-5a) | $X_{i(w)} = X_{i(n)} X_{i(w)}^0$   (2-5b) |
| $S_{i(w)} = \dfrac{\rho_w MW_i}{\gamma_{i(w)}^0 MW_w}$   (2-6a) | $C_{i(w)}^e = X_{i(n)} S_{i(w)}$   (2-6b) |

aqueous and NAPL phases is given in Equation (2-1a) if the NAPL consists of a single component $i$ and in Equation (2-1b) for a multicomponent NAPL. The chemical potentials are functions of chemical potential at standard state (liquid) and chemical activity, as shown in Equations (2-2a) through (2-3b). An expression for the mole fraction of $i$ in the aqueous phase is obtained by combining Equations (2-1a), (2-2a), and (2-3a) into Equation (2-4a) for a single component NAPL. The aqueous phase mole fraction of component $i$ in equilibrium with a multicomponent NAPL can be expressed in terms of the aqueous phase mole fraction of component $i$ in equilibrium with pure component $i$ (Equation 2-4b) by combining Equations (2-1b), (2-2b), and (2-3b) and dividing by Equation (2-4a).

Equation (2-5a) is a simplification of Equation (2-4a), assuming that negligible water is present in the NAPL phase ($X^0_{i(n)}$ and $\gamma^0_{i(n)}$ are unity). Equation (2-6a) is an expression for the aqueous solubility of component $i$. Equation (2-6a) is Equation (2-5a) written in terms of mass per volume with the additional assumption that the solution is dilute (e.g., the molar volume of the solution is approximately equal to the molar volume of water).

For multicomponent NAPLs, Equation (2-4b) can be simplified if the following assumptions are made. First, if negligible water is present in the NAPL phase, $X^0_{i(n)}$ and $\gamma^0_{i(n)}$ become unity. Second, if the aqueous solubility of component $i$ is not significantly affected by the presence of other solutes in the aqueous phase, $\gamma^0_{i(w)}$ equals $\gamma_{i(w)}$. Finally, if the component $i$ behaves ideally in the NAPL phase, $\gamma_{i(n)}$ is then unity. This results in Equation (2-5b), the expression of Raoult's law for

a liquid-liquid system. If the aqueous solution is sufficiently dilute, Equation (2-6b) results from converting to units of concentration for each component $i$. The Raoult's law approach for partitioning, simply stated, is that the equilibrium concentration of a component in water equals its aqueous solubility multiplied by its mole fraction in the NAPL.

In deriving Raoult's law for a liquid-liquid system, the standard state of the component $i$ is a liquid. If component $i$ is crystalline at normal temperatures and pressures, the aqueous solubility of that component must be adjusted for use in Raoult's law approach calculations. Upon dissolution in a liquid organic solvent, a component no longer has crystalline structure. Therefore, the solubility of a hypothetical super-cooled liquid is used (Mackay, 1977; Karickhoff, 1981; Chiou et al., 1982). Hypothetical super-cooled liquid solubility cannot be measured directly, but it can be estimated from a component's heat of fusion and melting point by the Van't Hoff equation (Equation 2-7):

$$\ln S_{scl} = \ln S_{i(w)} + \frac{\Delta H_f}{R_g \tau_m \tau} (\tau_m - \tau) \qquad \textbf{(2-7)}$$

Note that the $S_{i(w)}$ value used must be for the same temperature for which $S_{scl}$ is calculated. Also, the aqueous concentration of a component cannot exceed its crystalline aqueous solubility. This seems to suggest that NAPLs have a finite capacity for crystalline solutes; the mole fraction for a crystalline component in the NAPL cannot exceed $S_{i(w)}/S_{scl}$. Rather than a finite capacity, this "limitation" probably indicates that assumptions of ideal behavior are no longer valid when $X_{i(n)}$

approaches $S_{i(w)}/S_{scl}$. Several authors (Chiou et al., 1982; Vadas et al., 1991; Lee et al., 1992a) have used simplified versions of Equation (2-7). Vadas et al. (1991) and Lee et al. (1992a) noted that predictions of super-cooled liquid aqueous solubilities by methods similar to Equation (2-7) tend to be higher than those calculated from partitioning experiment measurements.

Adjustments to solubility must also be made if the "aqueous" phase contains a cosolvent. If a polar organic solvent, such as an alcohol, is added to the water, the equilibrium concentration of component $i$ is also affected. The aqueous solubility of component $i$ in Equation (2-6b) (Table 2-1) is replaced with the solvent mixture solubility for that component. The solubility ($S_{i(mix)}$) in the binary solvent mixture increases exponentially with increasing cosolvent fraction (Fu and Luthy, 1986; Morris et al., 1988) as shown in Equation (2-8):

$$\log S_{i(mix)} = \log S_{i(w)} + \sigma_c f_c \tag{2-8}$$

where the power of the cosolvent, $\sigma_c$, $= \log (S_{i(c)}/S_{i(w)})$. It can often be assumed that the effects of several cosolvents are additive. Increasing the solubility effects a decrease in the partitioning coefficient, as was shown by Rao et al. (1985) for sorption systems. However, since polar organic solvents are more soluble in organic NAPLs, significant fractions of cosolvents could invalidate assumptions for ideal behavior. (E.g., significant amounts of mixed solvent may completely dissolve in the NAPL phase.) Generally, deviations from ideal behavior are relatively small, and empirical constants are employed to make necessary corrections.

If a NAPL contains components with large cosolvency power (e.g., alcohol additives to gasoline), the dissolution of these compounds from the NAPL can decrease the polarity of the aqueous phase, enhancing the solubility of the NAPL constituents. Cline et al. (1991) and Poulsen et al. (1992) investigated cosolvency effects of oxygenated additives in gasoline. They found that the effects were negligible at NAPL saturations of less than 10 percent of porosity (typical of residual saturation or Zones II and III in Figure 2-1) due to dilution of the cosolvent by water. However, Poulsen et al. (1992) found that methanol added to gasoline at concentrations above 10 percent enhanced the "aqueous" concentrations of monoaromatics when the NAPL saturation was 50 percent of the porosity (typical of floating NAPL or Zone I in Figure 2-1). Cosolvent effects of proposed synthetic fuels such as M-85 (85 percent methanol and 15 percent gasoline) may therefore be significant when NAPL saturations are high.

Partition coefficients. Equilibrium chemistry commonly employs the use of equilibrium constants. The ratio of concentrations of a given component in the NAPL phase to its equilibrium concentration in the aqueous phase is known as the NAPL-water partition coefficient ($K_{n/w}$). The Raoult's law approach to organic partitioning allowed Cline et al. (1991) and Lee et al. (1992a,b) to develop Equation (2-6b) into an expression for $K_{n/w}$ based on the density and average molecular weight of the NAPL and the aqueous solubility of the component of interest (Equation 2-9):

$$K_{n/w} = \frac{C_{i(n)}}{C_{i(w)}^e} = \frac{\rho_n MW_i}{MW_n S_{i(w)}} \tag{2-9}$$

Mathematically identical partition coefficients have been proposed by Chiou et al. (1982) and Mackay et al. (1991).

Sorption equilibrium relationships also employ partition coefficients. The partition coefficient, $K_p$, is the ratio of the mass of a sorbed component per unit mass of soil to its equilibrium concentration in water. While $K_p$ values vary from soil to soil, partition coefficients that are normalized to fraction of organic carbon are consistent for a given component for most soils. The use of the organic carbon partition coefficient, $K_{oc}$, implies that physical composition of all soil organic matter is approximately the same and that organic compounds will partition into soil organic matter much more than they will adsorb to soil mineral surfaces (Chiou et al., 1979; Karickhoff et al., 1979; Means et al., 1980). Partitioning into organic matter tends to be the predominant sorption process unless the organic content of the soil is low, where reactions with soil mineral surfaces can become important (Means et al., 1982). The relationship between $K_p$ and $K_{oc}$ is given in Equation (2-10):

$$K_p = \frac{S_i}{C_{i(w)}^e} = f_{oc} K_{oc} \qquad (2\text{-}10)$$

An organic matter-water partition coefficient can be calculated from $K_{oc}$ by unit conversion (Equation 2-11):

$$K_{om/w} = \frac{C_{i(om)}}{C_{i(w)}^e} = K_{oc}\, \rho_{om}\, \frac{f_{oc}}{f_{om}} = \frac{K_{oc} f_{oc}\, \rho_s}{\theta_{om}} \qquad (2\text{-}11)$$

Schnitzer (1978) reports that $f_{oc}/f_{om}$ of humic acids range from 0.536 to 0.587, and Nelson and Sommers (1982) report that a value of 0.58 is commonly used for soil organic matter. Estimates of the density of soil organic matter range from 1.3 to 1.47 g/mL (Campbell, 1985; Kuipers, 1984). Therefore, $K_{om/w}$ ranges approximately from 0.70 $K_{oc}$ to 0.86 $K_{oc}$. Note that $K_{om/w}$ and $K_{n/w}$ have the same units. Use of $K_{om/w}$ instead of the more common $K_{oc}$ is necessary to make comparisons to NAPL water partition coefficients using Raoult's law convention.

The relationship between partition coefficient and aqueous solubility is demonstrated by Figure 2-4. Log hypothetical super-cooled liquid aqueous solubilities in mol/L are plotted on the X-axis versus log NAPL or organic matter partition coefficients on the Y-axis. Raoult's law convention states that, for a given NAPL, these parameters will plot on a straight line of slope -1 and intercept log $(\rho_n/MW_n)$. Deviations from the ideal line are caused both by errors (poor estimates of NAPL or solute parameters and measurement error) and nonideality (assumptions for Raoult's Law convention not valid).

Partition coefficients for various nonpolar aromatic compounds were obtained for gasoline (Cline et al., 1991), diesel fuel (Lee et al., 1992a), coal tar (Lee et al., 1992b), and soil organic matter (Gerstl, 1990a), and plotted versus their hypothetical super-cooled liquid aqueous solubilities on a log-log scale in Figure 2-5. Ideal lines based on Raoult's law convention fit the data very well for the fuels. Confidence intervals (not plotted) for the gasoline and diesel data are relatively tight, usually spanning just a few tenths of a log unit. The coal tar data fit less well, so Lee et al.
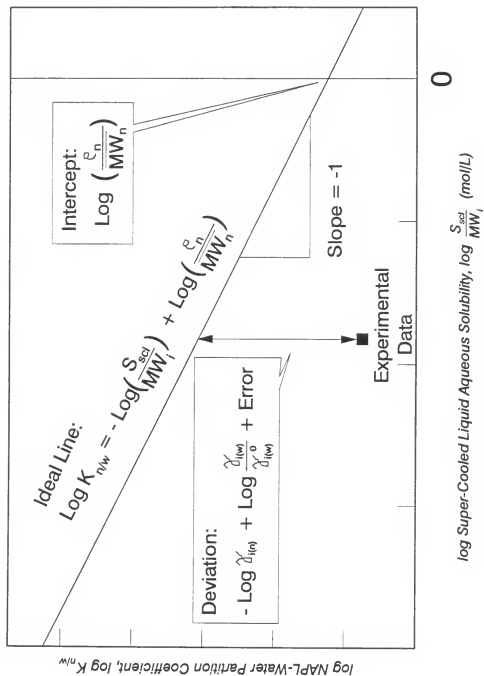
Figure 2-4.  Representation of ideal behavior (Raoult's law) and nonideality in liquid-liquid partitioning (adapted from Okuda et al, 1991, copyright by I. Okuda, reprinted with permission).
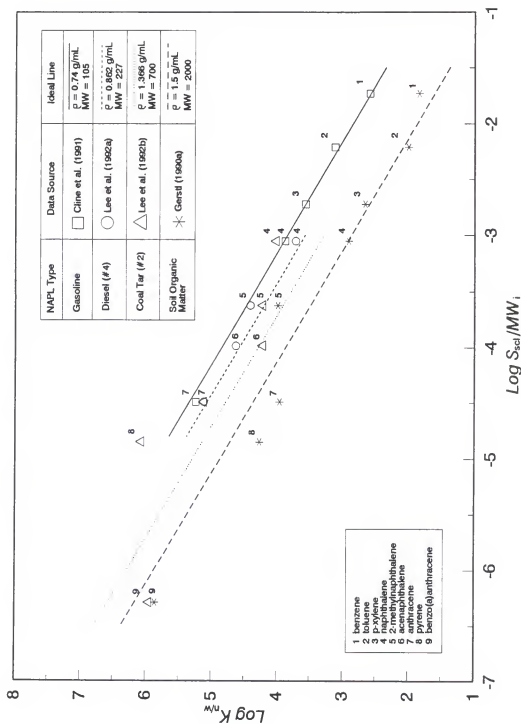
Figure 2-5. Relationship between partition coefficient and hypothetical super-cooled liquid aqueous solubility.

(1992b) suggested that the Raoult's Law approach was valid for coal tar only within a factor of two. The soil organic matter data followed the Raoult's Law trend, and fits an ideal line where the average molecular weight of the organic matter was assumed to be 2000 g/mol. Humic substances represent a significant fraction of soil organic matter and have molecular weights ranging from about 300 to over 30,000 g/mol (Stumm and Morgan, 1981). Therefore an average molecular weight for soil organic matter of 2000 g/mol would seem reasonable. Gerstl (1990a) compiled $K_{oc}$ values from up to 33 sources for each of the compounds plotted in Figure 2-5. The 95 percent confidence intervals on these data are necessarily wider than those experienced for a specific NAPL and often span an entire log unit.

Evidence of ideal behavior. Research in recent years has focused on the applicability of approaches based on Raoult's Law convention (i.e., how valid are the assumptions that were made in deriving Equation 2-6b). Burris and MacIntyre (1986a) stated that the assumption of water being negligible in the neat component phase is valid for temperatures below 150°C. Total solute concentrations must exceed 10,000 mg/L to introduce a one percent error in assuming the density of the solution is that of water. Since aqueous solubilities of nonpolar hydrocarbons are low, errors introduced by assuming a dilute solution are generally very small.

Researchers agree that solute-solute interactions in the aqueous phase explain at best only a small portion of nonideal behavior in octanol-water systems. Chiou et al. (1982) claimed these interactions helped explain nonideality observed for solutes with extremely low solubilities (e.g., DDT). However, Banerjee et al. (1980)

and Miller et al. (1985) discovered virtually no aqueous phase nonideality in octanol-water systems. Miller et al. (1985) suggested that concentrations of a given compound in water on the order of a few percent are necessary to observe a cosolvent effect on other solutes.

Research has concentrated on the assumptions of ideal behavior in the NAPL phase (i.e., there are no interactions between solutes in the NAPL). Chiou et al. (1977), Banerjee et al. (1980), Chiou et al. (1982), and Miller et al. (1984) performed regression calculations between log octanol-water partition coefficients and log aqueous solubilities for various solutes representing a wide range of aqueous solubilities. Slopes of these regressions ranged from -0.508 to -0.862, indicating nonideal behavior (slope equals -1 for ideal behavior). After aqueous solubilities were converted to hypothetical super-cooled liquid aqueous solubilities, the slopes were closer to -1 but still indicated nonideal behavior. By grouping and performing regressions for similarly structured solutes, Banerjee et al. (1980) and Chiou et al. (1982) showed that these regressions had slopes near -1, although each group had a different intercept. Miller et al. (1985) noted that deviations from the ideal increased with increasing difference in molecular sizes of the solute and octanol. These types of results lead a number of authors to conclude that the primary cause of nonideal behavior was nonunity values of the activity coefficients in the octanol phase (MacKay, 1977; Banerjee et al., 1980; Chiou et al., 1982; Miller et al., 1985).

Evidence of nonideal behavior in the NAPL phase was demonstrated by the work by Banerjee (1984) and Burris and MacIntyre (1985) with binary mixtures.

They determined that mixtures of similarly-structured compounds behaved ideally, but mixtures of compounds with dissimilar structure (e.g., alkanes and aromatics) deviated from ideal behavior. Banerjee (1984) and Burris and MacIntyre (1986b) determined that the nonideal behavior could be accounted for using estimates of $\gamma_{i(n)}$ values predicted by the UNIFAC model. The UNIFAC model (Fredenslund et al., 1975; Prausnitz et al., 1980) can predict activity coefficients involved in liquid-liquid partitioning equilibria based on contributions from both molecular geometry and functional group interactions.

Cline et al. (1991) and Lee et al. (1992a,b) determined that dissolution of organic components contained in gasoline, diesel, and coal tar (respectively) deviated from ideal partitioning behavior by no more than a factor of 2. Chen et al. (1994) similarly determined that partitioning of aromatics from motor oil deviated from ideal behavior by no more than a factor of 4. Lee et al. (1992a) determined that $\gamma_{i(n)}$ deviations from unity in gasoline and diesel fuels as determined by the UNIFAC model for polynuclear aromatic hydrocarbons (PAHs) smaller than fluoranthene caused negligible deviation from ideal behavior. Lee et al. (1992b) found that PAHs in coal tar exhibited reasonably ideal behavior, even though coal tar might not be expected to be an ideal mixture due to the large variety in molecular weights and functional groups of its components. Since the UNIFAC model predicted values of $\gamma_{i(n)}$ close to unity, and other assumptions for Raoult's Law appear valid, Lee et al. (1992b) attributed many of the deviations from ideality to poor parameter estimation and analytical problems. They suggested that the apparent nonideal behavior of

benzo(a)anthracene was probably an artifact of concentrations being near the detection limit and the low aqueous solubility made its literature $S_{i(w)}$ value less reliable (i.e., due to experimental error rather than nonideal behavior).

Linear isotherms prompted Chiou et al. (1979) to propose that sorption of nonpolar organic compounds by soil was a partitioning (dissolution) process rather than adsorption (involving chemical bonding) and that the sorption was occurring virtually exclusively in the soil organic matter. Chiou et al. (1979), Karickhoff et al. (1979) and Means et al. (1980) performed regression calculations of log organic carbon partition coefficients (log $K_{oc}$) versus log aqueous solubilities (log $S_{i(w)}/MW_i$) for various nonpolar organic compounds. While the regressions were linear, the slopes were not -1 (they ranged from -0.54 to -0.82). Karickhoff (1981) later described the need to perform these regressions using hypothetical super-cooled liquid aqueous solubilities. Better correlations were obtained by performing regressions between log organic carbon partition coefficients (log $K_{oc}$) and log octanol-water partition coefficients (log $K_{o/w}$). Karickhoff et al. (1979), Means et al. (1980), and Karickhoff (1981) all obtained slopes of unity or near unity and correlation coefficients greater than 0.98 for these correlations. The intercepts for these correlations ranged from -0.21 to -0.346. These correlations indicate not only that octanol is an excellent predictor for soil organic matter sorption of nonpolar organics, but also imply that the process of sorption of nonpolar organics into soil organic matter is indeed partitioning. Gerstl (1990a,b) could not improve the predictive ability of $K_{oc}$-$K_{o/w}$ and $K_{oc}$-$S_{scl}/MW_i$ relationships using correlations with

molecular connectivity indices, implying that nonideal behavior plays a negligible role in defining soil organic matter partition coefficients.

The various results just discussed indicate that equilibrium aqueous concentrations originating from the dissolution of multicomponent NAPLs can be reasonably predicted by approaches based on Raoult's law convention. Analytical technique limitations and unreliability of parameters may cause as much deviation from such estimates as do actual nonideal behavior. In field applications, complications of heterogeneities and mass transfer limitations will quickly mask any deviations from Raoult's law ideality.

## Effect of Partitioning Equilibria on Mass Transfer

Partitioning equilibria will affect mass transfer regardless of the cause of mass transfer constraints. The driving force for mass transfer depends on the equilibrium concentration in the aqueous phase, which is directly proportional to the concentration in the organic phase and inversely proportional to the partition coefficient (Equation 2-6b). Both the partition coefficient and the component concentration in a NAPL can change during the dissolution of multicomponent NAPLs. Nonlinear partition coefficients are also important for soil organic matter sorption systems.

Constituent dependent (non-linear) partition coefficient. The NAPL-water partition coefficient depends on the density and average molecular weight (or molar volume) of the NAPL (Equation 2-9). As component $i$ is depleted from the NAPL

by dissolution, the mole fractions of all constituent components of the NAPL change, and with them the properties of density and average molecular weight. This amounts to a constituent dependent partition coefficient or a nonlinear isotherm. This behavior has been noted in sorption systems. Karickhoff et al. (1979) noted that sorption (soil organic matter) isotherms were linear until the aqueous concentration exceeded approximately 60 percent of the aqueous solubility. At higher concentrations, the sorption coefficient increased.

To demonstrate the effect of component depletion on the NAPL-water partition coefficient, it is useful to rewrite Equation (2-9) in terms relating the properties of component $i$ to the properties of the other NAPL components. Assume that a NAPL is composed of a component $i$ and all other components $j$ ($j$ might represent the alkanes in gasoline, pitch in coal tar, or humic material in soil organic matter), and that molar volumes are conserved (Amagat's law). Characteristics of the NAPL can therefore be written in terms of these components as shown in Equation (2-12):

$$\frac{\overline{MW}_n}{\rho_n} = \overline{\upsilon}_n = X_{i(n)} \upsilon_i + (1 - X_{i(n)}) \upsilon_j \qquad \textbf{(2-12)}$$

Equation (2-13) defines molar volume of component $i$ relative to component(s) $j$:

$$f_{MV} = \frac{\upsilon_i}{\upsilon_j} \qquad \textbf{(2-13)}$$

Using these relationships, the NAPL-water partition coefficient, $K_{n/w}$ can be written in terms of the aqueous solubility of component $i$, the molar volume of all other NAPL components, and the relative molar volume defined in Equation (2-13). Further, a relative partition coefficient, $K_{n/w}^*$, can be defined as the ratio of partition coefficient for component $i$ at some mole fraction $X_{i(n)}$ to its partition coefficient at infinite dilution. Equation (2-9) is therefore rewritten as Equation (2-14):

$$K_{n/w} = \frac{1}{(1 + (f_{MV} - X_{i(n)}))} \frac{\rho_j MW_i}{MW_j S_{i(w)}} = K_{n/w}^* \frac{\rho_j MW_i}{MW_j S_{i(w)}} \qquad (2\text{-}14)$$

Densities of various NAPLs, organic matter, and organic compounds range only from about 0.7 g/mL to 1.5 g/mL, or over a factor of two. Molecular weights however can range over one order of magnitude. The molar volumes for various nonionic solutes and organic phases of environmental interest, and the resulting $f_{MV}$ values are provided in Table 2-2. Relative partition coefficient, $K_{n/w}^*$ (on the y-axis) is plotted versus fraction of mole fraction of component $i$ in the NAPL, $X_{i(n)}$ (on the x-axis) in Figure 2-6. The relative partition coefficients were calculated using Equation (2-14) for typical ranges of $f_{MV}$ illustrated in Table 2-2. A horizontal line at $K_{n/w}^* = 1$ (constant partition coefficient) represents a linear isotherm. This only truly occurs when the molar volumes of the solute and other NAPL components are equal. Deviation from the linear isotherm increases as the difference in the molar volumes of solute and NAPL increases. However, the mole fraction of the solute must exceed 50 percent before the relative partition coefficient changes by more than a factor of 2. This corresponds to the findings of Karickhoff et al. (1979) described
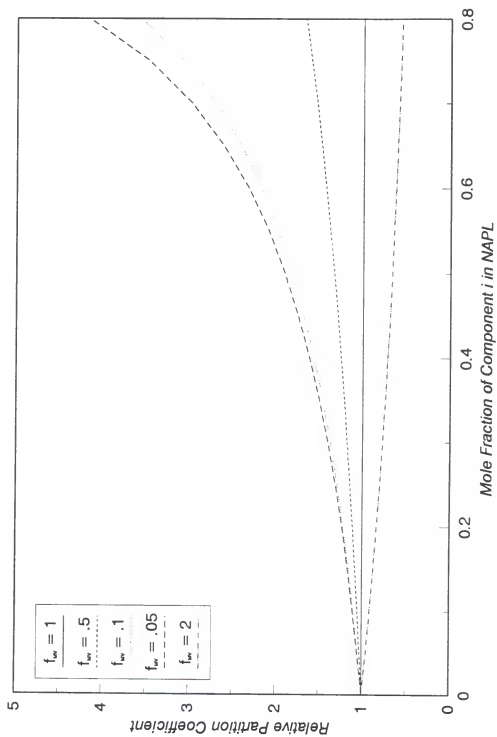
Figure 2-6.    Variation of partition coefficient with molar volume of constituent components.

Table 2-2. Ratios of molar volumes of solutes to molar volumes of NAPLs and soil organic matter, $f_{MV}$.

| Solute Component $i$ | NAPL | | | |
|---|---|---|---|---|
| | Trichloro-ethene $\upsilon = 90.1$ | Gasoline $\upsilon = 142$ | Coal Tar $\upsilon = 510$ | Soil Organic Matter $\upsilon = 1300$ |
| Benzene $\upsilon = 88.9$ | 0.99 | 0.66 | 0.17 | 0.068 |
| Anthracene $\upsilon = 143$ | | 1.01 | 0.28 | 0.11 |
| Tetrachloro-ethene $\upsilon = 102$ | 1.1 | | | 0.078 |
| Hexachloro-biphenyl $\upsilon = 231$ | | | | 0.18 |

Note: Molar volume in mL/mol.

above. Since the soluble fractions of many petroleum-derived NAPLs are usually only a few percent, the assumption of a constant partition coefficient is often valid. Constituent-dependent partition coefficients may be a significant factor for NAPLs that are composed of mostly soluble components, such as mixtures of synthetic solvents.

The observation of constituent dependency of partition coefficient by Karickhoff et al. (1979) is not universal; Chiou et al. (1979) observed linear isotherms at aqueous concentrations approaching the solubility limit. Since Figure 2-6 represents ideal conditions, when $X_{i(n)}$ approaches unity (solubility limit in the aqueous phase), the NAPL represents the neat component $i$ and $K_{n/w}^*$ equals $f_{MV}^{-1}$. The extreme nonlinear behavior as $C_{i(w)}/S_{i(w)}$ approaches unity represents the

replacement of all other NAPL molecules with component *i* molecules, a process that is unlikely to happen in natural systems containing insoluble components. As $X_{i(n)}$ increases, the likelihood for nonideal behavior also increases.

The implication of the Raoult's law approach is that the partition coefficient is a component (and therefore time) dependent variable. During the dissolution process, the most soluble constituents will have the lowest partition coefficients and will partition into the water more quickly than the less soluble constituents. This process will likely cause changes to the molar volume of the remaining NAPL. The changes will only be significant if the soluble fraction of the NAPL exceeds 50 percent. Increasing the average molar volume of the NAPL decreases the partition coefficients for all of the remaining constituents, speeding the dissolution of the larger compounds as the NAPL ages. However, the assumption of a constant partition coefficient is often valid for most petroleum derived NAPLs.

Changing component concentrations in NAPL. The equilibrium concentration of a component in water, and therefore its dissolution rate, will change in direct proportion to the mole fraction (or concentration) of that component in the NAPL. The equilibrium dissolution of a NAPL initially consisting of equimolar concentrations of benzene, toluene, and p-xylene was simulated by Mackay et al. (1991) and is shown in Figure 2-7. Since these compounds are relatively close in molecular weight, density, and structure, the partition coefficients would not be expected to change much during the dissolution process ($\upsilon_{benz} / \upsilon_{xyl} = 0.74$).
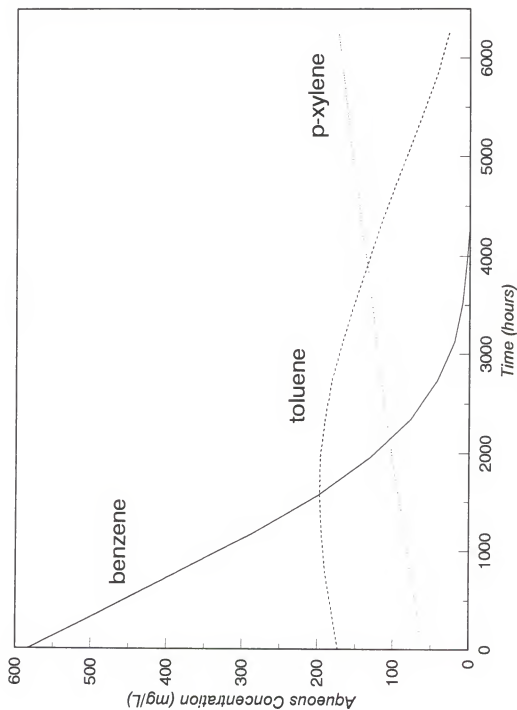
Figure 2-7. Changing concentrations of hydrocarbons in water caused by changing mole fractions of components in NAPL (Mackay et al., 1991, copyright by Elsevier Science, reprinted with permission).

The most soluble component (benzene in this case) is depleted first. Its concentration in the aqueous phase decreases exponentially with time, since as its NAPL concentration decreases, less and less is available to partition into the water. The tailing is therefore due to Raoult's law effect and not mass transfer limitations.

The aqueous concentration of next most soluble component, toluene, initially increases. Because the NAPL is being rapidly depleted of benzene, the mole fractions (or concentrations) of the remaining NAPL components increase, along with their dissolution rates. Eventually toluene is also depleted and its aqueous concentration and dissolution rate decrease. If the NAPL were composed of more than three components, one would observe the aqueous concentrations of the components initially increase then decrease in sequential order of decreasing aqueous solubility. This results in the "chromatographic effect" when aqueous concentrations are plotted versus time. This chromatographic effect was observed by Van der Waarden et al. (1971) and Borden and Piwoni (1992) during dissolution of petroleum and by Augustijn (1993) during dissolution of both synthetic multicomponent NAPLs and coal tar.

The aqueous concentration of the final component, p-xylene, approaches its solubility limit once most of the benzene and toluene have been depleted. At this point, the NAPL will consist of only p-xylene. The aqueous concentration of p-xylene will remain at its aqueous solubility until all of the xylene is dissolved. If an insoluble component were also present in the NAPL, the xylene concentration would

not reach the solubility limit but would begin to decrease as soon as most of the toluene was depleted.

The dependence of dissolution rate on the NAPL component concentration, and dependence of a NAPL component concentration on the concentrations of all other NAPL components, makes predicting dissolution of multicomponent NAPLs a very complicated task. Mackay et al. (1991) state that models involving multicomponent dissolution can only be solved numerically.

## Mass Transfer

### Liquid-Liquid Mass Transfer Processes

The process of NAPL dissolution is one of liquid-liquid mass transfer. Liquid-liquid mass transfer has been conceptualized by Giavedoni and Deiber (1986) as a series of several steps, including: (1) diffusion and advection through the bulk phase of the NAPL toward the interface; (2) accumulation, adsorption/desorption, advection, diffusion or chemical reaction at the interface; and (3) diffusion and advection away from the interface into the bulk phase of the water. Although NAPL dissolution is generally thought of in the direction from NAPL to water, these processes operate in both directions as illustrated in Figure 2-8. Soil organic matter is not a liquid, but the process of diffusion into voids in its open, polymer-like structure (Chiou et al., 1983; Brusseau and Rao, 1989b) is similar to that of diffusion into NAPL.
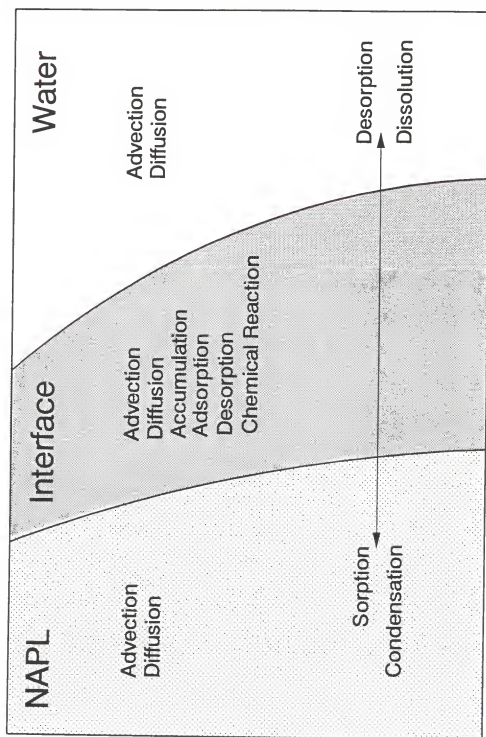
Figure 2-8. Liquid-liquid mass transfer processes.

Not all of the processes outlined by Giavedoni and Deiber (1986) are important for partitioning between organic and aqueous phases in porous media. Advection involves solute transport by momentum, which requires that the fluid have some velocity. There is no advective transport within soil organic matter. By defining NAPLs as immiscible, there is no fluid flow across the interfacial boundary, therefore no advective transport across the interface. NAPLs in porous media are often considered to be immobile, which would eliminate advective transport in the NAPL phase. This would particularly seem true in discontinuous NAPL ganglia, although observation of rapid movement of colloids near phase interfaces (Wan and Wilson, 1994) lead to speculation (J.L. Wilson, 1992 Darcy lecture, National Ground Water Association) that sheer stresses imposed by water advection on the ganglia surface might cause mixing within the ganglia. Induced mixing, if it occurs, would increase as pore water velocities increase and NAPL viscosity decreases. Advection is an important mass transport process in the water phase. Diffusion requires concentration gradients, which do not exist in the NAPL phase for single component NAPLs. Concentration gradients could occur within the organic phase (for multicomponent NAPLs and soil organic matter only), across the interface, and in the water phase. Diffusion is therefore an important process to liquid-liquid mass transfer. Diffusion at the interface would usually seem unimportant due to the very short diffusion path length, and interfacial processes are often assumed not to limit mass transfer. Chemical reactions do not occur in the case of partitioning of nonionic organic compounds. Adsorption and desorption at the interface are

similarly assumed to be instantaneous. Accumulation is the term that reflects the interfacial build up of certain compounds, which may be the solute of interest or other compounds that could affect mass transfer (e.g., film forming compounds discussed by Luthy et al., 1993). Accumulation can result in the establishment of a unique diffusion domain at the interface. The processes that definitely affect mass transfer are advection and diffusion in the water phase, and, in the case of multicomponent NAPLs and soil organic matter, diffusion in the organic phase. Other processes, such as advection (induced or otherwise) in the NAPL and accumulation/diffusion at the interface, may or may not be important to mass transfer. Mass transfer involves multiple processes in series and in parallel. Miller et al. (1990) argue that no one process can explain dissolution and that describing all processes by a grouped parameter (i.e., mass transfer rate coefficient) is justified.

Advection. The advective flux for solute $i$ in fluid $l$ is given by Equation (2-15):

$$J_{i(l)}^{adv} = v_l \theta_l C_{i(l)} \tag{2-15}$$

Mass transfer by advection is directly proportional to the fluid flux or fluid velocity and is a first-order process with respect to solute concentration. Several researchers (Miller et al., 1990; Powers et al., 1992; Guarnaccia et al., 1992) have found that the dissolution rate is dependent on the pore water velocity, indicating the influence of advection in the water phase. Similar velocity dependence for sorption mass transfer has been reported by Brusseau (1992b), Augustijn (1993) and Kookana et al. (1993). At low velocities, partitioning mass transfer is fast compared to advective transport;

the dissolution or desorption rate is dependent on the advection rate of solutes away from the interface. At high velocities, other processes (usually diffusion) limit mass transfer.

Diffusion. Diffusion mass transfer is governed by concentration gradient. The diffusive flux for solute $i$ in fluid $l$ is given by Fick's law in Equation (2-16):

$$J_{i(l)}^{dif} = -D_{i(l)} \theta_l \frac{dC_{i(l)}}{dx} \tag{2-16}$$

Dissolution mass transfer rates based on Fick's law, are first-order with respect to a concentration gradient, but not necessarily to concentration. However, an expression for dissolution mass transfer that is first-order with concentration can be derived by assuming a fixed interfacial area and a linear gradient between the average concentration of component $i$ in the bulk of the NAPL and the average concentration of component $i$ in the bulk of the water over the distance $\delta$. These assumptions are commonly made in the case of film diffusion. If mass transfer is limited by diffusion in the aqueous phase, the diffusive flux between the NAPL and water is approximated by Equation (2-17a):

$$\frac{d}{dt}(\theta_n C_{i(n)}) \approx -a_{n/w} \frac{D_{i(w)}}{\delta_w} \left(\frac{C_{i(n)}}{K_{n/w}} - C_{i(w)}\right) \tag{2-17a}$$

If mass transfer is limited by diffusion in the NAPL phase, the diffusive flux is approximated by Equation (2-17b):

$$\frac{d}{dt}(\theta_n C_{i(n)}) \approx -a_{n/w} \frac{D_{i(n)}}{\delta_n} (C_{i(n)} - K_{n/w} C_{i(w)}) \tag{2-17b}$$

Equations (2-17a) and (2-17b) are written in terms of the phase in which mass transfer is limited.

Equations (2-17a) and (2-17b) are first-order with respect to solute concentration because the concentration gradient is assumed to be linear. Concentration gradients are often nonlinear. Weber et al. (1991) discuss the implications of nonlinear concentration gradients to first-order approximations. Since first-order mass transfer rates are computationally convenient, approximations are often made to simulate first-order conditions.

Diffusive mass transfer occurs in multicomponent NAPLs and soil organic matter, across the interface, and in the water. Weber et al. (1991) discuss linking diffusion domains, however, Brusseau (1992a) demonstrates from an empirical approach that when mass transfer in one domain is much slower than in the other domains, the slower domain dominates the mass transfer process and the other domains experience equilibrium conditions. Since the diffusion path distance across the interface is very short, unless an interfacial film exists it is likely that mass transfer limitations exist either in the water or in a multicomponent organic phase. The mass transfer equation would then be written for diffusion in the fluid (water or organic) which limits mass transfer.

Various theories have been proposed claiming either water or soil organic matter is the phase in which sorption mass transfer is limited, and these theories are described in detail by Brusseau and Rao (1989a). The retarded intraparticle diffusion (RIPD) theory proposed by Ball and Roberts (1991) claims that diffusion

in micropores of soil aggregates is the rate limiting step to mass transfer. Weber et al. (1991) favor diffusion through stagnant films of water surrounding the soil organic matter. Brusseau and Rao (1989a) compiled evidence suggesting that intraorganic matter diffusion (IOMD) is often the rate limiting step. All of these concepts are probably correct to some extent depending on the geometry of the system being studied. Research with NAPLs has not yet produced the same level of debate as is found in the sorption literature. For systems involving single component NAPLs, diffusion gradients do not exist in the NAPL so any diffusion constraints must occur in the water. Hatfield et al. (1993) concluded that for soil columns containing residual saturation of decane, the limiting mass transfer resistance for various solutes was not in the NAPL ganglia. However, this conclusion was based on a literature correlation for a film mass transfer rate coefficient instead of an overall mass transfer rate coefficient estimated from their experimental data. Further, they assumed that the diffusion path length was the mean grain size radius, which fails to consider multipore ganglia. It is possible for diffusion limited mass transfer to occur in multicomponent NAPLs, but this process is only rarely considered. Brusseau (1992a) suggested that diffusion could be rate limiting in a viscous NAPL phase, such as coal tar. Conrad et al. (1992) discussed diffusion limited mass transport as a result of long transport distances in large multipore ganglia.

Equations (2-17a) and (2-17b) demonstrate that important factors in diffusive mass transfer are the diffusion coefficient, the diffusion path length, and the driving force or divergence from equilibrium. The coefficient of diffusion can be estimated

from the correlation developed by Wilke and Chang (1955) as shown in Equation (2-18):

$$D_{i(l)} = 7.4(10^{-10}) \frac{(x \, MW_l)^{0.5} \tau}{\lambda_l \, \tilde{\upsilon}_i^{0.6}} \qquad (2\text{-}18)$$

for $D_{i(l)}$ in cm$^2$/sec, $\tau$ in °K, $\lambda_l$ in g/(cm sec), and $\tilde{\upsilon}$ in mL/mol and where the association parameter, $x = 1$ for nonpolar solvents and 2.6 for water. Hayduk and Laudie (1974) suggested that the association parameter for water should be 2.26, and presented other similar regressions for diffusion coefficients of solutes in water. Since the molecular weight of water is very low compared to most NAPLs, the implication of Equation (2-18) is that, for mass transfer to be limited by diffusion in NAPL, either the viscosity of the NAPL must be high or the diffusion path length through the NAPL must be long.

In addition to causing advective transport, high pore water velocities can enhance diffusive transport. NAPL/water interfaces exposed to mobile water will have very short diffusive path lengths in the water phase. If shear stresses imposed on the NAPL/water interface induce mixing in the NAPL ganglia, concentration gradients within the NAPL may be eliminated. Both of these actions will result in faster mass transfer.

When estimating dissolution or desorption mass transfer, the phase which limits the mass transfer rate, the diffusion path length, and the interfacial area are usually unknown. Mass transfer is usually described in terms of an overall mass transfer rate and a driving force. The driving force can be written in terms of either

phase, and the driving force in terms of the aqueous phase is related to the driving force in terms of the NAPL phase by the NAPL-water partition coefficient. It may be useful to write the equations in terms of the aqueous phase since water is the phase in which contaminants are measured and of interest for risk assessment purposes. However, if attempts are made to correlate mass transfer rate coefficients with physical processes, it is important to reconcile the phase in which mass transfer is limited with the reference phase for the driving force.

<u>Aging Effects on Mass Transfer Rate</u>

<u>Changes in NAPL volume</u>. Dissolution mass transfer rates are dependent on the geometry or distribution of NAPL in the porous media. Dissolution mass transfer occurs across the NAPL/water interface; mass transfer rates are therefore proportional to the specific interfacial area, $a_{n/w}$. If mass transfer is limited by diffusion in the NAPL phase, the NAPL distribution effects the diffusion path length, $\delta_n$. As a NAPL dissolves, its mass is transferred from the NAPL phase to the water phase and the volume occupied by the NAPL, $\theta_n$, will decrease with time. Shrinking the NAPL volume means shorter intra-NAPL diffusion path lengths which could increase mass transfer rates, and ultimately smaller specific interfacial area which will decrease mass transfer rates. Lamarche (1991) investigated the effect of depletion of single-component NAPL residual saturation (i.e., decreasing interfacial area on a system where mass transfer is rate-limited in the aqueous phase) on dissolution rates. He found column effluent concentrations were initially at the solubility limit, then

rapidly dropped to a lower, stable concentration of about one percent of the solubility limit. The lower, stable concentration may represent desorption from the solid phase instead of NAPL dissolution. Lamarche (1991) was unable to quantify a relationship between dissolution kinetics and interfacial area.

Changes in interfacial area may not be perfectly correlated to the volume of the NAPL. Two examples help conceptualize how the poor correlation could occur. The first example involves NAPL distributed in large, irregular multipore ganglia which upon dissolution "break up" into more smaller ganglia. In this case, the interfacial area might actually increase over the short term. The second example involves the concept of an "effective" specific interfacial area equal to the portion of the interface that is in contact with mobile water. Miller et al. (1990), Conrad et al. (1992) and Powers et al. (1991) all speculated that of use an "effective" $a_{n/w}$ value would be appropriate as higher mass transfer rates would be expected through that portion of the interface. Again in the case of large, multipore ganglia, decreasing $\theta_n$ would cause the ganglia to retreat down various pore throats. A significant change in volume could conceptually occur with little or no change in the interfacial area contacting mobile water. It may be possible to assume that interfacial area does not change significantly over certain portions of the dissolution process.

If the NAPL contains a significant fraction of "insoluble" components, such as pitch or alkanes, the dissolution of a comparatively small mass of soluble components may not have a significant effect on the NAPL saturation or the interfacial area.

This would allow $a_{n/w}$ to be treated as a time-independent variable as it is for sorption by soil organic matter.

Depletion of soluble constituents. Depletion of the more soluble components from a multicomponent NAPL can change the average molar volume of the remaining NAPL, which will change the partition coefficient and mass transfer rates. In addition to altering equilibrium conditions, depletion of these more soluble components can effect other changes to mass transfer rates that are limited by diffusion in the NAPL phase. Equation (2-18) shows that diffusion coefficients are proportional to the square root of the average molecular weight of the NAPL, and inversely proportional to the NAPL viscosity. Since depletion of more soluble components is likely to increase both molecular weight and viscosity of the remaining NAPL, the ultimate effect on the diffusion coefficient will depend on the faster changing of the parameters.

Luthy et al. (1993) reported that a semirigid interfacial film was formed on the surface of coal tar after the coal tar had been aged in water (i.e., some dissolution occurred). The formation of the film was accompanied by a decrease in mass transfer rates. The composition of the film was not identified, but likely includes high molecular weight components of pitch such as asphaltenes. Similar films have been reported for multicomponent NAPLs such as crude oil and coal tar which contain these high molecular weight compounds. Formation of interfacial films may require reevaluation of mass transfer models which largely ignore

interfacial processes. Dissolution kinetics could be dependent on the film properties, not the properties of the bulk of the NAPL.

Oxidation of NAPL components. Organic NAPLs in the subsurface will likely come under attack by various biological agents, which will oxidize NAPL components to produce energy. Many remediation efforts may seek to enhance this process, or to oxidize the NAPL through chemical means. For example, remediation of coal tar contaminated soil by land farming seeks to convert coal tar pitch to something which more resembles soil organic matter. Transformation of nonpolar polyaromatic compounds to compounds containing polar functional groups may "open up" the structure of NAPL components, making the NAPL more porous and speeding mass transfer (Augustijn, 1993). The effect of chemical structure on partitioning kinetics is discussed by Carroll et al. (1994) for the case of soil organic matter. Soil organic matter is theorized to be composed of swollen (fast sorption) and condensed (slow sorption) humic polymers. Diffusion through the various regions is suggested to cause the observed variation in sorption kinetics.

Changes in wetability. Studies in clean (glass) porous media (Conrad et al., 1992) usually result in water being the wetting phase and NAPL existing as ganglia in large pore spaces. In actual soils, NAPLs may associate with organic matter on the mineral surface (Mercer and Cohen, 1990), changing the wetting fluid from water to NAPL or a NAPL/organic matter mixture. This change in distribution will affect mass transfer in several ways. Converting from ganglia to surface coatings will likely increase interfacial area and decrease diffusion path lengths, contributing to a

increase in mass transfer rates. NAPL may be drawn by capillary forces into intra-aggregate micropores, creating long diffusion path lengths which will act to reduce mass transfer rates. The NAPL may be less likely to interface mobile water, which also results in reduced mass transfer rates.

Mass Transfer Models

Various models have been proposed to describe NAPL dissolution and soil organic matter sorption mass transfer. Some of the more common models for both NAPL dissolution and sorption applications are illustrated in Figure 2-9. The models illustrated in Figure 2-9 and described below are not a complete; other models do exist. Brusseau and Rao (1989a) reported that mass transfer for sorption systems is described by diffusion models, first-order mass transfer models, and by incorporating mass transfer into hydrodynamic dispersion. Weber et al. (1991) describe mass transfer models which are not first-order. This discussion focuses on first-order models because advective and diffusive fluxes are often described as first-order with respect to solute concentration. Diffusion-based models would seem to be more accurate descriptions of the mass transfer process, but they require many independently determined parameters (e.g., diffusion coefficient, particle diameter, path length tortuosity, micropore volume fraction) which may be difficult to determine. Further, the true diffusion domains are too complex to describe and averaged conditions must be used. The more empirical approaches of first-order mass transfer models are commonly used and probably lose little to accuracy.
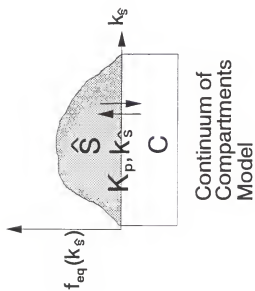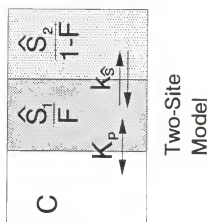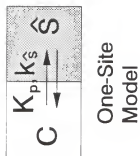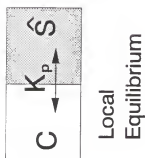
Figure 2-9. Sorption mass transfer models.

Models which employ other than first-order approaches may be necessary when isotherms are non-linear, but they create mathematical complications when coupled with flow models. Models which employ many mass transfer domains were omitted because Brusseau (1992a) found that the domain with the slowest rate dominates the mass transfer process.

First-order mass transfer models involve mass transfer coefficients that are dependent on the reference phase for the driving force term. The first-order mass transfer rate equations are presented in Equations (2-19a), (2-19b), and (2-19c) for NAPL dissolution referenced to the aqueous phase, NAPL dissolution referenced to the NAPL phase, and soil organic matter sorption, respectively:

$$\frac{dM_{i(n)}}{dt} = \frac{d}{dt}\theta_n C_{i(n)} = -a_{n/w}k_w\left(\frac{C_{i(n)}}{K_{n/w}} - C_{i(w)}\right) \qquad \textbf{(2-19a)}$$

$$\frac{dM_{i(n)}}{dt} = \frac{d}{dt}\theta_n C_{i(n)} = -a_{n/w}k_n(C_{i(n)} - K_{n/w}C_{i(w)}) \qquad \textbf{(2-19b)}$$

$$\frac{dM_{i(n)}}{dt} = \rho_s\frac{d\acute{S}_i}{dt} = \rho_s k_s(K_p C_{i(w)} - \acute{S}_i) \qquad \textbf{(2-19c)}$$

These equations all the mass transfer rate of solute $i$ between the aqueous and NAPL (or soil organic matter) phases per unit volume of porous media. If considered from a purely mathematical viewpoint, one can easily derive relationships between the mass transfer rate coefficients $k_w$, $k_n$, and $k_s$. However, if correlations

are to be made with process parameters (e.g., diffusion coefficients), care must be taken to use the appropriate form of the mass transfer equation.

Equations for various first-order mass transfer models are presented in Table 2-3. Equations describe time rate of mass of solute $i$ transferring between phases per unit volume of porous media for both NAPL dissolution and soil organic matter desorption. NAPL dissolution equations are written referenced to the aqueous phase. Equations for soil sorption models assume a constant partition coefficient.

Local equilibrium assumption. If all of the steps of the mass transfer process are very fast compared to the advective and dispersive transport in the aqueous phase, the water in the vicinity of the organic phase will always be at equilibrium with the organic phase. This is known as the Local Equilibrium Assumption (LEA) and is expressed using Equation (2-20a) for NAPL dissolution and Equation (2-20b) for soil organic matter sorption (Table 2-3). In many cases, the partition coefficient in Equation (2-20a) can be assumed constant. The NAPL volume fraction can sometimes be assumed constant with time if the NAPL contains a large fraction of insoluble components or the time scale of interest is relatively small.

Bahr and Rubin (1987) and Bahr (1990) conducted theoretical studies using dimensionless parameters to investigate applicability of LEA. They compared equilibrium and nonequilibrium mass transport models, isolated the kinetically influenced terms in the nonequilibrium models, and determined the conditions such that the kinetically influenced terms are not significant. When kinetically influenced terms are not significant, LEA is valid. Figure 2-10 illustrates the results of this

Table 2-3. Mass transfer rates for various dissolution and sorption models.

| Model | Dissolution | | Sorption | |
|---|---|---|---|---|
| Local Equilibrium Assumption | $\dfrac{dM_{i(o)}}{dt} = -\dfrac{d}{dt}(\theta_n K_{n/w} C_{i(w)})$ | (2-20a) | $\dfrac{dM_{i(s)}}{dt} = -\rho_s K_p \dfrac{dC_{i(w)}}{dt}$ | (2-20b) |
| One-Site Model | $\dfrac{dM_{i(o)}}{dt} = -a_{n/w} k_w \left(\dfrac{C_{i(n)}}{K_{n/w}} - C_{i(w)}\right)$ | (2-21a) | $\dfrac{dM_{i(s)}}{dt} = -\rho_s k_s (K_p C_{i(w)} - \hat{S}_i)$ | (2-21b) |
| Two-Site Model | $\dfrac{dM_{i(o)}}{dt} = -F K_{n/w} \dfrac{d}{dt}(\theta_n K_{n/w} C_{i(w)})$ $- a_{n/w} k_w \left(\dfrac{C_{i(n2)}}{K_{n2/w}} - C_{i(w)}\right)$ | (2-22a) | $\dfrac{dM_{i(s)}}{dt} = -F \rho_s K_p \dfrac{dC_{i(w)}}{dt}$ $+ \rho_s k_s \left(K_p C_{i(w)} - \dfrac{\hat{S}_{i(2)}}{(1 - F)}\right)$ | (2-22c) |
| | $C_{i(o)} = F K_{n/w} C_{i(w)} + (1 - F) C_{i(o2)}$ | (2-22b) | $\hat{S}_i = F K_p C_{i(w)} + \hat{S}_{i(2)}$ | (2-22d) |
| Continuum of Compartments | | | $\dfrac{dM_{i(o)}}{dt} = \rho_s [K_p C_{i(w)}) \int_0^\infty k_s f_{eq}(k_s)\,dk_s$ $- \hat{S}_i \int_0^\infty k_s f(k_s)\,dk_s]$ | (2-23) |

$$Pe = \frac{v_w L}{D_h}$$

$$Da = \frac{R k_s L}{v_w}$$

Region of LEA applicability

Damkohler Number, Da

Peclet Number, Pe
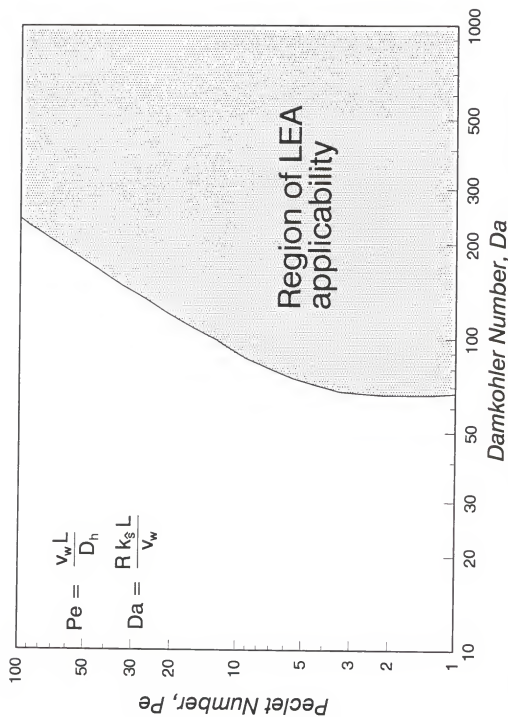
Figure 2-10. Conditions for LEA applicability for first-order one-site model (adapted from Bahr and Rubin, 1987, published by American Geophysical Union).

procedure for a one-dimensional transport and a one-site first-order sorption model. The region of LEA validity is defined by Peclet and Damkohler numbers. This solution is also valid for one-site first-order dissolution if the NAPL/water partition coefficient and volume fraction of NAPL do not change with time.

Experiments involving both single component NAPL ganglia (Hunt et al., 1988b; Anderson et al., 1992a; Guarnaccia et al., 1992) and multicomponent NAPL ganglia (Van der Waarden et al., 1971; Fried et al., 1979) indicated that equilibrium between NAPL and aqueous phases is achieved rapidly. Lamarche (1991) found that dissolution from trichloroethene ganglia was an equilibrium process over much his experiments, but mass transfer constraints became evident when NAPL saturation decreased to less than one percent of porosity. The mass transfer limitations may have been caused by desorption rather than dissolution. Borden and Piwoni (1992) found that dissolution of benzene from gasoline ganglia could be modeled using LEA, although other aromatics exhibited mass transfer limitations. These results seem to indicate that LEA is a reasonable assumption for many NAPL situations. These results contrast with soil organic matter sorption systems, where equilibrium conditions are rarely evidenced (Brusseau and Rao, 1989a). Since single component NAPL dissolution can only be rate limited by aqueous and interfacial processes, equilibrium conditions indicate that these processes are very fast. Nonequilibrium conditions observed for multicomponent NAPL dissolution and soil organic matter sorption is therefore evidence for mass transfer limited by organic phase diffusion.

Field data seldom reflects equilibrium conditions, prompting some researchers to investigate rate limited dissolution. Defending LEA, Anderson et al. (1992a,b) and Johnson and Pankow (1992) argued that dissolution is a rapid process, but as NAPL occupies only a small fraction of an aquifer, downgradient concentrations are probably diluted by water bypassing the NAPL. They attribute field observations of solute concentrations below the solubility limit to dissolution from pools of NAPL. Small interfacial areas normal to groundwater flow and the transverse dispersion process give the appearance of nonequilibrium. Dilution effects due to field observations are certainly probable as nonuniform distributions of NAPL are the norm. Poulsen and Kueper (1992) observed that saturations of a dyed NAPL released into an aquifer varied on a scale of millimeters.

If applicable, local equilibrium is a convenient assumption for two reasons; it does not require the estimation of mass transfer parameters, and it is computationally simple. For these reasons LEA has been widely used to model NAPL dissolution and solute sorption in porous media.

First-order kinetics, one-site model. The simplest nonequilibrium model, the one-site model, assumes that dissolution kinetics can be described by one average mass transfer rate. In its dissolution form (Equation 2-21a), the mass transfer rate equation features a single mass transfer rate coefficient, $k_w$, the specific interfacial area, $a_{n/w}$, and a driving force consisting of the difference of equilibrium and actual concentrations in the aqueous phase. Equation (2-21b), the sorption equivalent, is similar; the major difference is that interfacial area is a constant accounted for by the

mass of soil organic matter. Another difference is that the driving force for the sorption equation is written in terms of sorbed phase concentrations.

Several theoretical studies have employed the one-site model to demonstrate conditions where dissolution mass transfer is slow enough, compared to other contaminant transport mechanisms, for nonequilibrium conditions to exist. Hunt et al. (1988a) concluded that the dissolution mass transfer rate decreased with increasing ganglia diameter, and that ganglia could exist in porous media of sufficient size to cause dissolution to be the rate limiting process. Powers et al. (1991) investigated the effects of NAPL ganglia shape and mass transfer rate coefficient on rate limited mass transfer. Nonequilibrium mass transfer was predicted for small (areal extent) spills, high Darcy velocities, large ganglia sizes, and low NAPL saturations. Both Hunt et al. (1988a) and Powers et al. (1991) used correlations to determine mass transfer coefficients that were primarily developed for spheres or packed beds of solid organics. One of the correlation used by Powers et al. (1991) had been developed for NAPLs in groundwater, and mass transfer rate coefficients estimated with this correlation resulted in the fastest dissolution.

The one-site model has been used by several researchers to describe NAPL dissolution in column experiments. For single component NAPLs, studies include Miller et al. (1990) using toluene, Powers et al. (1992) using styrene and trichloroethene, and Guarnaccia et al. (1992) using trichloroethene. Observations of one-site nonequilibrium behavior of multicomponent NAPL systems include a gasoline study by Borden and Piwoni (1992), who noted that the degree of

nonequilibrium increased for the less soluble components, and Hatfield and Stauffer (1992), who observed nonequilibrium partitioning of various solutes in a column containing residual saturation of decane. Brusseau and Rao (1989a) report that two-site models are usually necessary to describe soil organic matter sorption.

The one-site model has the advantage of describing kinetics in a computationally simple way which appears to work reasonably well in certain cases for single component systems. However, it does not work well for soil sorption systems and cannot account for variable mass transfer rates in NAPL ganglia of different sizes.

First-order kinetics; two-site model. The two-site model assumes that the NAPL or soil organic matter is divided into two regions, each with its own characteristic mass transfer rate. Often one of the regions is assumed to be in equilibrium with the aqueous phase. The two-site model is represented in Table 2-3 by Equations (2-22a) and (2-22b) for NAPL dissolution and Equations (2-22c) and (2-22d) for sorption. The two-site model is a combination of the local equilibrium and one site models. If the fraction of sites experiencing equilibrium, F, equals unity, the two site model becomes the local equilibrium model. If the fraction of instantaneous sites is zero, the two-site model collapses to a one-site model. Note that the fraction of instantaneous sites, F, is a volume fraction for NAPL dissolution and mass fraction for soil organic matter sorption.

The conceptual justification for the two-site model for soil organic matter sorption has been that there are portions of the soil organic matter which are more

accessible to the solute than other portions. Ball and Roberts (1991) visualized soil organic matter located both on the outer surface of soil particles (more accessible, fast sites) and deep within micropores of soil aggregates (less accessible, slow sites) for the retarded intraparticle diffusion (RIPD) model. Intraorganic matter diffusion (IOMD) explanations of mass transfer conceptualize portions of the soil organic matter close to organic matter/water interface (short diffusion path, fast sites) and other portions distant from the interface (long diffusion path, slow sites) for the intraorganic matter diffusion model. Carroll et al. (1994) suggest that the two-site model works because of a bimodal distribution of diffusion coefficients resulting from both swollen (fast sorbing) and condensed (slow sorbing) polymeric structure of humic material constituting the organic matter. Although RIPD and IOMD are different conceptual models, both successfully employ the two-site model. The concept of sites of varying accessibility is easily extended to NAPLs in porous media; small droplets of NAPL might be considered fast sites while large multipore ganglia would be less accessible, slow sites (Borden and Kao, 1992).

The two-site model is very popular for soil organic matter sorption systems. Brusseau and Rao (1989a) review many of the researchers who have applied the model to soil sorption kinetics. Its use in NAPL dissolution is limited. Borden and Kao (1992) and Malone et al. (1993) used two-site models to describe dissolution of components from residual saturation of gasoline in laboratory columns. Borden and Kao used the two-site model as described in Equations (2-22a) and (2-22b), and further assumed that the NAPL/water partition coefficient did not change with time.

Malone et al. (1993) used a different version of the two-site model; dissolution of very small ganglia (fast sites) assumed a finite mass transfer rate estimated from a correlation by Miller et al. (1990) instead of using the local equilibrium assumption. The fast sites had mass transfer rates four orders of magnitude higher than the slow sites. Although the two-site model was necessary to describe the tailing observed during dissolution of gasoline components, both Borden and Kao (1992) and Malone et al. (1993) observed that over 90 percent volume fraction of the gasoline experienced equilibrium conditions.

Augustijn (1993) used the two-site model to describe sorption mass transfer by soils: (1) containing only natural soil organic matter, (2) contaminated with decane, (3) from a coal tar contaminated site, and (4) newly contaminated with coal tar. Mass transfer for soils contaminated with decane and aged coal tar-contaminated soils exhibited mass transfer characteristics similar to those typical of soil organic matter. However, the soil newly contaminated with coal tar soil exhibited mass transfer rates several orders of magnitude lower than would be typical of soil organic matter. Augustijn (1993) hypothesized that the aged coal tar had a more open structure due to oxidation. It is also possible that the soil newly contaminated with coal tar experienced mass transfer limitations due to formation of interfacial films as observed by Luthy et al. (1993).

To describe mass transfer, several steps in series and in parallel must be described. Weber et al. (1991) describe several approaches to linking mass transfer domains, and Brusseau (1992a) demonstrates several linked process, albeit from an

empirical approach. However, information on the subsurface systems and understanding of the dissolution process are too limited to provide values for so complex an approach. The usual approach is to assume that one of the steps is much slower than the others and limits the rate of the overall dissolution process, or that all processes can be grouped into one overall mass transfer rate. Brusseau (1992a) demonstrated how this may be a valid approach, but did not conduct a detailed sensitivity analysis to test the limits of the assumption.

The two-site model is a simple and versatile tool for describing partitioning mass transfer which exhibits the characteristics of partial equilibrium partitioning and partial tailing. Yet the two-site model is an empirical tool with limitations, notably in systems involving varying velocities (Brusseau, 1992b; Kookana et al., 1993) or long time periods for mass transfer (Karickhoff and Morris, 1985; Pavlostathis and Jaglal, 1991; Scribner et al., 1992; Connaughton et al., 1993). The two-site model fails under these conditions because a range of mass transfer rates is described by a parameter describing partitioning mass transfer relative to advective/dispersive transport (F) and by an averaged mass transfer rate coefficient.

Continuum of compartments model. To overcome the limitations of the two-site model, the number of sites may be increased, but this also increases the number of mass transfer parameters to be estimated. Connaughton et al. (1993) proposed that soil organic matter be treated as a continuum of compartments, each with its characteristic mass transfer rate. The size of each compartment is described by a frequency distribution with respect to the mass transfer rate, $f_{eq}(k_s)$. Connaughton

et al. (1993) proposed that the frequency distribution be described by a gamma function, which can be described by fitting only two parameters. The distribution of sorbate in the compartments is described by the time dependent distribution function, $f_s(k_s)$. Since $f_s(k_s)$ is time dependent, it cannot be described by a single distribution function. The sorption mass transfer rate (Equation 2-23) is dependent on the first moments of these two distributions. While the continuum of compartments model may overcome problems of velocity and time dependent sorption mass transfer inherent in the two-site model, it is computationally more rigorous and analytical solutions are probably not possible. Use of the continuum of compartments model has not yet been proposed for residual saturation of NAPL. Its form is probably more complex than Equation (2-23), since interfacial area ought to be combined with mass transfer rate and described by frequency distributions. If the ganglia size change during dissolution, mass transfer rate distributions both into and out of the NAPL would be time dependent. The time dependence of organic phase volume fractions again makes NAPL dissolution computationally more difficult than soil organic matter sorption.

<u>Quantifying Mass Transfer Rates</u>

In order to use the models described above, estimates of the mass transfer rates are necessary. Several researchers have tried to develop correlations to estimate mass transfer rates. Since the dissolution process is influenced by both the composition and geometry of the NAPL in the porous media, this topic is grouped

into three subsections: dissolution of single component NAPL ganglia, dissolution of multicomponent NAPL ganglia and soil organic matter sorption, and dissolution from NAPL pools.

Single component NAPL ganglia. Dissolution of single component NAPL ganglia is governed by aqueous phase mass transfer processes: advection and diffusion. Since the composition of the NAPL is constant, the NAPL-water partition coefficient is constant throughout the dissolution process. The volume occupied by the NAPL will necessarily decrease, causing changes in NAPL-water interfacial area as dissolution proceeds.

Several researchers have attempted to derive correlations for a one-site model mass transfer rate for a single component NAPL ganglia based on water phase advection and diffusion and NAPL/water interfacial area. Theoretical studies by Hunt et al. (1988a) and Powers et al. (1991) were based on correlations developed for flow around single spheres or packed beds of solid organic compounds to solve for the mass transfer rate, $k_w$. The correlations are written in dimensionless terms; commonly the Sherwood number, the Reynolds number, and the Schmidt number, respectively (Equations 2-24 through 2-26):

$$Sh = \frac{k_w d_c}{D_w} \qquad \textbf{(2-24)}$$

$$Re = \frac{v_w \rho_w d_c}{\lambda_w} \qquad \textbf{(2-25)}$$

$$Sc = \frac{\lambda_w}{\rho_w D_w} \qquad \textbf{(2-26)}$$

Powers et al. (1991) reported that the Sherwood numbers are related to the Reynolds and Schmidt numbers based on empirical correlations described in Equation (2-27):

$$Sh = a + b \, Re^m \, Sc^n \qquad \textbf{(2-27)}$$

where a, b, m, and n are empirical constants. Use of a mass transfer rate or rate coefficient based on Equation (2-27) is an empirical approach, but is probably better than a simple diffusion model because it incorporates more of the processes involved in dissolution mass transfer. All of the dimensionless numbers are defined in terms of aqueous phase because all mass transfer constraints are in that phase.

Equation (2-27) contains terms to relate mass transfer to advection and diffusion, but not to interfacial area. Researchers using real systems have been unable to independently estimate the interfacial area; Sleep and Sykes (1989), Miller et al. (1990), Guarnaccia et al. (1992), Borden and Piwoni (1992) and Powers et al. (1992) all combined the mass transfer rate coefficient and the specific surface area into a lumped parameter, the mass transfer rate, $k_{w-a}$ (Equation 2-28):

$$k_{w-a} = a_{n/w} k_w \qquad \textbf{(2-28)}$$

Miller et al. (1990) introduced a modified Sherwood number (Equation 2-29):

$$Sh' = \frac{k_{w-a} d_c^2}{D_w} \qquad \textbf{(2-29)}$$

The dimensionless numbers in Equations (2-24) - (2-26) and (2-29) employ a characteristic length to allow for scaling of relationships over varying system sizes. Miller et al. (1990) and subsequent researchers have defined the characteristic length as the mean particle diameter, $d_{50}$, even though characteristic length was expected to be a property of NAPL saturation and distribution. This approach was taken for lack of a way to estimate ganglia dimensions. The approach does invoke potential problems. To reconcile Equations (2-24) and (2-29), the characteristic length must equal the inverse of the specific interfacial area, $a_{n/w}$, which may not always be a constant value like $d_{50}$. Miller et al. (1990) and Powers et al. (1992) attempted to avoid the problems caused by the modified Sherwood number by conducting short-term, steady state experiments during which the NAPL volume fraction, $\theta_n$ and specific interfacial area, $a_{n/w}$ were assumed not to have changed.

Miller et al. (1990) recognized that the mass transfer rate coefficient had no obvious dependence on mean particle diameter. Assuming spherical ganglia, an alternative characteristic length in a saturated system might be estimated by Equation (2-30):

$$d_c = 6 \frac{\theta_n}{a_{n/w}} \tag{2-30}$$

This mean ganglia diameter would be descriptive of the system both in terms of advective transport by water (contact distance or time as water passes a ganglia) and, for a multi-component NAPL, diffusion in the NAPL phase (path length in the NAPL). This definition of characteristic length is similar to the longest blob diameter used in the theoretical study of Powers et al. (1991). However, until an independent method of estimating the interfacial area is developed, surrogates such as the mean particle diameter must be used.

Miller et al. (1990), Guarnaccia et al. (1992), and Powers et al. (1992) performed experiments with single component NAPLs and developed the regressions for Sh' shown in Equations (2-31) - (2-33) respectively:

$$Sh' = 12 \, \theta_w \, Re^{0.75} \theta_n^{0.60} Sc^{0.5} \tag{2-31}$$

$$Sh' = 3.18 \, Re^{0.98} \theta_n^{0.54} Sc^{0.5} \tag{2-32}$$

$$Sh' = 57.7 \, (Re \, \theta_w)^{0.61} d_{50}^{0.64} U_i^{0.41} \tag{2-33}$$

The $\theta_w$ term is included in some of the regressions because some of the authors defined parameters slightly different from those defined in this review. The uniformity index, $U_i$, is the ratio of particle diameters $d_{60}/d_{10}$.

All of the researchers found that the mass transfer rate was a strong function of the pore water velocity. Miller et al. (1990) found that the mass transfer rate

increased with pore water velocity to a point, after which it remained virtually constant. This indicates that mass transfer is limited by the rate that advection can remove solute at low velocities (i.e., local equilibrium), but by some other process(es) at higher velocities. This results in an exponent on the Re term of less than unity in the regressions of Miller et al. (1990) and Powers et al. (1992). Guarnaccia et al. (1992) conducted experiments at lower velocities, resulting in an Re exponent of near unity and observations of near LEA behavior. The relationship between Reynolds number and modified Sherwood numbers as determined in the three studies is shown in Figure 2-11.

Miller et al. (1990) and Guarnaccia et al. (1992) only conducted experiments with one NAPL, so they had data at only one Schmidt number. The inclusion of the Sc term in their regressions is not based on experimental data, and its exponent was one obtained from the literature. Powers et al. (1992) developed Equation (2-33) for data based on a NAPL composed of styrene. The regression fit their data from trichloroethene experiments reasonably well. As the fit could not be improved by accounting for the differences in the diffusion coefficients of styrene and trichloroethene in water, they elected not to include the Schmidt number in their regression.

One of the most interesting aspects of these correlations are the approaches taken to account for the specific surface area. As methods to directly measure $a_{n/w}$ have not been developed, researchers are forced to rely on surrogate parameters. Distribution of NAPL in a porous media, and therefore the specific surface area,
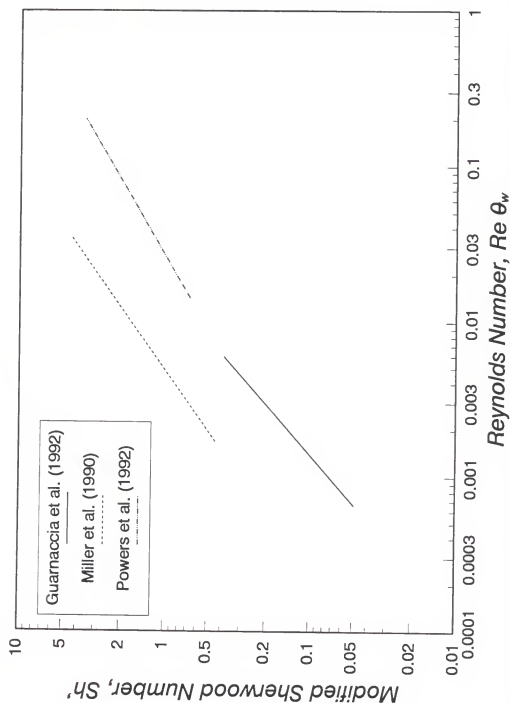
Figure 2-11. Comparison of modified Sherwood number predictions (adapted from Powers et al., 1992, copyright by American Geophysical Union, reprinted with permission).

depend on gradation and distribution of the pore spaces. A porous media composed of homogeneous particles will have small ganglia and the lowest residual saturation. As the distribution of the grain sizes (and therefore the pore sizes) increases, the residual saturation and ganglia size will also increase. If the medium is well sorted, NAPL will be trapped in large ganglia occupying the largest pore sizes. NAPL trapped in fewer, larger ganglia will have less surface area than NAPL in many small ganglia. This leads one to conclude that surface area is not directly proportional to NAPL saturation, and that capillary pressure-saturation relationships might be employed to estimate the surface area. Hunt et al. (1988a), Miller et al. (1990), Guarnaccia et al. (1992), and Powers et al. (1992) all discuss use of capillary pressure-saturation relationships to estimate $a_{n/w}$. However, the normal $p_c(\theta_w)$ relationships require that both immiscible phases be continuous. Since NAPL ganglia are discontinuous, use of these relationships as surrogates to describe NAPL-water interfacial area have not been developed.

Miller et al. (1990) and Guarnaccia et al. (1992) found that the mass transfer rate was a weak function of NAPL saturation, and included the NAPL volume fraction, $\theta_n$ in their regressions. Powers et al. (1992) rejected use of the $\theta_n$ term because, although increasing $\theta_n$ caused the mass transfer rate, $k_{w-a}$, to increase in uniform sands, $k_{w-a}$ decreased in graded sands. Various descriptors of the pore space gradation were tried including parameters from various $p_c(\theta_w)$ relationships, but grain size distribution parameters worked equally well. Powers et al. (1992) opted to use the mean grain size and uniformity index as surrogates for NAPL-water interfacial

area. Unfortunately, these parameters tell us nothing of the amount of NAPL present nor of the existence of pore size heterogeneities. It seems logical that reliable estimates of the NAPL-water interfacial area can be made using capillary pressure-saturation relationships, and these may be developed further in the future, possibly using data from direct measurement of NAPL ganglia using the NAPL polymerization techniques used by Conrad et al. (1992) and Powers et al. (1992).

Multicomponent NAPL ganglia and soil organic matter. Dissolution of individual components from multicomponent NAPL ganglia is the NAPL-water mass transfer system most analogous to soil organic matter sorption. The dissolution process is more complex; mass transfer constraints are possible in the NAPL and water phases and at the interface. Depletion of the more soluble components can change both equilibrium and mass transfer parameters (constituent dependent behavior). However, in many cases, the problem actually simplifies. For example, the molar volume of the constituents of many petroleum fuels are sufficiently similar that changes in partition coefficients can be ignored, and the fraction of soluble components is small enough that a constant interfacial area can be assumed. The system is therefore remarkably similar to soil organic matter sorption. These simplifications may not be valid if a large fraction of the NAPL constituents are soluble.

The two-site model, commonly used to describe soil organic matter sorption, has been applied to gasoline dissolution by Borden and Kao (1992) and to sorption by decane and coal tar contaminated soil by Augustijn (1993). Correlations for the

two-site model mass transfer parameters are not available for multicomponent NAPLs, but some have been developed for soil organic matter sorption. Brusseau and Rao (1989b) developed an empirical correlations between desorption mass transfer rate coefficient, $k_s/(1-F)$ (hr$^{-1}$), and the soil partitioning coefficient, $K_p$ (mL/g), for hydrophobic organics (Equation 2-34):

$$\log \left[ \frac{k_s}{(1-F)} \right] = 0.301 - 0.668 \log K_p \tag{2-34}$$

Augustijn (1993) attempted to further develop the correlation, writing it in terms of the mass transfer rate coefficient, $k_s$ (hr$^{-1}$), and the organic carbon equilibrium partitioning coefficient, $K_{oc}$ (mL/g) (Equation 2-35):

$$\log k_s = 3.53 - 0.97 K_{oc} \tag{2-35}$$

Augustijn (1993) also noted the dependence of the mass transfer rate on pore water velocity, but did not include a pore water velocity term in his regression.

The form of the sorption mass transfer equation used to create Equations (2-34) and (2-35) implies that mass transfer limitations are in the sorbed phase. If the mass transfer equation is rewritten in terms of organic material concentrations similar to Equation (2-19b), $k_s$ can be written in terms of an organic matter mass transfer rate coefficient, $k_{om}$ (Equation 2-36):

$$k_s = \frac{k_{om} \, a_{om/w}}{\theta_{om}} \tag{2-36}$$

By inserting Equations (2-11) and (2-36) into Equation (2-34), the Brusseau and Rao (1989b) correlation can be written in terms of the organic matter mass transfer rate (Equation 2-37):

$$k_{om} a_{om/w} = 2.00 (1-F) K_{om/w}^{-0.668} \theta_{om}^{0.332} \rho_s^{0.668} \qquad \textbf{(2-37)}$$

Similarly, the Augustijn (1993) correlation can be rewritten as Equation (2-38):

$$k_{om} a_{om/w} = 3390 K_{om/w}^{-0.97} \theta_{om}^{0.03} (\rho_s f_{oc})^{0.97}$$
$$= 3390 K_{om/w}^{-0.97} \theta_{om} (\rho_{om} \frac{f_{oc}}{f_{om}})^{0.97} \qquad \textbf{(2-38)}$$

The pore water velocity term was not included in these regressions, but Brusseau (1992b) and Augustijn (1993) both note that the sorption rate is dependent on the pore water velocity.

Equations (2-37) and (2-38) both include a positive correlation between mass transfer rate and organic matter volume fraction ($\theta_{om}$), which is similar to the work of Miller et al. (1990), and probably results as a measure of interfacial area. The two equations also indicate an inverse correlation between mass transfer rate and partition coefficient. Equation (2-38) includes some very intriguing terms. Dividing the equation through by the specific interfacial area results in the mass transfer rate coefficient being directly proportional to $\theta_{om}/a_{om/w}$, which as shown by Equation (2-30) is directly proportional to its diffusion path length. However, Equation (2-17b) indicates that the mass transfer rate coefficient should be inversely proportional to the square of the diffusion path length. Also, a positive correlation is indicated

between mass transfer rate and the density of organic carbon in the organic matter. This is an artifact of the correlation with organic carbon partition coefficient, but also seems counter-intuitive because a higher carbon content would seem to characteristic of an organic matter that has a higher density and hydrophobicity, and therefore slower mass transfer rates. Clearly more work is needed in developing and understanding these empirical correlations.

Sorption and dissolution processes are similar, and information from research in one area may be useful in promoting understanding in the other. Further research on correlations between sorption and dissolution mass transfer rate data may be helpful in understanding mass transfer from multicomponent NAPLs. This approach would seem especially useful for coal tar systems since, like natural organic matter, coal tar contains high molecular weight, insoluble compounds.

Dissolution from pools of NAPL. Mass transfer from NAPL ganglia and soil organic matter are pore scale processes. Dissolution from pools of NAPL is a process which operates at a much larger scale. In a series of papers, Anderson et al. (1992a,b) and Johnson and Pankow (1992) describe the process of dissolution from pools of NAPL. They claim that the dissolution process is rapid, and on a pore scale can be modeled by local equilibrium. However, pools of NAPL have very small interfacial areas in cross section to water flow. Dissolution is limited not by mass transfer, but by the rate that solute can be transported away from the interface (i.e., transverse dispersion). In other words, the rate of dissolution from pools of NAPL is controlled by aquifer hydrodynamics and not interphase diffusion. These claims

are consistent with the theoretical work of Powers et al. (1991) who predicted equilibrium conditions for large areal extent spills.

## Mass Transfer and Contaminant Remediation

Remediation of NAPL contaminated soil is a subject of great interest and continuing research and development. NAPL remediation technologies have been reviewed by Mercer and Cohen (1990). Since the majority of hydrophobic contaminants in contaminated soil exist in the NAPL or sorbed phases, recovery, destruction or at least isolation of the organic (particularly NAPL) phases would generally seem appropriate. Recovery technologies that have proven to be effective include excavation, vapor extraction of unsaturated soils (Baehr et al., 1989; Ho and Udell, 1992; Annable et al., 1993), and steam injection (Hunt et al., 1988b). Destruction technologies include bioventing of unsaturated soils (Dupont et al., 1991) and possibly vitrification. Isolation technologies include conventional hydraulic and physical barriers. Pump-and-treat technologies are very inefficient due to low solubility and hydrophobicity of the solutes and the heterogeneity of porous media (Mackay and Cherry, 1989). Although source treatment is desirable, the technologies will not be applicable for all sites, nor will they be completely effective. Remediation of sites contaminated with NAPLs or hydrophobic solutes will likely involve, at least as a component of the overall plan, pump-and-treat technology. When pump and treat is used, mass transfer processes become important. This review explores the

importance of mass transfer to various remediation approaches. The technologies discussed in this section and their attributes are summarized in Table 2-4.

Table 2-4. Remediation technologies and their effect on mass transfer processes.

| Remediation Technology | Impact on Mass Transfer |
|---|---|
| Increase Pumping Rate | Increase $k_w$, driving force |
| Pulsed Pumping | Allow equilibrium conditions to optimize volume pumped |
| Flooding Unsaturated Soil | Increase $a_{n/w}$ |
| Destroy aqueous contaminants | Max. driving force by minimizing $C_w$ |
| Surfactants | Partition into micelles, monomers; maximize $a_{n/w}$ |
| Cosolvents | Reduce $K_{n/w}$; possibly increase $k_s$ and $a_{n/w}$ |
| Dewatering | Decrease $a_{n/w}$ |
| Age NAPL | Increase $K_{n/w}$; possibly decrease $k_n$ |
| Subsurface Sorption Barrier | Add "insoluble" NAPL with high $K_{n/w}$, high $\theta_n$ |

Enhancing Mass Transfer

Mass transfer can be effected by controlling the transport of water through the contaminated zone. Various pumping schemes can be employed to enhance or decrease the dissolution and desorption processes. The variables that can be affected hydraulically are pore water velocity, contact time, and contact area.

Increase pumping rate. The mass transfer rate can be increased by increasing the hydraulic gradient and therefore the pore water velocity through the contaminated zone (Miller et al., 1990; Powers et al., 1992). Not only is the mass transfer rate increased, but by limiting contact time, the aqueous concentrations of the contaminant are kept low and therefore the driving force is kept as high as possible. Although this procedure will minimize the time required for clean up (Seagren et al., 1993), it results in large volumes of water which contain very low levels of contaminant (Borden and Kao, 1992). Treatment costs for water with low levels of contaminant will probably depend on the volume of water treated. Total treatment costs will therefore be disproportionately high.

Pulsed pumping. Recognizing the poor economy of maximizing the dissolution rate, optimization of the volume of water to be treated has been proposed using an approach called pulsed pumping (Borden and Kao, 1992). The ground water is not pumped continuously, but is cycled between pump and rest periods. During the rest period, the NAPL (or sorbed phase) and aqueous phase are allowed to approach equilibrium. Once water is contaminated with near saturation levels of contaminants, it is removed for treatment. Another constraint is that pumping would have to be sufficiently fast to prevent migration of contaminated water. The objective is to reduce cost by treating only highly contaminated water. This approach, though, results in longer time required to meet treatment objectives.

Flooding unsaturated soils. Another hydraulic control would be to affect the specific interfacial area. From Equations (2-19a) and (2-19b), mass transfer is

directly proportional to the specific interfacial area. Flooding unsaturated soils which contain residual NAPL to promote dissolution would be a way to take advantage of this property.

Destroy aqueous contaminants. The dissolution rate can only be manipulated by hydraulic control over a limited range. Therefore chemical methods have been proposed to effect the dissolution process. The simplest chemical method to enhance dissolution, at least in concept, is to ensure that the driving force is always near its maximum value. This would be achieved by making the aqueous phase concentration as near to zero as possible. Various methods for destroying the aqueous phase contaminants have been proposed, including enhanced biodegradation (Seagren et al., 1993) and chemical oxidation. To enhance dissolution, the contaminant destruction must take place in the immediate vicinity of the interface of the organic and aqueous phases. Also, the maximum driving force possible must be large enough to produce significant dissolution rates. Therefore, this approach will be most successful with single component NAPLs with relatively high aqueous solubilities. Achieving the necessary distribution of chemical oxidants or microbial nutrients in situ may be impossible due to media heterogeneities and reactions with inorganics. This method has a better chance of being successful in a completely mixed system. In such a system, contaminant destruction would likely be the goal, and enhanced dissolution by maximizing the driving force would be a side benefit. The problem with this method of enhancing mass transfer is that the partitioning coefficient and mass transfer rate coefficient are not affected.

The dissolution process could be enhanced by raising the temperature of the environment. This increases aqueous solubility (decreases the partitioning coefficient) and generally increases rates of mass transfer. However, raising the temperature of soil systems is expensive, and would probably involve raising temperatures in excess of the boiling point to remove NAPL, not to simply enhance mass transfer.

Surfactants. Addition of surfactants have been proposed to enhance both NAPL dissolution (Martel et al., 1993; Pennell et al., 1994) and desorption (Edwards et al., 1992a,b; Park and Jaffe, 1993) in porous media. Surfactant molecules have two structural moieties, one polar and the other nonpolar. Surfactants can dissolve in water as monomers, coat interfaces (e.g., NAPL/water and soil/water interfaces), and, at high enough concentrations, incorporate with other surfactant molecules to form micelles. The hydrophobic portion of the surfactant molecule is directed toward the interior of the micelle to form a liquid core with other hydrophobic moieties. Hydrophobic contaminants partition into, and are transported by, the micelles, thereby increasing their apparent aqueous solubilities and decreasing the apparent partition coefficient. As contaminants are removed from solution by partitioning into the micelles, more contaminant molecules dissolve or desorb to maintain equilibrium between the organic and water phases. When surfactant concentrations are below levels necessary to form micelles, hydrophobic compounds may combine with surfactant monomers (Edwards et al., 1992b). Partitioning into

surfactant monomers is not as strong as partitioning into micelles (Edwards et al., 1991; Park and Jaffe, 1993).

Use of surfactants for contaminant remediation faces several problems. Surfactants sorb to soil surfaces (Lui et al., 1992; Edwards et al., 1992b; Park and Jaffe, 1993) retarding their transport in porous media. Surfactant coating of the NAPL/water interface reduces surface tension and allows the formation of smaller NAPL particles. This process may increase the interfacial surface area and therefore the dissolution rate. Too much surfactant may result in the mobilization of NAPL ganglia (Pennell et al., 1994), which can exacerbate a contamination problems particularly in the case of DNAPLs. Surfactants can inhibit the biodegradation process (Laha and Luthy, 1992; Edwards et al., 1992a), which may cause problems if a treatment option seeks to combine enhanced solubilization and biodegradation.

Cosolvents. The use of cosolvents has also been proposed to enhance both NAPL dissolution (Augustijn et al., 1994a,b) and desorption (Rao et al, 1985; Nkedi-Kizza et al., 1985, 1987, 1989; Wood et al., 1990; Brusseau et al., 1991). This technology would affect the partitioning coefficient and possibly mass transfer rate coefficient and specific surface area. The aqueous phase would be replaced with a mixed solvent such as a methanol/water mixture. The contaminants have a greater solubility in the cosolvent mixture than in water alone, resulting in a decreased partition coefficient and increased driving force in the mass transfer equations (Equations 2-19a through 2-19c). Decreasing the partition coefficient to maximize the driving force is probably superior to approaches that seek to minimize the

aqueous concentration for those instances when the equilibrium concentration is very small in aqueous solutions (i.e., low solubility components of multicomponent NAPLs). Low values of equilibrium aqueous concentrations place such a great restraint on the driving force that, even at its maximum value, mass transfer is very limited. Increasing the saturation concentration is a more efficient method of enhancing mass transfer.

For sorption systems, several researchers (Nkedi-Kizza et al., 1989; Wood et al., 1990; Brusseau et al., 1991) have found that mass transfer rate coefficients increase with increasing cosolvent fractions. Brusseau et al. (1991) surmised that the presence of a cosolvent causes swelling of the organic matter, enhancing intraorganic matter diffusion. Further, they found that the correlation between mass transfer rate and partition coefficients derived by Brusseau and Rao (1989b) (Equation 2-34) held valid for cosolvent fractions below 70 percent. Presumably at very high cosolvent fractions the assumptions for ideal behavior are no longer valid.

Cosolvents decrease NAPL-water interfacial tension, possibly creating emulsions and increasing the specific surface area. Mobilizing NAPL ganglia may result in migration to previously uncontaminated zones, particularly in the case of DNAPLs. Tests of solvent flushing have been successful in the laboratory, but have yet to be tested *in situ*. Use of this technology *in situ* may be risky as contaminant migration is enhanced; if the cosolvents are not captured, contaminants could spread further and faster than they would under natural conditions. Further, cosolvents tend to shrink clays, possibly opening new migration pathways to mobilized NAPLs

(Augustijn et al., 1994a). As with all *in situ* technologies, delivery of the cosolvent may be difficult to achieve in a uniform manner due to media heterogeneities (Augustijn et al., 1994a). Density differences between cosolvents and water will further exacerbate this problem (Augustijn et al., 1994a).

Diminishing Mass Transfer

The alternative to enhancing dissolution to speed the contaminant recovery is to diminish the process to prevent significant migration from the source. Diminishing dissolution is not only difficult technically, it may be politically unacceptable as contaminants are left in place.

Dewatering. Diminishing dissolution hydraulically is most feasible by decreasing the interfacial contact area by dewatering a saturated contaminant zone. Given the success of venting technology, dewatering in conjunction with venting would likely be a successful approach.

Perhaps the most obvious chemical method would be to reduce the solubility of hydrophobic contaminants by increasing the polarity of the aqueous solution (i.e., "salting out" organic solutes). Adding electrolytes to water does decrease the solubility of many nonpolar organics. However, even at seawater salinity levels, the solubility of organics is only reduced by about 15 percent (Burris and MacIntyre, 1986b). When clean up objectives require reduction in concentrations over orders of magnitude, this approach is not likely to be successful. It would also render the water unsuitable for drinking because of high total dissolved solids.

Aging NAPL. Dissolution might be diminished if a NAPL could be altered to make the partitioning coefficient higher or the mass transfer rate lower. It is possible that this may be achieved by "aging" the NAPL, using treatment methods such as cosolvent washing or biodegradation. For example, if the NAPL following treatment is more viscous (reduced diffusion coefficient in NAPL), and the contaminant levels in the NAPL are low (reduced driving force), the dissolution rate may be slow enough to maintain aqueous concentrations below maximum contaminant levels. Formation of interfacial films (Luthy et al., 1993) could also inhibit mass transfer rates. It is therefore possible that use of certain remediation technologies, even though they are not totally effective at destroying or removing contaminants, could still result in meeting water quality objectives.

Subsurface sorption barrier. Another approach is to use partitioning principles to design a subsurface sorption barrier. A large mass of insoluble NAPL (e.g., decane, mineral oil) would be distributed as an immobile residual saturation in the porous media to intercept a groundwater plume. Laboratory experiments and modeling studies (Hatfield, et al., 1992) have indicated that these types of systems could be effective at sorbing plumes of organic contaminants for years. The contaminants concentrated in the NAPL may be removed, or possibly they would be destroyed by natural chemical and biological means. This technology has great potential for reducing the costs inherent in pump and treat systems. However, engineering development is required to ensure uniform distribution of NAPL,

conservation of hydraulic conductivity, and, if necessary, eventual removal of the system.

## Summary

Equilibrium partitioning of nonpolar compounds between organic (NAPLs or soil organic matter) and aqueous phases may be estimated by the Raoult's law approach. Mass transfer between organic and aqueous phases in porous media is a complex process. Dissolution from NAPLs seems to be rapid compared to groundwater advective/dispersive transport, and local equilibrium may often be a reasonable assumption.

Dissolution mass transfer may be rate limited in cases of: (1) high pore water velocity (limited contact time), (2) NAPL present as large multipore ganglia (low interfacial area and long transport distances within the ganglia), (3) low mole fraction of a NAPL component (small driving force), or (4) the dissolution process being in advanced stages (small interfacial area, formation of interfacial films, decrease in intra-NAPL diffusivity). Sorption and desorption from soil organic matter is usually a rate limited process.

Methods for estimating mass transfer rates generally involve empirically derived first-order kinetics. First-order models have the disadvantage that mass transfer rate coefficients are velocity or time dependent. Further research is needed to better understand and describe the distributions of organic phases in porous media

and to quantify the effects of diffusion limited transport in the ganglia of multicomponent NAPLs.

Dissolution and desorption processes will influence NAPL remediation, and technologies to enhance or diminish the mass transfer are being developed to help clean up the thousands of contaminated sites. Subsurface sorption barriers for collection of groundwater plume contaminants and use of cosolvents and surfactants for enhanced dissolution are promising remediation technologies that take advantage of partitioning and mass transfer principles to effect clean up.

# CHAPTER 3
## TWO-SITE MODEL PARAMETERS FROM STIR CELL EXPERIMENTS

### Introduction

The two-site model has been widely used to describe sorption mass transfer (Brusseau and Rao, 1989a). Sorption sites are classified in two groups by their mass transfer rates; "fast" sites that are at equilibrium with the aqueous phase and "slow" sites that experience first-order mass transfer. The two-site model is displayed schematically in Figure 3-1 and described mathematically by Equation (3-1):

$$M_s \frac{d\hat{S}_i}{dt} = FM_s K_p \frac{dC_{i(w)}}{dt} + M_s k_s (K_p C_{i(w)} - \frac{\hat{S}_{i(2)}}{(1-F)})$$  (3-1)

where notation for this and following equations are defined in the Glossary.

The three parameters needed to model two-site mass transfer are the equilibrium partition coefficient, $K_p$, the fraction of equilibrium sites, F, and the mass transfer rate coefficient for the "slow" sites, $k_s$. The partition coefficient can be obtained independently through batch isotherms, but F and $k_s$ are usually obtained by fitting models to experimental data. Experiments used for parameter prediction often include column tests, batch tests, or gas purge tests. All three methods have their limitations. In column experiments, the effects of mass transfer are combined with the effects of flow in porous media; hydrodynamic processes must be estimated

91
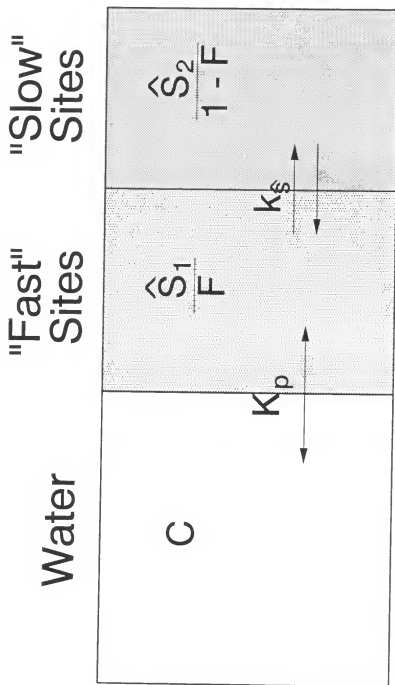
Figure 3-1. The two-site model.

separately using nonreactive tracers. Grain scale mass transfer resistances such as intraorganic matter diffusion and retarded intraparticle diffusion may be masked by diffusion through extra-aggregate immobile water. Batch methods are usually not amenable to perturbation analysis. The nature of mass transfer can be revealed by perturbation analysis, which can be performed by changing the flux of solute through the soil/water system and measuring the response. As there is no flux into or out of a batch system, batch methods generally cannot employ this technique. The gas purge method is a special case of the batch method where perturbation analysis is possible. However, perturbations are limited to removal of mass from the system and the technique can only be used for chemicals with a high Henry's constant since the component of interest must be removed from solution by volatilization.

An alternative technique to the three methods previously described is the stirred flow cell or continuously stirred tank reactor (CSTR). The stir cell consists of a chamber in which a soil/water slurry is continuously stirred. Water (or cosolvent) can flow through the cell but solids are retained in the cell. The stir cell has several advantages for the study of mass transfer:

1. Turbulent conditions in the cell preclude diffusion in extra-aggregate immobile water from being a limiting process. Mass transfer limitations will then be due to diffusion in organic matter or intraparticle micropores.

2. Low solid:liquid ratios (less than 0.2 g/mL) will result in lower retardation factors than experienced in columns. Experiments with

highly sorbing solutes can be accomplished faster in a stir cell than in a column.

3.  Perturbation analysis can be accomplished by varying flow rate, influent concentration, fluid composition, and temperature.

4.  Lack of space parameters (e.g., distance along column length) in the mass balance equation makes analytical solutions possible in some cases.

Only limited use of stir cells for studying soil/water systems has been reported to date. Miller et al. (1989) introduced a 30 mL plastic cell which used a shaft-driven impeller to suspend sediments. Bellin (1993) and Hoogeweg (1993) also used a shaft-driven impeller to stir their 4 mL steel stir cell for studies of sorption and biodegradation of quinoline. Carski and Sparks (1985) described a system which used a magnetic stir bar to study ion exchange kinetics. DiGrazia (1991) used a 0.75 L system to study sorption and biodegradation of naphthalene. While these stir cells demonstrated some success for studying sorption and/or degradation, all of the designs had to face the common problem of clogging. Deposition of solids on the effluent filter builds up back pressure, which causes leaks or even breakage of the cell. Further, the solids caked on the filter no longer experience completely mixed conditions, invalidating the governing equations. Miller et al. (1989) suggested that turbulence from the propeller could dislodge particles from the effluent filter. The design of Bellin (1993) and Hoogeweg (1993) attempted to use the impeller to physically brush the filter. Their steel design could withstand higher back pressures,

but prevented observation of the slurry. DiGrazia (1991) used a very large filter area to minimize clogging. All of these stir cells were designed for flow in one direction only; backwashing of the frits to resuspend the caked solids was not possible.

The objectives of this chapter are to:

1.  Describe a new, reversible-flow stir cell design that is compatible with standard high pressure liquid chromatography (HPLC) equipment;

2.  Compare two-site model parameter predictions obtained from stir cell experiments with parameters estimated from column experiments and published predictive methods; and

3.  Compare two methods of stir cell operation: flow interruption and flow-rate variation.

## Materials and Methods

### Solids, Solutes, and Solvents

Experiments were performed using two soils: Eustis sand and Zellwood muck. The Eustis soil was prepared by sieving with a 250 $\mu$m sieve, while the Zellwood muck was sieved with a 3 mm sieve. Both soils were allowed to air dry prior to use. The characteristics of the soils are summarized in Table 3-1.

The solvents used in all experiments were mixtures of HPLC grade methanol (MeOH) and distilled, deionized water ($H_2O$) in volume-to-volume ratios ranging from 0:100 to 50:50 MeOH/$H_2O$. Cosolvent ratios were chosen to result in partition coefficients of an optimum magnitude for stir cell experiments (retardation factors

Table 3-1. Soil characteristics.

|  | Eustis | Zellwood |
|---|---|---|
| Water Content (dry weight basis) | 0.0023 | 0.177 |
| Organic Carbon Content, $f_{oc}$ (Walkly-Black method) | 0.0054 | 0.43 |

in the range of 2 to 3). All solutions contained 0.01N $CaCl_2$ to provide a constant ionic strength, and were degassed with helium to inhibit biological activity and prevent cavitation.

Solutes used in the experiments were naphthalene, anthracene, pyrene, and pentafluorobenzoic acid (PFBA). All solutes were obtained from Aldrich Chemical Co., Milwaukee, WI, and were at least 99 percent pure.

Isotherms

Batch isotherm experiments were conducted to obtain independent estimates of the partition coefficient, $K_p$ (Equation 2-10). Linear isotherms were obtained over the concentration ranges and cosolvent mixtures of interest. Experimental procedures and isotherms are presented in the Appendix A.

Stir Cell Experiments

Stir cell construction. The component parts of the stir cell are listed in Table 3-2. The glass portion of the stir cell (roughly spherical with two threaded openings)

Table 3-2. Component parts of stir cell.

| Part | Small Cell | Large Cell | Source |
|------|-----------|-----------|--------|
| Glass Cell | Two #15 thread Glass Threaded Connectors [7644-15] | Two #25 thread Glass Threaded Connectors [7644-20] | Ace Glass, Inc. Vineland, NJ (fused by glass blower) |
| End Adapters | #15 thread Teflon Adapters [5838-47] | #25 thread Teflon Adapters [5838-51] | Ace Glass, Inc. Vineland, NJ |
| O-Rings | Teflon [T015 or T113] | Teflon [T023 or T121] | Sci. Instr. Services Ringoes, NJ |
| Frits | 1/2" OD x 1/32" thick x 2 μm pore size, Stainless Steel [721825] | 1" OD x 1/32" thick x 2 μm pore size, Stainless Steel [722205] | Alltech Assoc. Deefield, IL |
| Stir Bar | Nalgene teflon-coated Star-Head™ magnetic stir bar, 10 mm dia. [6600-0010] | Nalgene teflon-coated Star-Head™ magnetic stir bar, 22 mm dia. [6600-0012] | Fisher Scientific Pittsburgh, PA |

was fabricated by a glass blower from the threaded columns. Several stir cells were constructed and used, with sizes ranging from about 6.5 to 44 mL.

The edges of the stainless steel frits were wrapped with teflon tape to ensure a good seal with the teflon adapters. The frits served to retain the solids in the stir cell. The outside end of the adapters had female threads compatible with standard HPLC fittings.

Teflon o-rings assured a tight seal between the glass cell and the teflon adapters. During experiments, the stir cell assembly was located on a magnetic stir plate, and the teflon-coated stir bar kept the solid and liquid phases in a continuously mixed condition.

Experimental apparatus. The entire apparatus for stir cell experiments is illustrated in Figure 3-2. Solvents (either containing solute or solute-free) were pumped by separate HPLC positive displacement pumps (Gilson Model 302, 5 mL/min capacity). Direction of solvent flow was controlled by two six-way valves (Rheodyne 7000). The first valve was used to select the pump that sent solvent flow through the stir cell. The second valve was used to control flow reversal. Since fine particles collect on the downstream frit, it was necessary to periodically reverse the direction of flow through the stir cell to backwash each frit in turn. This procedure prevented clogging and leaking problems and maintained continuously mixed conditions in the cell. The system was plumbed so that only a small volume of solvent (0.04 mL or ≤ 0.7 percent of the stir cell liquid volume) was redirected back through the cell each time flow direction was reversed.
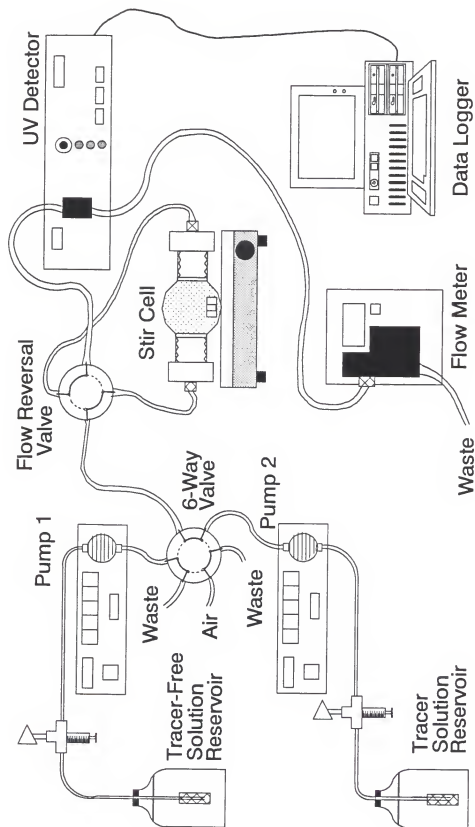
Figure 3-2. Stir cell apparatus.

Stir cell effluent was continuously monitored by an in-line ultra-violet (UV) detector (LDC/Milton Roy Spectromonitor III, Model 1204A). Continuous readings were recorded on a strip chart (Fisher Recordall Series 5000) and also digitally stored at 20 to 60 second intervals on an IBM PC computer using a Model 5508TC data acquisition card (ADAC Corp., Woburn, MA). All tubing between the first valve and the UV detector was 0.02 inch ID stainless steel to minimize dead volume and preclude sorption. Flow was measured by a Humonics 1000 digital flow meter.

Operation. The response of the UV detector to solute-containing and solute-free solutions was measured before and after each experiment when the stir cell was disconnected from the system. The stir cell was weighed empty and again after solid material was placed inside. Solute-free solvent was then introduced. Air bubbles were usually trapped in the cell, requiring removal by pumping degassed solvent through the stir cell for about an hour prior to starting an experiment. Pumping solute-free solvent through the stir cell also flushed dissolved organic matter from the soil in the cell, established a stable baseline for the in-line UV detector, and allowed hydration of soil organic matter. Flow direction through the stir cell was reversed periodically during all pumping operations, usually about every 10 minutes. However, flow reversals were not performed for blanks because fine material was not present in the stir cell.

Once a stable baseline was established, the solute-containing solvent was introduced. Two types of experiments were performed; flow interruption and flow-rate variation.

Flow interruption experiments were conducted at a single flow rate. The sequence of events was generally as follows:

1. Solute-containing solvent was directed through the stir cell until effluent concentration reached about 75 percent of the influent concentration.

2. Flow was stopped for about one hour.

3. Flow of solute-containing solvent was resumed until the effluent concentration was stable and approximately equal to the influent concentration. This usually involved pumping a total of 8 to 10 cell liquid volumes through the stir cell.

4. Solute-free solvent was pumped through the stir cell until the effluent concentration reached about 25 percent of the influent concentration.

5. Flow was stopped for about one hour.

6. Flow of solute-free solvent was resumed. The experiment was complete when the effluent concentration was stable and appeared to reflect baseline conditions.

Flow-rate variation experiments were generally conducted by directing two sequential pulses of solute through the stir cell. The flow rate was changed at least four times during the experiment; flow rates usually ranged between 0.5 and 2 mL/min. Changing the flow rate over a wider range was not practical. Higher flow rates increase hydrostatic pressure in the cell and could cause failure (leaking).

Lower flow rates allow diffusive mixing in the tubing between the stir cell and the detector (detector concentrations are no longer representative of stir cell conditions).

Grab samples for HPLC analysis were taken at strategic points throughout each experiment. Samples were collected directly after the in-line UV detector to minimize dead volume between the stir cell and the sampling location.

Experiments with PFBA, a nonsorbing solute, determined that the stir cell hydraulics were characteristic of a continuously mixed reactor (Figure 3-3).

Mass transfer parameters were estimated from break-through curve data using a modified version of TESTFIT, a University of Wisconsin nonlinear least squares regression program which uses the Marquadt technique.

## Column Experiments

The column experiments are described in detail by Dai (1993). Synopses of the experimental apparatus and operational parameters are provided below.

Column construction. The column consisted of a 0.99 cm ID by 7.41 cm long stainless steel cylinder. Soil was retained in the column using 2 $\mu$m pore size stainless steel frits. Eustis soil was packed in the column with a bulk density of 1.65 g/cm$^3$ and a saturated water content of 0.42.

Experiment apparatus. The system hardware was virtually identical to that described for the stir cell (Figure 3-2) except that the flow reversal valve was not needed and the column was placed in the location of the stir cell.
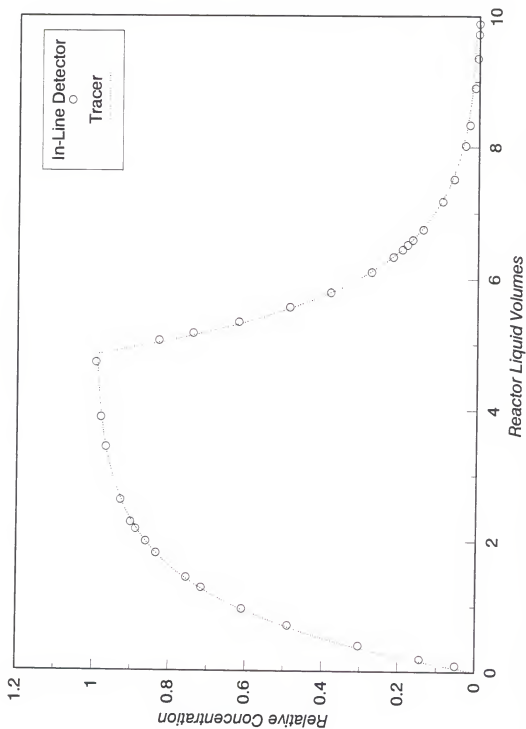
Figure 3-3.  Ideal mixing in stir cell shown by breakthrough curve of nonsorbing tracer (PFBA).

Operation. Experiments were run at a constant flow rate of 0.4 mL/min.
Solute was introduced as a short pulse of 0.046 pore volumes, except for one
experiment where solute was introduced as a long pulse of 83 pore volumes.
Experiments with a nonsorbing tracer (PFBA) were performed to determine the
Peclet number (an indicator of hydrodynamic dispersion) which was found to be 55.
Equilibrium partitioning was estimated by batch isotherms and moment analysis.
Two-site model parameters were estimated by fitting the breakthrough curve data
using the program CFITIM3 (van Genuchten, 1981).

## Models

The governing equation for the stir cell is given by Equation (3-2):

$$V\frac{dC}{dt} + M_s\frac{d\hat{S}_s}{dt} + M_R\frac{d\hat{S}_R}{dt} = Q(C_{in} - C) \tag{3-2}$$

The sorption onto the soil and the reactor walls (if significant) are both described by
the two-site model:

$$\hat{S}_s = \hat{S}_{s(1)} + \hat{S}_{s(2)} \tag{3-3}$$

and:

$$\hat{S}_R = \hat{S}_{R(1)} + \hat{S}_{R(2)} \tag{3-4}$$

where:

$$\hat{S}_{s(1)} = FK_p C \tag{3-5}$$

$$\hat{S}_{R(1)} = F_R K_R C \tag{3-6}$$

and:

$$\frac{d\hat{S}_{s(2)}}{dt} = k_s(K_p C - \frac{\hat{S}_{s(2)}}{(1-F)}) \tag{3-7}$$

$$\frac{d\hat{S}_{R(2)}}{dt} = k_R(K_R C - \frac{\hat{S}_{R(2)}}{(1-F_R)}) \tag{3-8}$$

It is often convenient to analyze experimental data in dimensionless terms. This is accomplished by defining the following dimensionless numbers:

$$R = 1 + \frac{M_s K_p}{V} + \frac{M_R K_R}{V} \tag{3-9a}$$

$$R_f = 1 + \frac{FM_s K_p}{V} + \frac{F_R M_R K_R}{V} \tag{3-9b}$$

$$R_s = \frac{(1-F)M_s K_p}{V} \tag{3-9c}$$

$$R_R = \frac{(1-F_R)M_R K_R}{V} \tag{3-9d}$$

$$\omega_s = \frac{M_s K_p k_s}{Q_{max}} \tag{3-9e}$$

$$\omega_R = \frac{M_R K_R k_R}{Q_{max}} \tag{3-9f}$$

$$\hat{S}_s^* = \frac{\hat{S}_{s(2)}}{(1-F)K_p C_{max}} \tag{3-9g}$$

$$\hat{S}_R^* = \frac{\hat{S}_{R(2)}}{(1-F_R)K_p C_{max}} \tag{3-9h}$$

$$C^* = \frac{C}{C_{max}} \tag{3-9i}$$

$$C_{in}^* = \frac{C_{in}}{C_{max}} \tag{3-9j}$$

$$T = \frac{Q_{max}t}{V} \tag{3-9k}$$

$$Q^* = \frac{Q}{Q_{max}} \tag{3-9l}$$

$$P = Q^*T \tag{3-9m}$$

$$C_0^* = C^*(T=0) \tag{3-9n}$$

$$\hat{S}_{s_0}^* = \hat{S}_s^*(T=0) \tag{3-9o}$$

$$\hat{S}_{R_0}^* = \hat{S}_R^*(T=0) \tag{3-9p}$$

Substituting appropriately, the governing equations become:

$$R_f \frac{dC^*}{dT} + R_s \frac{d\hat{S}_s^*}{dT} + R_R \frac{d\hat{S}_R^*}{dT} - Q^*(C_{in}^* - C^*) \tag{3-10}$$

$$R_s \frac{d\hat{S}_s^*}{dT} - \omega_s(C^* - \hat{S}_s^*) \tag{3-11}$$

and:

$$R_R \frac{d\hat{S}_R^*}{dT} - \omega_R(C^* - \hat{S}_R^*) \tag{3-12}$$

When one of the sorption sinks (solid phase or stir cell wall surfaces) is not present, the governing equations reduce to a second order differential equation which can be solved analytically. This condition is met when no soil is present in the reactor (blank) or when sorption onto the stir cell wall surfaces is not significant. Sorption onto the stir cell was found to be significant for naphthalene in water and anthracene in 30 percent methanol, and insignificant for all other solute/solvent combinations (see Appendix B). The analytical solution is given below, assuming that stir cell sorption is insignificant ($K_R \approx 0$).

$$C^* - (\frac{R_s n_1}{\omega_s} + 1)K_1 e^{n_1 T} + (\frac{R_s n_2}{\omega_s} + 1)K_2 e^{n_2 T} + C_{in}^* \tag{3-13}$$

and:

$$\hat{S}_s^* = K_1 e^{n_1 T} + K_2 e^{n_2 T} + C_{in}^* \tag{3-14}$$

where:

$$K_1 = \frac{\omega_s}{R_s} \frac{(C_0^* - \hat{S}_{s0}^*)}{(n_1 - n_2)} + \frac{n_2}{(n_1 - n_2)}(C_{in}^* - \hat{S}_{s0}^*) \tag{3-15a}$$

$$K_2 = \hat{S}_{s0}^* - K_1 - C_{in}^* \tag{3-15b}$$

$$n_2 = \frac{-b + \sqrt{b^2 - 4aQ^*}}{2a} \tag{3-15c}$$

$$n_2 = \frac{-b - \sqrt{b^2 - 4aQ^*}}{2a} \tag{3-15d}$$

$$a = \frac{R_f R_s}{\omega_s} \tag{3-15e}$$

$$b = R + \frac{Q^* R_s}{\omega_s} \qquad \text{(3-15f)}$$

Note that if there is no flow through the stir cell (i.e., $Q^* = 0$), then $C_{in}^*$ must be defined as zero.

When sorption to both soil and stir cell wall surfaces are significant, the governing equations are solved numerically using a forward differencing technique:

$$C^*(T + \Delta T) = \frac{1}{U_4}(U_1 C^*(T) + U_2 \hat{S}_s^*(T) + U_3 \hat{S}_R^*(T) + Q^* C_{in}^*) \qquad \text{(3-16)}$$

$$\hat{S}_s^*(T + \Delta T) = A_s(C^*(T + \Delta T) + C^*(T)) + B_s \hat{S}_s^*(T) \qquad \text{(3-17)}$$

and:

$$\hat{S}_R^*(T + \Delta T) = A_R(C^*(T + \Delta T) + C^*(T)) + B_R \hat{S}_R^*(T) \qquad \text{(3-18)}$$

where:

$$A_s = \frac{\dfrac{\omega_s}{2}}{\dfrac{R_s}{\Delta T} + \dfrac{\omega_s}{2}} \qquad \text{(3-19a)}$$

$$B_s = \frac{\dfrac{R_s}{\Delta T} - \dfrac{\omega_s}{2}}{\dfrac{R_s}{\Delta T} + \dfrac{\omega_s}{2}} \qquad \text{(3-19b)}$$

$$A_R = \frac{\dfrac{\omega_R}{2}}{\dfrac{R_R}{\Delta T} + \dfrac{\omega_R}{2}} \qquad \text{(3-19c)}$$

$$B_R = \frac{\dfrac{R_R}{\Delta T} - \dfrac{\omega_R}{2}}{\dfrac{R_R}{\Delta T} + \dfrac{\omega_R}{2}} \qquad \text{(3-19d)}$$

$$U_1 = \frac{R_f}{\Delta T} - \frac{R_s A_s}{\Delta T} - \frac{R_R A_R}{\Delta T} - \frac{Q^*}{2} \qquad \text{(3-19e)}$$

$$U_2 = \frac{R_s(1-B_s)}{\Delta T} \qquad \text{(3-19f)}$$

$$U_3 = \frac{R_R(1-B_R)}{\Delta T} \qquad \text{(3-19g)}$$

and:

$$U_4 = \frac{R_f}{\Delta T} + \frac{R_s A_s}{\Delta T} + \frac{R_R A_R}{\Delta T} + \frac{Q^*}{2} \qquad \text{(3-19h)}$$

## Results

### Stir Cell Breakthrough Curves

Typical stir cell breakthrough curves are depicted in Figure 3-4 for a flow interruption experiment and in Figure 3-5 for a flow-rate variation experiment. Data are plotted as relative aqueous concentration ($C^*$, Equation 3-9i) on the Y-axis versus cell liquid volumes (P, Equation 3-9m) on the X-axis. Both digitized in-line detector data and HPLC-analyzed grab sample data are displayed. Three curves are plotted: the tracer line represents behavior of a solute sorbing to the stir cell wall surfaces but not the soil; the equilibrium sorption line represents mass transfer-limited sorption onto the stir cell wall surfaces and equilibrium sorption onto the soil; and the two-site model line represents the fitted mass transfer parameters for soil and stir cell sorption.

Flow interruption breakthrough curves are characterized by the discontinuity in the exponential curve at the points where flow is stopped. Flow-rate variation experiments do not have this discontinuity.
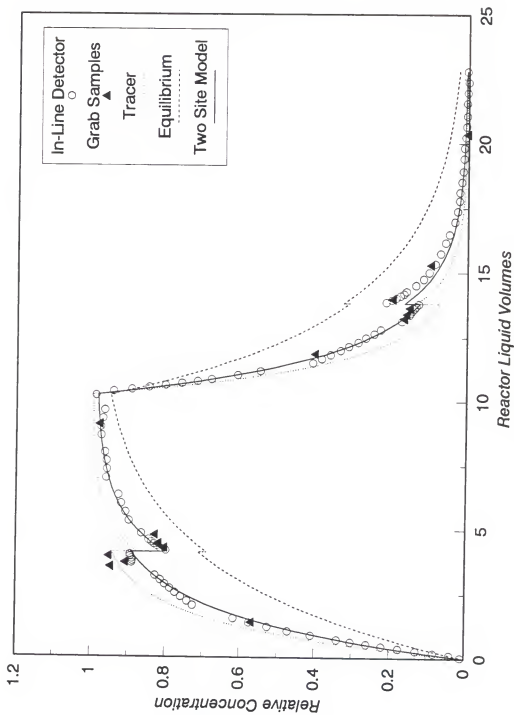
Figure 3-4. Typical flow interruption experiment breakthrough curve (Experiment AEI100).
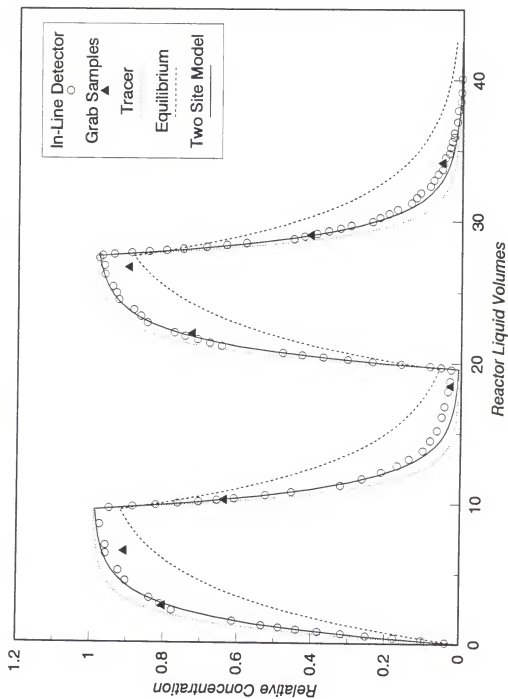
Figure 3-5.    Typical flow-rate variation experiment breakthrough curve (Experiment AEP200).

The data are characteristic of mass transfer-limited (nonequilibrium) sorption because the data plot between the tracer and equilibrium lines (Figure 3-4). The two-site model data fits generally describe this behavior, but seem to routinely under-predict the amount of concentration change that occurs during a flow interruption. If lower values of $K_p$ are used, the two-site model can be made to better fit (reduce the sum of squares of error) the flow interruptions. These better fits can be accomplished either by using $K_p$ values based on first moment analysis of the break-through curve, or by fitting $K_p$ with the other two mass transfer parameters. This in fact converts the two-site model to a three-site model, where the mass transfer rate into the third compartment is effectively zero. Since this approach is no longer truly a two-site model, it was rejected for further discussion here. The poor fit to the flow interruptions is characteristic of the failure of the two-site model to predict mass transfer in the event of changing flow rates.

## Summary of Two-Site Model Parameter Estimates

Estimates of mass transfer rates ($k_s$) and fraction of instantaneous sorbing sites (F) from both stir cell and column experiments are summarized in Table 3-3, with the standard error of these estimates. Also included in this table is a general description of experiment type (solute, solvent, soil, operation). Finally, the table includes results of moment analysis of the break-through curve. The recovery represents the total mass of solute observed in the effluent compared to the total

Table 3-3. Summary of soil sorption experiments.

| Run ID | Solute | Solvent[a] | Type | Partition Coef. $K_p$ (mL/g) | Mass Transfer Rate $k_s$ (hr$^{-1}$)[b] | Fraction Equilibrium Sites $F$[b] | Recovery[e] | Retard. Factor $R^d$ (batch) | Retard. Factor $R^e$ (obs) |
|---|---|---|---|---|---|---|---|---|---|
| Stir Cell: | Eustis | | | | | | | | |
| NEI100 | Naphthalene | water | Interrupt | 3.29 | 0.485 (0.0395) | 0.368 (0.0182) | 0.973 | 1.75 | 1.57 |
| NEP100 | Naphthalene | water | Flow Variation | 3.29 | 0.157 (0.0612) | 0.432 (0.0212) | 0.984 | 1.76 | 1.32 |
| AEI100 | Anthracene | 30:70 | Interrupt | 18.49 | 0.0460 (0.00757) | 0.213 (0.00799) | 0.988 | 3.42 | 1.92 |
| AEI203 | Anthracene | 30:70 | Interrupt | 18.49 | 0.0539 (0.00858) | 0.231 (0.00689) | 0.982 | 4.71 | 2.30 |
| AEI206 | Anthracene | 30:70 | Interrupt | 18.49 | 0.0491 (0.00890) | 0.333 (0.00827) | 0.989 | 4.53 | 2.87 |
| AEI210 | Anthracene | 30:70 | Interrupt | 18.49 | 0.00909 (0.00692) | 0.368 (0.00891) | 1.001 | 3.04 | 2.02 |
| AEI220 | Anthracene | 30:70 | Interrupt | 18.49 | 0.0701 (0.00724) | 0.423 (0.0106) | 0.987[f] | 2.96 | 2.19 |
| AEI240 | Anthracene | 30:70 | Interrupt | 18.49 | 0.0883 (0.00225) | 0.460 (0.00415) | 0.926[f] | 3.00 | 2.82 |
| AEP200 | Anthracene | 30:70 | Flow Variation | 18.49 | 0.000544 (0.0168) | 0.175 (0.00748) | 1.012 | 3.82 | 2.00 |
| YEI100 | Pyrene | 50:50 | Interrupt | 1.929 | 0.130 (0.0273) | 0.653 (0.0242) | 1.010 | 1.68 | 1.52 |

Table 3-3--continued.

| Run ID | Solute[a] | Solvent | Type | Partition Coef. $K_f$ (mL/g) | Mass Transfer Rate $k_s$ (hr$^{-1}$)[b] | Fraction Equilibrium Sites $f$[b] | Recovery[c] | Retard. Factor $R^d$ (batch) | Retard Factor $R^e$ (obs) |
|---|---|---|---|---|---|---|---|---|---|
| Stir Cell: | Zellwood | | | | | | | | |
| NZI100 | Naphthalene | 30:70 | Interrupt[g] | 47.43 | 0.0262 (0.0167) | 0.937 (0.0176) | | 2.25 | |
| NZP100 | Naphthalene | water | Flow Variation | 218.0 | 0.0603 (0.0222) | 0.526 (0.0161) | 0.928 | 4.58 | 2.70 |
| AZI100 | Anthracene | 30:70 | Interrupt[g] | 121.7 | 0.0227 (0.00161) | 0.380 (0.00965) | | 2.83 | |
| Column: | Eustis | (Dai,1993) | | | | | | | |
| NEC25A | Naphthalene | 25:75 | Short Pulse | 1.243 | 12.64 (1.48) | 0.313 (0.0377) | 1.000 | 5.88 | 6.73 |
| NEC40A | Naphthalene | 40:60 | Short Pulse | 0.3717 | 13.30 (0.802) | 0.454 (0.0141) | 1.000 | 2.46 | 3.11 |
| NEC40B | Naphthalene | 40:60 | Short Pulse | 0.3717 | 13.05 (0.815) | 0.431 (0.0149) | 1.000 | 2.46 | 3.28 |
| NEC50A | Naphthalene | 50:50 | Short Pulse | 0.1662 | 10.33 (0.547) | 0.590 (0.00844) | 1.000 | 1.65 | 1.65 |
| NEC50B | Naphthalene | 50:50 | Short Pulse | 0.1662 | 8.99 (0.570) | 0.575 (0.00983) | 1.000 | 1.65 | 1.65 |
| NEC50D | Naphthalene | 50:50 | Short Pulse | 0.1662 | 37.57 (4.04) | 0.225 (0.0378) | 1.000 | 1.65 | 1.74 |

Table 3-3--continued.

| Run ID | Solute[a] | Solvent | Type | Partition Coef. $K_p$ (mL/g) | Mass Transfer Rate $k_s$ (hr$^{-1}$)[b] | Fraction Equilibrium Sites $F$[b] | Recovery[c] | Retard. Factor $R^d$ (batch) | Retard. Factor $R^e$ (obs) |
|---|---|---|---|---|---|---|---|---|---|
| Column: | Eustis | (Dai, 1993) | | | | | | | |
| AEC25A | Anthracene | 25:75 | Long Pulse | 31.08 | 0.0477 (0.00240) | 0.493 (0.00521) | 1.000 | 123 | 106 |
| AEC50A | Anthracene | 50:50 | Short Pulse | 2.316 | 1.56 (0.106) | 0.316 (0.00832) | 1.000 | 10.1 | 7.19 |
| AEC50B | Anthracene | 50:50 | Short Pulse | 2.316 | 1.56 (0.0937) | 0.303 (0.00736) | 1.000 | 10.1 | 7.33 |
| AEC50C | Anthracene | 50:50 | Short Pulse | 2.316 | 1.37 (0.0951) | 0.493 (0.00521) | 1.000 | 10.1 | 6.48 |
| YEC50C | Pyrene | 50:50 | Short Pulse | 1.929 | 3.51 (0.122) | 0.473 (0.00739) | 1.000 | 8.58 | 8.55 |
| YEC50D | Pyrene | 50:50 | Short Pulse | 1.929 | 2.94 (0.113) | 0.368 (0.00891) | 1.000 | 8.58 | 8.80 |

Notes:
a. Percent by volume methanol and water. All solutions contained 0.01 N $CaCl_2$.
b. Standard error of estimate given in parentheses.
c. Ratio of mass of solute in effluent (zeroth moment analysis) to mass of solute in influent (pulse width).
d. Batch retardation factor includes sorption by stir cell (Equation (3-9a)).
e. Observed retardation factor determined by first moment analysis.
f. Experiment stopped before all effluent mass was recovered.
g. Sorption experiment only; moment analysis not possible.

mass of solute introduced into the system. The recovery is calculated by the ratio of the zero moments of column effluent and influent as described in Equation (3-20):

$$Recovery = \frac{\int_0^\infty C^* \, dP}{\int_0^\infty C_{in}^* \, dP} \tag{3-20}$$

The batch retardation factor is calculated using Equation (3-9a) with a $K_p$ value obtained from a batch isotherm. The observed retardation factor is calculated from first moment analysis as described in Equation (3-21):

$$R_{(obs)} = \int_0^\infty C^* \, P \, dP - \int_0^\infty C_{in}^* \, P \, dP \tag{3-21}$$

Characteristics of a well-performed experiment are a recovery near unity and batch and observed retardation factors that are equal. All solute mass to within 0.1 percent was recovered for all column (Dai, 1993) experiments. Mass recoveries for stir cell experiments were not as good as for column experiments, but divergence from complete recovery was generally less than 3 percent unless the experiment was truncated. Generally, analytical detection limitations prevent the long-term, low concentration desorption tailing from being fully defined and result in observed retardation factor being lower than those calculated from batch isotherm data. However, for some of the naphthalene and pyrene column experiments, Dai (1993) observed higher retardation factor than predicted by Equation (3-9a). This indicates either a poor estimate of $K_p$ or sorption to material other than the soil (e.g., column wall surfaces). Both possibilities indicate that the mass transfer rate predictions from

these experiments may be in error, so predictions based on these experiments should be used with caution.

## Discussion

### Comparison with Column Experiments

Brusseau and Rao (1989b) discovered a log-linear relationship between partition coefficient ($K_p$) and desorption rate coefficient ($k_s/(1-F)$) for nonpolar organic compounds. The data from which the relationship was derived came from a variety of published sources, including column, batch and gas purge studies. The column (Dai, 1993) and stir cell (this study) mass transfer parameter predictions are plotted in Figure 3-6 with the Brusseau and Rao (1989b) correlation and the 95 percent prediction intervals from that regression.

Magnitude of partition coefficient, $K_p$. Immediately obvious in Figure 3-6 is the fact that the $K_p$ values in the stir cell experiments are generally higher than those in the column experiments. Column (Dai, 1993) and stir cell experiments were conducted independently. Experiments were generally designed to achieve a system retardation factor in the range of two to three. Since the soil:water ratio in the column is higher than in the stir cell, combinations of solute and cosolvents were chosen that resulted in the lower $K_p$ values. While this makes comparison between methods difficult, it illustrates that the two techniques are suited for different sorption ranges.

Figure 3-6.  Two-site model fits for stir cell and Dai (1993) column experiments with Brusseau and Rao (1989b) regression

Magnitude of desorption rate, $k_2/(1-F)$. The parameter estimates may be compared by observing the value of the desorption rate with respect to the Brusseau and Rao (1989b) regression line. If extra-aggregate immobile water in packed columns imposes additional mass transfer restraint, column-derived mass transfer rates should be slower (lower) than those derived from stir cell experiments. However, all of the short pulse column experiments predicted very fast mass transfer rates (above the regression line in Figure 3-6) whereas all of the stir cell experiments with Eustis soil resulted in slower mass transfer rates (below the regression line in Figure 3-6). The one long pulse column experiment resulted in mass transfer rate predictions in about the same range as the stir cell experiments. Further, many of the short pulse column experiment predictions were outside the prediction interval for the Brusseau and Rao (1989b) regression, while the long pulse column and most of the stir cell mass transfer rates were within the prediction intervals.

These results indicate that experimental operation (pulse size or duration of exposure) is more important than experimental method (column or stir cell) in predicting two-site model parameters. Longer pulses supply more solute mass to the system, so that the tails of the break-through curve (where slow mass transfer rates are seen) are better defined and not lost to dilution and analytical detection limitations. Longer exposure times allow significant solute mass to be influenced by the slower sites. This theory may explain the slightly higher mass transfer rates obtained from stir cell experiments AEI220 and AEI240 (Table 3-3) where the break-through curve tails were truncated.

The Dai (1993) column experiments which resulted in desorption rates estimates outside the prediction bands of the Brusseau and Rao (1989b) regression are the same experiments wherein the observed retardation factor exceeded that predicted by isotherm experiments. The mass transfer rates obtained from these Dai (1993) experiments may therefore be in error. There appears no obvious explanation for the very low desorption rates resulting from stir cell experiments AEI210 and AEP200 (Table 3-3). However, when the observed retardation factor is higher than the theoretical retardation factor, faster mass transfer rates are seen. When the observed retardation factor is lower than the theoretical value, slower rates are estimated. Experiments AEI240, NEI100, YEC50C and YEC50D (Table 3-3) have observed and theoretical retardation factors which are approximately the same, and these experiments resulted in the desorption rate predictions that were the closest to the Brusseau and Rao (1989b) regression line. When observed retardation is lower than expected, very slow mass transfer rates were fitted to the two-site model which predict that most of the solute leaves the system before it can be affected by the slow sites. When observed retardation is high, the two-site model needs faster mass transfer rates so that the slow sites can be effective at retarding the solute transport.

Error bounds on estimates. The error bounds on the parameter estimates from Dai (1993) column experiments were all fairly small. Some of the parameter estimates from stir cell experiments also evidenced small error bounds, but a large number of the experiments, including AEI210, NZI100, AEP200, NEP100, and

NZP100 (Table 3-3), had very large error bounds. The larger error bounds on stir cell-derived parameter estimates may be related to the less-complete mass recoveries of these experiments. Also, all of the flow-rate variation experiments evidenced large error bounds on mass transfer rate parameter estimates, indicating a failure of the two-site model to predict breakthrough curves under conditions of changing velocity.

## Flow Interruption and Flow-Rate Variation Methods

Intentional perturbations (changes in flow-rate and influent concentration) to the stir cell results in system responses which provides information on mass transfer characteristics. Two types of flow perturbations were tested; flow interruption and flow-rate variation. The flow interruption method involves discontinuity in flow and concentration measurement. Information on concentration changes with time during the flow interruption are not available since the system design precludes sampling inside the cell. The flow-rate variation method, however, has the advantage that effluent concentration measurements were continuous throughout the experiment.

Both flow-rate variation and flow interruption experiments were conducted using Eustis soil for two solute/solvent combinations; naphthalene in water and anthracene in 30:70 MeOH/$H_2O$. The flow-rate variation experiments resulted in lower estimates of the mass transfer rate with larger error bounds than did the flow interruption experiments.

The flow-rate variation method was characterized by two short pulses and a changing flow rate. The time of exposure of the sorbent to the solute for each pulse

was shorter than in the flow interruption experiments, but usually only by a factor of 1.5 to 4. In the Dai (1993) column experiments, the short pulse experiments were shorter than the long pulse experiment by over three orders of magnitude, resulting in faster mass transfer rate predictions without increasing the error bounds of the estimate. Therefore, pulse width is probably not responsible for the trend seen between flow interruption and flow-rate variation experiments in the stir cell (Table 3-3). Further, fitting pulses separately changed the parameter estimates but not the trend of lower $k_s$ values and larger error bounds. Therefore the use of two sequential pulses is also not responsible for the trend.

The most likely cause of the trend lower $k_s$ values and larger error bounds is the changing flow rate. Brusseau (1992b) and Kookana et al. (1993) have documented the dependence of two-site model fits on pore water velocity. The results of the flow-rate variation method are probably a further indication of the failure of the two-site model to predict sorption mass transfer in the presence of a varying flow rate. The two-site model is an empirical model based loosely on diffusion mass transfer. Models which more accurately emulate the diffusive mass transfer process may be needed if a single model parameter estimate is to simulate mass transfer over varying flow rate conditions.

## General Observations on Stir Cell Operation

Separation of fines. The stirring process tends to separate fine particles from coarser particles. Soil organic matter tends to be associated with the finer particles.

Changing the grain size distribution of the soil (i.e., making finer particles from coarse particles) could increase mass transfer rates by increasing interfacial surface area and decreasing diffusion path lengths, but this effect was not evident from the stir cell experiments. Still, the potential of abnormally high mass transfer rates would argue for short term experiments to minimize any effects of separation of fines from prolonged stirring and grinding.

Accumulation of fines on frits. Finer particles collect on the effluent frit. This has two effects:

1. The pressure gradient across the frit increases to maintain a constant flow rate. Increased pressure will eventually cause the stir cell to fail by leaking or breaking.

2. Caked fines on the frits do not experience completely-mixed conditions, invalidating the fitting model.

The flow reversal technique helped minimize these effects. However, hydration of Zellwood muck organic matter resulted in a gelatinous-like film on the frits that eventually could not be dislodged by backwashing. The latter portions of the Zellwood muck experiments had to be discarded because complete-mixed assumptions were no longer valid, again arguing for shorter duration experiments.

Sorption onto the stir cell. The stir cell components (presumably the teflon) do sorb some solutes. Sorption onto stir cell wall surfaces appears to have mass transfer limitations which become more apparent as the sorption coefficient

increases. Blank experiments (Appendix B) have measured cell sorption contribution to the stir cell retardation factor as high as 0.5.

## Conclusions and Recommendations

The two-site mass transfer model parameter estimates obtained from the stir cell generally compare well with estimates obtained from other methods. The mass recoveries and error bounds on estimates were not as good for stir cell experiments as were realized for the Dai (1993) column experiments. However, the high mass transfer rate estimates obtained from the short pulse column experiments show that experimental procedures (i.e., long exposure time to define the desorption tail) are as important as hardware for obtaining parameter estimates. Stir cell operating conditions are best suited for short experiments using solids with high partition coefficients.

Conditions in the stir cell preclude mass transfer limitations in extra-aggregate water. Since the mass transfer model parameters estimated from stir cell experiments are similar to those estimated by column and other methods, extra-aggregate water diffusion does not have a limiting effect on mass transfer in most systems. Mass transfer limitations must be due to intraorganic matter diffusion or retarded intraparticle diffusion.

Experiments performed at a single flow rate with flow interruptions resulted in mass transfer parameter estimates that were consistent with the correlation of Brusseau and Rao (1989b), but the fitted parameters under-predicted concentration

changes during the flow interruptions. Experiments performed with a changing flow rate resulted in lower mass transfer rate estimates that had higher error bounds on the estimates. This behavior is related to failure of the two-site model to predict mass transfer in the presence of a varying flow rate.

Recommendations for future work include:

1. Replace teflon components of next generation stir cells with alternate materials such as polyether ether ketone (PEEK) or stainless steel to decrease sorption to stir cell wall surfaces; and

2. Develop models which better describe mass transfer processes to predict sorption during conditions of changing flow rates.

# CHAPTER 4
## MULTISITE MASS TRANSFER MODELS

### Introduction

The two-site model has been used widely to describe sorption mass transfer (Brusseau and Rao, 1989a) and in some instances to describe NAPL dissolution (Borden and Kao, 1992; Malone et al., 1993; Augustijn, 1993). However, the two-site model has two major deficiencies: (1) model parameters are dependent on pore water velocity (Brusseau, 1992b; Kookana et al., 1993), and (2) the model fails to reproduce the long-term slow desorption (known as tailing) of the breakthrough curve (Karickhoff and Morris, 1985; Pavlostathis and Jaglal, 1991; Scribner et al., 1992; Connaughton et al., 1993). The first model deficiency results from defining a fraction of sorption sites (F) at equilibrium with the aqueous phase relative to advective-dispersive transport. The second deficiency is caused by describing mass transfer from sites located at many different diffusion path distances and through phases with different diffusion coefficients by one averaged, first-order mass transfer rate.

A desirable improvement for modeling mass transfer would be development of a model which overcomes the deficiencies of the two-site model, but retains the attractive feature of needing only low number of defining parameters whose values

must be fitted. Connaughton et al. (1993) proposed such a model when they conceptualized sorption sites as a continuum of compartments, each defined by a first-order mass transfer rate. Connaughton et al. (1993) used a gamma distribution to describe their distribution of sorption sites. The gamma distribution, like the two-site model, is defined by only two parameters.

The concept of describing the mass transfer process using a frequency distribution of sorption sites will be further developed in this chapter. The Connaughton et al. (1993) approach will be expanded here in two ways:

1.  The Connaughton et al. (1993) model defined mass transfer as a process between the aqueous phase and each individual sorption compartment. Here, two variations of this approach are evaluated. The first, like the Connaughton model, has sorption compartments in parallel with the aqueous phase, and the second has sorption compartments arranged in series.

2.  An analytical solution for a specific desorption scenario was used in the Connaughton et al. (1993) study. Since the application of analytical models are limited, a numerical approach employing discretized frequency distributions is used.

The two models, multiple sites in parallel (MSP) and multiple sites in series (MSS) are illustrated in Figure 4-1, along with the conventional two-site model. The sizes of sorption site compartments for the MSP model are defined by a frequency distribution for mass transfer rates ($k_i$) as they were in the Connaughton et al.
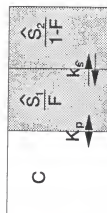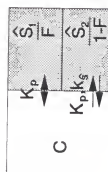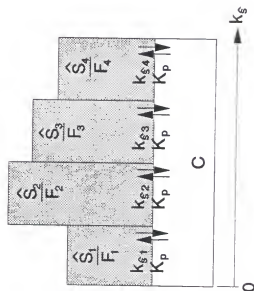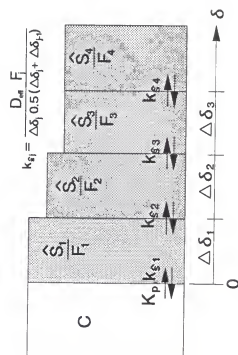
Figure 4-1. Two-site and multisite mass transfer models.

(1993) model. The sizes of sorption site compartments for the MSS model are defined by a frequency distribution of diffusion path lengths ($\delta$). The MSP and MSS models have the potential of being superior to the two-site model in several ways:

1.  Since all sites are defined by mass transfer rates instead of a relative measure of equilibrium, model parameters may be independent of pore water velocity (because equilibrium is relative to advective transport).

2.  Since multiple sites are defined by different mass transfer rates, overall mass transfer rates can change with time and long-term tailing may be modeled.

3.  Since sorption site compartment sizes are defined by standard frequency distributions (e.g., log-normal, gamma, spherical), using multiple sites does not increase the number of fitted parameters.

The multisite models will only be able to fulfill their potential if they describe the actual mass transfer processes with a reasonable degree of accuracy. Mass transfer is understood to be a diffusion-controlled process, whether in the organic phase (Brusseau and Rao, 1989b; Conrad et al., 1992) or in intraparticle micropores (Ball and Roberts, 1991). In the MSP model, it is assumed that the diffusion path between the bulk aqueous phase and each sorption site is independent of the diffusion path to all other sites. Further, it is assumed that the concentration gradient along each diffusion path is linear. This scenario seems an unlikely representation of reality. However, the parameters which govern mass transfer (e.g.,

diffusion coefficient, path length, tortuosity, geometric distribution of the organic phase) do not have a single value in natural systems. Use of a distribution of the grouped-parameter mass transfer rate coefficient accounts for variation and uncertainty in all of these parameters. It is in fact a stochastic approach to mass transfer. An additional advantage of the MSP model is its computational simplicity compared to the MSS model.

The MSS model describes diffusion through a sequence of compartments. While the concentration gradient between each adjacent compartment is linear, the concentration gradient over the entire diffusion path length can be nonlinear. The MSS model should accurately describe the process of diffusion into uniformly sized films, spheres, or micropores. The deficiency of the MSS model is that, unlike the stochastic approach of the MSP model, it can only represent one realization (at a time) of sorption sites distributed along a single diffusion path. The only "dead end" is the final compartment. Since all compartments are connected, the model does not account for variable diffusion path lengths such as would be encountered in micropores of variable length or NAPL ganglia of varying sizes. Further, the MSS model relies on a single coefficient of effective diffusion; different organic phase "density" (Carroll et al., 1994) or tortuosity over path length could result in a varying diffusion coefficient. Given these limitations, the multisite models must be carefully tested.

The ability of these multisite models to predict mass transfer using stir cell data is evaluated in this chapter. Results of three sets of experiments are presented:

1. Sorption of anthracene by Eustis soil was investigated under conditions of changing hydraulic residence times. The distribution of sorption compartments is unknown, but remains unchanged for each experiment. The ability of the multisite models to predict a common distribution (i.e., velocity independent parameters) for all experiments is tested.

2. Sorption of anthracene by various sizes of nylon balls was investigated. The balls have a known geometry (and therefore known distribution of sorption sites). The experiments were designed to determine if a distribution of sorption sites could be predicted from stir cell breakthrough curve data, and to examine the effect of modelling varying sorbent geometries with an averaged distribution.

3. Sorption and desorption of anthracene by paraffin beads was investigated. Experiments performed with different initial conditions were conducted to determine if similar mass transfer parameters could be obtained. This work represents initial development of techniques to use paraffin as a surrogate for soil organic matter or coal tar pitch.

## Model Development

The governing equation for the stir cell is given by Equation (4-1):

$$V\frac{dC}{dt} + M_s\frac{d\hat{S}_s}{dt} + M_R\frac{d\hat{S}_R}{dt} = Q(C_{in} - C) \qquad (4\text{-}1)$$

where notation for this and following equations are defined in the Glossary. Sorption by the stir cell components, if significant, is modeled by the two-site model as discussed in Chapter 3. The major difference between the multisite models discussed here and the two-site models of Chapter 3 is the method for handling sorption onto the solid of interest ($\hat{S}_s$). For both the MSP and MSS models, the total sorption into the solid is the sum of the amount sorbed in all compartments (Equation 4-2):

$$\hat{S}_s = \sum_{j=1}^{N} \hat{S}_{s(j)} \tag{4-2}$$

Also, the sum of the relative size of each compartment equals unity as shown in Equation (4-3):

$$\sum_{j=1}^{N} F_j = 1 \tag{4-3}$$

The two models also share a common definition of all dimensionless numbers except those dealing with mass transfer rates onto the solid of interest. These numbers have been defined previously in Equations (3-9a) through (3-9o), except that the definitions of $R_f$, $R_s$, and $\hat{S}_s^*$ are slightly changed:

$$R_f = 1 + \frac{F_R M_R K_R}{V} \tag{4-4a}$$

$$R_s = \frac{M_s K_p}{V} \tag{4-4b}$$

$$\hat{S}_s^* = \frac{\hat{S}_s}{K_p C_{\max}} \tag{4-4c}$$

$$\hat{S}_{s(j)}^* = \frac{\hat{S}_{s(j)}}{F_j K_p C_{\max}} \tag{4-4d}$$

$$\hat{S}_s^* = \sum_{j=1}^{N} F_j \hat{S}_{s(j)}^* \tag{4-4e}$$

The stir cell mass balance equation in dimensionless terms for both models is given by Equation (4-5):

$$R_f \frac{dC^*}{dT} + \sum_{j=1}^{N} F_j R_s \frac{d\hat{S}_{s(j)}^*}{dT} + R_R \frac{d\hat{S}_R^*}{dT} = Q^*(C_{in}^* - C^*) \tag{4-5}$$

Development of mass transfer expressions are specific to each model.

<u>MSP Model</u>

Mass transfer between the bulk aqueous phase and each sorption compartment is described by Equation (4-6):

$$\frac{d\hat{S}_{s(j)}}{dt} = k_{s(j)}(K_p C - \frac{\hat{S}_{s(j)}}{F_j})$$ (4-6)

The dimensionless mass transfer parameter for the MSP model is given by Equation (4-7):

$$\omega_{s(j)} = \frac{M_s K_p k_{s(j)}}{Q_{max}}$$ (4-7)

Equation (4-6) rewritten in dimensionless terms becomes Equation (4-8):

$$R_s F_j \frac{d\hat{S}_{s(j)}}{dT} = \omega_{s(j)}(C^* - \hat{S}_{s(j)}^*)$$ (4-8)

Equations (4-5), (4-8) and (3-12) are solved numerically using a forward differencing technique.

## MSS Model

The MSS model assumes that a linear concentration gradient exists between each compartment. Each compartment is defined by an average diffusion path length, $\delta$, from the aqueous phase/organic phase interface. The diffusion path distance across a compartment is $\Delta\delta_j$, and the average diffusion path distance between two compartments is $\frac{1}{2}(\Delta\delta_{j-1} + \Delta\delta_j)$. Equations (4-9a) through (4-9c) describe mass transfer between compartments. If $j = 1$:

$$\frac{d\hat{S}_{s(1)}}{dt} = - \frac{D_{eff}F_1}{0.5\,\Delta\delta_1^2}[\frac{\hat{S}_{s(1)}}{F_1} - K_p C]$$

$$- \frac{D_{eff}F_2}{\Delta\delta_2}[\frac{\frac{\hat{S}_{s(1)}}{F_1} - \frac{\hat{S}_{s(2)}}{F_2}}{0.5(\Delta\delta_1 + \Delta\delta_2)}]$$

$$(4\text{-}9a)$$

If $1 < j < N$:

$$\frac{d\hat{S}_{s(j)}}{dt} = - \frac{D_{eff}F_j}{\Delta\delta_j}[\frac{\frac{\hat{S}_{s(j)}}{F_j} - \frac{\hat{S}_{s(j-1)}}{F_{j-1}}}{0.5(\Delta\delta_j + \Delta\delta_{j-1})}]$$

$$- \frac{D_{eff}F_{j+1}}{\Delta\delta_{j+1}}[\frac{\frac{\hat{S}_{s(j)}}{F_j} - \frac{\hat{S}_{s(j+1)}}{F_{j+1}}}{0.5(\Delta\delta_j + \Delta\delta_{j+1})}]$$

$$(4\text{-}9b)$$

If $j = N$:

$$\frac{d\hat{S}_{s(N)}}{dt} = - \frac{D_{eff}F_N}{\Delta\delta_N}[\frac{\frac{\hat{S}_{s(N)}}{F_N} - \frac{\hat{S}_{s(N-1)}}{F_{N-1}}}{0.5(\Delta\delta_N + \Delta\delta_{N-1})}]$$

$$(4\text{-}9c)$$

The dimensionless mass transfer parameter for the MSS model is given by Equation (4-10):

$$\omega_{s(j)} = \frac{F_j M_s K_p D_{eff}}{Q_{max} \Delta \delta_j [0.5(\Delta \delta_j + \Delta \delta_{j-1})]} \tag{4-10}$$

Note that $\Delta \delta_0 = 0$.

Converted to dimensionless parameters, the governing equations for the MSS model are Equations (3-12), (4-5), and (4-11) through (4-13).

$$F_1 R_s \frac{d\hat{S}^*_{s(1)}}{dT} = - \omega_{s(1)}(\hat{S}^*_{s(1)} - C^*)$$
$$- \omega_{s(2)} (\hat{S}^*_{s(1)} - \hat{S}^*_{s(2)}) \tag{4-11}$$

$$F_N R_s \frac{d\hat{S}^*_{s(N)}}{dT} = -\omega_{s(N)} (\hat{S}^*_{s(N)} - \hat{S}^*_{s(N-1)}) \tag{4-12}$$

When $1 < j < N$:

$$F_j R_s \frac{d\hat{S}^*_{s(j)}}{dT} = - \omega_{s(j)} (\hat{S}^*_{s(j)} - \hat{S}^*_{s(j-1)})$$
$$- \omega_{s(j+1)} (\hat{S}^*_{s(j)} - \hat{S}^*_{s(j+1)}) \tag{4-13}$$

The equations are solved numerically using a forward differencing technique.

## MSS Dissolution Model

Since the paraffin beads had a known and relatively uniform geometry, the multiple-sites in series (MSS) model was used for fitting the breakthrough curves. However, the model was changed slightly to account for the fact that the concentration of anthracene in a solvent cannot exceed its crystalline solubility in that

solvent. Equation (4-11) was rewritten as Equations (4-14) through (4-16) to account for the solubility limit:

$$F_1 R_s \frac{d\hat{S}^*_{s(1)}}{dT} = -\omega_{s(1)}(C^*_s - C^*)$$
$$-\omega_{s(2)}(\hat{S}^*_{s(1)} - \hat{S}^*_{s(2)}) \qquad (4\text{-}14)$$

where:

$$\text{if } \hat{S}^*_{s(1)} > \frac{S}{C_{\max}}: \quad C^*_s = \frac{S}{C_{\max}} \qquad (4\text{-}15)$$

and:

$$\text{if } \hat{S}^*_{s(1)} < \frac{S}{C_{\max}}: \quad C^*_s = \hat{S}^*_{s(1)} \qquad (4\text{-}16)$$

## Materials and Methods

### Materials

Experiments were performed on Eustis sand, nylon balls, and paraffin beads. The Eustis soil ($f_{oc} = 0.0054$) was prepared by sieving with a 250 $\mu$m sieve and was allowed to air dry prior to use.

The type 66 nylon balls (Small Parts, Inc., Miami Lakes, FL) had a density of 1.14 g/cm$^3$. Balls of five different sizes were used: diameters were 2.381, 3.175, 4.762, 6.35, and 7.938 mm. Nylon balls were chosen for their known (spherical)

geometry and since diffusion into the polymer structure of nylon is a similar process to diffusion into the polymer-like structure of soil organic matter.

The use of paraffin as a surrogate organic matrix has several advantages: (1) the solute of interest can be dissolved in liquid (melted) paraffin, creating a homogenous and known distribution of solute in the organic phase; (2) paraffin can be molded into uniform shapes, creating a known and uniform geometrical distribution of the organic phase for testing mass transfer models; (3) paraffin is free of contaminants which would interfere with mass balance estimates; and (4) diffusion into the polymer-like structure of paraffin is a similar process to diffusion into the polymer-like structures of soil organic matter and coal tar pitch. Household paraffin was shredded and washed with methanol to remove any soluble impurities. The shredded paraffin was melted at a low temperature, then formed into beads by dropping molten paraffin from a pipette into a beaker of water. As the density of paraffin is less than that of water, the resulting beads were not spherical. The shape was that of a flattened sphere or disk, and the average size was about 5 mm in diameter and 2 mm in height. Some beads were formed of pure paraffin. Additionally, anthracene was dissolved in molten paraffin, and beads were formed which contained 5630 $\mu$g of anthracene per g of paraffin.

The solvents used in all experiments were mixtures of HPLC grade methanol and distilled, deionized water in volume-to-volume ratios of 30:70 MeOH/$H_2O$ for Eustis soil experiments and 50:50 MeOH/$H_2O$ for nylon ball and paraffin bead experiments. All solutions contained 0.01N $CaCl_2$ to provide a constant ionic

strength, and were degassed with helium to inhibit biological activity and prevent cavitation. The solute used in all experiments was 99+ percent pure anthracene (Aldrich Chemical Co., Milwaukee, WI).

Methods

Sorption isotherms experiments for all sorbents were conducted and are described in Appendix A. The stir cell apparatus and methods used were described previously in Chapter 3.

The Eustis soil experiments consisted of six flow interruption experiments. Each of these experiments was conducted at a different flow rate resulting in stir cell hydraulic residence times ranging from 0.0516 to 0.856 hours. The flow interruption experiments were used to calculate fits to the mass transfer models, and the fits were tested on data from a flow-rate variation experiment where hydraulic residence times ranged from 0.0525 to 0.175 hours.

The nylon ball experiments consisted of six flow interruption experiments all conducted at the same flow rate and time of operation. Five of the experiments were conducted using a single ball size and were used to calculate fits to the mass transfer models. The fits were tested on the sixth experiment which was performed on a mixture of all ball sizes.

Two stir cell experiments were conducted using paraffin beads. The first was a sorption/desorption experiment using the flow-interruption technique as described in Chapter 3. The second was a dissolution experiment. Paraffin beads containing

anthracene were placed in the stir cell and solute-free solution was pumped through the stir cell for three days, with periodic flow interruptions.

## Velocity Dependence of Parameters

### Defining the Frequency Distribution

Two-site model fits for Eustis sand experiments conducted at different hydraulic residence times (different velocities) were presented in Chapter 3; different parameter estimates were obtained for each experiment (Table 3-3) indicating velocity dependence of the two-site model parameters. To be successful, the multisite models must be described by the same frequency distribution for all velocities. The forms of the frequency distribution describing the sorption sites of Eustis sand for the MSP and MSS models are unknown. However, the two-site model is a simple ($N = 2$) version of both the MSP and MSS models. The frequency distribution of sites in parallel or in series can be determined by defining a mass transfer rate for the "fast" sites. Bahr and Rubin (1987) defined local equilibrium as the mass transfer rate that achieved 98 percent of the equilibrium sorbed phase concentration when the aqueous concentration was at 50 percent of its influent concentration. Using this definition, mass transfer rates for the "fast" sites were calculated for each experiment for two sites arranged both in parallel and in series with the aqueous phase, and the results are presented in Table 4-1. The mass transfer rates for the MSS model were converted to diffusion path lengths by combining Equations (4-7) and (4-10) and using a free liquid (tortuosity not

Table 4-1. Estimated mass transfer rate coefficients for two-site model.

| Run ID | Hydraulic Residence Time (hr) | Two-Site Model | | MSP | MSS | | |
|---|---|---|---|---|---|---|---|
| | | $k_{s(2)}$ (hr$^{-1}$) | F | $k_{s(1)}$ (hr$^{-1}$) | $k_{s(1)}$ (hr$^{-1}$) | $\Delta \delta_1$ (mm) | $\Delta \delta_2$ (mm) |
| AEI203 | 0.0516 | 0.0539 | 0.231 | 113 | 112 | 0.0127 | 1.052 |
| AEI206 | 0.0997 | 0.0491 | 0.333 | 70.8 | 73.2 | 0.0189 | 1.045 |
| AEI100 | 0.101 | 0.0460 | 0.213 | 61.2 | 63.6 | 0.0162 | 1.051 |
| AEI210 | 0.179 | 0.00912 | 0.368 | 56.1 | 56.5 | 0.0226 | 2.321 |
| AEI220 | 0.358 | 0.0702 | 0.423 | 29.5 | 32.8 | 0.0318 | 0.644 |
| AEI240 | 0.856 | 0.0882 | 0.460 | 12.1 | 15.8 | 0.0477 | 0.709 |

considered) diffusion coefficient of $1.09(10^{-7})$ cm$^2$/sec estimated by the method of Wilke and Chang (1955) (Equation 2-18).

The mass transfer rates and diffusion path lengths both vary over orders of magnitude, indicating that the distributions of the log transformed values should be studied. The cumulative frequency distributions for the log transformed mass transfer rate coefficients (sites in parallel) and log transformed diffusion path lengths (sites in series) are plotted in Figure 4-2. Connaughton et al. (1993) used a gamma distribution to describe the distribution of mass transfer rates (MSP model). However, a log normal distribution was used in the present study. Like the gamma distribution, the log-normal distribution requires only two fitting parameters. The two-site model distributions suggested a log-normal distribution of $\mu_{lnk} \approx$ -1.0 and $\sigma_{lnk}$ $\approx$ 8.0 might define a MSP model for these experiments.

The two-site model predictions of the diffusion path length distribution (Figure 4-2b) displayed some interesting characteristics. A large fraction of the sites was characterized by very short path lengths, but the total path length for all experiments was about 1 mm (within a factor of two). The maximum particle diameter was only 0.25 mm, but a longer path length was expected to account for tortuosity. This suggested a strong possibility of a velocity-independent MSS model fit since the total path length was the same for all experiments. Further, other diffusion models have required definition of equilibrium sorption sites to adequately fit break-through curve data (Ball, 1989). By discretizing the diffusion path in unequal increments, with very short increments near the organic phase/aqueous
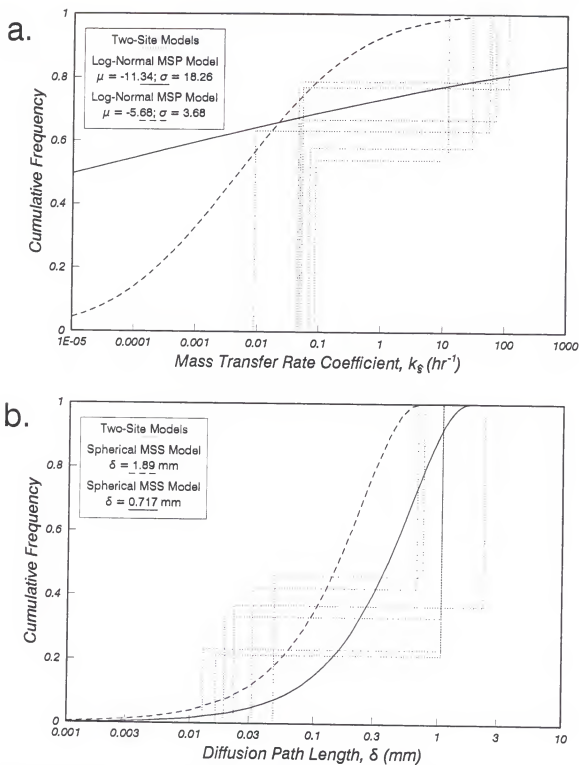
Figure 4-2. Multisite and two-site model cumulative frequency distributions: a) sites in parallel--mass transfer rate coefficient distribution, b) sites in series--diffusion path length distribution.

phase interface, it was hoped that a fraction of sorption sites would be effectively at equilibrium without having to independently define equilibrium sites. Spherical (i.e., distribution of sphere volume with radius) and uniform distributions, characteristic of retarded intraparticle diffusion and film diffusion respectively, and each requiring only one fitting parameter, were attempted for the MSS model. The spherical distribution resulted in slightly, but consistently, lower sums of squares of error of fit.

Model Parameter Estimates

The distribution of compartments for the MSP model was based on the log-normal distribution, having 500 total compartments and a compartment width of 0.012 standard deviations. The distribution of compartments for the MSS model was based on a spherical distribution, having 100 total compartments of equal volume. The fits for the two-site, MSP, and MSS models, and the total sum of squares of error for each fit, are presented in Table 4-2.

The fitted parameter estimates for the MSP model had much lower means and wider standard deviations than was expected, especially for the four faster experiments (AEI100, AEI203, AEI206, and AEI210 in Table 4-2). The distributions indicate a wide range of mass transfer rate coefficients. The effective diffusion path lengths (radii) estimated by fitting the MSS model were fairly consistent for all hydraulic residence times. Two distributions for each model representing the fitted distributions characterized by the widest and narrowest standard deviations are included in Figure 4-2.

Table 4.2. Fitted parameters for two-site, MSP, and MSS models.

| Run ID | Two-Site | | | MSP | | | MSS | |
|---|---|---|---|---|---|---|---|---|
| | $k_s$ | F | SSQ | $\mu_{link}$ | $\sigma_{link}$ | SSQ | $\delta$ | SSQ |
| AEI203 | 0.0539 (0.00858) | 0.231 (0.00689) | 0.0511 | -12.23 (0.666) | 10.87 (0.927) | 0.0237 | 1.062 (0.0921) | 0.283 |
| AEI206 | 0.0491 (0.00890) | 0.333 (0.00827) | 0.0514 | -11.33 (1.17) | 16.95 (2.89) | 0.0467 | 0.745 (0.0703) | 0.477 |
| AEI100 | 0.0460 (0.00757) | 0.213 (0.00799) | 0.0328 | -14.20 (1.27) | 12.13 (1.65) | 0.0273 | 1.886 (0.187) | 0.150 |
| AEI210 | 0.00909 (0.00692) | 0.368 (0.00891) | 0.0376 | -11.34 (1.28) | 18.26 (3.77) | 0.0298 | 1.025 (0.0815) | 0.245 |
| AEI220 | 0.0701 (0.00724) | 0.423 (0.0106) | 0.0294 | -6.29 (0.105) | 7.07 (0.425) | 0.0116 | 0.822 (0.0475) | 0.135 |
| AEI240 | 0.0883 (0.00225) | 0.460 (0.00415) | 0.00344 | -5.68 (0.0670) | 3.63 (0.156) | 0.0147 | 0.717 (0.0318) | 0.0594 |
| AEP200 | 0.000544 (0.0168) | 0.175 (0.00748) | 0.0441 | -167.10 (33.04) | 201.73 (45.59) | 0.0364 | 0.988 (0.120) | 0.286 |

Notes:    Mass transfer rate coefficient, $k_s$, in hr$^{-1}$; diffusion path length, $\delta$, in mm.
Standard error of estimate given in parentheses.
SSQ is sum of squares of error of fit.

The two-site model tended to under-predict the change in concentration resulting from flow interruptions (Figure 3-4), while the MSP model was able to better predict these concentration changes. The MSS model provided fits with higher sum of squares of error. Typical MSP and MSS model fits to stir cell breakthrough curves are illustrated by Figures 4-3 and 4-4 respectively.

Velocity Dependence of Parameter Estimates

The two-site and MSP models resulted in velocity dependent parameter estimates, but the MSS model parameters display velocity independence. The two-site, MSP, and MSS model parameter estimates and their 95 percent confidence intervals are plotted versus the minimum hydraulic residence time for the flow interruption experiments in Figures 4-5 through 4-7 respectively.

Two-site model. The velocity dependence of two-site model parameters has been documented by Brusseau (1992b) and Kookana et al. (1993). As the hydraulic residence time increases, the fraction of equilibrium sites, F, increases since there is time for more of the sites to approach equilibrium. The mass transfer rate coefficient, $k_2$, should decrease because the parameter is averaging over a population of slower mass transfer rates and there is more time for the influence of very slow rates to be realized. The trend of increasing F with increasing residence time is shown in Figure 4-5. However, $k_2$ values do not decrease. The two experiments with the longest hydraulic residence times were truncated. It may be that by not fully
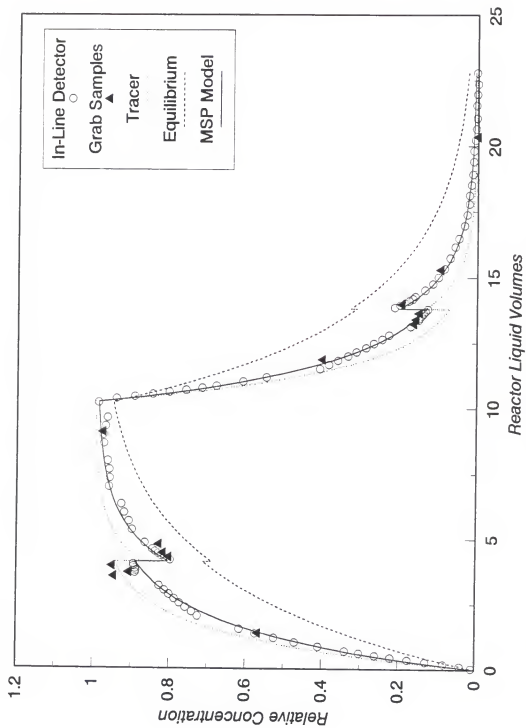
Figure 4-3. Typical MSP model fit for breakthrough curve (Experiment AEI100).
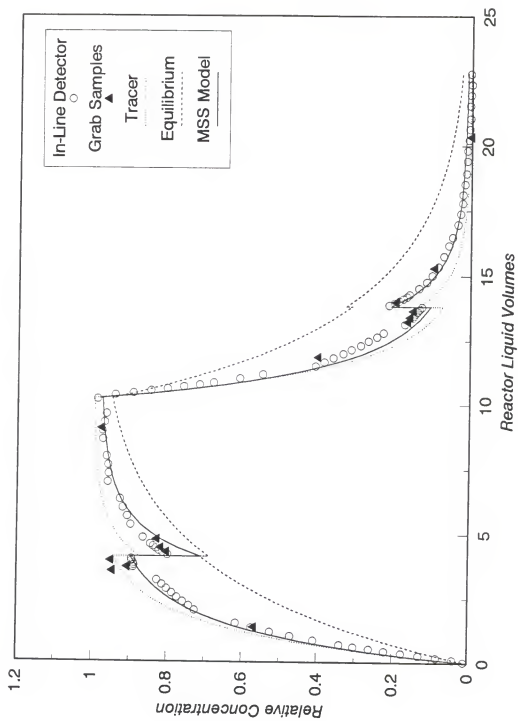
Figure 4-4. Typical MSS model fit for breakthrough curve (Experiment AEI100).
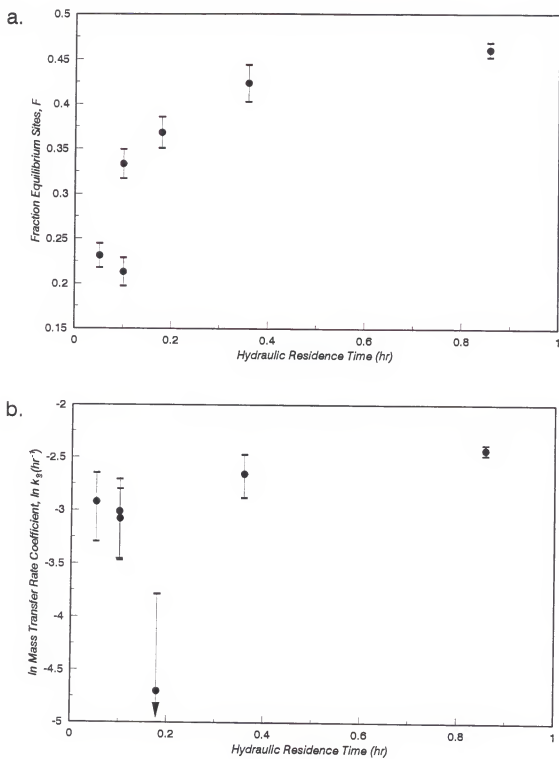
Figure 4-5. Velocity dependence of two-site model parameters: a) fraction of equilibrium sites, b) mass transfer rate coefficients.
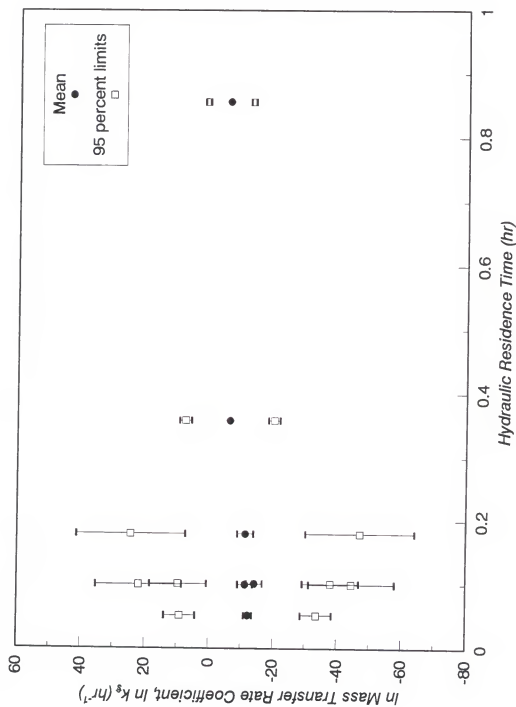
Figure 4-6.  Range of mass transfer rate coefficients determined by MSP model.
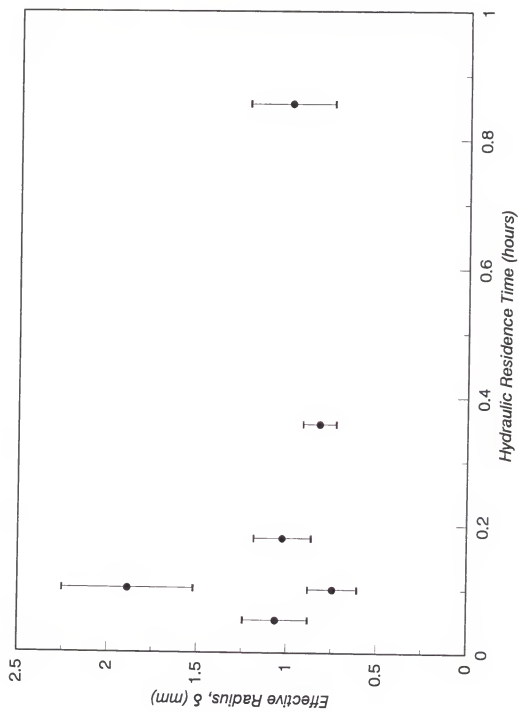
Figure 4-7. Range of diffusion path lengths determined by MSS model.

defining the tail of the break-through curve, estimates of erroneously high $k_\text{d}$ values were obtained for these two experiments (AEI220 and AEI240).

MSP model. The range of log-transformed mass transfer rate coefficients estimated by the MSP model are plotted in Figure 4-6. The expected behavior of these predictions would be that the mean of the log-transformed $k_\text{d}$ would sightly decrease with, and the range of log-transformed $k_\text{d}$ values would slightly increase with, increased hydraulic residence time. The reason for the expected trend is that the influence of slower mass transfer rates would be felt at the longer hydraulic residence times. The expected trend is somewhat apparent in Figure 4-6 for the fastest four (hydraulic residence time < 0.2 hours) experiments, but is reversed for the two slowest (hydraulic residence time > 0.2 hours) experiments. Like the two-site model predictions, the expected trend may have been influenced by truncating the longest two experiments (i.e., the mass transfer rate coefficient estimates were not influenced by slow desorption or "tailing"). Further, the increasing upper limit of mass transfer rates observed for the four faster experiments may be an artifact of the symmetry of the normal distribution; increasing the standard deviation to account for more slow sites causes results in a corresponding increase in fast sites. A distribution that is even more heavily weighted to lower values than the log-normal distribution may be needed.

MSS model. The effective diffusion path lengths (effective sphere radii) are plotted in Figure 4-7. The expected trend for these parameters is that they would be independent of hydraulic residence time. The total path length should be longer

than the mean particle radius since the diffusion coefficient used did not account for tortuosity. This behavior is exhibited in Figure 4-7. The effective diffusion path lengths are not the same for all experiments, but vary by no more than a factor of two and display no obvious trend with hydraulic residence time. However, the sums of squares of error for the MSS model fits were much larger than those obtained by using the two-site and MSP models (Table 4-2). The poor fits may result from using a spherical distribution which is defined by only one parameter, instead of a two parameter fit like the two-site and MSP models. The sorption sites are probably not spherically distributed, and other distributions may result in better fits. Also, the poor fits may result from variation in diffusion coefficient and diffusion path length which are not accounted for by the MSS model.

Test for Velocity-Independent Parameters

To improve on the performance of the two-site model, multisite models should be described by parameters that do not change with velocity. None of the models tested in this chapter provided mass transfer parameters that were exactly the same for all experiments, although the MSS model parameter estimates were relatively close. Therefore, the ability of parameters estimated from one data set to predict behavior of another experiment was tested. The "goodness of fits" were measured quantitatively by sums of squares of error.

First, parameters estimated from one experiment (AEI100) were used to predict behavior of all other experiments. Parameters derived from experiment

AEI100 were chosen for testing because it was one of the best fit experiments for all of the models, and, as a relatively fast experiment, it would be indicative of using parameters derived from fast laboratory experiments to predict behavior in slower field conditions. The sums of squares of error of fit are presented in Table 4-3.

Table 4-3.    Sums of squares of error for experiment AEI100-derived mass transfer parameters applied to all other experiments.

| Run ID | Two-Site | MSP | MSS |
|--------|----------|-------|-------|
| AEI100 | 0.0338 | 0.0273 | 0.150 |
| AEI203 | 0.0552 | 0.0314 | 0.349 |
| AEI206 | 0.191 | 0.201 | 0.700 |
| AEI210 | 0.152 | 0.124 | 0.327 |
| AEI220 | 0.261 | 0.244 | 0.321 |
| AEI240 | 0.456 | 0.497 | 0.386 |
| AEP200 | 0.0466 | 0.0549 | 0.329 |

The two-site and MSP model parameters derived from experiment AEI100 did a progressively poorer job of predicting the break-through curves as hydraulic residence time increased. Although the sums of squares of error were consistently high using MSS model parameters derived from experiment AEI100, there seems to be no correlation with hydraulic residence time. This indicates velocity-independence of MSS model parameters.

Next, the parameter estimates for each of the flow interruption experiments were used to predict the break-through curve of the flow-rate variation experiment

(AEP200). The fits were again measured by sum of squares of error and are presented in Table 4-4. The MSP model performed slightly better than the two-site

Table 4-4. Sums of squares of error for flow interruption experiment mass transfer parameters applied to flow-rate variation experiment (AEP200).

| Flow Interruption Experiment | Two-Site | MSP | MSS |
|---|---|---|---|
| AEI100 | 0.0466 | 0.0555 | 0.329 |
| AEI203 | 0.0514 | 0.0580 | 0.287 |
| AEI206 | 0.150 | 0.137 | 0.299 |
| AEI210 | 0.213 | 0.154 | 0.286 |
| AEI220 | 0.326 | 0.210 | 0.291 |
| AEI240 | 0.415 | 0.221 | 0.303 |

model, but both models demonstrated a correlation between sums of squares of error and hydraulic residence time indicating velocity-dependence of model parameters. The MSS model demonstrated high sums of squares for error but no velocity-dependence.

Discretizing the Distribution

Converting the continuous frequency distribution into a discrete distribution is called discretization. Using enough compartments (fine discretization) is important for achieving stable parameter estimates. Generally, stable estimates could be achieved with 50 to 100 compartments, although the log-normal distribution required

more. Since more compartments means longer computing time, a method to optimize the number of compartments would be desirable.

## Known Sorption Compartment Distributions

### Nature of Sorption

The nylon ball experiments were conducted to test the use of the MSS model on a sorbent with a known distribution of sorption sites (known geometry). In order to use the MSS model, it was necessary to determine if the nature of sorption of anthracene by the balls was a surface process (adsorption) or diffusion into the balls (partitioning). Batch isotherm studies (Appendix A) were conducted for each ball size over several weeks, and sorption coefficients were calculated both on a per mass (partition coefficient, $K_p$) and per surface area (adsorption coefficient, $K_a$) basis. If the sorption process was adsorption, the $K_p$ values would remain different for each ball size, with the smaller balls having the higher $K_p$ values. The $K_a$ values would be the same for all ball sizes. If the sorption process was partitioning, the $K_p$ values for each ball size would initially be different, but would eventually converge on a common value. The $K_a$ values would initially be the same for all ball sizes, but with time the $K_a$ values for the larger ball sizes would exceed the values for the smaller balls.

The isotherm data are displayed in Figure 4-8. The partition coefficient for the smallest ball, BN-1.5, appears to have approached a maximum value by day 36 (Figure 4-8a), while the partition coefficients for all of the other ball sizes are still
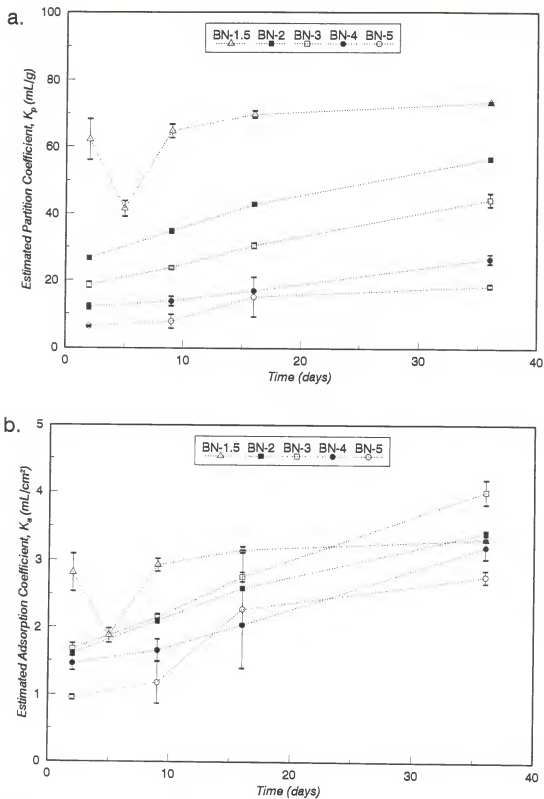
Figure 4-8. Sorption coefficient variation with equilibration time: a) partition coefficient, b) adsorption coefficient.

increasing. Also by day 36, the adsorption coefficient of the smallest ball is exceeded by those of the two next larger ball sizes (BN-2 and BN-3) (Figure 4-8b). This behavior was taken as evidence that the nature of sorption of anthracene by the nylon balls was partitioning, and therefore the MSS model could be used to simulate the sorption process. The partition coefficient for all balls was taken as the maximum value obtained for the smallest ball size, or 73.14 mL/g.

Stir Cell Experiments

Stir cell experiments were conducted using each ball size alone, and using a mixture of all ball sizes. The results of these experiments are summarized in Table 4-5.

Table 4-5. Summary of stir cell experiments using nylon balls.

| Run ID | Ball Name and Diameter (mm) | Recovery | Retard. Factor (batch) | Retard. Factor (obs) |
|---|---|---|---|---|
| ANI301 | BN-1.5 2.381 | 0.980 | 10.33 | 2.37 |
| ANI302 | BN-2 3.175 | 1.003 | 10.88 | 1.71 |
| ANI303R | BN-3 4.762 | 1.005 | 10.93 | 1.58 |
| ANI304 | BN-4 6.35 | 1.006 | 10.30 | 1.40 |
| ANI305 | BN-5 7.938 | 1.015 | 12.28 | 1.36 |
| ANI30X | Mixture | 1.003 | 12.19 | 1.64 |

The distribution of sorption sites for the MSS model was defined by the distribution of volume of a sphere with distance from the surface (i.e., diffusion path length, $\delta$). The cumulative distributions of sorption sites with diffusion path length for each individual ball size, and for the mixture of ball sizes, are illustrated in Figure 4-9.

The MSS model was used to estimate the effective diffusion coefficient for anthracene in the nylon balls for each of the five experiments with the single-sized balls. The MSS model divided the balls into 50 compartments of equal volume. The fitted diffusion coefficients and sum of squares of error of fit are shown in Table 4-6.

Table 4-6.     MSS model fits for the single-size nylon ball experiments.

| Run ID | Ball Name and Diameter (mm) | Diffusion Coefficient $D_{eff}$ (cm$^2$/sec) | Sum of Squares of Error |
|---|---|---|---|
| ANI301 | BN-1.5 2.381 | $1.269(10^{-8})$ $(0.664(10^{-9}))$ | 0.0494 |
| ANI302 | BN-2 3.175 | $0.892(10^{-8})$ $(0.574(10^{-9}))$ | 0.0380 |
| ANI303R | BN-3 4.762 | $1.393(10^{-8})$ $(0.939(10^{-9}))$ | 0.0351 |
| ANI304 | BN-4 6.35 | $1.389(10^{-8})$ $(1.092(10^{-9}))$ | 0.0293 |
| ANI305 | BN-5 7.938 | $0.937(10^{-8})$ $(1.075(10^{-9}))$ | 0.0392 |
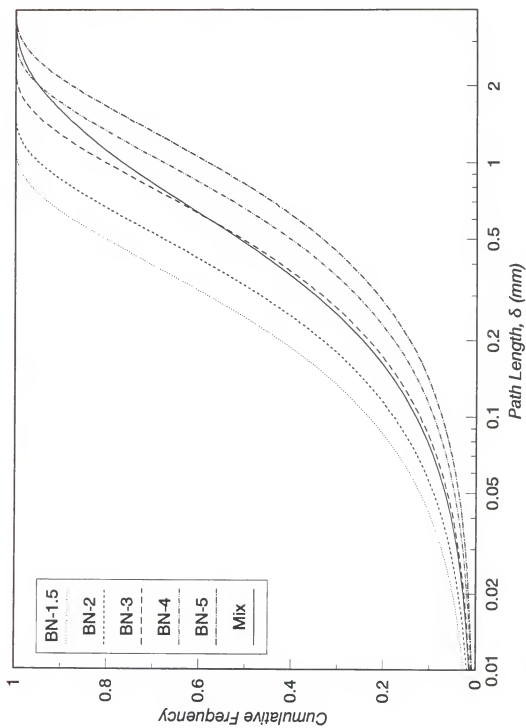
Figure 4-9.    Distribution of nylon ball sorption sites with diffusion path length.

The MSS model was able to fit all of the data sets well (sum of squares of error were always below 0.05). A typical break-through curve with MSS model fit is illustrated by Figure 4-10. The fitted effective diffusion coefficients for each ball size were very consistent, ranging from $0.892(10^{-8})$ to $1.39(10^{-8})$ cm$^2$/sec. The consistency of these fitted values would seem to indicate that the process of sorption of anthracene by nylon balls is partitioning and that the MSS model can successfully simulate this behavior. The diffusion coefficient for anthracene in a nylon should be less than that in the methanol/water phase. The fitted $D_{eff}$ values are an order of magnitude lower than the estimated free liquid diffusion coefficient for anthracene in 50:50 MeOH/H$_2$O ($1.16(10^{-7})$ cm$^2$/sec). Even so, the fitted $D_{eff}$ values are probably too high to represent diffusion in the nylon balls. At the fitted $D_{eff}$ values, the sorption isotherms experiments (Figure 4-8a) would have reached equilibrium in about 6 days for the BN-1.5 balls and in about 15 days for the BN-5 balls. Because diffusion in the balls is so slow, the short-term stir cell experiments are probably dominated by surface processes or diffusion in small pores in the balls. Stir cell experiments conducted over a period of days are necessary to get an accurate estimate of the diffusion coefficients in the balls.

The effective diffusion coefficients from these experiments were averaged, and the value of $1.176(10^{-8})$ cm$^2$/sec was used to attempt to predict the distribution of sorption sites for the stir cell experiment using a mixture of ball sizes (ANI30X, Table 4-5). The distributions tested were spherical, exponential, and log-normal. The results of these fits are presented in Table 4-7, and illustrated by the cumulative
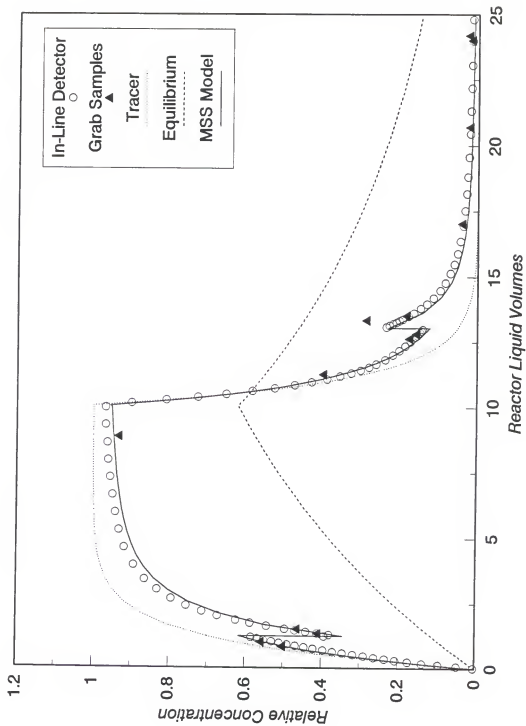
Figure 4-10. Typical MSS fit for breakthrough curve of nylon ball experiment (Experiment ANI301).

Table 4-7. Estimates of sorption site distribution for ANI30X.

| Distribution Type | Parameter Estimates | Sum of Squares of Error |
|---|---|---|
| Spherical | Radius = 2.13 mm (0.0757) | 0.0444 |
| Log-Normal | $\mu_{\ln\delta}$ = 1.71 (0.193) $\sigma_{\ln\delta}$ = 2.72 (0.110) | 0.0269 |
| Exponential | $\lambda$ = 0.566 (0.0233) | 0.0547 |

Note--Standard error of estimate given in parentheses.

distribution functions in Figure 4-11. While all three distributions fit predicted a similar distribution of short path lengths, the predicted distributions diverged as the path length increased. The short duration of the experiments prevented a significant mass of the solute from experiencing the sorption sites at the longer path lengths. Therefore the predictions for the longer path lengths are unreliable. Longer duration experiments would be necessary to allow accurate prediction this part of the sorption site distribution.

## Sorption and Dissolution

### Partition Coefficient

The expected result of the isotherm experiments was that the partition coefficient ($K_p$) of shredded paraffin would be greater that of paraffin beads due to mass transfer limitations in the beads. In fact, the $K_p$ value of the beads exceeded that of the shredded paraffin. The melting process in creating the beads likely volatilized low molecular weight components of the paraffin and created a more
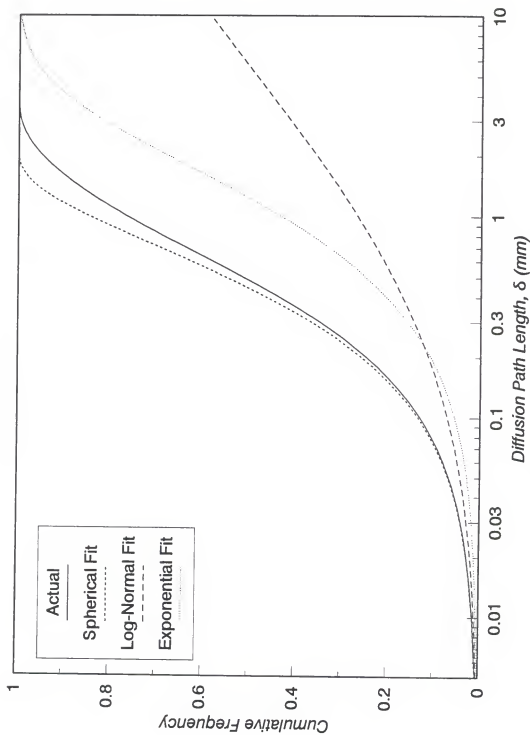
Figure 4-11. Predicted sorption site distributions for mixed sizes of nylon balls (Experiment ANI30X).

hydrophobic organic matrix. The increase in $K_p$ value was significant, being on the order of a factor of four to six. The value of $K_p$ used in simulations was the highest value obtained, 34 mL/g.

<u>Stir Cell Experiments</u>

<u>Characteristics of breakthrough curves</u>. The characteristics of the two stir cell experiments are presented in Table 4-8. Mass recovery was defined in Equation (3-

Table 4-8. Characteristics of stir cell experiments using paraffin beads.

| Run ID | Type | Recovery | Retard. Factor $R_{(obs)}$ | Retard. Factor $R_{(batch)}$ |
|--------|------|----------|--------------------------|------------------------------|
| API400 | Sorption | 0.996 | 1.53 | 7.43 |
| APD400 | Dissolution | 0.0512 | | 4.09 |

20), the observed retardation factor in Equation (3-21), and the batch retardation factor in Equation (3-9a). The sorption experiment was characterized by a good mass balance and a lower retardation factor than that predicted by equilibrium partitioning as characteristic of short-term experiments influenced by mass transfer limitations. The shape of the sorption experiment breakthrough curve was similar to the flow interruption breakthrough curves for Eustis soil and nylon balls.

Only five percent of the anthracene was recovered during the dissolution experiment despite flushing with over 170 cell volumes of solvent over a there day period. The low recovery was due both to the low crystalline solubility of anthracene

in the solvent and to mass transfer limitations. If the experiment had not been truncated, more anthracene would have been recovered. The observed retardation factor could not be calculated with any certainty because the experiment was truncated. The breakthrough curve (Figure 4-12) is characterized by a slowly declining baseline caused by a decreasing overall mass transfer rate as anthracene in the paraffin near the interface is depleted. Concentration increases during flow interruptions are generally proportional to the duration of the flow interruption with two exceptions: the concentration can never exceed the crystalline solubility of anthracene, and the amount concentration increase per minute of flow interruption decreases slightly in the latter stages of the experiment. The declining amounts of mass transfer during the later flow interruptions were again caused by depletion of anthracene near the interface and influence of mass transfer limitations within the paraffin bead.

MSS model predictions. The MSS model was used to fit the breakthrough curves. The geometry of the paraffin beads was assumed to be spherical. The maximum diffusion path length of the paraffin beads was 1 mm. However, since the beads were shaped more like a disk than a sphere, the diffusion path length (sphere radius) was adjusted to 1.667 mm so that the area to volume ratio of the disks would be preserved. The MSS model used 500 compartments of equal volume, and an effective diffusion coefficient was fit to the breakthrough curves. An excellent fit (low sum of squares) was obtained for the sorption experiment. The fit for the dissolution experiment (Figure 4-12) had a much higher sum of squares, but generally
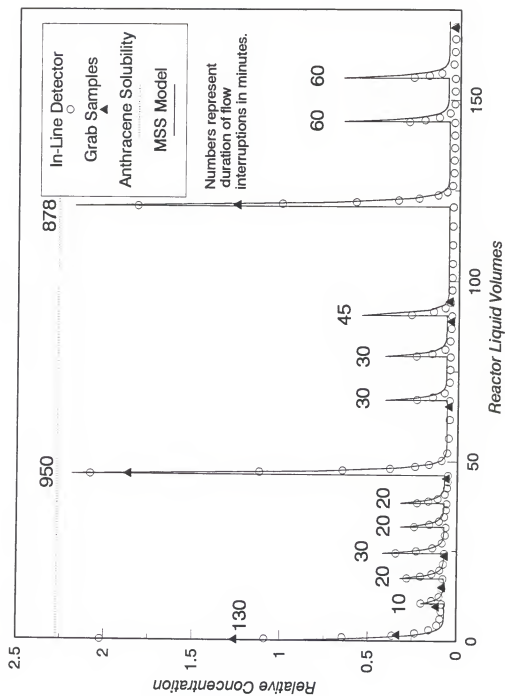
Figure 4-12. Breakthrough curve for paraffin dissolution experiment (Experiment APD400).

did a reasonable job predicting the breakthrough curve. Results of curve-fitting are presented in Table 4-9.

Table 4-9. Spherical model fits for paraffin bead experiments.

| Run ID | Sphere Radius $\delta$ (mm) | Effective Diffusion Coefficient $D_{eff}$ (cm$^2$/sec) | Sum of Squares of Error |
|--------|------------------------------|--------------------------------------------------------|--------------------------|
| API400 | 1.667 | $5.28(10^{-9})$ $(0.304(10^{-9}))$ | 0.0168 |
| APD400 | 1.667 | $0.226(10^{-9})$ $(0.0198(10^{-9}))$ | 1.93 |

The MSS model failed to fit the dissolution experiment breakthrough curve in two key areas. It failed to predict the full concentration increase during the initial flow interruption, and it failed to predict the steadily declining concentration that was evidenced when the flow was not interrupted. In other words, the model under-predicted the rate of mass transfer early in the experiment and over-predicted the rate of mass transfer later in the experiment. A possible explanation for the failure of the MSS model is that the spherical distribution used was not correct.

The effective diffusion coefficients ($D_{eff}$) predicted by the MSS model for the two experiments are presented in Table 4-9. The values are more than one order of magnitude less than the estimated free liquid diffusion coefficient for anthracene in 50:50 MeOH/H$_2$O ($1.16(10^{-7})$ cm$^2$/sec). The dissolution experiment resulted in a lower estimate of $D_{eff}$ than did the sorption experiment, probably because the

dissolution experiment was longer and the effects of diffusion to sites deeper in the paraffin were experienced.

## Conclusions and Recommendations

The MSP model generally provided better fits than the two-site model for individual experiments. Although the MSS model provided fits with higher sums of squares of error, its parameter estimates seem to be independent of velocity. The velocity-independence of MSS parameters is due to modeling mass transfer as diffusion instead of as a first-order process. The MSP model were very successful in describing the change in concentration during flow interruptions, which involves velocity changes within an experiment. The multisite models therefore hold some promise for development as mass transfer models with velocity-independent parameters.

The MSP model has two advantages over the MSS model: (1) the stochastic nature of the MSP model may allow better description of the highly varying parameters affecting mass transfer than can be achieved in the single realization allowed by the MSS model, and (2) it is computationally more simple. The MSS model will be more useful in cases where the geometry of the mass transfer domain is uniform and defined (e.g., diffusion into uniformly sized spheres).

Recommendations for further development of multisite models include:

1. Test multisite models using different data sets and frequency distributions to determine if they can describe mass transfer with parameters that are truly velocity-independent.

2. Develop a computer code to optimize the distribution discretization process. Fitting programs should be constructed so that the distribution is automatically more finely discretized in regions where mass transfer limitations are significant.

3. Conduct experiments over sufficiently long time frames so that slow mass transfer (remote sorption sites) can be characterized.

The use of paraffin as a surrogate organic matrix in desorption experiments will be useful calibrating mass transfer models. However, the paraffin/solute mixture require careful preparation. The MSS model used to simulate the breakthrough curves used the wrong distribution of sorption sites, but the longer experiment resulted in a significantly lower estimate of coefficient of effective diffusion of anthracene in paraffin.

Recommendations for use of paraffin as a surrogate organic matrix include:

1. Paraffin becomes more hydrophobic after being heated. To achieve a consistent partition coefficient, the paraffin should be heated for a fixed period of time at a fixed temperature.

2. Dropping molten paraffin into water creates flattened beads due to the greater density of water. More uniform sized beads may be obtained by dropping the molten paraffin into a liquid with a lower density than

paraffin. However, the liquid should not be able to extract the solute. Alternatively, the molten paraffin could be pored into a mold.

3.  The initial concentration of solute in the paraffin should be kept very low, so that the equilibrium concentration is less than half the crystalline solubility. This will allow the use of a linear isotherm without complications of solubility limitations.

4.  Longer experiments will experience the influence of more remote sites, and improve the estimate of mass transfer rates in the organic phase.

# CHAPTER 5
## SUMMARY AND CONCLUSIONS

This study was conducted to investigate the following questions concerning mass transfer:

1.   In what phase is mass transfer limited?

2.   Why are mass transfer rate coefficients a function of pore water velocity?

3.   Is the two-site sorption mass transfer model adequate?

A continuously stirred flow cell was designed and built with a flow reversal valve to keep fines in suspension. The turbulent conditions at the sorbent-water interface precluded mass transfer limitations in extra-aggregate water. Estimates of mass transfer parameters obtained from stir cell experiments were similar to estimates obtained from column experiments. Therefore, mass transfer is limited by diffusion in organic matter or in intraparticle micropores.

Are velocity-dependent parameters: (1) artifacts of relative rates of aqueous-phase advection and interphase mass transfer (i.e., hydraulic residence time), (2) artifacts of modeling a diffusion-controlled process with a first-order model, or (3) caused by changing shear forces at the sorbent-water interface (i.e., kinetic energy)? The turbulent conditions in the stir cell kept shear forces at the interface independent of hydraulic residence time. Parameter estimates of mass transfer rate

175

coefficients remained dependent on hydraulic residence time, indicating that "velocity" dependence is actually a modeling artifact. Further, both first-order models (two-site and multiple sites in parallel [MSP]) demonstrated velocity-dependent parameters. The two-site model simulates mass transfer relative to advection, but the MSP model only uses finite mass transfer rates. Only the diffusion model (multiple sites in series [MSS]) resulted in parameters which are independent of hydraulic residence time. Therefore, "velocity" dependence is an artifact of modeling a diffusion process with a first-order mass transfer model.

Two multisite models (MSP and MSS) were proposed which decouple advection from the mass transfer rate coefficients and allow mass transfer to occur at variable rates without increasing the number of fitted parameters. The MSP model was able to provide better (lower sum of squares of error) predictions of individual breakthrough curves, but only the MSS model exhibited velocity-independent parameters. Further testing of the models is recommended since both models demonstrate advantages over the conventional two-site model.

Specific conclusions of this study are:

1.  The continuously stirred flow cell, in combination with a flow reversal valve, is a viable design for studying soil-water systems.

2.  Mass transfer parameters estimated from stir cell breakthrough curves are similar to parameter values estimated by other techniques (i.e., column, batch, and gas purge methods).

3. The stir cell technique is best suited for short-term experiments (fast mass transfer) using solute/solvent/sorbent combinations which have high sorbent/solvent partition coefficients.

4. Mass transfer limitations in soil-water systems are caused by diffusion in organic matter, in intraparticle micropores, or both.

5. Estimation of long-term (slow) mass transfer rate coefficients require long-term experiments involving desorption (well defined "tail" of the breakthrough curve).

6. Flow interruption experiments provided mass transfer model parameter estimates with less standard error than did flow-rate variation experiments. Since flow rates can only be varied over a narrow range, the flow interruption tests actually achieve a larger and more effective exposure time perturbation than can be accomplished with the flow-rate variation technique.

7. Multisite models provide better predictions of individual breakthrough curves than does the two-site model because they allow the overall mass transfer rate to vary over the course of an experiment.

8. First-order mass transfer models result in velocity-dependent parameters. Only diffusion models have parameters that are independent of velocity or hydraulic residence time.

9. The MSP model has potential for further development because of its stochastic approach and computational simplicity.

10. The MSS model will be useful when mass transfer must be modeled as diffusion instead of as first-order process (e.g., changing pore water velocity).

## GLOSSARY

### Roman

a      Interfacial area per unit volume porous media, $L^{-1}$

C      Concentration, $M\ L^{-3}$

$d_c$      Characteristic length, L

$d_{10}$      Particle diameter (10 percent passing), L

$d_{50}$      Mean particle diameter (50 percent passing), L

$d_{60}$      Particle diameter (60 percent passing), L

$D_{eff}$      Effective coefficient of diffusion, $L^2\ t^{-1}$

$D_h$      Coefficient of hydrodynamic dispersion, $L^2\ t^{-1}$

$D_{i(l)}$      Coefficient of diffusion of solute $i$ in liquid $l$, $L^2\ t^{-1}$

$f_c$      Mass fraction of cosolvent in mixture

$f_{MV}$      Molar volume of species $i$ divided by average molar volume of all other components

$f_{oc}$      Mass of organic carbon per unit mass of solid

$f_{om}$      Mass of organic matter per unit mass of solid

F      Fraction of instantaneously sorbing sites (two-site model)

$F_j$      Fraction of sorption sites defined by compartment $j$ (multi-site models)

$\Delta H_f$      Heat of fusion, $M\ L^2\ t^{-2}\ mol^{-1}$

| J | Mass flux, $M\ L^{-2}\ t^{-1}$ |
|---|---|
| k | Mass transfer rate coefficient, $L\ t^{-1}$ |
| $k_2$ | Desorption mass transfer rate (two site model), $t^{-1}$ |
| $k_{w\text{-}a}$ | Mass transfer rate, $t^{-1}$ |
| $K_a$ | Adsorption coefficient, $L$ |
| $K_{n/w}$ | NAPL/water partitioning coefficient |
| $K_p$ | Sorption solid/water partitioning coefficient, $L^3\ M^{-1}$ |
| M | Mass, $M$ |
| MW | Molecular weight, $M\ mol^{-1}$ |
| $p_c$ | Capillary pressure, $M\ L^{-1}\ t^{-2}$ |
| P | Pore volumes or stir cell liquid volumes |
| Q | Volumetric flow rate, $L^3\ t^{-1}$ |
| R | Retardation factor |
| $R_g$ | Ideal gas constant, $M\ L^2\ t^{-1}\ mol^{-1}\ \tau^{-1}$ |
| Re | Reynolds number |
| S | Solubility of pure compound, $M\ L^{-3}$ |
| $\hat{S}$ | Mass component $i$ sorbed per mass of solid phase |
| Sc | Schmidt number |
| Sh | Sherwood number |
| Sh' | Modified Sherwood number |
| T | Dimensionless time |
| t | Time, $t$ |

| $U_i$ | Uniformity index |
| $v$ | Pore water velocity, $L\ t^{-1}$ |
| $V$ | Liquid volume in stir cell, $L^3$ |
| $X$ | Mole fraction |
| $x$ | Space dimension, $L$ |

## Greek

| $\gamma$ | Activity coefficient |
| $\delta$ | Diffusion transport distance, $L$ |
| $\varepsilon$ | Porosity |
| $\lambda$ | Absolute viscosity, $M\ L^{-1}\ t^{-1}$ |
| $\lambda$ | Exponential frequency distribution parameter (MSS model) |
| $\theta$ | Fluid/porous media volumetric ratio |
| $\mu$ | Mean |
| $\mu_i^*$ | Chemical potential of component $i$ at standard state, $M\ L^2\ t^{-2}\ mol^{-1}$ |
| $\mu_{i(l)}$ | Chemical potential of compenent $i$ in phase $l$, $M\ L^2\ t^{-2}\ mol^{-1}$ |
| $\rho$ | Density, $M\ L^{-3}$ |
| $\rho_a$ | Bulk density of solid, $M\ L^{-3}$ |
| $\sigma$ | Standard deviation |
| $\sigma_c$ | Power of cosolvent |
| $\tau$ | Temperature |
| $\upsilon$ | Molar volume, $L^3\ mol^{-1}$ |

| $\bar{v}$ | Molal volume, $L^3$ mol$^{-1}$ |
| $\omega$ | Dimensionless mass transfer rate |

## Subscripts

| c | Cosolvent |
| f | "fast" or equilibrium fraction |
| i | Component |
| in | Influent |
| j | Sorption compartment (multi-site models) |
| m | Melting point |
| max | Maximum or normalizing value |
| mix | Mixed aqueous/cosolvent phase |
| n | Nonaqueous phase liquid |
| oc | Organic carbon |
| om | Organic matter |
| R | Reactor or stir cell |
| s | Solid phase |
| scl | Super-cooled liquid |
| $\breve{\omega}$ | Sorbed (M/M) concentration |
| w | Aqueous phase |

## Superscripts

| | |
|---|---|
| adv | Advection |
| dif | Diffusion |
| e | Equilibrium |
| 0 | Single component NAPL system |
| * | Dimensionless or relative value |

## Methods

Isotherm experiments were conducted in 5 mL amber screw-top high pressure liquid chromatography (HPLC) vials with teflon lined septa. Vials were weighed empty, after the solid phase was added, and a third time after the solvent was added. The solvent contained a solute at an initial concentration of approximately 25, 50, 75 and 100 percent of saturation. Duplicates of each concentration were run.

Blanks, consisting of solution in vials containing no solid material, were prepared with the isotherm vials to define the initial concentration in the liquid phase. Isotherm vials were rotated for a period of days as indicated in Table A-1 so the solute could approach equilibrium between the solid and liquid phases.

Table A-1. Equilibration time for sorption isotherms.

| Solid Phase | Equilibration Time (days) |
|---|---|
| Eustis | 1 |
| Zellwood | 1 - 3 |
| Nylon Balls | 2 - 36 |
| Paraffin | 9 - 14 |

Following equilibration, vials containing soil were centrifuged for about 30 minutes on a Sorvall RT6000 refrigerated centrifuge. Equilibrium liquid phase concentrations were determined by HPLC analysis sampled directly from the isotherm vial. Sorbed phase concentrations were determined by mass balance using Equation (A-1):

$$\hat{S}_{(i)} = \frac{M_l}{\rho_l M_s}(C_{i(l)}^{blank} - C_{i(l)}^{eq}) \qquad \text{(A-1)}$$

Isotherms were constructed by plotting sorbed phase concentration, $\hat{S}_i$, versus equilibrium liquid phase concentration, $C_{i(l)}^{eq}$, and performing linear regression with intercept of zero. For soil isotherms conducted at several cosolvent fractions, linear regression was performed to determine the relationship between log partition coefficient (log $K_p$) and volume fraction of cosolvent methanol ($f_c$).

## Eustis Soil

Isotherms were performed on Eustis soil for naphthalene in water (Figure A-1), and for anthracene in 30:70, 40:60, and 50:50 methanol/water (MeOH/$H_2O$) (Figure A-2). The resulting partition coefficients, with additional $K_p$ data obtained from Dai (1993), is presented in Table A-2 and plotted versus fraction cosolvent in Figure A-3.

The log $K_p$ regressions with $f_c$ for naphthalene, anthracene, and pyrene are given in Equations (A-2a), (A-2b), and (A-2c) respectively.
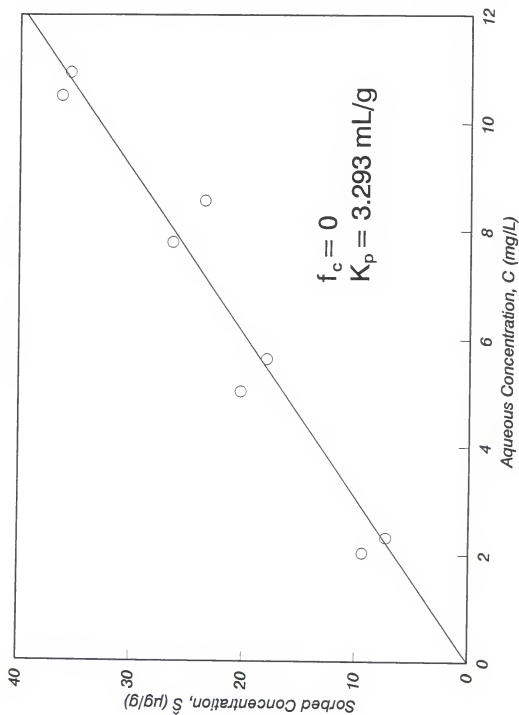
Figure A-1. Isotherm for naphthalene sorption onto Eustis soil.
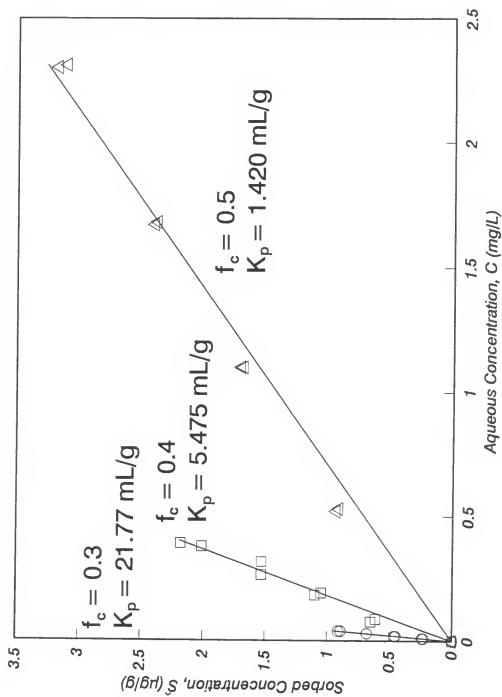
Figure A-2.   Isotherms for anthracene sorption onto Eustis soil.
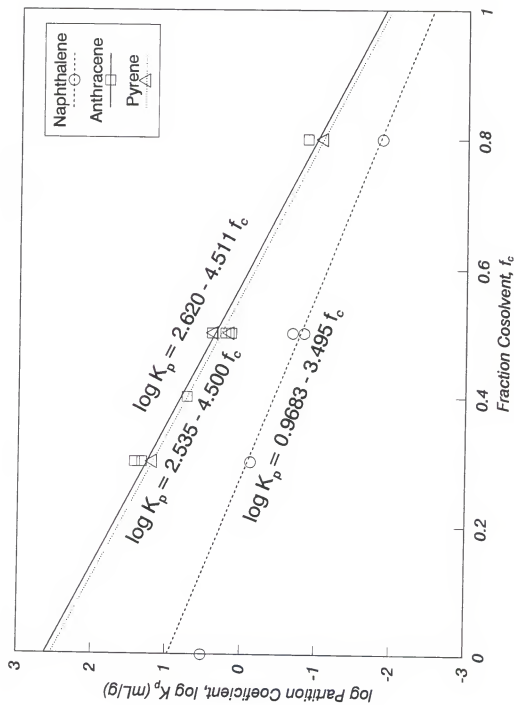
Figure A-3.   Eustis partition coefficient variation with cosolvent fraction.

Table A-2. Partition coefficients for Eustis soil, dry weight basis.

| $f_c$ | Naphthalene | Anthracene | Pyrene |
|-------|-------------|------------|--------|
| This Study | | | |
| 0 | 3.29[a] | | |
| 0.3 | | 21.8 | |
| 0.4 | | 5.48 | |
| 0.5 | | 1.42 | |
| Dai (1993) | | | |
| 0.3 | 0.76 | 27.3 | 15.6 |
| 0.5 | 0.15 | 2.59 | 1.48 |
| 0.5 | 0.214 | 1.70 | 2.45 |
| 0.8 | 0.014 | 0.14 | 0.087 |

a. Value not used in regression with $f_c$.

$$\log K_p \, (naph.) = 0.9683 - 3.495 f_c \qquad \textbf{(A-2a)}$$

$$\log K_p \, (anthr.) = 2.620 - 4.511 f_c \qquad \textbf{(A-2b)}$$

$$\log K_p \, (pyr.) = 2.535 - 4.500 f_c \qquad \textbf{(A-2c)}$$

## Zellwood Soil

Isotherms were performed on Zellwood soil for naphthalene in water, 25:75, 50:50, and 75:25 MeOH/$H_2$O (Figure A-4), and anthracene in 30:70, 50:50, 70:30, and 90:10 MeOH/$H_2$O (Figure A-5). Values for $K_p$ are presented in Table A-3.

Log $K_p$ regressions with $f_c$ are illustrated in Figure A-6, and are given as Equations (A-3a) and (A-3b) for naphthalene and anthracene respectively.
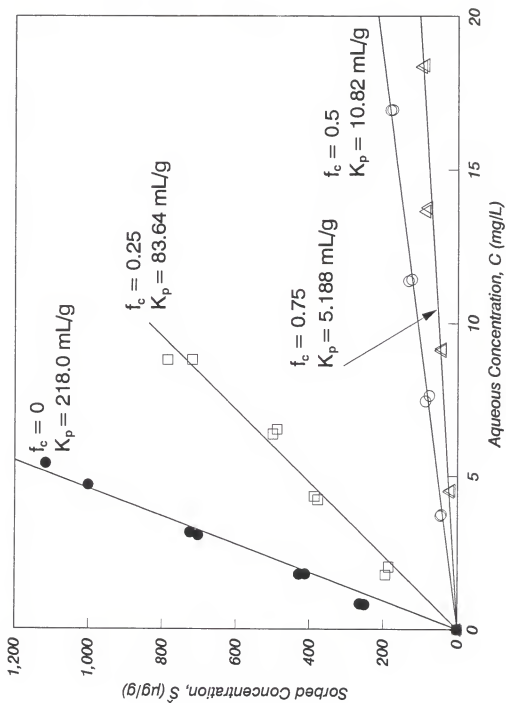
Figure A-4. Isotherms for naphthalene sorption onto Zellwood soil.
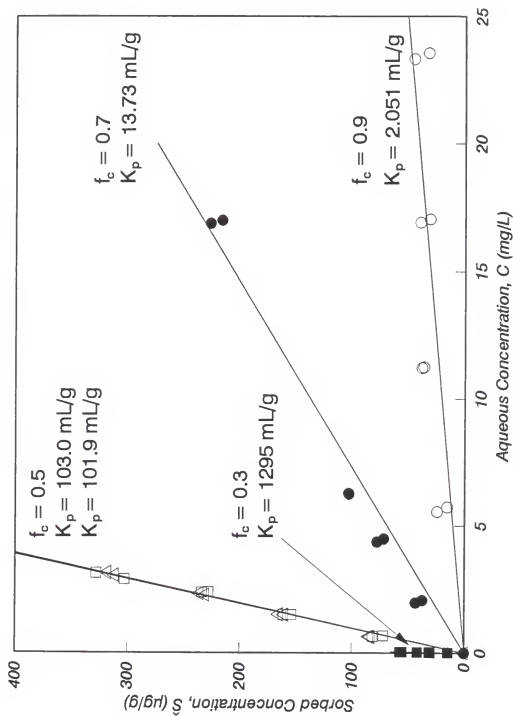
Figure A-5.   Isotherms for anthracene sorption onto Zellwood soil.
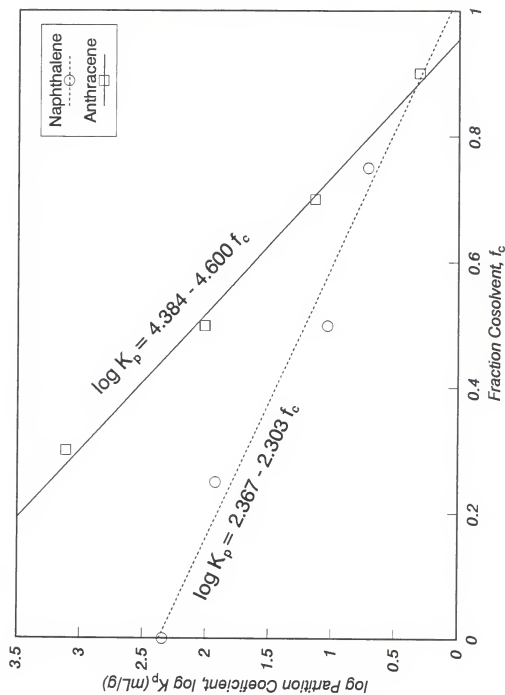
Figure A-6. Zellwood partition coefficient variation with cosolvent fraction.

Table A-3. Partition coefficients for Zellwood soil, dry weight basis.

| $f_c$ | Naphthalene | Anthracene |
|-------|-------------|------------|
| 0 | 218.0 | |
| 0.25 | 83.64 | |
| 0.3 | | 1295 |
| 0.5 | 10.82 | 103.0 |
| 0.5 | | 101.9 |
| 0.7 | | 13.73 |
| 0.75 | 5.188 | |
| 0.9 | | 2.051 |

$$\log K_p \, (naph.) = 2.367 - 2.303 f_c \qquad \textbf{(A-3a)}$$

$$\log K_p \, (anthr.) = 4.385 - 4.600 f_c \qquad \textbf{(A-3b)}$$

### Nylon Balls

A series of isotherms were conducted on nylon balls for anthracene in 50:50 MeOH/$H_2$O over a period of 2 to 36 days. Estimates of partition coefficients are presented in Table A-4. The long diffusion path distances in the nylon balls prevented the larger balls from reaching equilibrium. The partition coefficient used for all nylon balls was the largest partition coefficient estimated for the smallest ball size, or 73.14 mL/g. The 9-day isotherms are illustrated in Figure A-7.

Table A-4. Partition coefficients for nylon balls.

| Time/ No. Points | BN-1.5 2.381 mm | BN-2 3.175 mm | BN-3 4.762 mm | BN-4 6.35 mm | BN-5 7.938 mm |
|---|---|---|---|---|---|
| 2 days (3 pts) | 62.2 | 26.7 | 18.5 | 12.1 | 6.33 |
| 5 days (8 pts) | 41.5 | | | | |
| 9 days (8 pts) | 64.7 | 34.7 | 23.7 | 13.7 | 7.82 |
| 16 days (2 pts) | 69.7 | 42.9 | 30.4 | 16.9 | 15.1 |
| 36 days (2 pts) | 73.1 | 56.5 | 44.2 | 26.5 | 18.3 |

<u>Paraffin</u>

Isotherms were conducted on both shredded paraffin and paraffin beads for anthracene in 50:50 MeOH/$H_2O$ for a period of up to 14 days. The 14 day partition coefficient for the shredded paraffin (5.03 mL/g) was less than the 14 day partition coefficient for the paraffin beads (34.0 mL/g) despite the longer diffusion path distances in the beads. Presumably, heating (i.e., melting) the paraffin to form the beads made it more hydrophobic by volatilizing some of the lower molecular weight components. The isotherms are illustrated in Figure A-8.
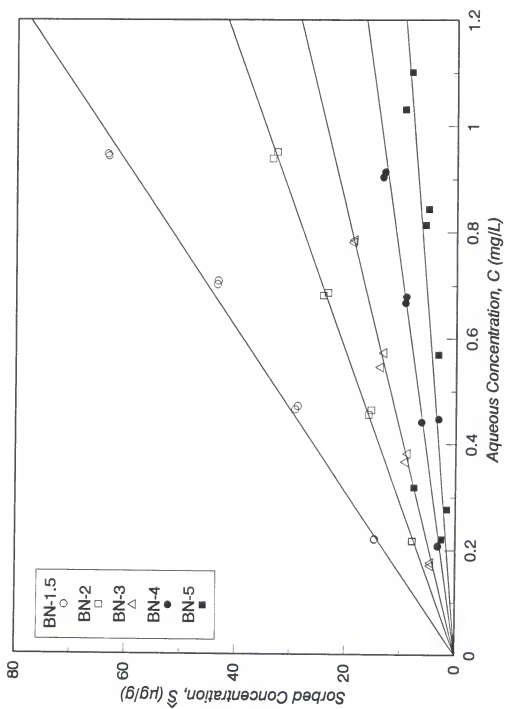
Figure A-7. Nine-day isotherms for anthracene sorption from 50:50 MeOH/$H_2O$ onto nylon balls.
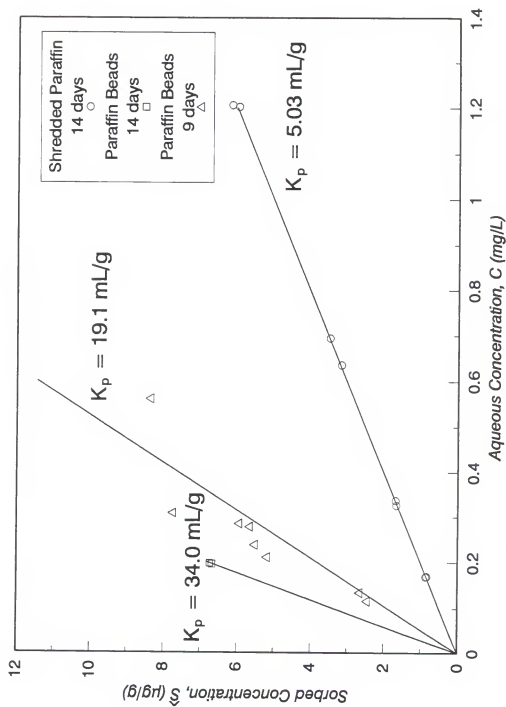
Figure A-8.  Isotherms for sorption of anthracene from 50:50 MeOH/H$_2$O methanol/water onto paraffin.

## APPENDIX B
## BLANKS

Stir cell experiments were performed for various solute and solvent combinations to determine sorption by the stir cell wall surfaces. Solute retardation was observed for solute/solvent combinations where $K_{oc} \geq 300$ mL/g. The sorption was limited by mass transfer. Sorption by stir cell wall surfaces was modeled using the two-site model. Model parameters were obtained by fitting the two-site model to break-through curves of blanks (stir cell experiments performed without sorbent in the reactor).

Eight blanks were conducted: one for pentafluorobenzoic acid (PFBA) in water, four for anthracene in 30:70 methanol/water (MeOH/H₂O), two for anthracene in 50:50 MeOH/H₂O, and one for naphthalene in water. All solutions contained 0.01 N CaCl₂. The characteristics of these experiments are summarized in Table B-1.

To estimate a sorption partition coefficient, it was necessary to define a measure of the sorbent (i.e. the stir cell wall surfaces). The actual wall surfaces would be difficult to measure. However, the sorption was assumed to occur on the teflon fittings of the reactor, which consisted of the end adapters, the o-rings, and the stir bar (Table 3-2). Only two sizes of these fittings were used, and the exposed surface area of the larger fittings were almost exactly four times that of the smaller

Table B-1. Characteristics of blank stir cell experiments.

| Run ID | Solute | Solvent[a] | Type[b] | Time of Exposure[c] (min) | $K_{oc}$[d] (mL/g) |
|--------|--------|-----------|---------|---------------------------|--------------------|
| POP100 | PFBA | water | Flow Var. | 43 | 0 |
| AOI203 | Anthracene | 30:70 | Inter. | 105 | 3424 |
| AOI206 | Anthracene | 30:70 | Inter. | 127 | 3424 |
| AOI206R | Anthracene | 30:70 | Inter. | 130 | 3424 |
| AOI210 | Anthracene | 30:70 | Inter. | 163 | 3424 |
| AOI300 | Anthracene | 50:50 | Inter. | 1277 | 429 |
| AOI301 | Anthracene | 50:50 | Inter. | 120 | 429 |
| NOP100 | Naphthalene | water | Flow Var. | 53 | 609 |

a.  Solvent is a volume to volume ratio of methanol and water. All solvents contained 0.01 N $CaCl_2$.
b.  Inter. = flow interruption experiment; Flow var. = flow-rate variation experiment.
c.  Time of exposure = time from start of experiment until solute-free solvent was introduced to the stir cell.
d.  Organic carbon partition coefficient for Eustis soil.

fittings. Therefore the "mass" of the stir cell wall surfaces, $M_R$, was assigned a value of one when the small fittings were used and a value of 4 when the larger fittings were used.

The tracer run using PFBA was used to study the hydraulic characteristics of the stir cell. There was no apparent sorption of the PFBA by the stir cell components. The break-through curve is characteristic of ideal mixing, and is presented as Figure 3-3.

The four blanks run for anthracene in 30:70 MeOH/$H_2O$ were conducted for different pulse durations. Pulse lengths were selected similar to those used in the experiments with Eustis soil (Tables 3-3 and 4-2). There was no apparent correlation between pulse length and fitted two-site model parameters. Presumably the pulse lengths of the experiments were sufficiently similar that parameter dependence on exposure time was not important. Therefore parameters were chosen that resulted in a minimum total sum of squares for all four blanks. Two site model parameter estimates are listed in Table B-2.

Table B-2. Fitted two-site model parameters for stir cell wall surface sorption.

| Solute/ Solvent | Partition Coefficient $K_R$ (mL/g) | Mass Transfer Rate Coef. $k_R$ (min$^{-1}$) | Fraction Equilibrium Sites $F_R$ |
|---|---|---|---|
| Anthracene 30:70 MeOH/$H_2O$ | 3.05 | 0.0088 | 0.58 |
| Anthracene 50:50 MeOH/$H_2O$ (long) | 0.288 | 0.0000253 | 0.478 |
| Anthracene 50:50 MeOH/$H_2O$ (short) | 0.0956 | 0.000356 | 0.611 |
| Naphthalene water | 1.244 | 0.0811 | 0.562 |

The two blanks run for anthracene in 50:50 MeOH/$H_2O$ were also conducted for different pulse durations. In this case, there did appear to be greater sorption for the longer exposure time, although both experiments indicated very little sorption by the stir cell wall surfaces. The parameters from the longer exposure time blank were used to model stir cell wall surface sorption for experiment AZI100 (Table 3-3). The parameters for the shorter exposure time blank were used to model stir cell wall surface sorption for experiments using nylon balls (Table 4-6). The fitted two-site model parameters are listed in Table B-2.

One blank was conducted for naphthalene in water. The fitted two-site model parameters are listed in Table B-2. These parameters were used to model stir cell wall surface sorption for experiments using the same solute/solvent combination and both Eustis and Zellwood soils (Table 3-3).

## APPENDIX C
## STIR CELL DATA

Stir cell data used for fitting mass transfer model parameters are listed in this appendix. Data sets are arranged by type of sorbent. Eustis soil experiments are listed first, followed by Zellwood soil, nylon ball, paraffin, and finally blanks. Notation used in the data sets are listed in the Glossary except for the following:

DV1   Dead volume between flow control valve and stir cell.

DV2   Dead volume between stir cell and in-line detector.

Y     Total in-line detector response.

$Y_b$    Baseline in-line detector response.

$Y_s$    In-line detector response for solute.

The detector response for the solute is total response minus the baseline response for the time of interest (Equation C-1).

$$Y_s = Y - Y_b \tag{C-1}$$

In-line detector response curves for most solutes were linear. However, a nonlinear response was noted for anthracene in 50:50 methanol/water. Its response curve was:

201

$$if \; Y_s \; < \; 0.02: \quad C \; - \; 11.9598 \, Y_s$$

$$if \; Y_s \; > \; 0.02: \quad C \; - \; 17.701 \, Y_s \; - \; 527.08 \, Y_s^2 \; + \; 12001 \, Y_s^3$$

(C-2)

Time was recorded in minutes. Times reflect actual times that valves were turned, samples were collected, or in-line detector responses were recorded. Times have not been adjusted for system dead volumes.

Run AEI100: Anthracene/Eustis/30:70/Interrupt
14Dec94

$Ms$ = .660 g   $V$ = 6.300 mL      $Kp$ = 18.490 mL/g
$C0$ = .000   $Ss0$ = .000      $Sr0$ = .000
$DV1$ = .180 mL  $DV2$ = .110 mL      $Mr$ = 1.000
$Kr$ = 3.050 mL  $kr$ = .8800E-02 min^-1  $Fr$ = .580

REACTOR OPERATION:

| Time Start | Flow | Cin |
|---|---|---|
| .0 | 1.040 | 1. |
| 25.0 | .000 | 1. |
| 85.0 | 1.040 | 1. |
| 122.0 | .000 | 0. |
| 123.0 | 1.030 | 0. |
| 145.0 | .000 | 0. |
| 205.0 | 1.030 | 0. |

EXPERIMENT DATA: In-Line Detector
Baseline: $Yb$ = .6084E-05 T + .1016E-02
Response Curve: Linear
$Ymax$ = .3149E-01

| T(min) | Y | T(min) | Y | T(min) | Y | T(min) | Y |
|---|---|---|---|---|---|---|---|
| .55 | .1318E-02 | 1.05 | .2246E-02 | 1.55 | .3613E-02 | 2.05 | .5078E-02 |
| 2.55 | .6543E-02 | 3.05 | .7959E-02 | 3.55 | .9229E-02 | 4.05 | .1055E-01 |
| 4.55 | .1172E-01 | 5.55 | .1392E-01 | 6.55 | .1587E-01 | 7.55 | .1758E-01 |
| 8.55 | .1914E-01 | 9.55 | .2046E-01 | 12.55 | .2393E-01 | 13.55 | .2441E-01 |
| 14.55 | .2495E-01 | 15.55 | .2544E-01 | 16.55 | .2588E-01 | 17.55 | .2632E-01 |
| 18.53 | .2671E-01 | 19.55 | .2715E-01 | 22.55 | .2915E-01 | 23.03 | .2910E-01 |
| 23.53 | .2915E-01 | 24.03 | .2930E-01 | 24.55 | .2930E-01 | 85.52 | .2666E-01 |
| 86.02 | .2710E-01 | 86.52 | .2739E-01 | 87.02 | .2764E-01 | 87.52 | .2788E-01 |
| 88.02 | .2813E-01 | 89.52 | .2876E-01 | 92.52 | .2983E-01 | 94.52 | .3013E-01 |
| 96.52 | .3052E-01 | 98.52 | .3076E-01 | 102.52 | .3184E-01 | 104.52 | .3179E-01 |
| 106.52 | .3184E-01 | 108.52 | .3198E-01 | 112.52 | .3232E-01 | 114.52 | .3237E-01 |
| 116.52 | .3223E-01 | 118.50 | .3208E-01 | 123.00 | .3286E-01 | 124.00 | .3140E-01 |
| 124.52 | .2988E-01 | 125.00 | .2842E-01 | 125.50 | .2705E-01 | 126.00 | .2568E-01 |
| 126.52 | .2437E-01 | 127.00 | .2319E-01 | 128.00 | .2100E-01 | 129.02 | .1909E-01 |
| 131.00 | .1470E-01 | 132.00 | .1397E-01 | 133.00 | .1323E-01 | 134.00 | .1240E-01 |
| 135.00 | .1172E-01 | 136.00 | .1094E-01 | 137.00 | .1030E-01 | 138.00 | .9619E-02 |
| 139.00 | .9082E-02 | 141.00 | .7324E-02 | 142.50 | .6689E-02 | 143.00 | .6592E-02 |
| 143.50 | .6445E-02 | 144.00 | .6299E-02 | 144.50 | .6152E-02 | 145.00 | .5957E-02 |
| 205.48 | .9033E-02 | 205.98 | .8594E-02 | 206.50 | .8203E-02 | 207.00 | .7861E-02 |
| 207.48 | .7568E-02 | 208.00 | .7373E-02 | 209.50 | .6592E-02 | 210.98 | .5957E-02 |

```
212.48 .5518E-02 214.50 .5029E-02 216.98 .4590E-02 219.50 .4199E-02
221.48 .3906E-02 224.48 .3467E-02 226.98 .3271E-02 229.48 .3125E-02
231.48 .3125E-02 233.98 .2979E-02 236.48 .2881E-02 239.48 .2832E-02
241.98 .2832E-02 244.48 .2734E-02 246.98 .2686E-02 249.48 .2637E-02
252.48 .2686E-02 254.98 .2637E-02 257.47 .2588E-02 259.98 .2686E-02
```

EXPERIMENT DATA: HPLC grab samples
Cmax = .2355E+00
```
T (min)   C       T(min)   C        T(min)   C       T(min)   C
  8.63  .1335E+00  21.64 .2224E+00  22.64 .2131E+00  24.13 .2234E+00
 86.14  .1886E+00  87.14 .1922E+00  89.13 .1947E+00 115.15 .2296E+00
133.14  .9461E-01 141.63 .3878E-01 142.62 .3732E-01 144.13 .3545E-01
206.18  .4615E-01 214.19 .2235E-01 245.17 .0000E+00
```

Run AEI203: Anthracene/Eustis/30:70/Interrupt
29Mar94

```
Ms  =  1.060 g   V  =  6.100 mL      Kp  =  18.490 mL/g
C0  =   .000    Ss0 =  .000      Sr0 =   .000
DV1 =   .180 mL  DV2 =   .110 mL     Mr  =  1.000
Kr  =  3.050 mL  kr =  .8800E-02 min^-1  Fr =   .580
```

REACTOR OPERATION:
```
Time Start   Flow    Cin
    .0       1.820    1.
  15.0        .000    1.
  76.0       1.820    1.
 105.0       1.970    0.
 115.0        .000    0.
 175.0       1.970    0.
```

EXPERIMENT DATA: In-Line Detector
Baseline: Yb = .6698E-05 T + .1179E-02
Response Curve: Linear
Ymax = .3194E-01
```
T(min)   Y       T(min)   Y        T(min)   Y       T(min)   Y
  .30  .1953E-02   .80  .3174E-02  1.30 .5225E-02  1.80 .7471E-02
 2.30  .9424E-02  2.80 .1133E-01  3.30 .1309E-01  3.80 .1465E-01
 4.30  .1621E-01  4.80 .1748E-01  5.30 .1870E-01  5.80 .1982E-01
 6.30  .2085E-01  6.80 .2183E-01  7.30 .2266E-01  7.80 .2334E-01
 8.30  .2402E-01  8.80 .2471E-01  9.30 .2515E-01  9.80 .2578E-01
```

```
12.30 .2827E-01   12.80 .2842E-01   13.30 .2861E-01   13.80 .2876E-01
14.30 .2896E-01   14.80 .2910E-01   76.63 .2642E-01   77.15 .2686E-01
77.63 .2730E-01   78.13 .2764E-01   78.63 .2803E-01   79.13 .2837E-01
82.13 .3057E-01   83.13 .3071E-01   84.13 .3086E-01   85.13 .3115E-01
86.13 .3140E-01   87.13 .3149E-01   90.63 .3228E-01   91.63 .3223E-01
92.63 .3232E-01   93.63 .3247E-01   94.63 .3242E-01   99.13 .3296E-01
100.13 .3296E-01  101.13 .3296E-01  102.13 .3291E-01  105.63 .3189E-01
106.13 .2944E-01  106.63 .2710E-01  107.13 .2485E-01  107.63 .2280E-01
108.13 .2105E-01  108.63 .1943E-01  109.13 .1792E-01  109.63 .1660E-01
111.63 .1206E-01  112.13 .1157E-01  112.63 .1099E-01  113.13 .1050E-01
113.63 .9912E-02  114.13 .9473E-02  114.63 .9033E-02  175.40 .1240E-01
175.90 .1143E-01  176.40 .1055E-01  176.90 .9766E-02  177.40 .9131E-02
177.92 .8594E-02  178.40 .8008E-02  178.90 .7520E-02  179.40 .7080E-02
179.90 .6641E-02  180.90 .6104E-02  181.40 .5811E-02  181.90 .5469E-02
182.40 .5225E-02  182.90 .4932E-02  183.40 .4590E-02  183.90 .4346E-02
187.40 .3662E-02  188.40 .3564E-02  190.90 .3418E-02  191.90 .3320E-02
192.90 .3223E-02  193.90 .3174E-02  194.90 .3027E-02  195.90 .3027E-02
196.90 .2930E-02  197.90 .2881E-02  199.40 .2881E-02  200.40 .2832E-02
201.40 .2783E-02  202.40 .2734E-02  203.40 .2734E-02  204.40 .2637E-02
205.40 .2588E-02  208.90 .2637E-02  209.88 .2637E-02  210.88 .2637E-02
```

EXPERIMENT DATA: HPLC grab samples
Cmax = .2481E+00

```
T (min)   C        T(min)   C        T(min)   C        T(min)   C
  5.13 .1283E+00   11.12 .2208E+00   14.15 .2307E+00   78.15 .2001E+00
 79.13 .2216E+00   84.16 .2336E+00   94.13 .2519E+00  109.15 .1293E+00
112.15 .8221E-01  113.12 .7384E-01  114.14 .6305E-01  176.13 .6551E-01
177.12 .5684E-01  178.12 .4708E-01  210.14 .0000E+00
```

Run AEI206: Anthracene/Eustis/30:70/Interrupt
17May94

```
Ms  =  1.010 g   V  =  6.160 mL      Kp  =  18.490 mL/g
C0  =   .000    Ss0 =   .000     Sr0 =   .000
DV1 =   .180 mL  DV2 =   .110 mL      Mr  =  1.000
Kr  =  3.050 mL  kr  = .8800E-02 min^-1  Fr =   .580
```

REACTOR OPERATION:

| Time Start | Flow | Cin |
|---|---|---|
| .0 | 1.030 | 1. |
| 15.0 | .000 | 1. |

| 85.0 | 1.030 | 1. |
| 139.0 | 1.030 | 0. |
| 165.0 | .000 | 0. |
| 227.0 | 1.030 | 0. |

EXPERIMENT DATA: In-Line Detector
Baseline: Yb = .8140E-05 T + .1344E-02
Response Curve: Linear
Ymax = .3121E-01

| T(min) | Y | T(min) | Y | T(min) | Y | T(min) | Y |
|---|---|---|---|---|---|---|---|
| .88 | .1563E-02 | 1.38 | .2539E-02 | 1.88 | .3516E-02 | 2.38 | .4639E-02 |
| 2.88 | .5713E-02 | 3.38 | .6787E-02 | 4.38 | .8887E-02 | 4.88 | .9766E-02 |
| 5.38 | .1065E-01 | 5.88 | .1157E-01 | 6.38 | .1240E-01 | 6.88 | .1328E-01 |
| 7.38 | .1397E-01 | 7.88 | .1470E-01 | 8.38 | .1553E-01 | 9.38 | .1694E-01 |
| 9.88 | .1748E-01 | 12.88 | .2197E-01 | 13.38 | .2222E-01 | 13.88 | .2251E-01 |
| 14.38 | .2275E-01 | 14.88 | .2290E-01 | 85.72 | .2022E-01 | 86.22 | .2061E-01 |
| 86.70 | .2100E-01 | 87.22 | .2144E-01 | 87.72 | .2178E-01 | 88.22 | .2212E-01 |
| 89.70 | .2310E-01 | 92.70 | .2568E-01 | 94.20 | .2612E-01 | 95.70 | .2676E-01 |
| 97.20 | .2734E-01 | 98.70 | .2778E-01 | 103.70 | .2993E-01 | 105.70 | .3018E-01 |
| 107.70 | .3047E-01 | 109.70 | .3066E-01 | 112.70 | .3145E-01 | 114.70 | .3140E-01 |
| 116.70 | .3145E-01 | 118.70 | .3154E-01 | 122.70 | .3232E-01 | 124.70 | .3232E-01 |
| 126.70 | .3237E-01 | 128.70 | .3232E-01 | 132.70 | .3286E-01 | 134.20 | .3272E-01 |
| 136.18 | .3296E-01 | 140.18 | .3232E-01 | 140.68 | .3125E-01 | 141.18 | .3008E-01 |
| 141.68 | .2905E-01 | 142.18 | .2793E-01 | 142.68 | .2686E-01 | 143.18 | .2583E-01 |
| 143.68 | .2485E-01 | 144.18 | .2393E-01 | 144.70 | .2295E-01 | 145.18 | .2217E-01 |
| 145.68 | .2129E-01 | 146.18 | .2051E-01 | 146.70 | .1973E-01 | 147.68 | .1836E-01 |
| 151.18 | .1431E-01 | 152.68 | .1343E-01 | 154.18 | .1240E-01 | 155.68 | .1143E-01 |
| 157.18 | .1060E-01 | 158.68 | .9863E-02 | 162.18 | .8496E-02 | 162.68 | .8301E-02 |
| 163.18 | .8154E-02 | 163.68 | .8057E-02 | 164.18 | .7861E-02 | 164.68 | .7715E-02 |
| 227.65 | .1001E-01 | 228.17 | .9766E-02 | 228.67 | .9521E-02 | 229.17 | .9277E-02 |
| 229.65 | .9131E-02 | 230.15 | .8887E-02 | 231.65 | .8252E-02 | 233.15 | .7666E-02 |
| 234.65 | .7178E-02 | 238.17 | .6348E-02 | 241.15 | .5957E-02 | 244.15 | .5566E-02 |
| 249.15 | .4932E-02 | 252.15 | .4785E-02 | 257.15 | .4492E-02 | 260.15 | .4346E-02 |
| 263.15 | .4346E-02 | 269.15 | .4248E-02 | 272.15 | .4199E-02 | 277.13 | .4199E-02 |
| 280.15 | .4150E-02 | 283.13 | .4150E-02 | 286.13 | .4102E-02 | 291.13 | .4102E-02 |

EXPERIMENT DATA: HPLC grab samples
Cmax = .1419E+00

| T(min) | C | T(min) | C | T(min) | C | T(min) | C |
|---|---|---|---|---|---|---|---|
| 7.27 | .5688E-01 | 12.28 | .9520E-01 | 13.28 | .9850E-01 | 87.27 | .8345E-01 |
| 134.26 | .1464E+00 | 147.24 | .7545E-01 | 161.24 | .2754E-01 | 162.29 | .2639E-01 |
| 163.26 | .2428E-01 | 228.28 | .2822E-01 | 229.28 | .2715E-01 | 230.30 | .2598E-01 |
| 290.30 | .2678E-02 | | | | | | |

Run AEI210: Anthracene/Eustis/30:70/Interrupt
28Apr94

Ms =   .998 g   V  =  10.570 mL       Kp  =  18.490 mL/g
C0 =   .000   Ss0 =   .000        Sr0 =   .000
DV1 =   .180 mL   DV2 =   .110 mL      Mr =  1.000
Kr =  3.050 mL   kr =  .8800E-02 min^-1   Fr =   .580

REACTOR OPERATION:

| Time Start | Flow | Cin |
|---|---|---|
| .0 | .895 | 1. |
| 27.0 | .000 | 1. |
| 87.0 | .895 | 1. |
| 163.0 | .984 | 0. |
| 196.0 | .000 | 0. |
| 262.0 | .984 | 0. |

EXPERIMENT DATA: In-Line Detector
Baseline: Yb = .3873E-05 T + .1912E-02
Response Curve: Linear
Ymax = .3753E-01

| T(min) | Y | T(min) | Y | T(min) | Y | T(min) | Y |
|---|---|---|---|---|---|---|---|
| 1.33 | .2490E-02 | 2.33 | .4053E-02 | 3.33 | .5713E-02 | 4.33 | .7324E-02 |
| 5.33 | .8887E-02 | 6.33 | .1040E-01 | 7.33 | .1191E-01 | 8.33 | .1328E-01 |
| 9.33 | .1460E-01 | 12.83 | .2022E-01 | 14.33 | .2100E-01 | 15.83 | .2188E-01 |
| 17.33 | .2280E-01 | 18.82 | .2368E-01 | 22.83 | .2798E-01 | 24.32 | .2837E-01 |
| 24.83 | .2856E-01 | 25.33 | .2871E-01 | 25.83 | .2891E-01 | 26.32 | .2910E-01 |
| 26.82 | .2930E-01 | 88.23 | .2783E-01 | 88.73 | .2808E-01 | 89.23 | .2837E-01 |
| 89.73 | .2866E-01 | 90.23 | .2891E-01 | 90.73 | .2915E-01 | 94.23 | .3091E-01 |
| 96.23 | .3140E-01 | 98.23 | .3189E-01 | 100.73 | .3272E-01 | 105.23 | .3457E-01 |
| 107.73 | .3491E-01 | 110.22 | .3530E-01 | 116.22 | .3613E-01 | 118.73 | .3618E-01 |
| 124.22 | .3745E-01 | 126.72 | .3750E-01 | 129.23 | .3765E-01 | 135.72 | .3789E-01 |
| 138.22 | .3794E-01 | 144.22 | .3867E-01 | 146.72 | .3867E-01 | 149.22 | .3867E-01 |
| 156.22 | .3877E-01 | 158.72 | .3877E-01 | 164.72 | .3774E-01 | 165.70 | .3594E-01 |
| 166.70 | .3418E-01 | 167.70 | .3252E-01 | 168.72 | .3086E-01 | 169.70 | .2935E-01 |
| 170.70 | .2783E-01 | 174.20 | .2246E-01 | 175.70 | .2144E-01 | 177.20 | .2036E-01 |
| 178.70 | .1924E-01 | 180.20 | .1807E-01 | 183.70 | .1436E-01 | 185.70 | .1357E-01 |
| 187.70 | .1279E-01 | 189.70 | .1206E-01 | 193.20 | .1045E-01 | 193.70 | .1040E-01 |
| 194.20 | .1030E-01 | 194.70 | .1021E-01 | 195.20 | .1016E-01 | 195.70 | .1011E-01 |
| 262.22 | .1240E-01 | 262.70 | .1187E-01 | 263.20 | .1152E-01 | 263.70 | .1133E-01 |
| 264.20 | .1113E-01 | 264.70 | .1094E-01 | 266.20 | .1040E-01 | 267.70 | .9912E-02 |
| 269.20 | .9424E-02 | 273.20 | .7568E-02 | 276.20 | .7080E-02 | 279.20 | .6787E-02 |
| 283.20 | .6152E-02 | 286.70 | .6055E-02 | 289.70 | .5908E-02 | 295.70 | .4883E-02 |
| 298.70 | .4834E-02 | 304.70 | .4736E-02 | 307.70 | .4736E-02 | 312.68 | .4150E-02 |

```
315.68 .4199E-02 318.68 .4199E-02 323.68 .4199E-02 326.68 .4248E-02
329.68 .4199E-02 334.68 .3906E-02 337.68 .3906E-02 342.68 .3955E-02
345.67 .3955E-02 348.68 .4004E-02 353.67 .3760E-02 356.67 .3760E-02
```

EXPERIMENT DATA: HPLC grab samples
Cmax = .2960E+00

| T (min) | C | T(min) | C | T(min) | C | T(min) | C |
|---|---|---|---|---|---|---|---|
| 15.27 | .1553E+00 | 24.29 | .2065E+00 | 25.28 | .2126E+00 | 26.25 | .2123E+00 |
| 89.29 | .2001E+00 | 90.26 | .2079E+00 | 95.27 | .2258E+00 | 127.27 | .2853E+00 |
| 176.25 | .1456E+00 | 193.25 | .5970E-01 | 194.25 | .6019E-01 | 195.27 | .5720E-01 |
| 263.25 | .6331E-01 | 264.23 | .5883E-01 | 265.24 | .5785E-01 | 325.25 | .8301E-02 |

Run AEI220: Anthracene/Eustis/30:70/Interrupt
14Jun94

$Ms$ = 4.000 g  $V$ = 43.860 mL    $Kp$ = 18.490 mL/g
$C0$ = .000    $Ss0$ = .000      $Sr0$ = .000
$DV1$ = .180 mL  $DV2$ = .110 mL    $Mr$ = 4.000
$Kr$ = 3.050 mL  $kr$ = .8800E-02 min^-1  $Fr$ = .580

REACTOR OPERATION:

| Time Start | Flow | Cin |
|---|---|---|
| .0 | 1.466 | 1. |
| 2.2 | 1.700 | 1. |
| 3.0 | 1.918 | 1. |
| 50.0 | .000 | 0. |
| 115.0 | 1.888 | 1. |
| 204.0 | 2.110 | 0. |
| 205.0 | 2.042 | 0. |
| 290.0 | .000 | 0. |
| 365.0 | 2.042 | 0. |

EXPERIMENT DATA: In-Line Detector
Baseline: $Yb$ = .8749E-05 T + .2804E-02
Response Curve:
Ymax = .2861E-01

| T(min) | Y | T(min) | Y | T(min) | Y | T(min) | Y |
|---|---|---|---|---|---|---|---|
| 1.08 | .2881E-02 | 3.08 | .3906E-02 | 4.58 | .4883E-02 | 6.08 | .5762E-02 |
| 7.58 | .6689E-02 | 9.08 | .7617E-02 | 13.58 | .1084E-01 | 15.58 | .1157E-01 |
| 17.58 | .1235E-01 | 19.58 | .1318E-01 | 23.58 | .1538E-01 | 25.58 | .1587E-01 |
| 27.57 | .1650E-01 | 29.58 | .1704E-01 | 33.57 | .1870E-01 | 35.57 | .1909E-01 |

```
37.57 .1953E-01   39.57 .1997E-01   43.57 .2148E-01   47.07 .2188E-01
47.57 .2197E-01   48.07 .2202E-01   48.57 .2212E-01   49.07 .2222E-01
49.57 .2231E-01  115.88 .2144E-01  116.38 .2158E-01  116.88 .2173E-01
117.38 .2183E-01  117.88 .2192E-01  118.38 .2197E-01  121.88 .2271E-01
125.37 .2378E-01  127.37 .2402E-01  129.87 .2432E-01  134.87 .2539E-01
139.87 .2588E-01  144.87 .2671E-01  149.87 .2705E-01  155.87 .2808E-01
159.87 .2832E-01  164.87 .2891E-01  169.85 .2910E-01  174.85 .2969E-01
179.85 .2983E-01  184.85 .3013E-01  189.85 .3023E-01  194.85 .3071E-01
199.85 .3086E-01  204.85 .3106E-01  206.35 .3008E-01  207.85 .2896E-01
209.85 .2759E-01  213.35 .2515E-01  215.33 .2417E-01  217.85 .2305E-01
220.33 .2192E-01  223.83 .2017E-01  227.33 .1914E-01  230.83 .1812E-01
234.83 .1655E-01  239.83 .1558E-01  244.83 .1455E-01  249.83 .1377E-01
254.83 .1289E-01  261.83 .1216E-01  266.83 .1143E-01  275.32 .1055E-01
281.82 .1016E-01  287.32 .9814E-02  287.82 .9766E-02  288.32 .9717E-02
288.82 .9766E-02  289.32 .9766E-02  289.82 .9717E-02  366.25 .1084E-01
366.75 .1069E-01  367.25 .1069E-01  367.75 .1060E-01  368.25 .1050E-01
368.75 .1060E-01  371.75 .1030E-01  374.75 .9912E-02  379.75 .9521E-02
384.75 .9229E-02  388.75 .8984E-02  393.75 .8887E-02  398.75 .8594E-02
403.75 .8496E-02  408.73 .8301E-02  413.73 .8203E-02  418.73 .8154E-02
423.73 .8057E-02  428.73 .7959E-02  433.73 .7959E-02  438.73 .7959E-02
443.73 .7910E-02  450.22 .7813E-02  456.72 .7861E-02  463.72 .7861E-02
```

EXPERIMENT DATA: HPLC grab samples
Cmax = .1000E+01

| T (min) | C | T(min) | C | T(min) | C | T(min) | C |
|---|---|---|---|---|---|---|---|
| 26.16 | .4805E+00 | 47.14 | .7545E+00 | 48.14 | .7086E+00 | 49.15 | .7303E+00 |
| 116.15 | .6266E+00 | 117.15 | .6467E+00 | 118.15 | .6980E+00 | 202.15 | .1016E+01 |
| 245.14 | .3180E+00 | 284.14 | .1453E+00 | 285.15 | .1543E+00 | 286.15 | .1406E+00 |
| 366.15 | .1724E+00 | 367.14 | .1595E+00 | 368.15 | .1587E+00 | 462.15 | .3539E-01 |

Run AEI240: Anthracene/Eustis/30:70/Interrupt
11May94

```
Ms  =  4.060 g   V  = 43.600 mL       Kp  = 18.490 mL/g
C0  =   .000    Ss0 =   .000       Sr0 =   .000
DV1 =   .180 mL  DV2 =   .110 mL        Mr  =  4.000
Kr  =  3.050 mL  kr  = .8800E-02 min^-1  Fr  =   .580
```

REACTOR OPERATION:

| Time Start | Flow | Cin |
|---|---|---|
| .0 | .849 | 1. |

| | | |
|---|---|---|
| 123.0 | .000 | 1. |
| 186.0 | .849 | 1. |
| 362.0 | .928 | 0. |
| 367.9 | .879 | 0. |
| 494.0 | .000 | 0. |
| 617.0 | .879 | 0. |

EXPERIMENT DATA: In-Line Detector
Baseline: $Yb = .1343E-05\ T + .3547E-02$
Response Curve: Linear
$Ymax = .3041E-01$

| T(min) | Y | T(min) | Y | T(min) | Y | T(min) | Y |
|---|---|---|---|---|---|---|---|
| 1.42 | .3369E-02 | 5.42 | .4346E-02 | 9.42 | .5859E-02 | 15.40 | .7813E-02 |
| 19.42 | .8545E-02 | 23.40 | .9424E-02 | 30.40 | .1148E-01 | 34.40 | .1226E-01 |
| 38.40 | .1279E-01 | 45.40 | .1436E-01 | 49.40 | .1484E-01 | 53.40 | .1533E-01 |
| 60.40 | .1675E-01 | 64.40 | .1738E-01 | 68.39 | .1792E-01 | 75.39 | .1885E-01 |
| 80.39 | .1924E-01 | 84.39 | .1963E-01 | 96.39 | .2056E-01 | 105.39 | .2212E-01 |
| 112.37 | .2261E-01 | 113.39 | .2266E-01 | 114.39 | .2271E-01 | 120.37 | .2334E-01 |
| 121.37 | .2349E-01 | 122.37 | .2358E-01 | 188.75 | .2251E-01 | 189.75 | .2261E-01 |
| 190.74 | .2271E-01 | 191.74 | .2280E-01 | 192.74 | .2310E-01 | 193.74 | .2315E-01 |
| 204.74 | .2407E-01 | 209.74 | .2437E-01 | 215.74 | .2495E-01 | 222.74 | .2568E-01 |
| 230.74 | .2593E-01 | 239.74 | .2627E-01 | 245.72 | .2690E-01 | 251.72 | .2739E-01 |
| 260.72 | .2749E-01 | 269.72 | .2773E-01 | 279.72 | .2832E-01 | 286.70 | .2852E-01 |
| 294.70 | .2871E-01 | 309.70 | .2935E-01 | 319.70 | .2944E-01 | 334.69 | .2983E-01 |
| 349.69 | .3023E-01 | 361.69 | .3052E-01 | 366.69 | .2974E-01 | 369.69 | .2886E-01 |
| 375.67 | .2695E-01 | 380.67 | .2593E-01 | 384.67 | .2500E-01 | 392.67 | .2300E-01 |
| 396.67 | .2236E-01 | 399.67 | .2183E-01 | 405.67 | .2056E-01 | 410.67 | .2002E-01 |
| 414.67 | .1948E-01 | 420.67 | .1826E-01 | 425.67 | .1782E-01 | 429.67 | .1733E-01 |
| 437.65 | .1636E-01 | 442.65 | .1592E-01 | 452.65 | .1475E-01 | 458.65 | .1440E-01 |
| 465.65 | .1387E-01 | 473.64 | .1294E-01 | 482.64 | .1250E-01 | 483.64 | .1235E-01 |
| 484.64 | .1235E-01 | 491.64 | .1167E-01 | 492.64 | .1162E-01 | 493.64 | .1162E-01 |
| 618.39 | .1270E-01 | 619.39 | .1265E-01 | 620.39 | .1255E-01 | 621.39 | .1250E-01 |
| 622.39 | .1240E-01 | 623.40 | .1231E-01 | 630.39 | .1172E-01 | 637.39 | .1133E-01 |
| 645.39 | .1084E-01 | 654.39 | .1021E-01 | 665.37 | .9619E-02 | 674.37 | .9473E-02 |
| 684.37 | .8984E-02 | 693.37 | .8740E-02 | 704.37 | .8350E-02 | 714.37 | .8203E-02 |
| 724.35 | .7715E-02 | 736.35 | .7520E-02 | 744.35 | .7422E-02 | 755.35 | .7178E-02 |
| 767.34 | .6982E-02 | 774.34 | .6934E-02 | 785.34 | .6738E-02 | 795.34 | .6641E-02 |

EXPERIMENT DATA: HPLC grab samples
$Cmax = .1382E+00$

| T (min) | C | T(min) | C | T(min) | C | T(min) | C |
|---|---|---|---|---|---|---|---|
| 62.34 | .6104E-01 | 119.30 | .9208E-01 | 120.28 | .9330E-01 | 121.30 | .9318E-01 |
| 188.27 | .8329E-01 | 189.32 | .8237E-01 | 190.32 | .8459E-01 | 333.32 | .1173E+00 |
| 353.31 | .1203E+00 | 451.31 | .4749E-01 | 490.30 | .3498E-01 | 491.29 | .3448E-01 |

492.31 .3319E-01  618.31 .3708E-01  619.33 .3740E-01  620.33 .3548E-01
796.30 .1115E-01

Run AEP200: Anthracene/Eustis/30:70/Flow-rate variation
11Apr94

Ms = .780 g  V = 6.200 mL      Kp = 18.490 mL/g
C0 = .000   Ss0 = .000      Sr0 = .000
DV1 = .180 mL  DV2 = .110 mL      Mr = 1.000
Kr = 3.050 mL  kr = .8800E-02 min^-1  Fr = .580

REACTOR OPERATION:

| Time Start | Flow | Cin |
|---|---|---|
| .0 | 1.840 | 1. |
| 32.0 | .000 | 0. |
| 34.0 | 1.490 | 0. |
| 76.0 | .960 | 1. |
| 127.0 | .590 | 0. |
| 220.0 | 1.970 | 0. |

EXPERIMENT DATA: In-Line Detector
Baseline: Yb = .1024E-04 T + .1713E-02
Response Curve: Linear
Ymax = .3137E-01

| T(min) | Y | T(min) | Y | T(min) | Y | T(min) | Y |
|---|---|---|---|---|---|---|---|
| .55 | .2881E-02 | 1.04 | .4883E-02 | 1.55 | .7275E-02 | 2.04 | .9619E-02 |
| 2.54 | .1172E-01 | 3.04 | .1372E-01 | 3.54 | .1553E-01 | 4.04 | .1704E-01 |
| 4.55 | .1851E-01 | 5.54 | .2100E-01 | 8.04 | .2617E-01 | 9.54 | .2720E-01 |
| 11.04 | .2813E-01 | 15.04 | .3023E-01 | 17.54 | .3086E-01 | 21.54 | .3198E-01 |
| 23.54 | .3203E-01 | 28.54 | .3257E-01 | 34.54 | .3184E-01 | 35.04 | .2983E-01 |
| 35.54 | .2788E-01 | 36.04 | .2603E-01 | 36.54 | .2427E-01 | 37.02 | .2271E-01 |
| 37.54 | .2124E-01 | 38.54 | .1860E-01 | 39.52 | .1641E-01 | 41.54 | .1226E-01 |
| 43.54 | .1045E-01 | 45.54 | .8838E-02 | 47.54 | .7520E-02 | 49.52 | .6543E-02 |
| 52.02 | .5420E-02 | 55.02 | .4834E-02 | 58.02 | .4297E-02 | 62.02 | .3955E-02 |
| 65.02 | .3760E-02 | 69.52 | .3516E-02 | 72.52 | .3369E-02 | 76.02 | .3320E-02 |
| 77.02 | .4199E-02 | 77.52 | .5127E-02 | 78.52 | .7568E-02 | 79.52 | .1001E-01 |
| 80.52 | .1211E-01 | 81.52 | .1421E-01 | 82.52 | .1602E-01 | 83.50 | .1768E-01 |
| 86.52 | .2290E-01 | 88.00 | .2393E-01 | 89.52 | .2500E-01 | 91.00 | .2607E-01 |
| 92.50 | .2700E-01 | 97.00 | .2935E-01 | 100.00 | .2993E-01 | 103.00 | .3057E-01 |
| 107.50 | .3189E-01 | 110.50 | .3213E-01 | 113.50 | .3247E-01 | 119.00 | .3320E-01 |
| 123.00 | .3330E-01 | 126.50 | .3374E-01 | 128.00 | .3350E-01 | 129.00 | .3252E-01 |

```
130.00 .3106E-01 131.00 .2959E-01 131.99 .2813E-01 133.00 .2671E-01
134.49 .2476E-01 135.99 .2305E-01 137.49 .2139E-01 140.49 .1738E-01
142.49 .1650E-01 144.50 .1548E-01 146.49 .1450E-01 148.49 .1353E-01
150.49 .1265E-01 153.49 .1084E-01 156.49 .1025E-01 159.49 .9521E-02
162.49 .8838E-02 167.49 .7715E-02 171.49 .7324E-02 174.99 .7031E-02
179.99 .6250E-02 184.47 .6006E-02 188.97 .5713E-02 192.47 .5371E-02
196.97 .5322E-02 201.47 .5225E-02 204.47 .4932E-02 208.97 .4883E-02
213.47 .4785E-02 216.97 .4639E-02 219.97 .4688E-02 222.47 .4443E-02
224.97 .4395E-02 226.97 .4199E-02 228.95 .4150E-02 231.97 .4150E-02
```

EXPERIMENT DATA: HPLC grab samples
Cmax = .2529E+00

| T (min) | C | T(min) | C | T(min) | C | T(min) | C |
|---|---|---|---|---|---|---|---|
| 9.14 | .2026E+00 | 22.14 | .2295E+00 | 37.18 | .1610E+00 | 71.16 | .6771E-02 |
| 92.28 | .1837E+00 | 122.29 | .2273E+00 | 143.40 | .1027E+00 | 197.46 | .1315E-01 |

Run NEI100: Naphthalene/Eustis/0:100/Interrupt
16Nov94

$Ms$ = 1.010 g   $V$ = 6.110 mL       $Kp$ = 3.293 mL/g
$C0$ = .000    $Ss0$ = .000      $Sr0$ = .000
$DV1$ = .180 mL  $DV2$ = .110 mL      $Mr$ = 1.000
$Kr$ = 1.240 mL  $kr$ = .8110E+00 min^-1  $Fr$ = .562

REACTOR OPERATION:

| Time Start | Flow | Cin |
|---|---|---|
| .0 | 1.010 | 1. |
| 35.0 | .000 | 0. |
| 95.0 | 1.010 | 1. |
| 112.0 | 1.030 | 0. |
| 132.0 | .000 | 0. |
| 192.0 | 1.030 | 0. |

EXPERIMENT DATA: In-Line Detector
Baseline: Yb = .2844E-05 T + .1466E-02
Response Curve: Linear
Ymax = .3667E-01

| T(min) | Y | T(min) | Y | T(min) | Y | T(min) | Y |
|---|---|---|---|---|---|---|---|
| .43 | .1904E-02 | .93 | .2930E-02 | 1.43 | .4736E-02 | 1.93 | .6641E-02 |
| 2.43 | .8496E-02 | 2.93 | .1025E-01 | 3.43 | .1191E-01 | 3.95 | .1348E-01 |
| 4.43 | .1494E-01 | 4.93 | .1641E-01 | 5.43 | .1773E-01 | 5.93 | .1890E-01 |

| 6.43 | .2002E-01 | 6.93 | .2109E-01 | 7.43 | .2207E-01 | 7.93 | .2315E-01 |
| 8.93 | .2476E-01 | 9.93 | .2622E-01 | 11.93 | .2949E-01 | 12.93 | .3008E-01 |
| 13.93 | .3071E-01 | 14.93 | .3130E-01 | 15.93 | .3189E-01 | 16.93 | .3242E-01 |
| 17.93 | .3291E-01 | 19.43 | .3350E-01 | 22.43 | .3467E-01 | 23.93 | .3481E-01 |
| 25.43 | .3516E-01 | 26.93 | .3540E-01 | 28.43 | .3569E-01 | 29.93 | .3594E-01 |
| 32.43 | .3652E-01 | 32.93 | .3643E-01 | 33.43 | .3638E-01 | 33.93 | .3643E-01 |
| 34.43 | .3643E-01 | 34.93 | .3648E-01 | 98.27 | .3506E-01 | 98.77 | .3506E-01 |
| 99.27 | .3511E-01 | 99.77 | .3521E-01 | 102.77 | .3594E-01 | 103.27 | .3599E-01 |
| 104.27 | .3604E-01 | 105.27 | .3613E-01 | 106.27 | .3628E-01 | 107.77 | .3648E-01 |
| 108.77 | .3657E-01 | 109.77 | .3677E-01 | 112.27 | .3706E-01 | 112.77 | .3618E-01 |
| 113.27 | .3428E-01 | 113.77 | .3232E-01 | 114.27 | .3047E-01 | 114.77 | .2861E-01 |
| 115.27 | .2695E-01 | 115.77 | .2539E-01 | 116.27 | .2388E-01 | 116.77 | .2251E-01 |
| 117.27 | .2124E-01 | 117.77 | .2002E-01 | 118.27 | .1890E-01 | 118.77 | .1782E-01 |
| 119.27 | .1685E-01 | 119.77 | .1592E-01 | 120.77 | .1401E-01 | 121.77 | .1294E-01 |
| 122.77 | .1196E-01 | 124.77 | .1030E-01 | 125.77 | .9131E-02 | 126.77 | .8350E-02 |
| 128.27 | .7324E-02 | 128.77 | .7031E-02 | 129.27 | .6738E-02 | 129.77 | .6494E-02 |
| 131.27 | .5811E-02 | 131.75 | .5322E-02 | 192.25 | .8984E-02 | 192.75 | .7422E-02 |
| 193.25 | .6982E-02 | 193.75 | .6641E-02 | 194.25 | .6348E-02 | 194.75 | .6055E-02 |
| 195.75 | .5566E-02 | 196.75 | .5127E-02 | 197.75 | .4736E-02 | 198.75 | .4443E-02 |
| 199.75 | .4102E-02 | 201.75 | .3662E-02 | 203.25 | .3418E-02 | 204.75 | .3174E-02 |
| 206.25 | .2979E-02 | 207.75 | .2832E-02 | 209.25 | .2637E-02 | 212.25 | .2490E-02 |
| 213.75 | .2344E-02 | 215.25 | .2246E-02 | 216.75 | .2148E-02 | 218.75 | .2100E-02 |

EXPERIMENT DATA: HPLC grab samples
Cmax = .1630E+02

| T (min) | C | T(min) | C | T(min) | C | T(min) | C |
| 4.20 | .5740E+01 | 11.17 | .1293E+02 | 33.13 | .1621E+02 | 96.16 | .1512E+02 |
| 98.18 | .1536E+02 | 108.65 | .1565E+02 | 121.17 | .4929E+01 | 131.19 | .1805E+01 |
| 193.17 | .2501E+01 | 219.16 | .0000E+00 | 239.67 | .0000E+00 | | |

Run NEP100: Naphthalene/Eustis/0:100 MeOH/H2O/flow-rate variation
19Nov93

Ms = 1.020 g   V = 6.060 mL       Kp = 3.293 mL/g
C0 = .000   Ss0 = .000       Sr0 = .000
DV1 = .180 mL   DV2 = .110 mL       Mr = 1.000
Kr = 1.240 mL   kr = .8110E-01 min^-1   Fr = .562

REACTOR OPERATION:
Time Start   Flow   Cin
     .0   1.000   1.

| 52.5 | 1.030 | 0. |
|---|---|---|
| 65.0 | .200 | 0. |
| 95.0 | 1.030 | 0. |
| 123.0 | .720 | 1. |
| 146.0 | .220 | 1. |
| 172.0 | .720 | 1. |
| 202.0 | .540 | 0. |

EXPERIMENT DATA: In-Line Detector
Baseline: $Yb = .4388E-05\ T + .1074E-02$
Response Curve: Linear
$Ymax = .3975E-01$

| T(min) | Y | T(min) | Y | T(min) | Y | T(min) | Y |
|---|---|---|---|---|---|---|---|
| .93 | .2686E-02 | 1.93 | .6787E-02 | 2.93 | .1084E-01 | 4.43 | .1616E-01 |
| 5.93 | .2056E-01 | 7.93 | .2515E-01 | 9.93 | .2861E-01 | 14.43 | .3389E-01 |
| 16.43 | .3525E-01 | 19.93 | .3696E-01 | 25.43 | .3853E-01 | 29.93 | .3921E-01 |
| 35.43 | .3999E-01 | 39.92 | .4009E-01 | 45.42 | .4043E-01 | 47.42 | .4038E-01 |
| 49.92 | .4038E-01 | 52.42 | .4082E-01 | 53.42 | .3901E-01 | 54.42 | .3442E-01 |
| 55.42 | .3032E-01 | 56.92 | .2500E-01 | 58.42 | .2065E-01 | 60.42 | .1567E-01 |
| 62.92 | .1235E-01 | 63.92 | .1113E-01 | 64.92 | .1001E-01 | 65.92 | .1001E-01 |
| 67.92 | .1016E-01 | 69.92 | .9912E-02 | 73.42 | .8887E-02 | 75.42 | .8594E-02 |
| 79.92 | .8252E-02 | 85.40 | .7813E-02 | 87.90 | .7715E-02 | 89.90 | .7520E-02 |
| 92.90 | .7227E-02 | 94.40 | .6885E-02 | 96.90 | .5908E-02 | 100.90 | .4004E-02 |
| 105.40 | .2979E-02 | 109.90 | .2344E-02 | 115.40 | .1855E-02 | 117.90 | .1758E-02 |
| 121.40 | .1709E-02 | 122.38 | .1660E-02 | 123.40 | .2344E-02 | 124.90 | .4492E-02 |
| 125.90 | .7422E-02 | 126.90 | .1035E-01 | 128.38 | .1426E-01 | 129.90 | .1777E-01 |
| 133.38 | .2476E-01 | 135.38 | .2715E-01 | 137.38 | .2930E-01 | 139.38 | .3130E-01 |
| 144.38 | .3433E-01 | 145.38 | .3481E-01 | 146.38 | .3496E-01 | 147.38 | .3491E-01 |
| 148.38 | .3486E-01 | 155.38 | .3599E-01 | 157.38 | .3599E-01 | 159.88 | .3608E-01 |
| 165.88 | .3652E-01 | 167.37 | .3652E-01 | 168.88 | .3662E-01 | 174.87 | .3765E-01 |
| 176.88 | .3799E-01 | 179.37 | .3848E-01 | 185.37 | .3936E-01 | 189.37 | .3975E-01 |
| 192.87 | .3999E-01 | 195.37 | .3999E-01 | 197.87 | .4014E-01 | 199.87 | .4014E-01 |
| 202.37 | .4033E-01 | 203.37 | .3975E-01 | 204.87 | .3672E-01 | 206.37 | .3350E-01 |
| 207.87 | .3047E-01 | 209.87 | .2681E-01 | 213.85 | .2036E-01 | 215.87 | .1826E-01 |
| 217.87 | .1631E-01 | 222.85 | .1260E-01 | 227.85 | .1006E-01 | 231.35 | .7813E-02 |
| 235.35 | .6934E-02 | 239.85 | .5811E-02 | 245.35 | .4980E-02 | 249.85 | .4297E-02 |
| 255.35 | .3613E-02 | 259.83 | .3271E-02 | 265.33 | .3027E-02 | 269.83 | .2832E-02 |
| 275.33 | .2588E-02 | 279.83 | .2441E-02 | 285.33 | .2344E-02 | 289.83 | .2295E-02 |

EXPERIMENT DATA: HPLC grab samples
$Cmax = .1000E+01$

| T (min) | C | T(min) | C |
|---|---|---|---|
| 121.17 | .0000E+00 | 286.29 | .0000E+00 |

Run YEI100: Pyrene/Eustis/50:50/Interrupt
24Feb94

$Ms$ = 2.020 g  $V$ = 5.760 mL   $Kp$ = 1.929 mL/g
$C0$ = .000  $Ss0$ = .000   $Sr0$ = .000
$DV1$ = .180 mL  $DV2$ = .110 mL   $Mr$ = 1.000
$Kr$ = .750 mL  $kr$ = .2400E+00 min^-1  $Fr$ = .580

REACTOR OPERATION:

| Time Start | Flow | Cin |
|---|---|---|
| .0 | 1.010 | 1. |
| 15.0 | .000 | 0. |
| 76.0 | 1.010 | 1. |
| 122.0 | 1.030 | 0. |
| 144.0 | .000 | 0. |
| 210.0 | 1.030 | 0. |

EXPERIMENT DATA: In-Line Detector
Baseline: $Yb$ = .6482E-06 T + .9853E-03
Response Curve: Linear
$Ymax$ = .5164E-01

| T(min) | Y | T(min) | Y | T(min) | Y | T(min) | Y |
|---|---|---|---|---|---|---|---|
| .63 | .1465E-02 | 1.12 | .3906E-02 | 1.63 | .7031E-02 | 2.13 | .1011E-01 |
| 2.62 | .1299E-01 | 3.13 | .1572E-01 | 3.62 | .1821E-01 | 4.12 | .2056E-01 |
| 4.62 | .2271E-01 | 5.13 | .2476E-01 | 5.63 | .2666E-01 | 6.62 | .2998E-01 |
| 7.62 | .3286E-01 | 8.62 | .3535E-01 | 9.62 | .3755E-01 | 11.62 | .4194E-01 |
| 12.12 | .4243E-01 | 12.62 | .4297E-01 | 13.12 | .4390E-01 | 13.62 | .4395E-01 |
| 14.12 | .4439E-01 | 14.62 | .4482E-01 | 76.65 | .4458E-01 | 77.15 | .4497E-01 |
| 77.65 | .4546E-01 | 78.15 | .4585E-01 | 78.65 | .4624E-01 | 79.15 | .4663E-01 |
| 81.65 | .4819E-01 | 83.15 | .4888E-01 | 84.65 | .4932E-01 | 86.15 | .4976E-01 |
| 87.63 | .5024E-01 | 89.15 | .5059E-01 | 91.63 | .5132E-01 | 93.65 | .5147E-01 |
| 95.63 | .5166E-01 | 97.63 | .5176E-01 | 99.63 | .5190E-01 | 101.63 | .5210E-01 |
| 103.63 | .5210E-01 | 105.63 | .5215E-01 | 107.63 | .5220E-01 | 109.63 | .5225E-01 |
| 112.13 | .5244E-01 | 114.13 | .5239E-01 | 116.13 | .5239E-01 | 118.13 | .5239E-01 |
| 119.63 | .5249E-01 | 122.13 | .5259E-01 | 123.13 | .4981E-01 | 123.63 | .4688E-01 |
| 124.13 | .4390E-01 | 124.63 | .4116E-01 | 125.13 | .3857E-01 | 125.63 | .3613E-01 |
| 126.13 | .3384E-01 | 126.63 | .3174E-01 | 127.13 | .2974E-01 | 127.63 | .2783E-01 |
| 128.63 | .2446E-01 | 129.63 | .2153E-01 | 131.13 | .1641E-01 | 132.13 | .1499E-01 |
| 133.13 | .1348E-01 | 134.13 | .1216E-01 | 135.13 | .1094E-01 | 136.13 | .9863E-02 |
| 137.13 | .8936E-02 | 138.13 | .8057E-02 | 139.13 | .7324E-02 | 141.13 | .6104E-02 |
| 141.62 | .6055E-02 | 142.13 | .5957E-02 | 142.63 | .5713E-02 | 143.13 | .5518E-02 |
| 143.62 | .5322E-02 | 210.57 | .7422E-02 | 211.07 | .7080E-02 | 211.57 | .6689E-02 |
| 212.07 | .6396E-02 | 212.57 | .6055E-02 | 213.07 | .5762E-02 | 214.57 | .5078E-02 |
| 216.57 | .4248E-02 | 218.57 | .3174E-02 | 221.07 | .2734E-02 | 223.57 | .2393E-02 |

```
226.07 .2100E-02  228.57 .1904E-02  232.07 .1855E-02  234.57 .1807E-02
237.07 .1709E-02  239.57 .1563E-02  243.55 .1416E-02  246.05 .1367E-02
248.57 .1318E-02  252.55 .1367E-02  255.05 .1367E-02  257.55 .1318E-02
```

EXPERIMENT DATA: HPLC grab samples
$C_{max}$ = .8955E+01

| T (min) | C | T(min) | C | T(min) | C | T(min) | C |
|---|---|---|---|---|---|---|---|
| 7.21 | .5186E+01 | 12.26 | .7245E+01 | 13.22 | .7451E+01 | 14.23 | .7551E+01 |
| 77.19 | .7419E+01 | 78.24 | .7422E+01 | 83.20 | .8116E+01 | 115.25 | .9082E+01 |
| 128.21 | .4212E+01 | 137.26 | .1322E+01 | 142.22 | .8605E+00 | 143.21 | .7598E+00 |
| 211.73 | .7846E+00 | 212.72 | .7217E+00 | 213.73 | .7294E+00 | 245.25 | .6030E-01 |

Run AZI100: Anthracene/Zellwood/50:50 MeOH-$H_2O$
20Jan94

$M_s$ = .096 g  $V$ = 6.550 mL    $K_p$ = 121.690 mL/g
$C_0$ = .000  $S_{s0}$ = .000    $S_{r0}$ = .000
$DV1$ = .180 mL  $DV2$ = .110 mL    $M_r$ = 1.000
$K_r$ = .288 mL  $k_r$ = .2530E-04 min^-1  $F_r$ = .478

REACTOR OPERATION:

| Time Start | Flow | Cin |
|---|---|---|
| .0 | 1.030 | 1. |
| 35.0 | .000 | 0. |
| 135.0 | 1.020 | 1. |
| 165.0 | .000 | 0. |
| 1226.0 | .997 | 1. |
| 1261.0 | 1.030 | 0. |

EXPERIMENT DATA: In-Line Detector
Baseline: $Y_b$ = .3251E-06 T + .6357E-03
Response Curve: Equation (C-2)
$Y_{max}$ = .5654E-01

| T(min) | Y | T(min) | Y | T(min) | Y | T(min) | Y |
|---|---|---|---|---|---|---|---|
| .40 | .7810E-03 | .90 | .5469E-02 | 1.40 | .1133E-01 | 1.90 | .1650E-01 |
| 2.40 | .2095E-01 | 2.90 | .2485E-01 | 3.40 | .2822E-01 | 3.90 | .3115E-01 |
| 4.40 | .3364E-01 | 4.90 | .3584E-01 | 5.40 | .3774E-01 | 5.90 | .3936E-01 |
| 6.40 | .4082E-01 | 6.90 | .4209E-01 | 7.40 | .4321E-01 | 7.90 | .4424E-01 |
| 8.40 | .4512E-01 | 8.90 | .4595E-01 | 9.40 | .4668E-01 | 9.90 | .4731E-01 |
| 11.40 | .4976E-01 | 11.90 | .5005E-01 | 12.40 | .5029E-01 | 12.90 | .5059E-01 |
| 13.40 | .5088E-01 | 13.90 | .5117E-01 | 14.40 | .5142E-01 | 14.90 | .5166E-01 |

| | | | | | | | |
|---|---|---|---|---|---|---|---|
| 15.90 | .5215E-01 | 16.90 | .5259E-01 | 17.90 | .5293E-01 | 18.90 | .5327E-01 |
| 19.90 | .5361E-01 | 21.40 | .5420E-01 | 22.40 | .5435E-01 | 23.40 | .5449E-01 |
| 24.40 | .5469E-01 | 25.40 | .5483E-01 | 26.40 | .5503E-01 | 27.40 | .5518E-01 |
| 28.40 | .5527E-01 | 29.40 | .5547E-01 | 31.40 | .5581E-01 | 32.40 | .5586E-01 |
| 32.90 | .5586E-01 | 33.40 | .5591E-01 | 33.90 | .5596E-01 | 34.38 | .5601E-01 |
| 34.88 | .5601E-01 | 135.75 | .5488E-01 | 136.25 | .5503E-01 | 136.75 | .5513E-01 |
| 137.25 | .5523E-01 | 137.75 | .5527E-01 | 138.25 | .5537E-01 | 139.27 | .5552E-01 |
| 143.75 | .5610E-01 | 144.75 | .5615E-01 | 145.75 | .5620E-01 | 146.75 | .5625E-01 |
| 147.75 | .5630E-01 | 148.75 | .5635E-01 | 149.75 | .5640E-01 | 152.75 | .5654E-01 |
| 153.75 | .5654E-01 | 154.75 | .5654E-01 | 155.75 | .5659E-01 | 156.75 | .5664E-01 |
| 157.75 | .5664E-01 | 158.75 | .5664E-01 | 159.75 | .5664E-01 | 160.75 | .5674E-01 |
| 161.75 | .5669E-01 | 162.75 | .5669E-01 | 163.25 | .5669E-01 | 163.75 | .5674E-01 |
| 164.25 | .5674E-01 | 164.75 | .5674E-01 | 165.25 | .5669E-01 | 1226.92 | .5361E-01 |
| 1227.42 | .5366E-01 | 1227.90 | .5366E-01 | 1228.40 | .5371E-01 | 1228.90 | .5381E-01 |
| 1229.40 | .5386E-01 | 1232.90 | .5479E-01 | 1233.92 | .5483E-01 | 1234.90 | .5498E-01 |
| 1235.90 | .5508E-01 | 1236.90 | .5518E-01 | 1237.90 | .5532E-01 | 1238.90 | .5547E-01 |
| 1239.90 | .5557E-01 | 1247.40 | .5610E-01 | 1248.40 | .5625E-01 | 1249.40 | .5630E-01 |
| 1256.40 | .5659E-01 | 1257.40 | .5664E-01 | 1258.40 | .5669E-01 | 1259.40 | .5674E-01 |

EXPERIMENT DATA: HPLC grab samples
Cmax = .4424E+01

| T (min) | C | T(min) | C | T(min) | C | T(min) | C |
|---|---|---|---|---|---|---|---|
| 4.15 | .1190E+01 | 32.16 | .4229E+01 | 33.16 | .4265E+01 | 34.17 | .3901E+01 |
| 136.64 | .3672E+01 | 137.67 | .3769E+01 | 138.66 | .3800E+01 | 161.17 | .4416E+01 |
| 162.17 | .4372E+01 | 163.22 | .4430E+01 | 1227.15 | .3434E+01 | 1228.13 | .3412E+01 |
| 1229.19 | .3761E+01 | 1246.19 | .4280E+01 | | | | |

Run NZI100: Naphthalene/Zellwood/30:70 MeOH-H2O/interupt
2Feb94

Ms =   .171 g   V =   6.500 mL      Kp = 47.429 mL/g
C0 =   .000    Ss0 =   .000       Sr0 =   .000
DV1 =   .180 mL  DV2 =   .110 mL       Mr = 1.000
Kr =   .480 mL   kr = .6700E+00 min^-1   Fr =   .580

REACTOR OPERATION:

| Time Start | Flow | Cin |
|---|---|---|
| .0 | 1.050 | 1. |
| 25.0 | .000 | 0. |
| 125.0 | 1.050 | 1. |
| 165.0 | .000 | 0. |

| | | |
|---|---|---|
| 1390.0 | .960 | 1. |
| 1411.0 | 1.030 | 0. |

EXPERIMENT DATA: In-Line Detector
Baseline: $Yb = -.2067E-06\ T + .2294E-02$
Response Curve: Linear
$Ymax = .4143E-01$

| T(min) | Y | T(min) | Y | T(min) | Y | T(min) | Y |
|---|---|---|---|---|---|---|---|
| .27 | .2246E-02 | .77 | .2441E-02 | 1.28 | .3320E-02 | 1.77 | .4590E-02 |
| 2.27 | .6006E-02 | 2.77 | .7520E-02 | 3.27 | .8984E-02 | 3.78 | .1035E-01 |
| 4.27 | .1167E-01 | 4.77 | .1294E-01 | 5.27 | .1421E-01 | 5.77 | .1538E-01 |
| 6.27 | .1650E-01 | 6.77 | .1763E-01 | 7.27 | .1865E-01 | 7.77 | .1963E-01 |
| 8.27 | .2065E-01 | 8.77 | .2158E-01 | 9.27 | .2241E-01 | 9.77 | .2329E-01 |
| 11.77 | .2715E-01 | 12.77 | .2817E-01 | 13.77 | .2920E-01 | 14.77 | .3013E-01 |
| 15.77 | .3091E-01 | 16.77 | .3174E-01 | 17.77 | .3252E-01 | 18.77 | .3325E-01 |
| 19.77 | .3389E-01 | 21.77 | .3545E-01 | 22.77 | .3579E-01 | 23.27 | .3599E-01 |
| 23.77 | .3618E-01 | 24.27 | .3633E-01 | 24.77 | .3652E-01 | 25.27 | .3672E-01 |
| 126.33 | .3750E-01 | 126.83 | .3755E-01 | 127.33 | .3765E-01 | 127.83 | .3774E-01 |
| 128.33 | .3789E-01 | 128.83 | .3799E-01 | 129.33 | .3814E-01 | 129.83 | .3828E-01 |
| 131.83 | .3906E-01 | 132.33 | .3916E-01 | 132.83 | .3931E-01 | 133.33 | .3945E-01 |
| 133.83 | .3950E-01 | 134.82 | .3975E-01 | 135.83 | .3994E-01 | 136.83 | .4014E-01 |
| 137.82 | .4033E-01 | 138.83 | .4058E-01 | 139.83 | .4077E-01 | 141.83 | .4116E-01 |
| 142.83 | .4126E-01 | 143.82 | .4136E-01 | 144.82 | .4150E-01 | 145.82 | .4155E-01 |
| 146.82 | .4165E-01 | 147.82 | .4180E-01 | 148.83 | .4185E-01 | 149.82 | .4194E-01 |
| 153.32 | .4219E-01 | 154.33 | .4229E-01 | 155.32 | .4238E-01 | 156.32 | .4243E-01 |
| 157.32 | .4248E-01 | 157.82 | .4253E-01 | 158.32 | .4253E-01 | 158.82 | .4253E-01 |
| 159.32 | .4253E-01 | 161.32 | .4229E-01 | 161.82 | .4229E-01 | 162.32 | .4229E-01 |
| 162.82 | .4229E-01 | 163.32 | .4229E-01 | 163.82 | .4229E-01 | 164.32 | .4233E-01 |
| 164.82 | .4229E-01 | 1398.00 | .4219E-01 | 1398.50 | .4219E-01 | 1399.00 | .4219E-01 |
| 1399.50 | .4219E-01 | 1400.00 | .4219E-01 | 1400.50 | .4219E-01 | 1401.00 | .4219E-01 |
| 1401.50 | .4219E-01 | 1402.00 | .4219E-01 | 1402.50 | .4219E-01 | 1406.00 | .4263E-01 |
| 1406.50 | .4258E-01 | 1407.00 | .4273E-01 | 1407.50 | .4277E-01 | 1408.00 | .4277E-01 |
| 1408.50 | .4273E-01 | 1409.00 | .4268E-01 | 1409.50 | .4268E-01 | 1410.50 | .4277E-01 |

EXPERIMENT DATA: HPLC grab samples
$Cmax = .1953E+02$

| T(min) | C | T(min) | C | T(min) | C | T(min) | C |
|---|---|---|---|---|---|---|---|
| 8.18 | .8879E+01 | 22.21 | .1715E+02 | 23.20 | .1657E+02 | 24.22 | .1654E+02 |
| 127.16 | .1598E+02 | 128.21 | .1639E+02 | 133.25 | .1622E+02 | 157.17 | .2007E+02 |
| 163.21 | .2067E+02 | 164.21 | .1873E+02 | 1392.18 | .2062E+02 | 1393.20 | .1718E+02 |
| 1398.23 | .1814E+02 | | | | | | |

Run NZP100: Naphthalene/Zellwood/0:100/flow-rate variation
21Oct93

$Ms$ = .101 g    $V$ = 6.500 mL        $Kp$ = 218.010 mL/g
$C0$ = .000    $Ss0$ = .000        $Sr0$ = .000
$DV1$ = .180 mL    $DV2$ = .110 mL        $Mr$ = 1.000
$Kr$ = 1.240 mL    $kr$ = .8110E-01 min^-1    $Fr$ = .562

REACTOR OPERATION:

| Time Start | Flow | Cin |
|---|---|---|
| .0 | .990 | 1. |
| 30.0 | .000 | 0. |
| 55.0 | .990 | 1. |
| 95.0 | 1.030 | 0. |
| 156.0 | .580 | 1. |
| 215.0 | .780 | 0. |

EXPERIMENT DATA: In-Line Detector
Baseline: $Yb$ = .0000E+00 T + .2637E-02
Response Curve: Linear
$Ymax$ = .3833E-01

| T(min) | Y | T(min) | Y | T(min) | Y | T(min) | Y |
|---|---|---|---|---|---|---|---|
| .85 | .2686E-02 | 2.85 | .4102E-02 | 4.85 | .6641E-02 | 6.85 | .1001E-01 |
| 8.85 | .1348E-01 | 10.85 | .1665E-01 | 12.85 | .1939E-01 | 14.85 | .2183E-01 |
| 16.85 | .2398E-01 | 18.85 | .2578E-01 | 23.35 | .3013E-01 | 25.33 | .3086E-01 |
| 27.33 | .3159E-01 | 27.83 | .3179E-01 | 28.33 | .3193E-01 | 28.83 | .3213E-01 |
| 29.33 | .3232E-01 | 29.83 | .3252E-01 | 55.83 | .3315E-01 | 56.33 | .3325E-01 |
| 56.83 | .3330E-01 | 57.32 | .3335E-01 | 57.83 | .3345E-01 | 58.33 | .3355E-01 |
| 60.33 | .3394E-01 | 62.33 | .3442E-01 | 64.82 | .3501E-01 | 71.32 | .3604E-01 |
| 74.33 | .3652E-01 | 78.82 | .3701E-01 | 84.32 | .3745E-01 | 89.32 | .3779E-01 |
| 93.32 | .3789E-01 | 95.32 | .3794E-01 | 96.82 | .3721E-01 | 98.32 | .3525E-01 |
| 99.82 | .3257E-01 | 101.32 | .2969E-01 | 102.82 | .2700E-01 | 104.32 | .2466E-01 |
| 107.32 | .1792E-01 | 109.30 | .1694E-01 | 111.32 | .1602E-01 | 113.32 | .1499E-01 |
| 115.80 | .1353E-01 | 118.80 | .1187E-01 | 121.30 | .1060E-01 | 123.80 | .9570E-02 |
| 128.30 | .7471E-02 | 133.30 | .6885E-02 | 137.30 | .6201E-02 | 140.80 | .5615E-02 |
| 144.30 | .5078E-02 | 148.30 | .4199E-02 | 154.30 | .4053E-02 | 156.30 | .4053E-02 |
| 158.28 | .4248E-02 | 160.28 | .5029E-02 | 162.30 | .6006E-02 | 164.30 | .7373E-02 |
| 169.78 | .1499E-01 | 172.28 | .1636E-01 | 174.78 | .1787E-01 | 177.28 | .1939E-01 |
| 180.28 | .2100E-01 | 182.78 | .2236E-01 | 184.78 | .2339E-01 | 190.28 | .2676E-01 |
| 195.28 | .2778E-01 | 200.27 | .2900E-01 | 204.28 | .3003E-01 | 210.27 | .3247E-01 |
| 213.27 | .3276E-01 | 215.27 | .3301E-01 | 217.27 | .3228E-01 | 218.77 | .3076E-01 |
| 220.27 | .2905E-01 | 221.77 | .2725E-01 | 223.27 | .2554E-01 | 224.77 | .2393E-01 |
| 226.77 | .1934E-01 | 229.27 | .1816E-01 | 231.77 | .1699E-01 | 234.27 | .1587E-01 |
| 236.77 | .1465E-01 | 239.27 | .1357E-01 | 242.77 | .1206E-01 | 247.77 | .9131E-02 |

| | | | | | | | |
|---|---|---|---|---|---|---|---|
| 252.75 | .8594E-02 | 257.75 | .7764E-02 | 262.75 | .6885E-02 | 272.75 | .5322E-02 |
| 277.25 | .5078E-02 | 282.75 | .4639E-02 | 290.75 | .3711E-02 | 297.25 | .3564E-02 |
| 302.75 | .3320E-02 | 312.73 | .2734E-02 | 317.23 | .2783E-02 | 322.73 | .2686E-02 |

ANI301: anthracene/BN-1.5/Interrupt/50:50
1Jul94

$Ms$ = .750 g   $V$ = 5.890 mL        $Kp$ = 73.140 mL/g
$C0$ = .000    $Ss0$ = .000        $Sr0$ = .000
$DV1$ = .180 mL   $DV2$ = .110 mL        $Mr$ = 1.000
$Kr$ = .096 mL   $kr$ = .3560E-03 min^-1   $Fr$ = .611

REACTOR OPERATION:

| Time Start | Flow | Cin |
|---|---|---|
| .0 | .984 | 1. |
| 7.5 | .000 | 1. |
| 67.5 | .984 | 1. |
| 120.0 | 1.030 | 0. |
| 137.5 | .000 | 0. |
| 197.5 | 1.030 | 0. |

EXPERIMENT DATA: In-Line Detector
Baseline: $Yb$ = -.8003E-06 T + -.1772E-04
Response Curve: Equation (C-2)
$Ymax$ = .5172E-01

| T(min) | Y | T(min) | Y | T(min) | Y | T(min) | Y |
|---|---|---|---|---|---|---|---|
| .42 | .2930E-03 | .75 | .4492E-02 | 1.08 | .9180E-02 | 1.42 | .1328E-01 |
| 1.75 | .1690E-01 | 2.08 | .2012E-01 | 2.42 | .2285E-01 | 2.75 | .2529E-01 |
| 3.08 | .2744E-01 | 3.42 | .2935E-01 | 3.75 | .3106E-01 | 4.08 | .3252E-01 |
| 4.42 | .3384E-01 | 4.75 | .3506E-01 | 5.08 | .3613E-01 | 5.42 | .3711E-01 |
| 5.75 | .3799E-01 | 6.08 | .3877E-01 | 6.42 | .3950E-01 | 6.75 | .4023E-01 |
| 7.08 | .4082E-01 | 7.40 | .4136E-01 | 67.63 | .3364E-01 | 67.97 | .3301E-01 |
| 68.32 | .3457E-01 | 68.63 | .3589E-01 | 68.98 | .3711E-01 | 69.30 | .3818E-01 |
| 69.97 | .3994E-01 | 70.63 | .4141E-01 | 71.30 | .4258E-01 | 72.30 | .4399E-01 |
| 73.30 | .4512E-01 | 74.63 | .4619E-01 | 76.30 | .4717E-01 | 78.30 | .4805E-01 |
| 80.63 | .4878E-01 | 83.97 | .4941E-01 | 87.97 | .4995E-01 | 91.97 | .5024E-01 |
| 95.97 | .5044E-01 | 99.97 | .5059E-01 | 103.97 | .5073E-01 | 107.97 | .5083E-01 |
| 111.95 | .5088E-01 | 115.95 | .5098E-01 | 119.95 | .5098E-01 | 120.95 | .4956E-01 |
| 121.62 | .4751E-01 | 122.28 | .4546E-01 | 122.95 | .4341E-01 | 123.63 | .4131E-01 |
| 124.28 | .3931E-01 | 124.95 | .3731E-01 | 125.62 | .3540E-01 | 126.28 | .3345E-01 |
| 126.95 | .3164E-01 | 127.62 | .2988E-01 | 128.28 | .2827E-01 | 128.95 | .2666E-01 |

```
129.62 .2520E-01 130.62 .2315E-01 131.62 .2124E-01 132.62 .1953E-01
133.62 .1802E-01 134.62 .1665E-01 135.62 .1543E-01 135.95 .1504E-01
136.28 .1465E-01 136.62 .1431E-01 136.95 .1397E-01 137.28 .1367E-01
197.83 .2285E-01 198.18 .2207E-01 198.52 .2114E-01 198.85 .2026E-01
199.18 .1943E-01 199.52 .1865E-01 200.17 .1714E-01 200.83 .1582E-01
201.85 .1411E-01 202.85 .1255E-01 204.17 .1094E-01 205.85 .9229E-02
207.50 .7959E-02 209.52 .6689E-02 211.50 .5713E-02 213.83 .4883E-02
216.50 .4199E-02 219.83 .3516E-02 223.17 .3027E-02 226.83 .2637E-02
230.50 .2393E-02 234.83 .2100E-02 239.83 .1807E-02 244.83 .1660E-02
249.83 .1465E-02 254.83 .1367E-02 260.17 .1221E-02 264.82 .1172E-02
```

EXPERIMENT DATA: HPLC grab samples
Cmax = .1968E+01

| T (min) | C | T(min) | C | T(min) | C | T(min) | C |
|---|---|---|---|---|---|---|---|
| 5.28 | .9840E+00 | 6.28 | .1095E+01 | 68.27 | .8021E+00 | 69.27 | .9099E+00 |
| 113.27 | .1835E+01 | 127.27 | .7828E+01 | 135.26 | .3412E+00 | 136.26 | .3066E+00 |
| 199.26 | .5621E+00 | 200.26 | .3564E+00 | 220.26 | .7666E-01 | 241.26 | .3839E-01 |
| 260.27 | .2803E-01 | 261.28 | .4182E-01 | | | | |

ANI302: Anthracene/BN-2/50:50/Interrupt
13Jul94

Ms = .800 g    V = 5.930 mL       Kp = 73.140 mL/g
C0 = .000    Ss0 = .000        Sr0 = .000
DV1 = .180 mL  DV2 = .110 mL        Mr = 1.000
Kr = .096 mL   kr = .3560E-03 min^-1  Fr = .611

REACTOR OPERATION:

| Time Start | Flow | Cin |
|---|---|---|
| .0 | 1.030 | 1. |
| 7.5 | .000 | 1. |
| 67.5 | 1.030 | 1. |
| 120.0 | 1.030 | 0. |
| 137.5 | .000 | 0. |
| 197.5 | 1.030 | 0. |

EXPERIMENT DATA: In-Line Detector
Baseline: Yb = -.3023E-06 T + .1819E-03
Response Curve: Equation (C-2)
Ymax = .4863E-01

| T(min) | Y | T(min) | Y | T(min) | Y | T(min) | Y |
|---|---|---|---|---|---|---|---|

```
 .53 .1953E-02    .87 .6641E-02   1.20 .1113E-01   1.53 .1480E-01
1.87 .1826E-01   2.20 .2119E-01   2.53 .2378E-01   2.87 .2607E-01
3.20 .2808E-01   3.53 .2979E-01   3.87 .3135E-01   4.20 .3272E-01
4.53 .3398E-01   4.87 .3506E-01   5.20 .3604E-01   5.53 .3691E-01
5.87 .3770E-01   6.20 .3848E-01   6.53 .3911E-01   6.87 .3970E-01
7.20 .4023E-01  68.02 .3491E-01  68.53 .3662E-01  69.02 .3799E-01
69.52 .3916E-01  70.02 .4014E-01  70.53 .4102E-01  71.52 .4238E-01
72.53 .4346E-01  74.02 .4463E-01  75.52 .4551E-01  77.52 .4629E-01
80.02 .4688E-01  83.02 .4736E-01  86.52 .4771E-01  90.52 .4795E-01
94.52 .4810E-01  98.52 .4824E-01 102.52 .4829E-01 106.52 .4834E-01
110.52 .4829E-01 114.52 .4839E-01 117.73 .4844E-01 120.07 .4844E-01
120.73 .4756E-01 121.40 .4541E-01 122.07 .4321E-01 122.73 .4097E-01
123.42 .3867E-01 124.07 .3648E-01 124.73 .3423E-01 125.40 .3208E-01
126.08 .3003E-01 126.73 .2803E-01 127.40 .2612E-01 128.07 .2441E-01
128.73 .2271E-01 129.73 .2041E-01 130.73 .1841E-01 131.73 .1660E-01
132.73 .1504E-01 133.73 .1362E-01 134.73 .1240E-01 135.73 .1133E-01
136.07 .1099E-01 136.40 .1065E-01 136.73 .1040E-01 137.07 .1006E-01
137.40 .9814E-02 198.20 .1904E-01 198.70 .1777E-01 199.20 .1655E-01
199.70 .1543E-01 200.20 .1445E-01 200.70 .1353E-01 201.70 .1187E-01
202.68 .1040E-01 204.20 .8691E-02 205.70 .7324E-02 207.18 .6250E-02
209.20 .5127E-02 211.70 .4150E-02 215.18 .3223E-02 220.18 .2441E-02
225.18 .2002E-02 230.18 .1758E-02 235.18 .1514E-02 240.18 .1367E-02
245.18 .1270E-02 250.18 .1172E-02 255.17 .1074E-02 260.17 .1025E-02
265.17 .9770E-03 270.17 .8790E-03 275.17 .8300E-03 280.17 .8300E-03
285.17 .7320E-03 290.17 .7320E-03 295.17 .7320E-03 299.65 .6840E-03
```

EXPERIMENT DATA: HPLC grab samples
Cmax = .1844E+01

| T (min) | C | T(min) | C | T(min) | C | T(min) | C |
|---|---|---|---|---|---|---|---|
| 5.26 | .9535E+00 | 130.26 | .3977E+00 | 200.25 | .2981E+00 | 210.26 | .9768E-01 |
| 225.26 | .4086E-01 | 250.25 | .2380E-01 | 297.26 | .1366E-01 | | |

AEI303R: Anthracene/BN-3/50:50/Interrupt
1Aug94

Ms = .800 g    V = 5.900 mL      Kp = 73.140 mL/g
C0 = .000    Ss0 = .000        Sr0 = .000
DV1 = .180 mL  DV2 = .110 mL      Mr = 1.000
Kr = .096 mL  kr = .3560E-03 min^-1  Fr = .611

REACTOR OPERATION:

| Time Start | Flow | Cin |
|---|---|---|
| .0 | 1.030 | 1. |
| 7.5 | .000 | 1. |
| 67.5 | 1.030 | 1. |
| 120.0 | 1.030 | 0. |
| 137.5 | .000 | 0. |
| 197.5 | 1.030 | 0. |

EXPERIMENT DATA: In-Line Detector
Baseline: $Yb = .4243E-06\ T + .1981E-03$
Response Curve: Equation (C-2)
$Ymax = .4842E-01$

| T(min) | Y | T(min) | Y | T(min) | Y | T(min) | Y |
|---|---|---|---|---|---|---|---|
| .42 | .4390E-03 | .92 | .6885E-02 | 1.40 | .1338E-01 | 1.92 | .1875E-01 |
| 2.42 | .2319E-01 | 2.92 | .2676E-01 | 3.42 | .2954E-01 | 3.92 | .3203E-01 |
| 4.40 | .3398E-01 | 4.92 | .3565E-01 | 5.40 | .3706E-01 | 5.92 | .3828E-01 |
| 6.42 | .3931E-01 | 6.90 | .4019E-01 | 7.40 | .4102E-01 | 68.10 | .3599E-01 |
| 68.60 | .3750E-01 | 69.10 | .3877E-01 | 69.60 | .3989E-01 | 70.12 | .4082E-01 |
| 70.60 | .4160E-01 | 71.10 | .4233E-01 | 72.10 | .4346E-01 | 73.10 | .4434E-01 |
| 74.10 | .4502E-01 | 75.60 | .4575E-01 | 77.10 | .4634E-01 | 78.60 | .4673E-01 |
| 81.10 | .4727E-01 | 84.10 | .4761E-01 | 87.60 | .4790E-01 | 91.60 | .4805E-01 |
| 95.10 | .4815E-01 | 98.58 | .4824E-01 | 102.10 | .4829E-01 | 106.08 | .4829E-01 |
| 110.08 | .4834E-01 | 114.08 | .4839E-01 | 117.08 | .4839E-01 | 120.08 | .4839E-01 |
| 121.08 | .4653E-01 | 121.58 | .4492E-01 | 122.08 | .4321E-01 | 122.58 | .4146E-01 |
| 123.08 | .3975E-01 | 123.58 | .3799E-01 | 124.08 | .3623E-01 | 124.58 | .3447E-01 |
| 125.08 | .3281E-01 | 125.58 | .3110E-01 | 126.58 | .2788E-01 | 127.58 | .2490E-01 |
| 128.58 | .2217E-01 | 129.58 | .1978E-01 | 130.58 | .1763E-01 | 131.58 | .1577E-01 |
| 132.58 | .1411E-01 | 133.58 | .1265E-01 | 134.58 | .1138E-01 | 135.08 | .1084E-01 |
| 135.58 | .1030E-01 | 136.08 | .9814E-02 | 136.58 | .9375E-02 | 137.08 | .8936E-02 |
| 197.97 | .1802E-01 | 198.47 | .1685E-01 | 198.97 | .1563E-01 | 199.47 | .1455E-01 |
| 199.95 | .1357E-01 | 200.47 | .1265E-01 | 200.97 | .1182E-01 | 201.45 | .1099E-01 |
| 201.95 | .1030E-01 | 202.45 | .9619E-02 | 203.45 | .8447E-02 | 204.45 | .7471E-02 |
| 205.45 | .6641E-02 | 206.45 | .5908E-02 | 207.45 | .5273E-02 | 208.95 | .4541E-02 |
| 210.45 | .3955E-02 | 212.95 | .3223E-02 | 215.45 | .2734E-02 | 218.45 | .2344E-02 |
| 221.45 | .2051E-02 | 224.95 | .1807E-02 | 228.45 | .1660E-02 | 232.45 | .1514E-02 |
| 236.45 | .1416E-02 | 240.95 | .1367E-02 | 245.43 | .1270E-02 | 250.45 | .1172E-02 |
| 255.43 | .1123E-02 | 260.43 | .1074E-02 | 265.43 | .1025E-02 | 270.43 | .9770E-03 |
| 275.43 | .9770E-03 | 280.43 | .9770E-03 | 285.43 | .9280E-03 | 289.92 | .8790E-03 |

EXPERIMENT DATA: HPLC grab samples
$Cmax = .2858E+01$

| T(min) | C | T(min) | C | T(min) | C | T(min) | C |
|---|---|---|---|---|---|---|---|
| 5.31 | .1443E+01 | 105.27 | .2751E+01 | 130.27 | .6188E+00 | 200.27 | .4110E+00 |
| 210.29 | .1160E+00 | 220.28 | .5691E-01 | 240.27 | .3611E-01 | 270.28 | .2446E-01 |

ANI304: Anthracene\BN-4\Interrupt\50:50
18Jul94

Ms = .750 g   V = 5.910 mL      Kp = 73.140 mL/g
C0 = .000   Ss0 = .000      Sr0 = .000
DV1 = .180 mL   DV2 = .110 mL      Mr = 1.000
Kr = .096 mL   kr = .3560E-03 min^-1   Fr = .611

REACTOR OPERATION:

| Time Start | Flow | Cin |
|---|---|---|
| .0 | 1.030 | 1. |
| 7.5 | .000 | 1. |
| 67.5 | 1.030 | 1. |
| 120.0 | 1.030 | 0. |
| 137.5 | .000 | 0. |
| 197.5 | 1.030 | 0. |

EXPERIMENT DATA: In-Line Detector
Baseline: Yb = .6220E-06 T + .9859E-04
Response Curve: Equation (C-2)
Ymax = .4858E-01

| T(min) | Y | T(min) | Y | T(min) | Y | T(min) | Y |
|---|---|---|---|---|---|---|---|
| .22 | .9800E-04 | .55 | .1953E-02 | .88 | .6738E-02 | 1.22 | .1128E-01 |
| 1.55 | .1528E-01 | 1.88 | .1880E-01 | 2.22 | .2188E-01 | 2.55 | .2446E-01 |
| 2.88 | .2676E-01 | 3.22 | .2881E-01 | 3.55 | .3062E-01 | 3.88 | .3223E-01 |
| 4.22 | .3355E-01 | 4.55 | .3481E-01 | 4.88 | .3594E-01 | 5.22 | .3691E-01 |
| 5.55 | .3779E-01 | 5.88 | .3857E-01 | 6.22 | .3931E-01 | 6.55 | .3994E-01 |
| 6.88 | .4058E-01 | 7.22 | .4106E-01 | 7.55 | .4141E-01 | 67.90 | .3750E-01 |
| 68.42 | .3887E-01 | 68.92 | .3994E-01 | 69.42 | .4092E-01 | 69.92 | .4185E-01 |
| 70.42 | .4248E-01 | 70.90 | .4307E-01 | 71.90 | .4414E-01 | 72.92 | .4492E-01 |
| 74.40 | .4580E-01 | 75.92 | .4648E-01 | 77.40 | .4707E-01 | 79.42 | .4741E-01 |
| 81.40 | .4780E-01 | 83.90 | .4800E-01 | 86.40 | .4815E-01 | 89.40 | .4829E-01 |
| 92.40 | .4844E-01 | 95.90 | .4849E-01 | 99.40 | .4849E-01 | 103.40 | .4854E-01 |
| 107.40 | .4863E-01 | 111.90 | .4863E-01 | 116.40 | .4863E-01 | 119.53 | .4868E-01 |
| 120.53 | .4839E-01 | 121.22 | .4629E-01 | 121.88 | .4399E-01 | 122.55 | .4165E-01 |
| 123.20 | .3926E-01 | 123.87 | .3691E-01 | 124.87 | .3330E-01 | 125.87 | .2979E-01 |
| 126.88 | .2647E-01 | 127.87 | .2349E-01 | 128.87 | .2075E-01 | 129.87 | .1831E-01 |
| 130.87 | .1621E-01 | 131.87 | .1431E-01 | 132.87 | .1270E-01 | 133.87 | .1128E-01 |
| 134.87 | .1001E-01 | 135.87 | .8984E-02 | 136.20 | .8643E-02 | 136.53 | .8398E-02 |
| 136.87 | .8057E-02 | 137.20 | .7813E-02 | 137.53 | .7617E-02 | 197.72 | .1543E-01 |
| 198.22 | .1504E-01 | 198.72 | .1392E-01 | 199.22 | .1289E-01 | 199.72 | .1201E-01 |
| 200.22 | .1113E-01 | 201.22 | .9619E-02 | 202.22 | .8301E-02 | 203.22 | .7227E-02 |
| 204.22 | .6299E-02 | 205.72 | .5225E-02 | 207.22 | .4346E-02 | 209.20 | .3467E-02 |
| 211.70 | .2734E-02 | 214.70 | .2148E-02 | 218.70 | .1660E-02 | 222.72 | .1367E-02 |

```
226.70 .1221E-02  230.70 .1123E-02  234.70 .1025E-02  239.70 .9770E-03
244.70 .9770E-03  249.70 .8790E-03  254.70 .7810E-03  259.68 .7810E-03
264.68 .7810E-03  269.68 .7320E-03  274.68 .6840E-03  279.68 .6840E-03
```

EXPERIMENT DATA: HPLC grab samples
Cmax = .1865E+01

| T (min) | C | T(min) | C | T(min) | C | T(min) | C |
|---|---|---|---|---|---|---|---|
| 5.27 | .9737E+00 | 114.25 | .1840E+01 | 130.28 | .3711E+00 | 200.27 | .2340E+00 |
| 210.27 | .5923E-01 | 220.26 | .2836E-01 | 240.28 | .1618E-01 | 260.29 | .1190E-01 |

AEI305: Anthracene/BN-5/Interrupt/50:50
20Jul94

$Ms$ = .880 g   $V$ = 5.715 mL      $Kp$ = 73.140 mL/g
$C0$ = .000    $Ss0$ = .000      $Sr0$ = .000
$DV1$ = .180 mL  $DV2$ = .110 mL      $Mr$ = 1.000
$Kr$ = .096 mL  $kr$ = .3560E-03 min^-1  $Fr$ = .611

REACTOR OPERATION:

| Time Start | Flow | Cin |
|---|---|---|
| .0 | 1.030 | 1. |
| 7.5 | .000 | 1. |
| 67.5 | 1.030 | 1. |
| 120.0 | 1.030 | 0. |
| 137.5 | .000 | 0. |
| 197.5 | 1.030 | 0. |

EXPERIMENT DATA: In-Line Detector
Baseline: $Yb$ = .4382E-06 $T$ + .1981E-03
Response Curve: Equation (C-2)
Ymax = .4850E-01

| T(min) | Y | T(min) | Y | T(min) | Y | T(min) | Y |
|---|---|---|---|---|---|---|---|
| .27 | .1950E-03 | .58 | .2881E-02 | .92 | .7813E-02 | 1.25 | .1235E-01 |
| 1.58 | .1631E-01 | 1.92 | .1982E-01 | 2.25 | .2285E-01 | 2.58 | .2534E-01 |
| 2.93 | .2773E-01 | 3.25 | .2964E-01 | 3.60 | .3145E-01 | 3.93 | .3296E-01 |
| 4.25 | .3433E-01 | 4.58 | .3550E-01 | 4.92 | .3657E-01 | 5.25 | .3750E-01 |
| 5.58 | .3838E-01 | 5.92 | .3916E-01 | 6.25 | .3984E-01 | 6.58 | .4048E-01 |
| 6.92 | .4102E-01 | 7.25 | .4155E-01 | 67.98 | .3965E-01 | 68.48 | .4063E-01 |
| 68.98 | .4146E-01 | 69.48 | .4233E-01 | 69.98 | .4297E-01 | 70.48 | .4356E-01 |
| 71.48 | .4458E-01 | 72.48 | .4536E-01 | 73.98 | .4609E-01 | 75.48 | .4678E-01 |
| 77.48 | .4736E-01 | 79.48 | .4780E-01 | 82.48 | .4819E-01 | 85.48 | .4834E-01 |

| | | | | | | | |
|---|---|---|---|---|---|---|---|
| 88.97 | .4854E-01 | 92.47 | .4863E-01 | 95.98 | .4863E-01 | 99.47 | .4868E-01 |
| 102.97 | .4873E-01 | 106.47 | .4873E-01 | 109.97 | .4878E-01 | 113.47 | .4878E-01 |
| 116.97 | .4883E-01 | 119.97 | .4883E-01 | 120.97 | .4722E-01 | 121.47 | .4551E-01 |
| 121.97 | .4375E-01 | 122.47 | .4199E-01 | 122.97 | .4023E-01 | 123.47 | .3838E-01 |
| 123.97 | .3652E-01 | 124.47 | .3462E-01 | 124.97 | .3286E-01 | 125.47 | .3106E-01 |
| 126.47 | .2773E-01 | 127.47 | .2456E-01 | 128.47 | .2168E-01 | 129.47 | .1914E-01 |
| 130.47 | .1690E-01 | 131.97 | .1406E-01 | 133.47 | .1172E-01 | 134.95 | .9814E-02 |
| 135.47 | .9277E-02 | 135.95 | .8789E-02 | 136.47 | .8350E-02 | 136.97 | .7910E-02 |
| 137.47 | .7520E-02 | 197.80 | .1416E-01 | 198.30 | .1328E-01 | 198.80 | .1231E-01 |
| 199.30 | .1148E-01 | 199.80 | .1055E-01 | 200.30 | .9766E-02 | 200.80 | .8984E-02 |
| 201.80 | .7910E-02 | 202.80 | .6738E-02 | 203.80 | .6006E-02 | 205.30 | .4785E-02 |
| 206.80 | .3955E-02 | 208.30 | .3369E-02 | 210.30 | .2686E-02 | 212.80 | .2148E-02 |
| 215.80 | .1758E-02 | 219.30 | .1367E-02 | 223.30 | .1172E-02 | 227.78 | .1025E-02 |
| 232.28 | .9280E-03 | 236.78 | .8300E-03 | 241.28 | .7810E-03 | 245.78 | .7810E-03 |
| 250.28 | .7320E-03 | 254.78 | .7320E-03 | 259.78 | .6840E-03 | 264.78 | .6840E-03 |
| 269.78 | .6350E-03 | 274.78 | .6350E-03 | 279.77 | .6350E-03 | 284.77 | .3910E-03 |

EXPERIMENT DATA: HPLC grab samples

$Cmax = .1765E+01$

| T(min) | C | T(min) | C | T(min) | C | T(min) | C |
|---|---|---|---|---|---|---|---|
| 5.27 | .1001E+01 | 110.27 | .1778E+01 | 130.26 | .3516E+00 | 210.27 | .4958E-01 |
| 220.26 | .2021E-01 | 235.27 | .1179E-01 | 266.27 | .7343E-02 | | |

ANI30X: Anthracene/mixed nylon balls/50:50/interrupt
27Jul94

| | | | | | | |
|---|---|---|---|---|---|---|
| $Ms =$ | .880 g | $V =$ | 5.758 mL | $Kp =$ | 70.000 mL/g | |
| $C0 =$ | .000 | $Ss0 =$ | .000 | $Sr0 =$ | .000 | |
| $DV1 =$ | .180 mL | $DV2 =$ | .110 mL | $Mr =$ | 1.000 | |
| $Kr =$ | .096 mL | $kr =$ | .3560E-03 min^-1 | $Fr =$ | .611 | |

REACTOR OPERATION:

| Time Start | Flow | Cin |
|---|---|---|
| .0 | 1.030 | 1. |
| 7.5 | .000 | 1. |
| 67.5 | 1.030 | 1. |
| 120.0 | 1.030 | 0. |
| 137.5 | .000 | 0. |
| 197.5 | 1.030 | 0. |

EXPERIMENT DATA: In-Line Detector

Baseline: Yb = .9473E-07 T + .1439E-03
Response Curve: Equation (C-2)
Ymax = .4997E-01

| T(min) | Y | T(min) | Y | T(min) | Y | T(min) | Y |
|---|---|---|---|---|---|---|---|
| .33 | .1460E-03 | .67 | .2881E-02 | 1.00 | .8008E-02 | 1.33 | .1270E-01 |
| 1.67 | .1670E-01 | 2.00 | .2022E-01 | 2.33 | .2329E-01 | 2.67 | .2598E-01 |
| 3.00 | .2822E-01 | 3.33 | .3018E-01 | 3.67 | .3198E-01 | 4.00 | .3345E-01 |
| 4.33 | .3481E-01 | 4.67 | .3604E-01 | 5.00 | .3711E-01 | 5.33 | .3809E-01 |
| 5.67 | .3892E-01 | 6.00 | .3965E-01 | 6.33 | .4043E-01 | 6.67 | .4102E-01 |
| 7.00 | .4160E-01 | 7.33 | .4209E-01 | 68.13 | .3716E-01 | 68.63 | .3872E-01 |
| 69.12 | .3994E-01 | 69.63 | .4102E-01 | 70.12 | .4199E-01 | 70.62 | .4277E-01 |
| 71.13 | .4356E-01 | 72.12 | .4473E-01 | 73.12 | .4561E-01 | 74.12 | .4629E-01 |
| 75.62 | .4707E-01 | 77.12 | .4766E-01 | 78.62 | .4810E-01 | 80.62 | .4854E-01 |
| 82.62 | .4883E-01 | 85.12 | .4907E-01 | 88.62 | .4941E-01 | 92.12 | .4951E-01 |
| 96.12 | .4961E-01 | 100.12 | .4971E-01 | 104.12 | .4976E-01 | 108.12 | .4981E-01 |
| 112.10 | .4985E-01 | 116.10 | .4985E-01 | 120.10 | .4990E-01 | 121.10 | .4805E-01 |
| 121.60 | .4634E-01 | 122.10 | .4473E-01 | 122.60 | .4297E-01 | 123.12 | .4121E-01 |
| 123.60 | .3945E-01 | 124.10 | .3770E-01 | 124.60 | .3599E-01 | 125.10 | .3428E-01 |
| 126.10 | .3106E-01 | 127.10 | .2793E-01 | 128.10 | .2510E-01 | 129.10 | .2251E-01 |
| 130.10 | .2022E-01 | 131.10 | .1816E-01 | 132.10 | .1641E-01 | 133.10 | .1480E-01 |
| 134.60 | .1279E-01 | 135.10 | .1221E-01 | 135.60 | .1162E-01 | 136.10 | .1113E-01 |
| 136.60 | .1060E-01 | 137.10 | .1016E-01 | 198.13 | .1939E-01 | 198.63 | .1797E-01 |
| 199.13 | .1675E-01 | 199.63 | .1558E-01 | 200.13 | .1445E-01 | 200.63 | .1353E-01 |
| 201.63 | .1177E-01 | 202.63 | .1035E-01 | 204.13 | .8496E-02 | 205.62 | .7080E-02 |
| 207.13 | .6006E-02 | 208.63 | .5127E-02 | 210.62 | .4297E-02 | 213.13 | .3467E-02 |
| 215.62 | .2930E-02 | 220.12 | .2295E-02 | 224.62 | .1904E-02 | 229.62 | .1611E-02 |
| 234.62 | .1416E-02 | 239.62 | .1270E-02 | 244.62 | .1221E-02 | 249.62 | .1123E-02 |
| 254.60 | .1025E-02 | 259.60 | .9770E-03 | 264.60 | .9770E-03 | 269.60 | .8790E-03 |
| 274.60 | .8300E-03 | 279.60 | .7810E-03 | 284.60 | .7320E-03 | 289.60 | .7320E-03 |

EXPERIMENT DATA: HPLC grab samples
Cmax = .1914E+01

| T(min) | C | T(min) | C | T(min) | C | T(min) | C |
|---|---|---|---|---|---|---|---|
| 5.29 | .1050E+01 | 110.30 | .1830E+01 | 130.26 | .4138E+00 | 200.27 | .2975E+00 |
| 210.27 | .8541E-01 | 220.28 | .4239E-01 | 240.29 | .2396E-01 | 270.27 | .1488E-01 |

API400: anthracene/paraffin beads/Interrupt/50:50
23Aug94

Ms = 1.020 g    V = 5.410 mL        Kp = 34.000 mL/g
C0 = .000    Ss0 = .000        Sr0 = .000

DV1 = .180 mL  DV2 = .110 mL       Mr = 1.000
Kr = .096 mL  kr = .3560E-03 min^-1  Fr = .611

REACTOR OPERATION:

| Time Start | Flow | Cin |
|---|---|---|
| .0 | 1.030 | 1. |
| 7.5 | .000 | 1. |
| 67.5 | 1.030 | 1. |
| 120.0 | 1.030 | 0. |
| 137.5 | .000 | 0. |
| 197.5 | 1.030 | 0. |

EXPERIMENT DATA: In-Line Detector
Baseline: Yb = -.1147E-07 T + .1118E-03
Response Curve: Equation (C-2)
Ymax = .4856E-01

| T(min) | Y | T(min) | Y | T(min) | Y | T(min) | Y |
|---|---|---|---|---|---|---|---|
| .45 | .1221E-02 | .95 | .8740E-02 | 1.45 | .1538E-01 | 1.95 | .2070E-01 |
| 2.45 | .2500E-01 | 2.95 | .2852E-01 | 3.45 | .3120E-01 | 3.95 | .3355E-01 |
| 4.45 | .3545E-01 | 4.95 | .3701E-01 | 5.45 | .3833E-01 | 5.95 | .3945E-01 |
| 6.45 | .4043E-01 | 6.95 | .4126E-01 | 7.45 | .4199E-01 | 67.62 | .3731E-01 |
| 68.12 | .3838E-01 | 68.62 | .3965E-01 | 69.12 | .4063E-01 | 69.62 | .4150E-01 |
| 70.12 | .4224E-01 | 70.62 | .4292E-01 | 71.12 | .4346E-01 | 72.12 | .4439E-01 |
| 73.12 | .4517E-01 | 74.10 | .4570E-01 | 75.62 | .4634E-01 | 77.12 | .4683E-01 |
| 78.62 | .4717E-01 | 80.62 | .4751E-01 | 82.62 | .4775E-01 | 85.10 | .4795E-01 |
| 87.60 | .4810E-01 | 90.10 | .4815E-01 | 93.10 | .4824E-01 | 96.10 | .4829E-01 |
| 99.10 | .4834E-01 | 102.10 | .4834E-01 | 105.10 | .4839E-01 | 108.10 | .4844E-01 |
| 111.10 | .4844E-01 | 114.10 | .4844E-01 | 117.10 | .4844E-01 | 120.10 | .4844E-01 |
| 120.60 | .4790E-01 | 121.10 | .4619E-01 | 121.60 | .4443E-01 | 122.10 | .4268E-01 |
| 122.58 | .4082E-01 | 123.10 | .3897E-01 | 123.60 | .3711E-01 | 124.08 | .3525E-01 |
| 124.60 | .3345E-01 | 125.10 | .3159E-01 | 125.58 | .2983E-01 | 126.08 | .2813E-01 |
| 126.60 | .2647E-01 | 127.58 | .2334E-01 | 128.58 | .2056E-01 | 129.60 | .1802E-01 |
| 130.58 | .1582E-01 | 131.58 | .1392E-01 | 132.58 | .1226E-01 | 133.58 | .1079E-01 |
| 134.58 | .9570E-02 | 135.08 | .9033E-02 | 135.58 | .8496E-02 | 136.08 | .8008E-02 |
| 136.58 | .7568E-02 | 137.08 | .7178E-02 | 197.77 | .1406E-01 | 198.27 | .1299E-01 |
| 198.77 | .1196E-01 | 199.27 | .1104E-01 | 199.77 | .1021E-01 | 200.27 | .9424E-02 |
| 201.27 | .8057E-02 | 202.27 | .6934E-02 | 203.27 | .6006E-02 | 204.27 | .5225E-02 |
| 205.27 | .4492E-02 | 206.77 | .3711E-02 | 208.27 | .3125E-02 | 209.77 | .2637E-02 |
| 211.77 | .2148E-02 | 213.77 | .1758E-02 | 216.27 | .1465E-02 | 218.77 | .1221E-02 |
| 221.77 | .1025E-02 | 225.75 | .9280E-03 | 229.75 | .8300E-03 | 233.75 | .7810E-03 |
| 237.75 | .6840E-03 | 241.75 | .6350E-03 | 245.75 | .6350E-03 | 249.75 | .5860E-03 |
| 253.75 | .5860E-03 | 257.75 | .5860E-03 | 261.75 | .5370E-03 | 265.75 | .5370E-03 |

EXPERIMENT DATA: HPLC grab samples
Cmax = .1632E+01

| T (min) | C | T(min) | C | T(min) | C | T(min) | C |
|---|---|---|---|---|---|---|---|
| 5.25 | .9319E+00 | 114.25 | .1614E+01 | 130.25 | .3078E+00 | 203.25 | .1062E+00 |
| 210.25 | .4467E-01 | 220.25 | .1930E-01 | 264.25 | .9793E-02 | | |

APD400: anthracene/paraffin beads/Dissolution/50:50
29Aug94

Ms = .530 g   V  =  5.920 mL      Kp =  34.000 mL/g
C0 =  .000    Ss0 = 104.480        Sr0 =  .000
DV1 =  .180 mL   DV2 =  .110 mL        Mr =  1.000
Kr =  .288 mL   kr =  .2530E-04 min^-1   Fr =  .478

REACTOR OPERATION:

| Time Start | Flow | Cin |
|---|---|---|
| .0 | .000 | 0. |
| 130.0 | 1.030 | 0. |
| 190.0 | .000 | 0. |
| 200.0 | 1.030 | 0. |
| 240.0 | .000 | 0. |
| 260.0 | 1.030 | 0. |
| 300.0 | .000 | 0. |
| 330.0 | 1.030 | 0. |
| 372.0 | .000 | 0. |
| 392.0 | 1.030 | 0. |
| 430.0 | .000 | 0. |
| 450.0 | 1.030 | 0. |
| 495.0 | .000 | 0. |
| 1445.0 | 1.030 | 0. |
| 1565.0 | .000 | 0. |
| 1595.0 | 1.030 | 0. |
| 1665.0 | .000 | 0. |
| 1695.0 | 1.030 | 0. |
| 1760.0 | .000 | 0. |
| 1805.0 | 1.030 | 0. |
| 1978.0 | .000 | 0. |
| 2856.0 | 1.030 | 0. |
| 2990.0 | .000 | 0. |
| 3050.0 | 1.030 | 0. |
| 3120.0 | .000 | 0. |
| 3180.0 | 1.030 | 0. |

EXPERIMENT DATA: In-Line Detector
Baseline: Yb = .3085E-07 T + .1629E-03
Response Curve: Equation (C-2)
Ymax = .4847E-01

| T(min) | Y | T(min) | Y | T(min) | Y | T(min) | Y |
|---|---|---|---|---|---|---|---|
| 130.68 | .6284E-01 | 132.68 | .5029E-01 | 135.68 | .4028E-01 | 139.18 | .2891E-01 |
| 143.17 | .1943E-01 | 148.17 | .1299E-01 | 155.67 | .9229E-02 | 165.67 | .7813E-02 |
| 177.67 | .7227E-02 | 189.67 | .6934E-02 | 200.65 | .1660E-01 | 204.65 | .1167E-01 |
| 211.15 | .8203E-02 | 224.15 | .6836E-02 | 239.65 | .6445E-02 | 260.45 | .2334E-01 |
| 263.45 | .1699E-01 | 267.45 | .1167E-01 | 273.45 | .8008E-02 | 283.45 | .6348E-02 |
| 299.93 | .5859E-02 | 330.42 | .2773E-01 | 333.93 | .1895E-01 | 338.92 | .1138E-01 |
| 346.92 | .6982E-02 | 359.42 | .5566E-02 | 371.92 | .5322E-02 | 392.53 | .1997E-01 |
| 396.53 | .1294E-01 | 401.53 | .8447E-02 | 408.53 | .6055E-02 | 419.53 | .5225E-02 |
| 429.53 | .5029E-02 | 450.50 | .1880E-01 | 453.50 | .1353E-01 | 457.50 | .9180E-02 |
| 465.00 | .5908E-02 | 475.00 | .4883E-02 | 484.98 | .4590E-02 | 494.98 | .4541E-02 |
| 1445.62 | .6353E-01 | 1449.62 | .5093E-01 | 1452.62 | .4048E-01 | 1455.62 | .2988E-01 |
| 1459.12 | .1987E-01 | 1462.62 | .1343E-01 | 1469.10 | .7617E-02 | 1481.10 | .4980E-02 |
| 1504.58 | .4346E-02 | 1534.58 | .4004E-02 | 1564.57 | .4053E-02 | 1596.18 | .1934E-01 |
| 1600.18 | .1206E-01 | 1607.17 | .6543E-02 | 1624.17 | .4199E-02 | 1644.17 | .4004E-02 |
| 1664.15 | .3906E-02 | 1695.38 | .1978E-01 | 1699.40 | .1250E-01 | 1706.38 | .6445E-02 |
| 1719.38 | .4053E-02 | 1739.37 | .3564E-02 | 1759.37 | .3418E-02 | 1806.03 | .2227E-01 |
| 1811.03 | .1191E-01 | 1817.03 | .6494E-02 | 1826.03 | .4004E-02 | 1846.02 | .3369E-02 |
| 1866.02 | .3320E-02 | 1888.00 | .3271E-02 | 1918.00 | .3223E-02 | 1947.98 | .3174E-02 |
| 1977.97 | .3125E-02 | 2856.28 | .6074E-02 | 2860.28 | .4878E-01 | 2863.28 | .3843E-01 |
| 2866.28 | .2788E-01 | 2869.27 | .1919E-01 | 2874.27 | .1030E-01 | 2879.27 | .6152E-02 |
| 2889.27 | .3516E-02 | 2909.27 | .2930E-02 | 2929.25 | .2881E-02 | 2949.25 | .2783E-02 |
| 2969.23 | .2734E-02 | 2989.23 | .2734E-02 | 3050.38 | .2383E-01 | 3053.38 | .1665E-01 |
| 3057.38 | .9961E-02 | 3064.37 | .4883E-02 | 3079.37 | .2783E-02 | 3099.35 | .2686E-02 |
| 3119.35 | .2637E-02 | 3181.02 | .2192E-01 | 3184.02 | .1480E-01 | 3188.02 | .8984E-02 |
| 3202.00 | .3320E-02 | 3222.00 | .2734E-02 | 3241.98 | .2637E-02 | 3261.98 | .2588E-02 |

EXPERIMENT DATA: HPLC grab samples
Cmax = .1585E+01

| T (min) | C | T(min) | C | T(min) | C | T(min) | C |
|---|---|---|---|---|---|---|---|
| 131.25 | .1994E+01 | 140.25 | .5268E+00 | 185.25 | .1764E+00 | 226.25 | .1235E+00 |
| 296.25 | .1016E+00 | 490.25 | .9252E-01 | 1446.25 | .2956E+01 | 1555.55 | .7387E-01 |
| 1750.25 | .6124E-01 | 1827.25 | .7394E-01 | 2858.25 | .1988E+01 | 3260.25 | .4425E-01 |
| 3261.25 | .4241E-01 | | | | | | |

RUN POP100:  PFBA\blank\0:100\flow-rate variation
18Aug93

Ms =   .000 g   V  =  6.300 mL
C0 =   .000    Ss0 =   .000           Sr0 =   .000
DV1 =   .180 mL  DV2 =   .110 mL       Mr =  1.000
Kr =       mL  kr =       min^-1    Fr =  1.000

REACTOR OPERATION:

| Time Start | Flow | Cin |
|---|---|---|
| .0 | .916 | 1. |
| 15.0 | .087 | 1. |
| 27.0 | .981 | 1. |
| 43.0 | 1.038 | 0. |
| 53.0 | .088 | 0. |
| 65.0 | 1.032 | 0. |

EXPERIMENT DATA: In-Line Detector
Baseline: Yb =  .0000E+00 T +  .2000E-01
Response Curve: Linear
Ymax =  .7520E+01

| T(min) | Y | T(min) | Y | T(min) | Y | T(min) | Y |
|---|---|---|---|---|---|---|---|
| .29 | .2000E-01 | .99 | .4000E+00 | 1.68 | .1100E+01 | 3.06 | .2300E+01 |
| 5.14 | .3700E+01 | 6.87 | .4600E+01 | 9.12 | .5400E+01 | 10.15 | .5700E+01 |
| 12.75 | .6300E+01 | 13.96 | .6500E+01 | 17.59 | .6700E+01 | 25.20 | .6800E+01 |
| 29.01 | .7000E+01 | 34.20 | .7300E+01 | 37.14 | .7400E+01 | 42.50 | .7500E+01 |
| 44.58 | .6270E+01 | 45.27 | .5600E+01 | 46.31 | .4700E+01 | 47.69 | .3700E+01 |
| 49.07 | .2900E+01 | 50.98 | .2100E+01 | 52.36 | .1680E+01 | 53.40 | .1500E+01 |
| 58.59 | .1400E+01 | 63.78 | .1300E+01 | 65.85 | .1100E+01 | 68.45 | .7200E+00 |
| 70.52 | .5000E+00 | 73.64 | .2800E+00 | 75.54 | .2000E+00 | 79.00 | .1000E+00 |
| 81.77 | .5000E-01 | 84.01 | .3000E-01 | 85.00 | .2000E-01 | | |

Run NOP100:  Naphthalene/blank/0:100/flow-rate variation
12 Dec 93

Ms =   .000 g   V  =  6.570 mL
C0 =   .000    Ss0 =   .000           Sr0 =   .000
DV1 =   .180 mL  DV2 =   .110 mL       Mr =  1.000
Kr =       mL  kr =       min^-1   Fr =  1.000

REACTOR OPERATION:

| Time Start | Flow | Cin |
|---|---|---|
| .0 | 2.100 | 1. |
| 7.0 | .160 | 1. |
| 28.0 | 2.100 | 1. |
| 53.0 | 2.200 | 0. |
| 60.5 | .150 | 0. |
| 80.0 | 2.200 | 0. |

EXPERIMENT DATA: In-Line Detector
Baseline: $Yb = .0000E+00\ T + .3910E-03$
Response Curve: Linear
$Ymax = .3408E-01$

| T(min) | Y | T(min) | Y | T(min) | Y | T(min) | Y |
|---|---|---|---|---|---|---|---|
| .70 | .4736E-02 | 1.70 | .1250E-01 | 2.72 | .1821E-01 | 3.72 | .2246E-01 |
| 4.70 | .2549E-01 | 5.70 | .2778E-01 | 6.72 | .2949E-01 | 7.70 | .2959E-01 |
| 8.70 | .2910E-01 | 9.70 | .2896E-01 | 10.70 | .2896E-01 | 11.70 | .2905E-01 |
| 12.70 | .2910E-01 | 13.70 | .2920E-01 | 14.70 | .2930E-01 | 15.70 | .2935E-01 |
| 16.70 | .2944E-01 | 17.70 | .2954E-01 | 18.70 | .2959E-01 | 19.70 | .2969E-01 |
| 20.70 | .2974E-01 | 21.70 | .2983E-01 | 22.70 | .2988E-01 | 23.70 | .2998E-01 |
| 24.70 | .3003E-01 | 25.70 | .3008E-01 | 26.70 | .3018E-01 | 27.70 | .3023E-01 |
| 28.70 | .3154E-01 | 29.70 | .3232E-01 | 30.70 | .3291E-01 | 31.70 | .3330E-01 |
| 32.70 | .3364E-01 | 33.70 | .3389E-01 | 34.70 | .3408E-01 | 35.70 | .3418E-01 |
| 36.70 | .3428E-01 | 37.70 | .3438E-01 | 38.70 | .3442E-01 | 39.70 | .3438E-01 |
| 40.70 | .3447E-01 | 41.70 | .3442E-01 | 43.70 | .3447E-01 | 44.70 | .3447E-01 |
| 46.70 | .3447E-01 | 47.70 | .3447E-01 | 48.70 | .3452E-01 | 50.68 | .3452E-01 |
| 51.68 | .3452E-01 | 52.68 | .3447E-01 | 53.70 | .3027E-01 | 54.70 | .2256E-01 |
| 55.68 | .1680E-01 | 56.68 | .1250E-01 | 57.68 | .9375E-02 | 58.68 | .7080E-02 |
| 59.68 | .5420E-02 | 60.68 | .4248E-02 | 61.68 | .4590E-02 | 62.68 | .4932E-02 |
| 64.68 | .4932E-02 | 65.68 | .4883E-02 | 66.68 | .4834E-02 | 67.68 | .4736E-02 |
| 68.68 | .4688E-02 | 69.68 | .4590E-02 | 70.68 | .4541E-02 | 71.68 | .4492E-02 |
| 72.68 | .4492E-02 | 73.68 | .4297E-02 | 74.68 | .4297E-02 | 75.68 | .4199E-02 |
| 76.68 | .4102E-02 | 77.68 | .4004E-02 | 78.68 | .3955E-02 | 79.68 | .3906E-02 |
| 80.68 | .2979E-02 | 81.68 | .2344E-02 | 82.68 | .1855E-02 | 83.68 | .1514E-02 |
| 84.68 | .1221E-02 | 85.68 | .1074E-02 | 86.68 | .8790E-03 | 87.68 | .8300E-03 |
| 88.68 | .7320E-03 | 89.68 | .6840E-03 | 90.68 | .5860E-03 | 91.68 | .5860E-03 |
| 92.68 | .5370E-03 | 94.67 | .5370E-03 | 95.68 | .4880E-03 | 96.67 | .4880E-03 |
| 98.68 | .4880E-03 | 99.67 | .4390E-03 | 101.67 | .4390E-03 | 102.67 | .4880E-03 |
| 104.67 | .4390E-03 | 105.67 | .4390E-03 | 107.67 | .4390E-03 | 108.67 | .4390E-03 |

Run AOI203: Anthracene/blank/30:70/Interrupt
6Jul94

$Ms$ = .000 g   $V$ = 6.560 mL
$C0$ = .000   $Ss0$ = .000     $Sr0$ = .000
$DV1$ = .180 mL   $DV2$ = .110 mL     $Mr$ = 1.000
$Kr$ =   mL   $kr$ =   min^-1   $Fr$ = 1.000

REACTOR OPERATION:

| Time Start | Flow | Cin |
|---|---|---|
| .0 | .970 | 1. |
| 15.0 | .000 | 1. |
| 76.0 | .970 | 1. |
| 105.0 | 1.030 | 0. |
| 115.0 | .000 | 0. |
| 175.0 | 1.030 | 0. |

EXPERIMENT DATA: In-Line Detector
Baseline: $Yb$ = .1903E-05 $T$ + -.3909E-03
Response Curve: Linear
$Ymax$ = .3581E-01

| T(min) | Y | T(min) | Y | T(min) | Y | T(min) | Y |
|---|---|---|---|---|---|---|---|
| .65 | .1950E-03 | 1.15 | .2002E-02 | 1.65 | .3955E-02 | 2.15 | .5908E-02 |
| 2.65 | .7617E-02 | 3.15 | .9375E-02 | 3.65 | .1089E-01 | 4.15 | .1240E-01 |
| 4.65 | .1377E-01 | 5.15 | .1504E-01 | 5.65 | .1621E-01 | 6.15 | .1738E-01 |
| 6.65 | .1846E-01 | 7.15 | .1939E-01 | 7.65 | .2036E-01 | 8.15 | .2114E-01 |
| 9.15 | .2275E-01 | 10.15 | .2417E-01 | 11.15 | .2534E-01 | 12.13 | .2637E-01 |
| 12.63 | .2681E-01 | 13.13 | .2725E-01 | 13.65 | .2773E-01 | 14.15 | .2808E-01 |
| 14.65 | .2852E-01 | 75.60 | .2690E-01 | 76.10 | .2744E-01 | 76.60 | .2793E-01 |
| 77.10 | .2832E-01 | 77.60 | .2881E-01 | 78.10 | .2910E-01 | 79.10 | .2983E-01 |
| 80.10 | .3037E-01 | 81.10 | .3091E-01 | 82.10 | .3140E-01 | 83.10 | .3174E-01 |
| 84.10 | .3218E-01 | 85.60 | .3262E-01 | 87.10 | .3311E-01 | 88.60 | .3340E-01 |
| 90.10 | .3364E-01 | 91.60 | .3389E-01 | 93.10 | .3408E-01 | 94.60 | .3428E-01 |
| 96.10 | .3438E-01 | 97.60 | .3457E-01 | 99.10 | .3462E-01 | 101.10 | .3477E-01 |
| 103.08 | .3481E-01 | 105.10 | .3496E-01 | 105.58 | .3457E-01 | 106.08 | .3276E-01 |
| 106.58 | .3086E-01 | 107.10 | .2896E-01 | 107.60 | .2720E-01 | 108.08 | .2559E-01 |
| 108.58 | .2402E-01 | 109.08 | .2256E-01 | 109.58 | .2119E-01 | 110.08 | .1992E-01 |
| 110.58 | .1870E-01 | 111.08 | .1758E-01 | 111.58 | .1650E-01 | 112.08 | .1553E-01 |
| 112.58 | .1460E-01 | 113.08 | .1372E-01 | 113.58 | .1289E-01 | 114.08 | .1216E-01 |
| 114.58 | .1148E-01 | 175.48 | .1196E-01 | 175.98 | .1123E-01 | 176.48 | .1055E-01 |
| 176.98 | .9912E-02 | 177.48 | .9277E-02 | 177.98 | .8691E-02 | 178.98 | .7715E-02 |
| 179.98 | .6787E-02 | 180.98 | .6055E-02 | 181.98 | .5371E-02 | 183.48 | .4492E-02 |
| 184.98 | .3809E-02 | 186.48 | .3223E-02 | 188.48 | .2637E-02 | 190.48 | .2148E-02 |
| 192.48 | .1758E-02 | 194.48 | .1465E-02 | 196.98 | .1221E-02 | 199.47 | .9770E-03 |

201.97 .8790E-03 204.47 .7810E-03 207.48 .6350E-03 210.47 .5860E-03
213.47 .4390E-03 216.47 .4880E-03 219.47 .4390E-03 222.47 .3420E-03
225.47 .3910E-03 228.47 .2930E-03 231.47 .2930E-03 234.47 .2930E-03

EXPERIMENT DATA: HPLC grab samples
Cmax = .1502E+00

| T (min) | C | T(min) | C | T(min) | C | T(min) | C |
|---|---|---|---|---|---|---|---|
| 13.28 | .1235E+00 | 95.31 | .1560E+00 | 112.28 | .6192E-01 | 185.26 | .1565E-01 |
| 195.26 | .5938E-02 | 214.27 | .0000E+00 | 223.27 | .0000E+00 | | |

Run AOI206: Anthracene/blank/30:70/Interrupt
2Jun94

$Ms$ = .000 g   $V$ = 6.520 mL
$C0$ = .000   $Ss0$ = .000   $Sr0$ = .000
$DV1$ = .180 mL   $DV2$ = .110 mL   $Mr$ = 1.000
$Kr$ =   mL   $kr$ =   min^-1   $Fr$ = 1.000

REACTOR OPERATION:

| Time Start | Flow | Cin |
|---|---|---|
| .0 | 1.064 | 1. |
| 11.0 | .000 | 1. |
| 71.0 | 1.064 | 1. |
| 127.0 | 1.033 | 0. |
| 138.0 | .000 | 0. |
| 198.0 | 1.033 | 0. |

EXPERIMENT DATA: In-Line Detector
Baseline: $Yb$ = .6792E-06 T + .8150E-06
Response Curve: Linear
Ymax = .3461E-01

| T(min) | Y | T(min) | Y | T(min) | Y | T(min) | Y |
|---|---|---|---|---|---|---|---|
| .80 | .1465E-02 | 1.30 | .3613E-02 | 1.80 | .5811E-02 | 2.30 | .7813E-02 |
| 2.80 | .9668E-02 | 3.30 | .1138E-01 | 3.80 | .1294E-01 | 4.28 | .1445E-01 |
| 4.78 | .1587E-01 | 5.28 | .1714E-01 | 5.78 | .1831E-01 | 6.28 | .1934E-01 |
| 6.80 | .2041E-01 | 7.28 | .2129E-01 | 7.78 | .2222E-01 | 8.30 | .2305E-01 |
| 8.78 | .2368E-01 | 9.28 | .2437E-01 | 9.78 | .2505E-01 | 10.28 | .2564E-01 |
| 10.78 | .2617E-01 | 71.60 | .2354E-01 | 72.10 | .2437E-01 | 72.60 | .2510E-01 |
| 73.10 | .2578E-01 | 73.60 | .2627E-01 | 74.10 | .2686E-01 | 74.60 | .2734E-01 |
| 75.60 | .2827E-01 | 76.60 | .2905E-01 | 78.10 | .3008E-01 | 79.60 | .3086E-01 |
| 81.60 | .3164E-01 | 83.60 | .3218E-01 | 85.60 | .3267E-01 | 88.10 | .3306E-01 |

```
 91.10 .3350E-01  94.60 .3374E-01  98.08 .3389E-01 102.08 .3408E-01
106.08 .3418E-01 110.08 .3428E-01 114.08 .3428E-01 118.08 .3438E-01
122.08 .3438E-01 126.08 .3447E-01 127.58 .3389E-01 128.08 .3184E-01
128.58 .2974E-01 129.08 .2773E-01 129.58 .2583E-01 130.08 .2417E-01
130.58 .2256E-01 131.08 .2100E-01 131.58 .1963E-01 132.08 .1836E-01
132.58 .1719E-01 133.08 .1602E-01 133.58 .1499E-01 134.08 .1401E-01
134.58 .1318E-01 135.08 .1231E-01 135.58 .1157E-01 136.08 .1089E-01
136.58 .1021E-01 137.08 .9619E-02 137.58 .9082E-02 198.43 .1040E-01
198.93 .9668E-02 199.45 .8984E-02 199.93 .8447E-02 200.45 .7861E-02
200.93 .7422E-02 201.43 .6934E-02 202.43 .6055E-02 203.43 .5420E-02
204.43 .4785E-02 205.93 .4004E-02 207.43 .3418E-02 208.93 .2881E-02
210.93 .2441E-02 212.93 .2002E-02 214.93 .1709E-02 216.93 .1465E-02
219.43 .1172E-02 222.43 .1025E-02 225.43 .8300E-03 228.43 .7320E-03
231.93 .6350E-03 235.93 .4880E-03 239.42 .4880E-03 243.43 .4390E-03
248.42 .3910E-03 253.42 .3420E-03 258.42 .3420E-03 263.42 .2440E-03
268.42 .2930E-03 273.42 .2440E-03 278.42 .1950E-03 283.42 .1950E-03
```

Run AOI206r: Anthracene/blank/30:70/Interruption
20Jun94

$M_s$ =   .000 g   V =  6.530 mL
$C_0$ =   .000   $S_{s0}$ =   .000      $S_{r0}$ =   .000
$DV_1$ =  .180 mL  $DV_2$ =   .110 mL      $M_r$ =  1.000
$K_r$ =        $k_r$ =      min^-1    $F_r$ =  1.000

REACTOR OPERATION:

| Time Start | Flow | Cin |
|---|---|---|
| .0 | .950 | 1. |
| 12.0 | .000 | 1. |
| 73.0 | .950 | 1. |
| 130.0 | 1.030 | 0. |
| 142.0 | .000 | 0. |
| 202.0 | 1.030 | 0. |

EXPERIMENT DATA: In-Line Detector
Baseline: $Y_b$ = .2502E-05 T + -.1940E-03
Response Curve: Linear
$Y_{max}$ = .3705E-01

| T(min) | Y | T(min) | Y | T(min) | Y | T(min) | Y |
|---|---|---|---|---|---|---|---|
| .60 | -0.000098 | 1.10 | .1465E-02 | 1.60 | .3369E-02 | 2.10 | .5322E-02 |
| 2.60 | .7178E-02 | 3.10 | .8838E-02 | 3.60 | .1055E-01 | 4.10 | .1211E-01 |

| | | | | | | | |
|---|---|---|---|---|---|---|---|
| 4.60 | .1353E-01 | 5.10 | .1494E-01 | 5.60 | .1616E-01 | 6.10 | .1743E-01 |
| 6.60 | .1841E-01 | 7.10 | .1953E-01 | 7.60 | .2041E-01 | 8.10 | .2139E-01 |
| 8.60 | .2217E-01 | 9.10 | .2300E-01 | 9.60 | .2383E-01 | 10.10 | .2441E-01 |
| 10.60 | .2515E-01 | 11.10 | .2568E-01 | 11.60 | .2637E-01 | 12.10 | .2681E-01 |
| 73.80 | .2466E-01 | 74.32 | .2539E-01 | 74.82 | .2607E-01 | 75.32 | .2666E-01 |
| 75.82 | .2725E-01 | 76.32 | .2773E-01 | 77.32 | .2871E-01 | 78.32 | .2959E-01 |
| 79.32 | .3037E-01 | 80.80 | .3130E-01 | 82.32 | .3208E-01 | 84.30 | .3286E-01 |
| 86.30 | .3359E-01 | 88.80 | .3423E-01 | 91.30 | .3477E-01 | 93.80 | .3506E-01 |
| 96.80 | .3545E-01 | 100.30 | .3579E-01 | 104.30 | .3599E-01 | 108.30 | .3613E-01 |
| 112.30 | .3633E-01 | 116.30 | .3638E-01 | 120.30 | .3643E-01 | 124.28 | .3652E-01 |
| 129.78 | .3657E-01 | 130.28 | .3652E-01 | 130.78 | .3604E-01 | 131.28 | .3403E-01 |
| 131.80 | .3203E-01 | 132.28 | .3008E-01 | 132.78 | .2822E-01 | 133.30 | .2647E-01 |
| 133.78 | .2485E-01 | 134.30 | .2344E-01 | 134.78 | .2197E-01 | 135.28 | .2061E-01 |
| 135.78 | .1939E-01 | 136.28 | .1821E-01 | 136.78 | .1719E-01 | 137.28 | .1611E-01 |
| 137.78 | .1519E-01 | 138.28 | .1426E-01 | 138.78 | .1348E-01 | 139.28 | .1274E-01 |
| 139.78 | .1196E-01 | 140.28 | .1138E-01 | 140.78 | .1069E-01 | 141.28 | .1016E-01 |
| 141.78 | .9521E-02 | 202.52 | .1162E-01 | 203.02 | .1079E-01 | 203.52 | .1006E-01 |
| 204.02 | .9424E-02 | 204.52 | .8887E-02 | 205.02 | .8350E-02 | 206.02 | .7422E-02 |
| 207.02 | .6543E-02 | 208.02 | .5859E-02 | 209.02 | .5176E-02 | 210.52 | .4395E-02 |
| 212.02 | .3760E-02 | 213.50 | .3223E-02 | 215.52 | .2686E-02 | 217.52 | .2246E-02 |
| 219.52 | .1855E-02 | 222.00 | .1563E-02 | 225.00 | .1270E-02 | 228.00 | .1074E-02 |
| 231.50 | .9280E-03 | 234.50 | .7810E-03 | 237.50 | .6840E-03 | 240.50 | .6350E-03 |
| 243.50 | .6350E-03 | 246.50 | .5370E-03 | 249.50 | .5370E-03 | 252.50 | .4880E-03 |

Run AEO210: Anthracene/blank/30:70/Interrupt
8Jul94

Ms  =  1.000 g    V  =  11.040 mL       Kp  =   3.050 mL/g
C0 =   .000    Ss0 =   .000      Sr0 =   .000
DV1 =   .180 mL   DV2 =   .110 mL      Mr  =  1.000
Kr  =  1.000 mL   kr  =  .1000E+01 min^-1   Fr  =   1.000

REACTOR OPERATION:

| Time Start | Flow | Cin |
|---|---|---|
| .0 | .890 | 1. |
| 27.0 | .000 | 1. |
| 87.0 | .890 | 1. |
| 163.0 | 1.030 | 0. |
| 190.0 | .000 | 0. |
| 250.0 | 1.030 | 0. |

EXPERIMENT DATA: In-Line Detector
Baseline: $Yb$ = .1090E-05 T + .2399E-03
Response Curve: Linear
$Ymax$ = .3588E-01

| T(min) | Y | T(min) | Y | T(min) | Y | T(min) | Y |
|---|---|---|---|---|---|---|---|
| .67 | .5370E-03 | 1.67 | .2832E-02 | 2.67 | .5176E-02 | 3.67 | .7373E-02 |
| 4.67 | .9473E-02 | 5.67 | .1133E-01 | 6.67 | .1314E-01 | 7.65 | .1475E-01 |
| 8.67 | .1626E-01 | 9.67 | .1768E-01 | 10.67 | .1895E-01 | 11.65 | .2022E-01 |
| 13.17 | .2183E-01 | 14.67 | .2324E-01 | 16.17 | .2456E-01 | 17.67 | .2578E-01 |
| 19.15 | .2676E-01 | 20.65 | .2773E-01 | 22.15 | .2852E-01 | 24.15 | .2954E-01 |
| 24.65 | .2969E-01 | 25.15 | .2993E-01 | 25.65 | .3013E-01 | 26.15 | .3037E-01 |
| 26.65 | .3057E-01 | 87.28 | .2974E-01 | 87.78 | .3027E-01 | 88.28 | .3052E-01 |
| 88.78 | .3076E-01 | 89.28 | .3091E-01 | 89.78 | .3110E-01 | 91.78 | .3184E-01 |
| 93.78 | .3242E-01 | 95.78 | .3286E-01 | 97.78 | .3335E-01 | 100.28 | .3379E-01 |
| 103.28 | .3423E-01 | 106.78 | .3467E-01 | 110.78 | .3501E-01 | 114.77 | .3525E-01 |
| 118.77 | .3550E-01 | 123.27 | .3574E-01 | 128.27 | .3594E-01 | 133.27 | .3599E-01 |
| 138.27 | .3613E-01 | 143.27 | .3618E-01 | 148.27 | .3628E-01 | 153.25 | .3628E-01 |
| 158.25 | .3638E-01 | 162.75 | .3643E-01 | 163.75 | .3579E-01 | 164.25 | .3457E-01 |
| 164.77 | .3320E-01 | 165.25 | .3193E-01 | 165.77 | .3076E-01 | 166.75 | .2842E-01 |
| 167.75 | .2622E-01 | 168.75 | .2427E-01 | 169.75 | .2246E-01 | 170.75 | .2070E-01 |
| 172.25 | .1846E-01 | 173.75 | .1646E-01 | 175.25 | .1465E-01 | 176.75 | .1309E-01 |
| 178.25 | .1172E-01 | 179.75 | .1050E-01 | 181.25 | .9375E-02 | 183.25 | .8154E-02 |
| 185.25 | .7080E-02 | 187.25 | .6201E-02 | 187.75 | .5957E-02 | 188.25 | .5811E-02 |
| 188.75 | .5664E-02 | 189.25 | .5420E-02 | 189.75 | .5273E-02 | 250.63 | .6104E-02 |
| 251.15 | .5811E-02 | 251.63 | .5566E-02 | 252.15 | .5371E-02 | 252.63 | .5176E-02 |
| 253.13 | .5029E-02 | 254.13 | .4688E-02 | 255.63 | .4248E-02 | 257.13 | .3906E-02 |
| 258.65 | .3516E-02 | 260.63 | .3174E-02 | 263.13 | .2783E-02 | 265.63 | .2441E-02 |
| 268.63 | .2148E-02 | 271.63 | .1855E-02 | 275.13 | .1660E-02 | 278.63 | .1465E-02 |
| 282.63 | .1367E-02 | 286.63 | .1172E-02 | 290.63 | .1172E-02 | 294.63 | .1074E-02 |
| 298.62 | .1025E-02 | 302.62 | .1025E-02 | 306.62 | .9770E-03 | 309.62 | .9770E-03 |

EXPERIMENT DATA: HPLC grab samples
$Cmax$ = .1564E+00

| T(min) | C | T(min) | C | T(min) | C | T(min) | C |
|---|---|---|---|---|---|---|---|
| 23.29 | .1113E+00 | 153.30 | .1569E+00 | 179.24 | .4002E-01 | 260.28 | .1027E-01 |
| 275.25 | .4978E-02 | 290.28 | .2786E-02 | 308.28 | .1539E-02 | | |

Run AOI300: Anthracene Blank/50:50/Interruption
29Jun94

Ms = 1.000 g   V = 6.370 mL       Kp =  .288 mL/g
C0 =  .000   Ss0 =  .000     Sr0 =  .000
DV1 =  .180 mL   DV2 =  .110 mL     Mr = 1.000
Kr = 1.000 mL   kr = .1000E+01 min^-1   Fr = 1.000

REACTOR OPERATION:

| Time Start | Flow | Cin |
|---|---|---|
| .0 | 1.040 | 1. |
| 7.0 | .000 | 1. |
| 67.0 | 1.040 | 1. |
| 71.0 | .000 | 1. |
| 315.0 | 1.040 | 1. |
| 319.0 | .000 | 1. |
| 1200.0 | 1.040 | 1. |
| 1277.0 | 1.030 | 0. |
| 1297.0 | .000 | 0. |
| 1380.0 | 1.030 | 0. |

EXPERIMENT DATA: In-Line Detector
Baseline: Yb = .0000E+00 T + -.3430E-04
Response Curve: Equation (C-2)
Ymax = .5153E-01

| T(min) | Y | T(min) | Y | T(min) | Y | T(min) | Y |
|---|---|---|---|---|---|---|---|
| .78 | .5469E-02 | 1.27 | .1245E-01 | 1.77 | .1841E-01 | 2.27 | .2334E-01 |
| 2.77 | .2739E-01 | 3.28 | .3076E-01 | 3.77 | .3355E-01 | 4.27 | .3584E-01 |
| 4.77 | .3779E-01 | 5.28 | .3945E-01 | 5.77 | .4082E-01 | 6.27 | .4199E-01 |
| 6.77 | .4302E-01 | 67.37 | .4409E-01 | 67.87 | .4492E-01 | 68.37 | .4556E-01 |
| 68.87 | .4614E-01 | 69.37 | .4668E-01 | 69.87 | .4712E-01 | 70.37 | .4751E-01 |
| 70.87 | .4790E-01 | 315.30 | .4824E-01 | 315.80 | .4849E-01 | 316.30 | .4873E-01 |
| 316.80 | .4902E-01 | 317.30 | .4922E-01 | 317.80 | .4941E-01 | 318.30 | .4956E-01 |
| 318.80 | .4971E-01 | 1200.35 | .5000E-01 | 1200.85 | .5000E-01 | 1203.35 | .5049E-01 |
| 1208.35 | .5098E-01 | 1213.35 | .5122E-01 | 1218.35 | .5132E-01 | 1223.33 | .5137E-01 |
| 1228.33 | .5137E-01 | 1233.33 | .5137E-01 | 1238.33 | .5137E-01 | 1243.33 | .5137E-01 |
| 1248.33 | .5142E-01 | 1253.33 | .5137E-01 | 1258.33 | .5137E-01 | 1263.32 | .5137E-01 |
| 1268.32 | .5137E-01 | 1273.32 | .5137E-01 | 1277.32 | .5137E-01 | 1277.82 | .5010E-01 |
| 1278.32 | .4868E-01 | 1278.82 | .4717E-01 | 1279.32 | .4556E-01 | 1279.82 | .4395E-01 |
| 1280.32 | .4224E-01 | 1280.82 | .4048E-01 | 1281.32 | .3877E-01 | 1281.82 | .3696E-01 |
| 1282.32 | .3516E-01 | 1282.82 | .3340E-01 | 1283.32 | .3154E-01 | 1283.82 | .2979E-01 |
| 1284.32 | .2808E-01 | 1284.82 | .2647E-01 | 1285.32 | .2481E-01 | 1285.82 | .2324E-01 |
| 1286.32 | .2173E-01 | 1286.82 | .2031E-01 | 1287.32 | .1895E-01 | 1287.82 | .1768E-01 |
| 1288.32 | .1646E-01 | 1289.32 | .1426E-01 | 1290.32 | .1231E-01 | 1291.32 | .1060E-01 |

```
1292.32 .9082E-02 1293.32 .7813E-02 1294.32 .6641E-02 1294.82 .6152E-02
1295.32 .5713E-02 1295.82 .5273E-02 1296.32 .4883E-02 1296.82 .4492E-02
1380.43 .4883E-02 1380.93 .4346E-02 1381.43 .3955E-02 1381.93 .3662E-02
1382.43 .3369E-02 1382.93 .3125E-02 1383.93 .2637E-02 1384.93 .2295E-02
1385.93 .1953E-02 1387.43 .1514E-02 1389.43 .1074E-02 1391.43 .7810E-03
1393.43 .5860E-03 1398.43 .2440E-03 1403.43 .9800E-04 1408.42 .4900E-04
1413.42 .0000E+00 1418.42 .0000E+00 1423.42 .0000E+00 1428.42 .0000E+00
```

EXPERIMENT DATA: HPLC grab samples
Cmax = .2184E+01

| T (min) | C | T(min) | C | T(min) | C | T(min) | C |
|---|---|---|---|---|---|---|---|
| 6.30 | .1267E+01 | 70.29 | .1664E+01 | 315.32 | .1756E+01 | 318.30 | .1904E+01 |
| 1201.29 | .2101E+01 | 1275.28 | .2297E+01 | 1296.28 | .1236E+00 | 1380.48 | .1587E+00 |
| 1461.30 | .7275E-02 | | | | | | |

Run AOI301: Anthracene Blank/50:50/Interruption
29Jul94

Ms = 1.000 g   V = 6.510 mL      Kp = .096 mL/g
C0 = .000   Ss0 = .000      Sr0 = .000
DV1 = .180 mL   DV2 = .110 mL      Mr = 1.000
Kr = 1.000 mL   kr = .1000E+01 min^-1   Fr = 1.000

REACTOR OPERATION:

| Time Start | Flow | Cin |
|---|---|---|
| .0 | 1.030 | 1. |
| 7.5 | .000 | 1. |
| 67.5 | 1.030 | 1. |
| 120.0 | 1.030 | 0. |
| 137.5 | .000 | 0. |
| 197.5 | 1.030 | 0. |

EXPERIMENT DATA: In-Line Detector
Baseline: Yb = -.1046E-06 T + .4911E-04
Response Curve: Equation (C-2)
Ymax = .5001E-01

| T(min) | Y | T(min) | Y | T(min) | Y | T(min) | Y |
|---|---|---|---|---|---|---|---|
| .63 | .3125E-02 | 1.15 | .1016E-01 | 1.63 | .1611E-01 | 2.13 | .2109E-01 |
| 2.63 | .2524E-01 | 3.13 | .2871E-01 | 3.63 | .3154E-01 | 4.13 | .3389E-01 |
| 4.63 | .3589E-01 | 5.13 | .3755E-01 | 5.63 | .3897E-01 | 6.13 | .4019E-01 |
| 6.63 | .4126E-01 | 7.13 | .4219E-01 | 68.03 | .4360E-01 | 68.53 | .4424E-01 |

| | | | | | | | |
|---|---|---|---|---|---|---|---|
| 69.03 | .4473E-01 | 69.53 | .4522E-01 | 70.03 | .4565E-01 | 70.53 | .4605E-01 |
| 71.03 | .4644E-01 | 71.53 | .4678E-01 | 72.03 | .4707E-01 | 72.53 | .4731E-01 |
| 73.53 | .4785E-01 | 74.53 | .4815E-01 | 75.53 | .4849E-01 | 77.03 | .4883E-01 |
| 78.53 | .4912E-01 | 80.53 | .4941E-01 | 83.03 | .4966E-01 | 85.53 | .4981E-01 |
| 88.03 | .4990E-01 | 90.52 | .5000E-01 | 93.03 | .5000E-01 | 95.52 | .5005E-01 |
| 98.03 | .5005E-01 | 100.53 | .5010E-01 | 103.02 | .5010E-01 | 105.52 | .5010E-01 |
| 108.02 | .5010E-01 | 110.52 | .5010E-01 | 113.02 | .5010E-01 | 115.52 | .5010E-01 |
| 118.02 | .5010E-01 | 120.02 | .5010E-01 | 120.52 | .4990E-01 | 121.02 | .4854E-01 |
| 121.52 | .4707E-01 | 122.02 | .4551E-01 | 122.52 | .4385E-01 | 123.02 | .4219E-01 |
| 123.52 | .4048E-01 | 124.02 | .3877E-01 | 124.52 | .3696E-01 | 125.02 | .3525E-01 |
| 125.52 | .3350E-01 | 126.02 | .3174E-01 | 126.52 | .2998E-01 | 127.02 | .2832E-01 |
| 127.52 | .2666E-01 | 128.02 | .2505E-01 | 128.52 | .2349E-01 | 129.02 | .2202E-01 |
| 129.52 | .2061E-01 | 130.02 | .1924E-01 | 130.52 | .1797E-01 | 131.02 | .1670E-01 |
| 132.02 | .1450E-01 | 133.02 | .1255E-01 | 134.00 | .1084E-01 | 135.02 | .9326E-02 |
| 135.52 | .8643E-02 | 136.00 | .8008E-02 | 136.52 | .7471E-02 | 137.02 | .6885E-02 |
| 137.50 | .6445E-02 | 197.93 | .6592E-02 | 198.43 | .5908E-02 | 198.93 | .5469E-02 |
| 199.43 | .5029E-02 | 199.93 | .4688E-02 | 200.43 | .4297E-02 | 200.93 | .4004E-02 |
| 201.43 | .3711E-02 | 201.93 | .3418E-02 | 202.43 | .3174E-02 | 203.43 | .2734E-02 |
| 204.43 | .2344E-02 | 205.93 | .1904E-02 | 207.43 | .1514E-02 | 209.43 | .1172E-02 |
| 211.93 | .8300E-03 | 214.43 | .5860E-03 | 216.93 | .4390E-03 | 219.43 | .3420E-03 |
| 221.93 | .2930E-03 | 224.43 | .2440E-03 | 226.93 | .1950E-03 | 229.43 | .1950E-03 |

EXPERIMENT DATA: HPLC grab samples

$C_{max}$ = .1750E+01

| T(min) | C | T(min) | C | T(min) | C | T(min) | C |
|---|---|---|---|---|---|---|---|
| 5.30 | .8894E+00 | 105.25 | .1619E+01 | 130.27 | .3466E+00 | 200.28 | .7793E-01 |
| 205.28 | .3798E-01 | 210.29 | .1919E-01 | 220.27 | .6085E-02 | 230.27 | .3405E-02 |

## APPENDIX D
## COMPUTER PROGRAMS

Four FORTRAN computer programs used during the course of this research are presented in this appendix. The first program, DATAMAN, was used to convert raw data into a form that could be used by the fitting models. The primary function of this program was to account for dead volumes in the experimental apparatus and to convert time and concentration units to those used by the model (Equations 3-9i and 3-9k). The remaining three programs are the University of Wisconsin nonlinear least-squares fitting program, TESTFIT, which was adapted to fit mass transfer parameters to stir cell breakthrough curves. The complete program is listed for the version designated TWOSITE, which fits breakthrough curve data to the two-site model (Equations 3-16 through 3-18). The program TESTFIT is essentially unchanged for the last two programs, so only the relevant subroutine, MODEL, is listed. These last two programs are designated MSPLN, which fits the MSP model (Equations 3-12, 4-5, and 4-8) using a log-normal distribution, and MSSSP, which fits the MSS model (Equations 3-12, 4-5, and 4-11 through 4-13) using a spherical distribution.

```
********************************************************************
*
*    FROM: EDWARD HEYSE
*         DEPARTMENT OF ENVIRONMENTAL ENGINEERING SCIENCES
*         UNIVERSITY OF FLORIDA
*         GAINEVILLE, FLORIDA 32611 U.S.A.
*
********************************************************************
********************************************************************
      PROGRAM DATAMAN
********************************************************************
C
C   Program to create data file from CSTR flow perturbation experiments
C   Special program for anthracene in 50:50 MeOH/H20
C   Nonlinear response curve on in-line detector data
C   for R>0.02: C = a1 R + a2 R^2 + a3 R^3
C   a1 = 17.701   a2 = -527.08   a3 =12001.
C   for R<0.02: C = 11.9598 R
C   Unit 30 = Input file for Test fit program
C
********************************************************************
*
*    Variable Declarations
*
********************************************************************
C
      IMPLICIT DOUBLE PRECISION (A-H, O-Z)
      PARAMETER (PI=3.1415926538D0)
      PARAMETER (NR=20, ND=50*NR)
      DIMENSION TS(0:NR), Q(0:NR), CIN(0:NR), DT(0:ND)
      DIMENSION XT(0:NR), XPV(0:NR), XFDT(0:NR), XQ(0:NR), XCIN(0:NR)
      DIMENSION SQ(0:ND), CC(0:ND), T(0:ND), PV(0:ND), C(0:ND)
      CHARACTER*15 INFIL, OUTFIL, OUT2FIL, INPUT, OUTPUT, OUT2
      CHARACTER*10 TITLE(6), DATE
      QMAX=1.d0
C
********************************************************************
*    INPUT - OUTPUT FILES
********************************************************************
C
      WRITE(6,*) 'Name of input file'
      READ(5,1000) INFIL
      INPUT = INFIL
      WRITE(6,*) 'Name of testfit input file'
```

```
      READ(5,1000) OUT2FIL
      OUT2 = OUT2FIL
 c    OPEN (UNIT = 10, FILE = OUTPUT, STATUS = 'NEW')
      OPEN (UNIT = 20, FILE = INPUT, STATUS = 'OLD')
      OPEN (UNIT = 30, FILE = OUT2, STATUS = 'NEW')
 C
 ***********************************************************************
 *    INPUT FORMAT
 *
 *    Title of Experiment
 *    Date
 *    M V DV1 DV2
 *    Co Sso Sro
 *    Koc k F foc
 *    Mr Kpr kr Fr
 *    #flow changes
 *    TS(1) Q(1) Cin(1)  (note: TS = time new flow starts)
 *    TS(2) Q(2) Cin(2)
 *    .....
 *    T1 SQ1 C1      (t=T1; Squ.# @ t=T1, Conc. @T1)
 *    T2 SQ2 C2      (note: C1 and C2 must represent the baseline!)
 *    CCO            (normalizing concentration)
 *    # observations
 *    SQ(1) CC(1)    (squ #; chart concentration)
 *    SQ(2) CC(2)
 *    .....
 *
 *
 ***********************************************************************
 *
 *       ASSUMED UNITS:
 *
 *    Mass = g    Volume = mL    Flow Rate = mL/min
 *
 *    Time = min   Kd = mL/g   k2 = hr^-1   k = min^-1
 *
 ***********************************************************************
 C
 C DATA IDENTIFICATION
 C
      READ(20,1500)TITLE(1),TITLE(2),TITLE(3),TITLE(4),TITLE(5),TITLE(6)
      READ(20,1100) DATE
      WRITE(30,2500) TITLE(1),TITLE(2),TITLE(3),TITLE(4),TITLE(5),TITLE
     +(6),DATE
```

```
C
C
C  READ REACTOR DIMENSIONS/CONDITIONS
C
      READ(20,*) XM,V,DV1,DV2
      READ(20,*) PC0,PS0,PSR0
C
C  READ SOLIDS PROPERTIES
C
      READ(20,*) XKOC,XK,F,FOC
      XKD = XKOC*FOC
      XK2 = XK*60.d0/(1.d0-F)
      IF (XK2.EQ.0) GO TO 50
      GO TO 70
   50 XK2 = 2.d0*(XKD**(-0.668d0))
      XK = XK2*(1.d0-F)/60.d0
   70 CONTINUE
C
C  READ REACTOR PROPERTIES
C
      READ(20,*) XMR,XKPR,XKR,XFR
      R = 1.d0 + XM*XKD/V
      BETA = (1.d0 + F*XM*XKD/V)/R
      OMEGA = R*(1.d0-BETA)*XK2*V/(QMAX*60.d0)
      WRITE(30,2700) XKOC,XK,F,PS0,PSR0
      WRITE(30,6000) FOC,XM,V,PC0
      WRITE(30,6000) XMR,XKPR,XKR,XFR
C
C  READ EXPERIMENT OPERATION DATA
C
      READ(20,*) NFR
      DO 100 I = 1,NFR
      READ(20,*) TS(I),Q(I),CIN(I)
  100 CONTINUE
C
C  ESTABLISH TEMPORAL COORDINATE SYSTEMS
C
c     WRITE(10,3500)
      TS(NFR + 1) = TS(NFR) + 30.d0
      J = 0
      DPV = 0.d0
      DO 300 I = 1,NFR
      J = J + 1
      IF (I.EQ.1) GO TO 210
```

```
      GO TO 220
  210 XT(J)=TS(I)+(DV1+DV2)/Q(I)
      XPV(J)=0
      DPV=-DV1/V
      GO TO 280
  220 CONTINUE
      IF (Q(I).EQ.0.) GO TO 230
      GO TO 240
  230 XT(J)=TS(I+1)+DV2/Q(I+1)
      XFDT(J)=QMAX*(TS(I+1)-TS(I))/V
      GO TO 260
  240 CONTINUE
      XT(J)=TS(I)+DV2/Q(I)
  260 XPV(J)=XPV(J-1)+DPV+Q(I-1)*(TS(I)-TS(I-1))/V
      DPV=0.d0
      IF (CIN(I).NE.CIN(I-1)) GO TO 270
      GO TO 280
  270 CONTINUE
      IF (Q(I).EQ.0.) GO TO 280
      IF (Q(I-1).EQ.0.) GO TO 280
      XCIN(J)=CIN(I-1)
      XQ(J)=Q(I)
      J=J+1
      XT(J)=TS(I)+(DV1+DV2)/Q(I)
      XPV(J)=XPV(J-1)+DV1/V
      DPV=-DV1/V
  280 XCIN(J)=CIN(I)
      IF (Q(I).EQ.0.) XCIN(J)=0.
      XQ(J)=Q(I)
  290 CONTINUE
  300 CONTINUE
C
C   CALCULATE NO. EFFECTIVE FLOW DOMAINS
C
      NEFD=J
      WRITE(30,2900) NEFD
C
C   READ CHART SPEED AND BASELINE INFORMATION
C
      READ(20,*) T1,SQ1,C1,T2,SQ2,C2
      CHTSPD=(SQ2-SQ1)/(T2-T1)
      BSLN=(C2-C1)/(T2-T1)
C
C  CALCULATE FINAL DIMENSIONLESS TIMES
```

```fortran
C
    XPV(J+1)=XPV(J)+Q(NFR)*(T2-TS(NFR))/V
    DO 310 I=1,NEFD
    IF (XQ(I).EQ.0.) GO TO 303
    XFDT(I)=QMAX*(XPV(I+1)-XPV(I))/XQ(I)
303 CONTINUE
310 WRITE(30,6100) I,XFDT(I),XQ(I),XCIN(I)
    WRITE(30,2800)
C
C CONCENTRATION NORMALIZATION
C
    READ(20,*) CCO
C
C READ EXPERIMENTAL RESULTS
C
    READ(20,*) NOBS
    DO 400 I=1,NOBS
    READ(20,*) SQ(I), CC(I)
    PV(I)=-(DV1+DV2)/V
    T(I)=(SQ(I)-SQ1)/CHTSPD+T1
    RESP0=17.701*CCO-527.08*CCO**2.+12001.*CCO**3.
    RESP=(CC(I)-(C1+(T(I)-T1)*BSLN))
    RESP1=17.701*RESP-527.08*RESP**2.+12001.*RESP**3.
    IF (RESP.LT.0.02) RESP1=11.9598*RESP
    C(I)=(RESP1/RESP0)
    J=NFR
320 IF (T(I).GE.TS(J)) GO TO 350
    J=J-1
    GO TO 320
350 PV(I)=PV(I)+Q(J)*(T(I)-TS(J))/V
    IF (J-1.LT.1) GO TO 380
    DO 370 K=1,J-1
    PV(I)=PV(I)+Q(K)*(TS(K+1)-TS(K))/V
370 CONTINUE
380 CONTINUE
    JJ=NEFD
    IF (PV(I).LT.0) GO TO 397
390 IF (PV(I).GE.XPV(JJ)) GO TO 395
    JJ=JJ-1
    GO TO 390
395 DT(I)=(PV(I)-XPV(JJ))*QMAX/XQ(JJ)
    WRITE(30,6200)JJ,DT(I),C(I)
397 CONTINUE
400 CONTINUE
```

```
*****************************************************************
*
*       FORMAT STATEMENTS
*
*****************************************************************
C
 1000 FORMAT(A15)
 1100 FORMAT(A10)
 1500 FORMAT(6A10)
 2000 FORMAT(6A10,/,A10,//)
 2500 FORMAT(7A10,/'+----Koc---+----k-----+----F-----+---Sso---+---Sro-
     +--+')
 2700 FORMAT(5(1X,E10.4),/,'---- 1 means fit parameter, 0 means keep it
     +fixed',/,'    0        1        1        0       0 ',/,/,'-
     +---CONSTANTS----')
 2800 FORMAT('+Flow Cond-+DMLS Time-+----C-----+')
 2900 FORMAT(I10)
 3300 FORMAT(3(1X,E10.4))
 4000 FORMAT(1X,I3,5(1X,E10.4,1X))
 5000 FORMAT(I2,7(E10.4))
 6000 FORMAT(4(1X,E10.4))
 6100 FORMAT(1X,I10,3(1X,E10.4))
 6200 FORMAT(1X,I10,2(1X,E10.4))
C
*****************************************************************
      STOP
      END
*****************************************************************
```

```
C
C   Program Testfit (TWOSITE)
C
C   Adapted for CSTR experiencing:
C       Bicontinuum sorption
C       Flow and inlet concentration perturbations
C       Bicontinuum sorption on reactor walls
C
C       NUMERICAL SOLUTION
C
C   BY: E. Heyse
C   University of Florida, 23 AUG 93
C
C
C dim scrat = 5*np +np*np +(2+np)*nob
C signs = 1  means parms cannot change sign
C P(IPOINT(I)) = VAL(I) = = PNAME(I)
C
C       IMPLICIT DOUBLE PRECISION (A-H,O-Z)
        DOUBLE PRECISION FOC,XM,V,PC0,XFDT(20),XQ(20),XCIN(20)
        DOUBLE PRECISION XMR,XKPR,XKR,XFR,X(100)
        DOUBLE PRECISION XKOC,XK,XF,XSS0,XSR0
        DIMENSION IX(100),Y(100),P(7),DIFF(7),SIGNS(7),SCRAT(1999)
        DIMENSION IFC(20)
        CHARACTER*8 PNAME(7)
        DIMENSION VAL(7),IPOINT(7),IVARY(7)
        COMMON /BMOD/FOC,XM,V,PC0,NEFD,XFDT,XQ,XCIN
        COMMON /BMODA/XMR,XKPR,XKR,XFR
        COMMON /VALUE/ VAL,IPOINT,IVARY,PNAME,NFIX
        COMMON /BDAT/ IX,X
        CHARACTER*80 TIT,LIN1,LIN2,LIN3,LIN4
        NFIX=5
        PNAME(1)=' Koc '
        PNAME(2)=' k '
        PNAME(3)=' F '
        PNAME(4)=' Sso '
        PNAME(5)=' Sro '
        WRITE(*,'(/A)') ' UNIT 3 is the  Input File'
        WRITE(*,'(A)') ' UNIT 4 is the Output File'
        READ(3,'(A)') TIT
C
C   Read parameters to be fitted
C
C   XKOC = Soil Organic carbon partition coefficient, Koc, mL/g
```

```
C    XK = Soil Mass transfer rate coefficient, k (= k2*(1-F)), min^-1
C    XF = Fraction of instantaneous sorbing soil sites, F
C    XSS0 = Initial dmls Concentration in slow soil sites, Sso, ug/g
C    XSR0 = Initial dmsl Conc. in slow reactor sites, Sro, ug/g
C
     READ(3,'(A)') LIN1
     READ(3,*) XKOC,XK,XF,XSS0,XSR0
C
C    Read Constants
C
C    FOC = Mass fraction organic carbon on soil, foc
C    XM = Mass of soil in reactor, g
C    V = Volume of solvent in reactor, mL
C    PC0 = Dimensionless initial concentration of solute on soil
C    NEFD = Number of effective flow domains
C    IFC = Flow condition number
C    XFDT = Final dimensionless time for flow condition
C    XQ = Flow rate, mL/min
C    XCIN = Dimensionless inlet concentration
C    XMR = Mass of reactor, g
C    XKPR = Linear partition coef. on reactor, mL/g
C    XKR = 1st order mass transfer rate onto reactor, min^-1
C    XFR = Fraction instaneous sorbing reactor sites
C
     READ(3,'(A)') LIN2
     READ(3,*) (IVARY(I),I=1,NFIX)
     READ(3,'(A)') LIN3
     READ(3,*) FOC,XM,V,PC0
     READ(3,*) XMR,XKPR,XKR,XFR
     READ(3,*) NEFD
     DO 6 I=1,NEFD
   6 READ(3,*) IFC(I),XFDT(I),XQ(I),XCIN(I)
C
C    Read Data to be fitted
C
C    IX = Flow Condition
C    X = Dimensionless time (Qmax*t/V)  (Qmax = 1)
C    Y = Relative Concentration (C*)
C
     READ(3,'(A)') LIN4
     NOB=0
     DO 3 I=1,100
     READ(3,*,END=4) IX(I),X(I),Y(I)
   3  NOB=NOB+1
```

```
4      WRITE(4,1) TIT
1      FORMAT(/' ',A)
       WRITE(4,1) LIN1
       WRITE(4,2) XKOC,XK,XF,XSS0,XSR0
2      FORMAT(' ',7F11.6)
       WRITE(4,1) LIN2
       WRITE(4,5) (IVARY(I),I=1,NFIX)
5      FORMAT(' ',7I10)
       WRITE(4,1) LIN3
       WRITE(4,777) FOC,XM,V,PC0,XMR,XKPR,XKR,XFR,NEFD
 777   FORMAT(' ',2(4F11.6,/),I10)
       DO 778 I=1,NEFD
       WRITE(4,779) IFC(I),XFDT(I),XQ(I),XCIN(I)
 778   CONTINUE
 779   FORMAT(' ',I10,3F11.6)
       VAL(1)=XKOC
       VAL(2)=XK
       VAL(3)=XF
       VAL(4)=XSS0
       VAL(5)=XSR0
       NP=0
       JFIX=NFIX
       DO 20 I=1,NFIX
        IF (IVARY(I).EQ.1) THEN
          NP=NP+1
          IPOINT(I)=NP
        ELSE
          IPOINT(I)=JFIX
          JFIX=JFIX-1
        ENDIF
20     CONTINUE
       DO 22 I=1,NFIX
        P(IPOINT(I))=VAL(I)
22     CONTINUE
       NPROB=1
       MIT=0
       EPS1=0.0
       EPS2=0.0
       FLAM=0.0
       IF(EPS1.LT.1.E-9) EPS1=0.0
       IF(EPS2.LT.1.E-9) EPS2=1.E-3
       IF(MIT.EQ.0) MIT=15
       IF(FLAM.LT.1.E-9) FLAM=0.01
       FNU=10.
```

```
     DO 9 I=1,6
     SIGNS(I)=1.0
9    DIFF(I)=0.01
     WRITE(4,7) NPROB
7    FORMAT(' PROBLEM NUMBER',I3,T26,'IX',T38,'X',T50,'Y'/)

     WRITE(4,8) (IX(I),X(I),Y(I),I=1,NOB)
8    FORMAT(' ',T19,I12,2F12.5)
     WRITE(*,12) (PNAME(I),I=1,NFIX)
12   FORMAT(/T6,'SSQ',T11,7A12)
     WRITE(*,15) (P(IPOINT(I)),I=1,NFIX)
15   FORMAT(T11,7E12.5)
     CALLUWHAUS(NPROB,NOB,Y,NP,P,DIFF,SIGNS,EPS1,EPS2,MIT,FLAM,

    *FNU,SCRAT)
     WRITE(*,14) TIT
14   FORMAT(/' END: ',A)
999  STOP
     END

     SUBROUTINE UWHAUS(NPROB,NOB,Y,NP,TH,DIFF,SIGNS,EPS1,EPS2,

1    MIT, FLAM, FNU, SCRAT)
     DIMENSION SCRAT(1),Y(1),TH(1),DIFF(1),SIGNS(1)
     IA=1
     IB=IA+NP
     IC=IB+NP
     ID=IC+NP
     IE=ID+NP
     IF=IE+NP
     IG=IF+NOB
     IH=IG+NOB
     II = IH + NP * NOB
     IJ = IH
        CALL   HAUS59(NPROB,NOB,Y,NP,TH,DIFF,SIGNS,EPS1,EPS2,MIT

1    ,FLAM,FNU,SCRAT(IA), SCRAT(IB), SCRAT(IC), SCRAT(ID),

2    SCRAT(IE), SCRAT(IF), SCRAT(IG), SCRAT(IH), SCRAT(II),

3    SCRAT(IJ)  )
     RETURN
     END
     SUBROUTINE HAUS59(NPRBO, NBO, Y,NQ,TH,DIFZ,SIGNS,EP1S,EP2S,
```

```
    1MIT,FLAM,FNU,   Q,P,E,PHI,TB,F,R,A,D,DELZ)
     DIMENSION TH(1), DIFZ(1), SIGNS(1), Y(1), Q(1), P(1), E(1),
    1   PHI(1), TB(1), F(1), R(1), A(1), D(1), DELZ(1)
     CHARACTER*8 PNAME(7)
     DIMENSION VAL(7),IPOINT(7),IVARY(7)
     COMMON /VALUE/ VAL,IPOINT,IVARY,PNAME,NFIX
     DATA MAXCNT/6/
     ACOS(X) = ATAN(SQRT(1.0/X**2 - 1.0))
     NP = NQ
     NPROB = NPRBO
     NOB = NBO
     EPS1 = EP1S
     EPS2 = EP2S
     NPSQ = NP * NP
     NSCRAC = 5*NP+NPSQ +2*NOB+NP*NOB

     WRITE(4, 1000) NPROB, NOB, NP, NSCRAC
     WRITE(4, 1001)
     CALL GASS60(1, NP, TH, TEMP, TMEP)
     WRITE(4, 1002)
     CALL GASS60(1, NP, DIFZ, TEMP, TEMP)
     IF(MIN0(NP-1,50-NP,NOB-NP,MIT-1,999-MIT))99,15,15
15   IF(FNU-1.0)99, 99, 16
16   CONTINUE
     DO 19 I=1,NP
     TEMP = ABS(DIFZ(I))
     IF(AMIN1(1.0-TEMP, ABS(TH(I))))99, 99, 19
19   CONTINUE
     GA = FLAM
     NIT = 1
     ASSIGN 131 TO LAOS
     ASSIGN 225 TO IRAN
     ASSIGN 265 TO JORDAN
     IF(EPS1) 5, 10, 10
5    EPS1 = 0
10   IF(EPS2) 40, 40, 30
40   IF(EPS1) 60, 60, 50
  60 ASSIGN 270 TO IRAN
     GO TO 70
  50 ASSIGN 265 TO IRAN
     GO TO 70
30   IF(EPS1) 80, 80, 70
  80 ASSIGN 270 TO JORDAN
```

```
  70 SSQ = 0
     DO 71 I=1,NFIX
     IF(IVARY(I).EQ.1) VAL(I)=TH(IPOINT(I))
  71    CONTINUE
     CALL MODEL(NPROB, TH, F, NOB, NP)
     DO 90 I = 1, NOB
     R(I) = Y(I) - F(I)
  90 SSQ=SSQ+R(I)*R(I)
     WRITE(4, 1003) SSQ
     WRITE(*,3003) SSQ,(TH(IPOINT(I)),I=1,NFIX)
3003 FORMAT(' ',1PE9.2,0P7E12.5)
     WRITE(4, 1011)
     WRITE(4, 2006) (F(I),I=1,NOB)
C                              BEGIN ITERATION
 100  GA = GA / FNU
     INTCNT = 0
     WRITE(4, 1004)  NIT
 101  JS = 1 - NOB
     DO 130 J=1,NP
     TEMP = TH(J)
     P(J)=DIFZ(J)*TH(J)
     TH(J)= TH(J)+P(J)
     Q(J)=0
     JS = JS + NOB
     DO 102 I=1,NFIX
     IF(IVARY(I).EQ.1) VAL(I)=TH(IPOINT(I))
 102    CONTINUE
     CALL MODEL(NPROB, TH, DELZ(JS), NOB, NP)

     IJ = JS-1
     DO 120 I = 1, NOB
     IJ = IJ + 1
     DELZ(IJ) = DELZ(IJ) - F(I)
 120  Q(J) = Q(J) + DELZ(IJ) * R(I)
     Q(J)= Q(J)/P(J)
C                         Q=XT*R (STEEPEST DESCENT)
 130 TH(J) = TEMP
     GO TO LAOS,(131,414)
 131  DO 150 I = 1, NP
     DO 151 J=1,I
     SUM = 0
     KJ = NOB*(J-1)
     KI = NOB*(I-1)
     DO 160 K = 1, NOB
```

```
      KI = KI + 1
      KJ = KJ + 1
  160 SUM = SUM + DELZ(KI) * DELZ(KJ)
      TEMP = SUM/(P(I)*P(J))
      JI = J + NP*(I-1)
      D(JI) = TEMP
      IJ = I + NP*(J-1)
  151 D(IJ) = TEMP
  150 E(I) = SQRT(D(JI))
  666 CONTINUE
      DO 153 I = 1, NP
      IJ = I-NP
      DO 153 J = 1,I
      IJ = IJ + NP
      A(IJ) = D(IJ) / (E(I)*E(J))
      JI = J + NP*(I-1)
  153 A(JI) = A(IJ)
C                         A = SCALED MOMENT MATRIX
      II = - NP
      DO 155 I = 1,NP
      P(I) = Q(I)/E(I)
      PHI(I) = P(I)
      II = NP + 1 + II
  155 A(II) = A(II) + GA
      I = 1
      CALL MATIN(A, NP, P, I, DET)
C                         P/E = CORRECTION VECTOR
      STEP = 1.0
      SUM1 = 0.
      SUM2 = 0.
      SUM3 = 0.
      DO 231 I = 1,NP
      SUM1 = P(I)*PHI(I) + SUM1
      SUM2 = P(I)*P(I) + SUM2
      SUM3 = PHI(I) * PHI(I) + SUM3
  231 PHI(I) = P(I)
      TEMP = SUM1/SQRT(SUM2*SUM3)
      TEMP = AMIN1(TEMP, 1.0)
      TEMP = 57.295*ACOS(TEMP)
      WRITE(4, 1041) DET, TEMP
  170 DO 220 I = 1, NP
      P(I) = PHI(I) *STEP / E(I)
      TB(I) = TH(I) + P(I)
  220 CONTINUE
```

```
      WRITE(4, 7000)
7000 FORMAT(' TEST POINT PARAMETER VALUES')
      WRITE(4, 2006)  (TB(I), I = 1, NP)
      DO 221 I = 1, NP
      IF(SIGNS(I)) 221, 221, 222
222 IF(SIGN(1.0,TH(I))*SIGN(1.0,TB(I))) 663, 221, 221
221 CONTINUE
      SUMB=0
      DO 223 I=1,NFIX
      IF(IVARY(I).EQ.1) VAL(I)=TB(IPOINT(I))
223    CONTINUE
      CALL MODEL(NPROB, TB, F, NOB, NP)
      DO 230 I=1,NOB
      R(I)=Y(I)-F(I)
230 SUMB=SUMB+R(I)*R(I)
      WRITE(4, 1043)  SUMB
      WRITE(*,3002) SUMB,(VAL(I),I=1,NFIX)
3002 FORMAT(' ',1PE9.2,0P7E12.5)
      WRITE(4, 1011)
      WRITE(4, 2006) (F(I),I=1,NOB)
      IF(SUMB - (1.0+EPS1)*SSQ) 662, 662, 663
663 IF( AMIN1(TEMP-30.0, GA)) 665, 665, 664
665 STEP=STEP/2.0
      INTCNT = INTCNT + 1
      IF(INTCNT-MAXCNT) 170,2700,2700
664 GA=GA*FNU
      INTCNT = INTCNT + 1
      IF(INTCNT-MAXCNT) 666,2700,2700
662 WRITE(4, 1007)
      DO 669 I=1,NP
669 TH(I)=TB(I)
      CALL GASS60(1, NP, TH, TEMP, TEMP)
      WRITE(4, 1040)  GA, SUMB
      GO TO IRAN,(225,270,265)
225 DO 240 I = 1, NP
      IF(ABS(P(I))/(1.E-20+ABS(TH(I)))-EPS2) 240, 240, 241
241 GO TO JORDAN,(265,270)
240 CONTINUE
      WRITE(4, 1009) EPS2
      GO TO 280
265 IF(ABS(SUMB - SSQ) - EPS1*SSQ) 266, 266, 270
266 WRITE(4, 1010) EPS1
      GO TO 280
270 SSQ=SUMB
```

```
    NIT=NIT+1
    IF(NIT - MIT) 100, 100, 280
2700 WRITE(4, 2710)
2710 FORMAT(///115H **** THE SUM OF SQUARES CANNOT BE
REDUCED TO THE SUM
    10F SQUARES AT THE END OF THE LAST ITERATION - ITERATING
STOPS  /)
C                              END ITERATION
 280 WRITE(4, 1011)
    WRITE(4, 2001) (F(I), I = 1, NOB)
    WRITE(4, 1012)
    WRITE(4, 2001)  (R(I), I = 1, NOB)
    SSQ=SUMB
    IDF=NOB-NP
    WRITE(4, 1015)
    I=0
     CALL MATIN(D, NP, P, I, DET)
    DO 7692 I=1,NP
    II = I + NP*(I-1)
7692 E(I) = SQRT(D(II))
    DO 340 I=1,NP
    JI = I + NP*(I-1) - 1
    IJ = I + NP*(I-2)
    DO 340 J = I, NP
    JI = JI + 1
    A(JI) = D(JI) / (E(I)*E(J))
    IJ = IJ + NP
 340   A(IJ) = A(JI)
     CALL GASS60(3, NP, TEMP, TEMP, A)
     WRITE(4, 1016)
     CALL GASS60(1, NP, E, TEMP, TEMP)
     IF(IDF) 341, 410, 341
 341 SDEV = SSQ / IDF
     WRITE(4, 1014) SDEV, IDF
     SDEV = SQRT(SDEV)
     WRITE(4,3007) (PNAME(I),I=1,NFIX)
     WRITE(*,3007) (PNAME(I),I=1,NFIX)
3007 FORMAT(/T6,'SSQ',T11,7A12)
     DO 3008 I=1,NFIX
     IF(IVARY(I).EQ.1) VAL(I)=TH(IPOINT(I))
3008 CONTINUE
     WRITE(*,3004) SSQ,(VAL(I),I=1,NFIX)
     WRITE(4,3004) SSQ,(VAL(I),I=1,NFIX)
3004 FORMAT(1PE10.2,0P7E12.5)
```

```
      DO 3005 I=1,NP
3005  P(I)=E(I)*SDEV
      DO 3009 I=1,NFIX
      VAL(I)=0.0
      IF(IVARY(I).EQ.1) VAL(I)=P(IPOINT(I))
3009  CONTINUE
      WRITE(*,3006) (VAL(I),I=1,NFIX)
      WRITE(4,3006) (VAL(I),I=1,NFIX)
3006  FORMAT(' Std. Dev.',7E12.5)
      DO 391 I=1,NP
      P(I)=TH(I)+2.0*E(I)*SDEV
391   TB(I)=TH(I)-2.0*E(I)*SDEV
      WRITE(4, 1039)
      CALL GASS60(2, NP, TB, P, TEMP)
C returns with out confidence limits on function values
      RETURN
      ASSIGN 414 TO LAOS
      GO TO 101
414   DO 415 K = 1, NOB
      TEMP = 0
      DO 420 I=1,NP
      DO 420 J=1,NP
      ISUB = K+NOB*(I-1)
      DEBUG1 = DELZ(ISUB)
      ISUB = K+NOB*(J-1)
      DEBUG2 = DELZ(ISUB)
      IJ = I + NP*(J-1)
      DEBUG3 = D(IJ)/(DIFZ(I)*TH(I)*DIFZ(J)*TH(J))
420   TEMP = TEMP + DEBUG1 * DEBUG2 * DEBUG3

      TEMP = 2.0*SQRT(TEMP)*SDEV
      R(K)=F(K)+TEMP
415   F(K)=F(K)-TEMP
      WRITE(4, 1008)
      IE=0
      DO 425 I=1,NOB,10
      IE=IE+10
      IF(NOB-IE) 430,435,435
430   IE=NOB
435   WRITE(4, 2001) (R(J), J = I, IE)
425   WRITE(4, 2006) (F(J), J = I, IE)
410   WRITE(4, 1033) NPROB
      RETURN
99    WRITE(4, 1034)
```

```
      GO TO 410
  10000FORMAT(38H NON-LINEAR ESTIMATION, PROBLEM NUMBER  I3,//
 I5,
     1  14H OBSERVATIONS, I5, 11H PARAMETERS   I14, 17H SCRATCH
 REQUIRED)
  1001 FORMAT(/25H INITIAL PARAMETER VALUES  )

  1002 FORMAT(/54H PROPORTIONS USED IN CALCULATING DIFFERENCE
 QUOTIENTS )
  1003 FORMAT(/25H INITIAL SUM OF SQUARES =   E12.4)

  1004 FORMAT(/////45X,13HITERATION NO.  I4)
  1007 FORMAT(/32H PARAMETER VALUES VIA REGRESSION  )

  1008 FORMAT(/////54H APPROXIMATE CONFIDENCE LIMITS FOR EACH
 FUNCTION VAL
     1UE   )
  10090FORMAT(/62H ITERATION STOPS - RELATIVE CHANGE IN EACH
 PARAMETER LE
      1SS THAN  E12.4)
  10100FORMAT(/62H ITERATION STOPS - RELATIVE CHANGE IN SUM OF
 SQUARES LE
      1SS THAN  E12.4)
  1011 FORMAT(22H0     FUNCTION VALUES  )
  1012 FORMAT(////10H RESIDUALS  )
  1014 FORMAT(//24H VARIANCE OF RESIDUALS =    ,E12.4,1H,I4,

     120H DEGREES OF FREEDOM   )
  1015 FORMAT(////19H CORRELATION MATRIX   )

  1016 FORMAT(////21H NORMALIZING ELEMENTS    )

  1033 FORMAT(//19H END OF PROBLEM NO.  I3)

  1034 FORMAT(/16H PARAMETER ERROR  )

  10390FORMAT(/71H INDIVIDUAL CONFIDENCE LIMITS FOR EACH
 PARAMETER (ON LI
     1NEAR HYPOTHESIS)   )
  10400FORMAT(/9H LAMBDA =E10.3,40X,33HSUM OF SQUARES AFTER
 REGRESSION =
     1E15.7)
  1041 FORMAT(14H DETERMINANT =  E12.4, 6X, 25H ANGLE IN SCALED
 COORD. =
```

```
   1 F5.2, 8HDEGREES   )
1043 FORMAT(28H TEST POINT SUM OF SQUARES =   E12.4)

2001 FORMAT(/10E12.4)
2006 FORMAT(10E12.4)
     END
     SUBROUTINE MATIN(A, NVAR, B, NB, DET)
     DIMENSION A(NVAR, 1), B(NVAR, 1)
      PIVOTM = A(1,1)
      DET = 1.0
     DO 550 ICOL = 1, NVAR
      PIVOT = A(ICOL, ICOL)
     PIVOTM = AMIN1(PIVOT, PIVOTM)
      DET = PIVOT * DET
C    DIVIDE PIVOT ROW BY PIVOT ELEMENT

     A(ICOL, ICOL) = 1.0
     PIVOT = AMAX1(PIVOT, 1.E-20)
      PIVOT = A(ICOL, ICOL)/PIVOT
     DO 350 L=1,NVAR
 350  A(ICOL, L) = A(ICOL, L)*PIVOT
     IF(NB .EQ. 0) GO TO 371
     DO 370 L=1,NB
 370  B(ICOL, L) = B(ICOL, L)*PIVOT
C    REDUCE NON-PIVOT ROWS
 371  DO 550 L1=1,NVAR
     IF(L1 .EQ. ICOL) GO TO 550
     T = A(L1, ICOL)
      A(L1, ICOL) = 0.
     DO 450 L=1,NVAR
 450  A(L1, L) = A(L1, L) - A(ICOL, L)*T
     IF(NB .EQ. 0) GO TO 550
     DO 500 L=1,NB
 500  B(L1, L) = B(L1, L)-B(ICOL,L)*T
 550  CONTINUE
     RETURN
     END
     SUBROUTINE GASS60(ITYPE, NQ, A, B, C)
     DIMENSION A(NQ),B(NQ),C(NQ,NQ)
      NP = NQ
      NR = NP/10
      LOW = 1
      LUP = 10
 10   IF( NR )15,20,30
```

```
 15   RETURN
 20   LUP=NP
      IF(LOW .GT. LUP) RETURN
 30   WRITE(4, 500) (J,J=LOW,LUP)
      GO TO (40,60,80),ITYPE
 40   WRITE(4, 600) (A(J),J=LOW,LUP)
      GO TO 100
 60   WRITE(4, 600) (B(J),J=LOW,LUP)
      GO TO 40
 80   DO 90 I=LOW,LUP
 90   WRITE(4, 720) I,(C(J,I),J=LOW,LUP)
      LOW2=LUP+1
      IF(LOW2 .GT. NP) GO TO 100
      DO 95 I=LOW2,NP
 95   WRITE(4, 720) I,(C(J,I),J=LOW,LUP)
100   LOW = LOW + 10
      LUP = LUP + 10
      NR = NR - 1
      GO TO 10
500   FORMAT(/I8,9I12)
600   FORMAT(10E12.4)
720   FORMAT(1H0,I3,1X,F7.4,9F12.4)
  1   CONTINUE
      RETURN
      END

C THE MODEL

      SUBROUTINE MODEL(NPROB,P,F,NOB,NP)
      DOUBLE PRECISION FOC,XM,V,PC0,XFDT(20),XQ(20),XCIN(20)
      DOUBLE PRECISION XMR,XKPR,XKR,XFR,X(100)
      DOUBLE PRECISION XKOC,XK,XF,XSS0,XSR0
      DOUBLE PRECISION QMAX,RF,RS,RR,WS,WR,DELT,
      DOUBLE PRECISION AS,AR,BS,BR,XNA,XNB,XNC
      DOUBLE PRECISION XD,TX,XXC(0:100),XXSS(0:100),XXSR(0:100)
      DIMENSION P(1),F(1)
      DIMENSION VAL(7),IPOINT(7),IVARY(7)
      CHARACTER*8 PNAME(7)
      COMMON /VALUE/ VAL,IPOINT,IVARY,PNAME,NFIX
      COMMON /BMOD/FOC,XM,V,PC0,NEFD,XFDT,XQ,XCIN
      COMMON /BMODA/XMR,XKPR,XKR,XFR
      COMMON /BDAT/ IX(100),X
      XKOC=VAL(1)
      XK=VAL(2)
```

```
      XF=VAL(3)
      XSS0=VAL(4)
      XSR0=VAL(5)
      QMAX=1.d0
C
C     Establish parameter values for analytical solutions
C
      RF=1.d0+XM*XKOC*FOC*XF/V+XMR*XKPR*XFR/V
      RS=(1.d0-XF)*XM*XKOC*FOC/V
      RR=(1.d0-XFR)*XMR*XKPR/V
      WS=XM*XKOC*FOC*XK/QMAX
      WR=XMR*XKPR*XKR/QMAX
      DO 100 I=1,NOB
      NK=IX(I)
      XXC(0)=PC0
      XXSS(0)=XSS0
      XXSR(0)=XSR0
      DO 95 K=1,NK
      NITER=100
      IF(XFDT(K).LT.0.1) NITER=5
      DELT=XFDT(K)/NITER
      AS=(WS/2.d0)/(RS/DELT+WS/2.d0)
      BS=(RS/DELT-WS/2.d0)/(RS/DELT+WS/2.d0)
      AR=(WR/2.d0)/(RR/DELT+WR/2.d0)
      BR=(RR/DELT-WR/2.d0)/(RR/DELT+WR/2.d0)
      DO 90 L=1,NITER
      XNA=((RF-RS*AS-RR*AR)/DELT-XQ(K)/2.d0)*XXC(L-1)
      XNB=(1.d0-BS)*RS*XXSS(L-1)/DELT
      XNC=(1.d0-BR)*RR*XXSR(L-1)/DELT
      XD=(RF+RS*AS+RR*AR)/DELT+XQ(K)/2.d0
      XXC(L)=(XNA+XNB+XNC+XQ(K)*XCIN(K))/XD
      XXSS(L)=AS*(XXC(L)+XXC(L-1))+BS*XXSS(L-1)
      XXSR(L)=AR*(XXC(L)+XXC(L-1))+BR*XXSR(L-1)
      IF (K.EQ.NK) GO TO 80
      GO TO 90
   80 CONTINUE
      TX=L*DELT
      IF(X(I).LE.TX) GO TO 82
      GO TO 90
   82 F(I)=(XXC(L)-XXC(L-1))*(X(I)-(L-1)*DELT)/DELT+XXC(L-1)
      GO TO 100
   90 CONTINUE
      XXC(0)=XXC(NITER)
      XXSS(0)=XXSS(NITER)
```

```
      XXSR(0) = XXSR(NITER)
  95  CONTINUE
 100  CONTINUE
C
      RETURN
      END
```

```
C
C  Program Testfit  (MSPLN)
C
C  Adapted for CSTR experiencing:
C       Multisite sorption on soil (lognormal distribution)
C       Flow and inlet concentration perturbations
C       Bicontinuum sorption on reactor walls
C
C       NUMERICAL SOLUTION
C
C  BY: E. Heyse
C  University of Florida, 23 AUG 93
C

C THE MODEL

      SUBROUTINE MODEL(NPROB,P,F,NOB,NP)
      DOUBLE PRECISION FOC,XM,V,PC0,XFDT(20),XQ(20),XCIN(20)
      DOUBLE PRECISION XMR,XKPR,XKR,XFR,X(100)
      DOUBLE PRECISION XKOC,ULNK,SLNK,XSS0,XSR0
      DOUBLE PRECISION QMAX,RF,RS,RR,WR,DELT
      DOUBLE PRECISION AR,BR,U1,U3,U4,SUMAS
      DOUBLE PRECISION WS(501),AS(501),BS(501)
      DOUBLE PRECISION XFRAC(501),U2(501),SUMU2S
      DOUBLE PRECISION TX,XXC(0:100),XXSS(501,0:100),XXSR(0:100)
      DOUBLE PRECISION A1,A2,A3,A4,A5,A6,DELKL,DELKU
      DOUBLE PRECISION XFRACL,XFRACU,SIGN,XIII,XXX,ERFX
      DIMENSION P(1),F(1)
      DIMENSION VAL(7),IPOINT(7),IVARY(7)
      CHARACTER*8 PNAME(7)
      COMMON /VALUE/ VAL,IPOINT,IVARY,PNAME,NFIX
      COMMON /BMOD/FOC,XM,V,PC0,NEFD,XFDT,XQ,XCIN
      COMMON /BMODA/XMR,XKPR,XKR,XFR
      COMMON /BDAT/ IX(100),X
      XKOC=VAL(1)
      ULNK=VAL(2)
      SLNK=VAL(3)
      XSS0=VAL(4)
      XSR0=VAL(5)
      QMAX=1.d0
C
C  Establish constants for numerical solution
C
      RF=1.d0+XMR*XKPR*XFR/V
```

```
      RS = XM*XKOC*FOC/V
      RR = (1.d0-XFR)*XMR*XKPR/V
      WR = XMR*XKPR*XKR/QMAX
C
C     sizes of compartments based on log normal distribution
C
C         parameters for polynomial estimator of error function
C
      A1 = 0.0705230784000000
      A2 = 0.0422820123000000
      A3 = 0.0092705272000000
      A4 = 0.0001520143000000
      A5 = 0.0002765672000000
      A6 = 0.0000430638000000
      XFRACL = 0.d0
      DELKL = 0.d0
      NFRAC = 500
      XNFRAC = NFRAC
      DO 20 I = 1,NFRAC
      SIGN = 1.d0
      XIII = I
      DELKU = ULNK + (6.d0*XIII/XNFRAC-3.d0)*SLNK
      XXX = (DELKU-ULNK)/((2.d0**0.5d0)*SLNK)
c     WRITE(10,*) 'I = ',I,'DelKu = ',DELKU,' XXX = ',XXX
      IF (XXX.LT.0.d0) SIGN = -1.d0
      XXX = SIGN*XXX
c     WRITE(10,*) 'XXX = ',XXX
      ERFX = SIGN*(1.d0-(1.d0+(A1*XXX)+(A2*XXX**2.d0)+
     +(A3*XXX**3.d0)+(A4*XXX**4.d0)+(A5*XXX**5.d0)+
     +(A6*XXX*6.d0))**(-16.d0))
c     WRITE(10,*) 'ERF(X) = ',ERFX
      XFRACU = 0.5*(1.d0+ERFX)
      XFRAC(I) = XFRACU-XFRACL
      XFRACL = XFRACU
      DELKL = DELKU
   20 CONTINUE
C
C     Damkohler for each compartment
C
      DO 50 IW = 1,NFRAC
      XIW = IW
      WS(IW) = (XM*XKOC*FOC/QMAX)*(DEXP(ULNK+((6.d0*XIW-3.d0)/
     +XNFRAC-3.d0)*SLNK))/60.d0
c     WRITE(10,*) ' WS(',IW,') = ',WS(IW)
```

```
   50 CONTINUE
C
C    Loop for each observation
C
     DO 100 I=1,NOB
     NK=IX(I)
c    WRITE(6,*) 'Observation # = ',I
C
C    Initial values
C
     XXC(0)=PC0
     DO 30 IS=1,NFRAC
     XXSS(IS,0)=XSS0
   30 CONTINUE
     XXSR(0)=XSR0
C
C    Loop for each flow domain (to flow domain of obs)
C
     DO 95 K=1,NK
     NITER=100
c    WRITE(6,*)' flow domain # = ', K
     IF(XFDT(K).LT.0.1) NITER=5
C
C    size of dT
C
     DELT=XFDT(K)/NITER
C
C    dT dependent constants
C
     SUMAS=0.d0
     DO 70 J=1,NFRAC
     AS(J)=(WS(J)/2.d0)/(XFRAC(J)*RS/DELT+WS(J)/2.d0)
     BS(J)=(XFRAC(J)*RS/DELT-WS(J)/2.d0)/
    +(XFRAC(J)*RS/DELT+WS(J)/2.d0)
     SUMAS=SUMAS+XFRAC(J)*AS(J)
     U2(J)=RS*XFRAC(J)*(1.d0-BS(J))/DELT
c    WRITE(4,*)' AS(',J,') = ',AS(J)
c    WRITE(4,*)' BS(',J,') = ',BS(J)
c    WRITE(4,*)' U2(',J,') = ',U2(J)
   70 CONTINUE
     AR=(WR/2.d0)/(RR/DELT+WR/2.d0)
     BR=(RR/DELT-WR/2.d0)/(RR/DELT+WR/2.d0)
     U1=(RF-RS*SUMAS-RR*AR)/DELT-XQ(K)/2.d0
     U3=RR*(1.d0-BR)/DELT
```

```fortran
      U4 = (RF + RS*SUMAS + RR*AR)/DELT + XQ(K)/2.d0
c     WRITE(4,*) '---AR, BR, U1, U3, U4, SUMAS = ',AR,BR,U1,U3,U4,SUMAS
C
C     Loop for each dT in a flow domain
C
      DO 90 L=1,NITER
c     WRITE(6,*) '  dT # = ',L
      SUMU2S=0.d0
      DO 75 IU=1,NFRAC
c     WRITE(6,*) '  Compartment # = ',IU
      SUMU2S=SUMU2S+U2(IU)*XXSS(IU,L-1)
   75 CONTINUE
c     WRITE(4,*) '  SUMU2S = ',SUMU2S
      XXC(L)=(U1*XXC(L-1)+SUMU2S+U3*XXSR(L-1)+XQ(K)*XCIN(K))/U4
c     WRITE(4,*) L,L,'XXC = ',XXC(L)
      DO 77 IU=1,NFRAC
      XXSS(IU,L)=AS(IU)*(XXC(L)+XXC(L-1))+BS(IU)*XXSS(IU,L-1)
c     WRITE(4,*) IU,'  XXSS = ',XXSS(IU,L)
   77 CONTINUE
      XXSR(L)=AR*(XXC(L)+XXC(L-1))+BR*XXSR(L-1)
      IF (K.EQ.NK) GO TO 80
      GO TO 90
   80 CONTINUE
      TX=L*DELT
      IF(X(I).LE.TX) GO TO 82
      GO TO 90
   82 F(I)=(XXC(L)-XXC(L-1))*(X(I)-(L-1)*DELT)/DELT+XXC(L-1)
c     WRITE(4,*) I,X(I),F(I)
c     WRITE(4,*) XXSS(1,L-1),XXSS(2,L-1),XXSS(3,L-1),XXSS(4,L-1)
      GO TO 100
   90 CONTINUE
      XXC(0)=XXC(NITER)
      DO 97 JS=1,NFRAC
      XXSS(JS,0)=XXSS(JS,NITER)
   97 CONTINUE
      XXSR(0)=XXSR(NITER)
   95 CONTINUE
  100 CONTINUE
C
      RETURN
      END
```

```
C
C   Program Testfit (MSSSP)
C
C   Adapted for CSTR experiencing:
C      Multisite (series) sorption on soil (spherical distribution)
C      Driving force limited by chrystalline solubility of solute
C        Flow and inlet concentration perturbations
C        Bicontinuum sorption on reactor walls
C
C        NUMERICAL SOLUTION
C
C   BY: E. Heyse
C   University of Florida, 23 AUG 93
C
C

C THE MODEL

      SUBROUTINE MODEL(NPROB,P,F,NOB,NP)
      DOUBLE PRECISION FOC,XM,V,PC0,XFDT(30),XQ(30),XCIN(30)
      DOUBLE PRECISION XMR,XKPR,XKR,XFR,X(100)
      DOUBLE PRECISION XKOC,DEFF,DPATH,XSS0,XSR0
      DOUBLE PRECISION QMAX,RF,RS,RR,WR,DELT,AR,BR,U1,U2,U3,U4
      DOUBLE PRECISION WS(51),AS(51),BS(51),CS(51),XFRAC(51)
      DOUBLE PRECISION TX,XXC1,XXC0,XXCT
      DOUBLE PRECISION XXSS0(51),XXSS1(51),XXSST(51)
      DOUBLE PRECISION XXSR0,XXSR1,XXSRT,XNFRAC,VNORM,DELPU
      DOUBLE PRECISION DELPL,DELP(0:51),WSA,WSB,AAAA,AAAN,AAA1
      DOUBLE PRECISION DDD(53),DDR(53),U2SUM,CSATT,CSAT0
      DIMENSION P(1),F(1)
      DIMENSION VAL(7),IPOINT(7),IVARY(7)
      CHARACTER*8 PNAME(7)
      COMMON /VALUE/ VAL,IPOINT,IVARY,PNAME,NFIX
      COMMON /BMOD/FOC,XM,V,PC0,NEFD,XFDT,XQ,XCIN
      COMMON /BMODA/XMR,XKPR,XKR,XFR
      COMMON /BDAT/ IX(100),X
      XKOC=VAL(1)
      DEFF=VAL(2)
      DPATH=VAL(3)
      XSS0=VAL(4)
      XSR0=VAL(5)
      QMAX=1.d0
C
C      Establish constants for numerical solution
```

```
C
      RF=1.d0+XMR*XKPR*XFR/V
      RS=XM*XKOC*FOC/V
      RR=(1.d0-XFR)*XMR*XKPR/V
      WR=XMR*XKPR*XKR/QMAX
C
C     sizes of compartments based on spherical distribution
C     Each compartment = equal size/each delta P is different
C
      NFRAC=100
      XNFRAC=NFRAC
      VNORM=DPATH**3.d0
      DELPU=DPATH
      DO 20 ISP=1,NFRAC-1
      XFRAC(ISP)=1.d0/XNFRAC
      DELPL=(DELPU**3.d0-XFRAC(ISP)*VNORM)**(1.d0/3.d0)
      DELP(ISP)=DELPU-DELPL
      DELPU=DELPL
   20 CONTINUE
      XFRAC(NFRAC)=1.d0/XNFRAC
      DELP(NFRAC)=DELPU
C
C     Damkohler for each compartment
C
      DELP(0)=0.d0
      DO 50 IW=1,NFRAC
C
C     Deff (mm^2/min) = Deff (cm^2/sec)*6000
C
      WSA=XFRAC(IW)*XM*XKOC*FOC*DEFF*6000.d0/QMAX
      WSB=DELP(IW)*0.5d0*(DELP(IW)+DELP(IW-1))
      WS(IW)=WSA/WSB
   50 CONTINUE
C
C     Loop for each observation
C
      DO 100 I=1,NOB
      NK=IX(I)
C
C     Initial values
C
      XXC0=PC0
      DO 30 IS=1,NFRAC
      XXSS0(IS)=XSS0
```

```
   30 CONTINUE
      XXSR0=XSR0
C
C    Loop for each flow domain (to flow domain of obs)
C
      DO 95 K=1,NK
      NITER=100
      IF(XFDT(K).LT.0.1) NITER=5
C
C     size of dT
C
      DELT=XFDT(K)/NITER
C
C     dT dependent constants
C
      DO 70 J=2,NFRAC-1
      AAAA=XFRAC(J)*RS/DELT+WS(J)/2.d0+WS(J+1)/2.d0
      AS(J)=(XFRAC(J)*RS/DELT-WS(J)/2.d0-WS(J+1)/2.d0)/AAAA
      BS(J)=(WS(J)/2.d0)/AAAA
      CS(J)=(WS(J+1)/2.d0)/AAAA
   70 CONTINUE
      AAAN=XFRAC(NFRAC)*RS/DELT+WS(NFRAC)/2.d0
      AS(NFRAC)=(XFRAC(NFRAC)*RS/DELT-WS(NFRAC)/2.d0)/AAAN
      BS(NFRAC)=(WS(NFRAC)/2.d0)/AAAN
      AR=(WR/2.d0)/(RR/DELT+WR/2.d0)
      BR=(RR/DELT-WR/2.d0)/(RR/DELT+WR/2.d0)
      U1=RF/DELT-XQ(K)/2.d0
      U2=-RS/DELT
      U3=-RR/DELT
      U4=RF/DELT+XQ(K)/2.d0
C
C    Loop for each dT in a flow domain
C
      DO 90 L=1,NITER
C
C    Iterative solution
C
C       inital estimate X(t+del t) = X(t)
C
      XXCT=XXC0
      XXSRT=XXSR0
      DO 71 IST=1,NFRAC
      XXSST(IST)=XXSS0(IST)
   71 CONTINUE
```

```
C
C        iteration loop
C
      DO 78 ITTT = 1,2000
C
C        evaluate step t + del t
C
      U2SUM = 0.d0
      DO 201 IUU = 1,NFRAC
      U2SUM = U2SUM + XFRAC(IUU)*U2*(XXSST(IUU)-XXSS0(IUU))
  201 CONTINUE
      XXC1 = (U1*XXC0 + U2SUM + U3*(XXSRT-XXSR0) + XQ(K)*XCIN(K))/U4
      CSATT = 2.271500000000000
      CSAT0 = 2.271500000000000
      IF (XXSS0(1).LT.CSAT0) GO TO 721
      IF (XXSST(1).LT.CSATT) GO TO 722
      AAA1 = XFRAC(1)*RS/DELT + WS(2)/2.d0
      AS(1) = (XFRAC(1)*RS/DELT-WS(2)/2.d0)/AAA1
      BS(1) = (WS(1)/2.d0)/AAA1
      CS(1) = (WS(2)/2.d0)/AAA1
      XXSS1(1) = AS(1)*XXSS0(1) + BS(2)*(XXC0 + XXC1-CSAT0-CSATT)
      + + CS(1)*(XXSST(2) + XXSS0(2))
      GO TO 723
  721 CONTINUE
      AAAA = XFRAC(1)*RS/DELT + WS(1)/2.d0 + WS(2)/2.d0
      AS(1) = (XFRAC(1)*RS/DELT-WS(1)/2.d0-WS(2)/2.d0)/AAAA
      BS(1) = (WS(1)/2.d0)/AAAA
      CS(1) = (WS(2)/2.d0)/AAAA
      XXSS1(1) = AS(1)*XXSS0(1) + BS(2)*(XXC0 + XXC1)
      + + CS(1)*(XXSST(2) + XXSS0(2))
      GO TO 723
  722 CONTINUE
      AAAA = XFRAC(1)*RS/DELT + WS(1)/2.d0 + WS(2)/2.d0
      AS(1) = (XFRAC(1)*RS/DELT-WS(2)/2.d0)/AAAA
      BS(1) = (WS(1)/2.d0)/AAAA
      CS(1) = (WS(2)/2.d0)/AAAA
      XXSS1(1) = AS(1)*XXSS0(1) + BS(2)*(XXC0 + XXC1-CSAT0)
      + + CS(1)*(XXSST(2) + XXSS0(2))
      GO TO 723
  723 CONTINUE
      DO 72 IU = 2,NFRAC-1
      XXSS1(IU) = AS(IU)*XXSS0(IU) + BS(IU)*(XXSS1(IU-1) + XXSS0(IU-1))
      + + CS(IU)*(XXSST(IU + 1) + XXSS0(IU + 1))
   72 CONTINUE
```

```
    XXSS1(NFRAC)=AS(NFRAC)*XXSS0(NFRAC)+BS(NFRAC)*
   +(XXSS1(NFRAC-1)+XXSS0(NFRAC-1))
    XXSR1=AR*(XXC0+XXC1)+BR*XXSR0
C
C      test estimate
C
    DDD(1)=XXC1-XXCT
    DDD(2)=XXSR1-XXSRT
    DO 73 IU=3,NFRAC+2
    DDD(IU)=XXSS1(IU-2)-XXSST(IU-2)
  73 CONTINUE
    DO 301 IABS=1,NFRAC+2
    IF (DDD(IABS).LT.0.d0) DDD(IABS)=-1.d0*DDD(IABS)
 301 CONTINUE
    DO 74 IU=1,NFRAC+2
    IF (DDD(IU).EQ.0.d0) GO TO 74
    IF (IU.EQ.1) DDR(IU)=DDD(IU)/XXC1
    IF (IU.EQ.2) DDR(IU)=DDD(IU)/XXSR1
    IF (IU.GT.2) DDR(IU)=DDD(IU)/XXSS1(IU-2)
    IF (DDR(IU).LT.0.0001) GO TO 74
    GO TO 75
  74 CONTINUE
c     IF (ITTT.GE.100) WRITE(6,7075) I,K,L,ITTT
c     IF (ITTT.GE.20) WRITE(4,7075) I,K,L,ITTT
    GO TO 79
  75 CONTINUE
C
C ----- establish new test values
C
    XXCT=XXC1
    XXSRT=XXSR1
    DO 76 IU=1,NFRAC
    XXSST(IU)=XXSS1(IU)
  76 CONTINUE
    IF (ITTT.EQ.2000) WRITE(6,7070)
C
C      End iterative solution loop
C
  78 CONTINUE
  79 CONTINUE
C
C      Determine if you are at a point to make estimate
C
C      Check flow domain
```

```
C
      IF (K.EQ.NK) GO TO 80
      GO TO 89
   80 CONTINUE
C
C     Check for time in flow domain
C
      TX=L*DELT
      IF(X(I).LE.TX) GO TO 82
      GO TO 89
C
C     Model estimate of Y(I) (Concentration at T)
C
   82 F(I)=(XXC1-XXC0)*(X(I)-(L-1)*DELT)/DELT+XXC0
      GO TO 100
   89 CONTINUE
C
C   Adjust initial values at end of dT step
C
      XXC0=XXC1
      XXSR0=XXSR1
      DO 88 IU=1,NFRAC
      XXSS0(IU)=XXSS1(IU)
   88 CONTINUE
C
C     End dT loop
C
   90 CONTINUE
C
C   Adjust initial values at end of flow domain
C
      XXC0=XXC1
      DO 93 JS=1,NFRAC
      XXSS0(JS)=XXSS1(JS)
   93 CONTINUE
      XXSR0=XXSR1
C
C     End flow domain loop
C
   95 CONTINUE
C
C     End observation loop
C
  100 CONTINUE
```

```
 7070 FORMAT(//,' The solution did not converge in 2000 iterations')
 7075 FORMAT(1X,' Obs# = ',I4,' Flow dom. = ',I4,' dT = ',I4,' itteratio
     +n = ',I4)
C
      RETURN
      END
```

# REFERENCES

Anderson, M.R., Johnson, R.L., and Pankow, J.F. (1992a) "Dissolution of dense chlorinated solvents into ground water: 1. Dissolution from a well defined source," *Ground Water*, 30(2):250-256.

Anderson, M.R., Johnson, R.L., and Pankow, J.F. (1992b) "Dissolution of dense chlorinated solvents into ground water: 3. Modeling contaminant plumes from fingers and pools of solvent," *Environmental Science and Technology*, 26(5):901-908.

Annable, M.D., Wallace, R.B., Hayden, N.J., and Voice, T.C. (1993) "Reduction of gasoline component leaching potential by soil venting," *Journal of Contaminant Hydrology*, 12(1/2):151-170.

Augustijn, D.C.M. (1993) *Chemodynamics of Complex Waste Mixtures: Applications to Contamination and Remediation of Soils and Aquifer Media*, Ph.D. Dissertation, University of Florida, Gainesville.

Augustijn, D.C.M., Dai, D., Rao, P.S.C., and Wood, A.L. (1994a) "Solvent flushing dynamics in contaminated soils," In: *Proceedings of the IAHR/AIRH Symposium on Transport and Reactive Processes in Aquifers, Zurich, Switzerland (11 - 15 April, 1994)*, (Th. Dracos and F. Stauffer, Editors), A.A. Balkema, Rotterdam, pp. 557-562.

Augustijn, D.C.M., Jessup, R.E., Rao, P.S.C., and Wood, A.L. (1994b) "Remediation of contaminated soils by solvent flushing," *Journal of Environmental Engineering (ASCE)*, 120(1):42-57.

Baehr, A.L., Hoag, G.E., and Marley, M.C. (1989) "Removing volatile contaminants from the unsaturated zone by inducing advective air-phase transport," *Journal of Contaminant Hydrology*, 4(1):1-26.

Bahr, J.M. (1990) "Kinetically influenced terms for solute transport affected by heterogeneous and homogeneous classical reactions," *Water Resources Research*, 26(1):21-34.

274

Bahr, J.M., and Rubin, J. (1987) "Direct comparison of kinetic and local equilibrium formulation for solute transport affected by surface reactions," *Water Resources Research*, 23(3):438-452.

Ball, W.P. (1989) *Equilibrium Sorption and Diffusion Rate Studies with Halogenated Organic Chemicals and Sandy Aquifer Material*, Ph.D. Dissertation, Stanford University, Stanford, CA.

Ball, W.P., and Roberts, P.V. (1991) "Long-term sorption of halogenated organic chemicals by aquifer material. 2. Intraparticle diffusion," *Environmental Science and Technology*, 25(7):1237-1249.

Banerjee, S. (1984) "Solubility of organic mixtures in water," *Environmental Science and Technology*, 18(8):587-591.

Banerjee, S., Yalkowsky, S.H., and Valvani, S.C. (1980) "Water solubility and octanol/water partition coefficients of organics. Limitations of the solubility-partition coefficient correlation," *Environmental Science and Technology*, 14(10):1227-1229.

Bellin, C.A. (1993) *Coupled-Processes: Interactions of Contaminants, Bacteria, and Surfaces*, Ph.D. Dissertation, University of Florida, Gainesville.

Borden, R.C., and Kao, C.-M. (1992) "Evaluation of groundwater extraction for remediation of petroleum-contaminated aquifers," *Water Environment Research*, 64(1):28-36.

Borden, R.C., and Piwoni, M.D. (1992) "Hydrocarbon dissolution and transport: A comparison of equilibrium and kinetic models," *Journal of Contaminant Hydrology*, 10(4):309-323.

Brusseau, M.L. (1992a) "Rate limited mass transfer and transport of organic solutes in porous media that contain immobile immiscible organic liquid," *Water Resources Research*, 28(1):33-45.

Brusseau, M.L. (1992b) "Nonequilibrium transport of organic chemicals: The impact of pore-water velocity," *Journal of Contaminant Hydrology*, 9(4):353-368.

Brusseau, M.L., and Rao, P.S.C. (1989a) "Sorption nonideality during organic contaminant transport in porous media," *CRC Critical Reviews in Environmental Control*, 19(1):33-99

Brusseau, M.L., and Rao, P.S.C. (1989b) "The influence of sorbate-organic matter interactions on sorption nonequilibrium," *Chemosphere*, 18(9/10):1691-1706.

Brusseau, M.L., Wood, A.L., and Rao, P.S.C. (1991) "Influence of organic cosolvents on the sorption kinetics of hydrophobic organic chemicals," *Environmental Science and Technology*, 25(5):903-910.

Burris, D.R., and MacIntyre, W.G. (1985) "Water solubility behavior of binary hydrocarbon mixtures," *Environmental Toxicology and Chemistry*, 4(3):371-377.

Burris, D.R., and MacIntyre, W.G. (1986a) "A thermodynamic study of solutions of liquid hydrocarbon mixtures in water," *Geochimica et Cosmochimica Acta*, 50(7):1545-1549.

Burris, D.R., and MacIntyre, W.G. (1986b) "Water solubility behavior of hydrocarbon mixtures - Implications for petroleum dissolution," In: *Oil in Fresh Water: Chemistry, Biology, Countermeasure Technology, Proceedings of the Symposium of Oil Pollution in Freshwater, Edmonton, Alberta, Canada*, (J.H. vanderMeulen and S.E. Hrudey, Editors), Pergamon Press, New York, pp. 85-94.

Campbell, G.S. (1985) *Soil Physics with Basic Transport Models for Soil-Plant Systems*, Elsevier Scientific Publishing Company, Amsterdam, 150p.

Carroll, K.M., Harkness, M.R., Bracco, A.A., and Balcarcel, R.R. (1994) "Application of a permeant/polymer diffusional model to the desorption of polychlorinated biphenyls from Hudson River sediments," *Environmental Science and Technology*, 28(2):253-258.

Carski, T.H., and Sparks, D.L. (1985) "A modified miscible displacement technique for investigating adsorption-desorption kinetics in soils," *Soil Science Society of America Journal*, 49(5):1114-1116.

Chen, C. S.-H., Delfino, J.J., and Rao, P.S.C. (1994) "Partitioning of organic and inorganic components from motor oil into water," *Chemosphere*, 28(7):1385-1400.

Chiou, C.T., Freed, V.H., Schmedding, D.W., and Kohnert, R.L. (1977) "Partition coefficient and bioaccumulation of selected organic chemicals," *Environmental Science and Technology*, 11(5):475-478; 11(13):1220.

Chiou, C.T., Peters, L.J., and Freed, V.H. (1979) "A physical concept of soil-water equilibria for nonionic organic compounds," *Science*, 206:831-832.

Chiou, C.T., Porter, P.E., and Schmedding, D.W. (1983) "Partition equilibria of nonionic organic compounds between soil organic matter and water," *Environmental Science and Technology*, 17(4):227-231.

Chiou, C.T., Schmedding, D.W., and Manes, M. (1982) "Partitioning of organic compounds in octanol-water systems," *Environmental Science and Technology*, 16(1):4-10.

Cline, P.V., Delfino, J.J., and Rao, P.S.C. (1991) "Partitioning of aromatic constituents into water from gasoline and other complex solvent mixtures," *Environmental Science and Technology*, 25(5):914-920.

Connaughton, D.F., Stedinger, J.R., Lion, L.W., and Shuler, M.L. (1993) "Description of time-varying desorption kinetics: Release of naphthalene from contaminated soils," *Environmental Science and Technology*, 27(12):2397-2403.

Conrad, S.H., Wilson, J.L., Mason, W.R., and Peplinski, W.J. (1992) "Visualization of residual organic liquid trapped in aquifers," *Water Resources Research*, 28(2):467-478.

Dai, D. (1993) *Sorption of Hydrophobic Organic Chemicals: Effects of Sorbent and Solute Structure*, M.S. Thesis, University of Florida, Gainesville, FL.

DiGrazia, P.M. (1991) *Microbial Systems Analysis of Naphthalene Degradation in a Continuous Flow Soil Slurry Reactor*, Ph.D. Dissertation, University of Tennessee, Knoxville.

Dupont, R.R., Dulcett, W.J., and Hinchee, R.E. (1991) "Assessment of in situ bioremediation potential and the application of bioventing at a fuel-contaminated site," In: *In Situ Bioreclamation: Applications and Investigations for Hydrocarbon and Contaminated Site Remediation*, (R.E. Hinchee and R.F. Olfenbuttel, Editors), Butterworth-Heinemann, Stoneham, MA, pp. 262-282.

Edwards, D.A., Laha, S., Liu, Z., and Luthy, R.G. (1992a) "Solubilization and biodegradation of hydrophobic organic compounds in soil-aqueous systems with nonionic surfactants," In: *Transport and Remediation of Subsurface Contaminants: Colloidal, Interfacial, and Surfactant Phenomena*, ACS Symposium Series No. 491, (D.A. Sabatini and R.C. Knox, Editors), American Chemical Society, pp. 159-168.

Edwards, D.A., Liu, Z., and Luthy, R.G. (1992b) "Interactions between nonionic surfactant monomers, hydrophobic organic compounds and soil," *Water Science and Technology*, 26(1/2):147-158.

Edwards, D.A., Luthy, R.G., and Liu, Z. (1991) "Solubilization of polycyclic aromatic hydrocarbons in micellar nonionic surfactant solutions," *Environmental Science and Technology*, 25(1):127-133.

Falta, R.W., Javendel, I., Pruess, K., and Witherspoon, P.A. (1989) "Density-driven flow in gas in the unsaturated zone due to evaporation of volatile organic compounds," *Water Resources Research*, 25(10):2159-2170.

Fredenslund, A., Jones, R.L., and Prausnitz, J.M. (1975) "Group estimation of activity coefficients in nonideal liquid mixtures," *AIChE Journal*, 21(6):1086-1099.

Fried, J.J., Muntzer, P., and Zillox, L. (1979) "Groundwater pollution by transfer of oil-hydrocarbons," *Ground Water*, 17(6):586-594.

Fu, J.-K., and Luthy, R.G. (1986) "Aromatic compound solubility in solvent/water mixtures," *Journal of Environmental Engineering (ASCE)*, 112(2):328-345.

Gerstl, Z. (1990a) *Evaluating the Groundwater Pollution Hazard of Toxic Organics by Molecular Connectivity*, Final report, Institute of Soils and Water, The Volcani Centre, Ben Dagan, Israel, 196p.

Gerstl, Z. (1990b) "Estimation of organic chemical sorption by soils," *Journal of Contaminant Hydrology*, 6(4):357-375.

Giavedoni, M.D., and Deiber, J.A. (1986) "A model of mass transfer through a fluid-fluid interface," *Chemical Engineering Science*, 41(7):1921-1925.

Guarnaccia, J.F., Imhoff, P.T., Missildine, B.C., Oostrom, M., Celia, M.A., Dane, J.H., Jaffe, P.R., and Pinder, G.F. (1992) *Multiphase Chemical Transport in Porous Media*, U.S. Environmental Protection Agency Research Brief, EPA/600/S-92/002, R.S. Kerr Environmental Research Laboratory, Ada, OK.

Hatfield, K., Burris, D., Stauffer, T.B., and Ziegler, J. (1992) "Theory and experiments on subsurface contaminant sorption systems," *Journal of Environmental Engineering (ASCE)*, 118(3):322-337.

Hatfield, K., and Stauffer, T.B. (1992) "Nonequilibrium modeling of transport in sand containing residual decane," *Hazardous Waste and Hazardous Materials*, 9(4):369-382.

Hatfield, K., Ziegler, J., and Burris, D.R. (1993) "Transport in porous media containing residual hydrocarbon. II: Experiments," *Journal of Environmental Engineering (ASCE)*, 119(3):559-575.

Hayduk, W., and Laudie, H. (1974) "Prediction of diffusion coefficients for nonelectrolytes in dilute aqueous solutions," *AIChE Journal*, 20(3):611-615.

Ho, C.K., and Udell, K.S. (1992) "An experimental investigation of air venting of volatile liquid hydrocarbon mixtures from homogeneous and heterogeneous porous media," *Journal of Contaminant Hydrology*, 11(3/4):291-316.

Hoogweg, G. (1993) *Coupling Sorption and Biodegradation of Organic Chemicals in a Dynamic Soil System*, Internship Thesis, Wageningen Agricultural University, Wageningen, The Netherlands.

Hunt, J.R., Sittar, N., and Udell, K.S. (1988a) "Nonaqueous phase liquid transport and cleanup, 1. Analysis of mechanisms," *Water Resources Research*, 24(8):1247-1258.

Hunt, J.R., Sittar, N., and Udell, K.S. (1988b) "Nonaqueous phase liquid transport and cleanup, 2. Experimental studies," *Water Resources Research*, 24(8):1259-1269.

Johnson, R.L., and Pankow, J.F. (1992) "Dissolution of dense chlorinated solvents into ground water: 2. Source functions for pools of solvent," *Environmental Science and Technology*, 26(5):896-901.

Karickhoff, S.W. (1981) "Semi-empirical estimation of sorption of hydrophobic pollutants on natural sediments and soils," *Chemosphere*, 10(8):833-846.

Karickhoff, S.W., Brown, D.S., and Scott, T.A. (1979) "Sorption of hydrophobic pollutants on natural sediments," *Water Research*, 13(3):241-248.

Karickhoff, S.W., and Morris, K.R. (1985) "Sorption dynamics of hydrophobic pollutants in sediment suspensions," *Environmental Toxicology and Chemistry*, 4(4):469-479.

Kookana, R.S., Schuller, R.D., and Alymore, L.A.G. (1993) "Simulation of simazine transport through soil columns using time-dependant sorption data measured under flow conditions," *Journal of Contaminant Hydrology*, 14(2):93-116.

Kuipers, S.F. (1984) *Bodemkunde*, Educaboek B.V., Culemborg, Netherlands, 305p.

Laha, S., and Luthy, R.G. (1992) "Effects of nonionic surfactants on the solubilization and mineralization of phenanthrene in soil-water systems," *Biotechnology and Bioengineering*, 40(11):1367-1380.

Lamarche, P. (1991) *Dissolution of Immiscible Organics in Porous Media*, PhD Dissertation, University of Waterloo, Waterloo, Ontario, Canada.

Lee, L.S., Hagwall, M., Delfino, J.J., and Rao, P.S.C. (1992a) "Partitioning of polycyclic aromatic hydrocarbons from diesel fuel into water," *Environmental Science and Technology*, 26(11):2104-2110.

Lee, L.S., Rao, P.S.C., and Okuda, I. (1992b) "Equilibrium partitioning of polycyclic aromatic hydrocarbons from coal tar," *Environmental Science and Technology*, 26(11):2110-2115.

Liu, Z., and Luthy, R.G. (1992) "Sorption of nonionic surfactants onto soil," *Water Research*, 26(10)1337-1345.

Luthy, R.G., Ramaswami, A., Ghoshal, S., and Merkel, W. (1993) "Interfacial films in coal tar nonaqueous-phase liquid-water systems," *Environmental Science and Technology*, 27(13):2914-2918.

Mackay, D. (1977) Untitled letter, *Environmental Science and Technology*, 11(13):1219.

Mackay, D.M., and Cherry, J.A. (1989) "Groundwater contamination: Pump-and-treat remediation," *Environmental Science and Technology*, 23(6):630-636.

Mackay, D.M., Roberts, P.V., and Cherry, J.A. (1985) "Transport of organic contaminants in groundwater," *Environmental Science and Technology*, 19(5):384-392.

Mackay, D., Shiu, W.Y., Maijanen, A., and Feenstra, S. (1991) "Dissolution of non-aqueous phase liquids in groundwater," *Journal of Contaminant Hydrology*, 8(1):23-42.

Malone, D.R., Kao, C.-M., and Borden, R.C. (1993) "Dissolution and biorestoration of nonaqueous phase hydrocarbons: Model development and laboratory evaluation," *Water Resources Research*, 29(7):2203-2213.

Martel, R., Gelinas, P.J., Desnoyers, J.E., and Masson, A. (1993) "Phase diagrams to optimize surfactant solutions for oil and DNAPL recovery in aquifers," *Ground Water*, 31(5):789-800.

Means, J.C., Wood, S.G., Hassett, J.J., and Banwart, W.L. (1980) "Sorption of polynuclear aromatic hydrocarbons by sediments and soils," *Environmental Science and Technology*, 14(12):1524-1528.

Means, J.C., Wood, S.G., Hassett, J.J., and Banwart, W.L. (1982) "Sorption of amino- and carboxy-substituted polynuclear aromatic hydrocarbons by sediments and soil," *Environmental Science and Technology*, 16(2):93-98.

Mendoza, C.A., and Frind, E.O. (1990) "Advective-dispersive transport of dense organic vapors in the unsaturated zone, 1. Model development," *Water Resources Research*, 26(3):379-387.

Mercer, J.M., and Cohen, R.M. (1990) "Review paper: A review of immiscible fluids in the subsurface: Properties, models, characterization and remediation," *Journal of Contaminant Hydrology*, 6(2):107-163.

Miller, C.T., Poirier-McNeill, M.M., and Mayer, A.S. (1990) "Dissolution of trapped nonaqueous phase liquids: Mass transfer characteristics," *Water Resources Research*, 26(11):2783-2796.

Miller, D.M., Miller, W.P., and Sumner, M.E. (1989) "A continuous-flow stirred reaction cell for studying adsorption in suspensions," *Soil Science Society of America Journal*, 53(5):1407-1411.

Miller, M.M., Ghodbane, S., Wasik, S.P., Tewari, Y.B., and Martire, D.E. (1984) "Aqueous solubilities, octanol/water partition coefficients, and entropies of melting of chlorinated benzenes and biphenyls," *Journal of Chemical Engineering Data*, 29(2):184-190.

Miller, M.M., Wasik, S.P., Huang, G.-L., Shiu, W.-Y., and Mackay, D. (1985) "Relationships between octanol/water partition coefficient and aqueous solubility," *Environmental Science and Technology*, 19(6):522-529.

Morris, K.R., Abramowitz, R., Pinal, R., Davis, P., and Yalkowski, S.H. (1988) "Solubility of aromatic pollutants in mixed solvents," *Chemosphere*, 17(2):285-298.

Nelson, D.W., and Sommers, L.E. (1982) "Total carbon, organic carbon, and organic matter," In: *Methods of Soil Analysis; Part 2, Chemical and Microbiological Properties*, (A.L. Page, Editor), 2nd Edition, American Society of Agronomy, Inc., Madison WI, pp. 539-579.

Nkedi-Kizza, P., Brusseau, M.L., Rao, P.S.C., and Hornsby, A.G. (1989) "Nonequilibrium sorption during displacement of hydrophobic organic chemicals and $^{45}$Ca through soil columns with aqueous and mixed solvents," *Environmental Science and Technology*, 23(7):814-820.

Nkedi-Kizza, P., Rao, P.S.C., and Hornsby, A.G. (1985) "Influence of organic cosolvents on sorption of hydrophobic organic chemicals by soils," *Environmental Science and Technology*, 19(10):975-979.

Nkedi-Kizza, P., Rao, P.S.C., and Hornsby, A.G. (1987) "Influence of organic cosolvents on leaching of hydrophobic organic chemicals through soils," *Environmental Science and Technology*, 21(11):1107-1111.

Okuda, I., Lee, L.S., and Rao, P.S.C. (1991) "Dissolution and desorption of polyaromatic hydrocarbons from nonaqueous liquid wastes," In: *American Chemical Society, Division of Environmental Chemistry, Preprints of Papers Presented at the 201st National Meeting, Atlanta, GA, (April 14-19, 1991)*, 31(1):467-469.

Park, J.-W., and Jaffe, P.R. (1993) "Partitioning of three nonionic organic compounds between adsorbed surfactants, micelles, and water," *Environmental Science and Technology*, 27(12):2559-2565.

Pavlostathis, S.G. and Jaglal, K. (1991) "Desorptive behavior of trichloroethylene in contaminated soil," *Environmental Science and Technology*, 25(2):274-279.

Pennell, K.D., Jin, M., Abriola, L.M., and Pope, G.A. (1994) "Surfactant enhanced remediation of soil columns contaminated by residual tetrachloroethylene," *Journal of Contaminant Hydrology*, 16(1):35-53.

Pennell, K.D., Rhue, R.D., Rao, P.S.C., and Johnston, C.T. (1992) "Vapor-phase sorption of p-xylene and water on soils and clay minerals," *Environmental Science and Technology*, 26(4):756-763.

Poulsen, M.M., and Kueper, B.H. (1992) "A field experiment to study the behavior of tetrachloroethylene in unsaturated porous media," *Environmental Science and Technology*, 25(5):889-895.

Poulsen, M., Lemon, L., and Barker, J.F. (1992) "Dissolution of monoaromatic hydrocarbons into groundwater from gasoline-oxygenate mixtures," *Environmental Science and Technology*, 26(12):2483-2489.

Powers, S.E., Abriola, L.M., and Weber, W.J., Jr. (1992) "An experimental investigation of nonaqueous phase liquid dissolution in saturated subsurface systems: Steady state mass transfer rates," *Water Resources Research*, 28(10):2691-2705.

Powers, S.E., Loureiro, C.O., Abriola, L.M., and Weber, W.J., Jr. (1991) "Theoretical study of the significance of nonequilibrium dissolution on nonaqueous phase liquids in subsurface systems," *Water Resources Research*, 27(4):463-477; 27(8):2169.

Prausnitz, J.M., Anderson, T.F., Grens, E.A., Eckert, C.A., Hsieh, R., and O'Connel, J.P. (1980) *Computer Calculations for Multicomponent Vapor-Liquid and Liquid-Liquid Equilibria*, Prentice-Hall, Inc., Englewood Cliffs, NJ.

Rao, P.S.C., Hornesby, A.G., Kilcrease, D.P., and Nkedi-Kizza, P. (1985) "Sorption and transport of hydrophobic organic chemicals in aqueous and mixed solvent systems: Model development and preliminary evaluation," *Journal of Environmental Quality*, 14(3):376-383.

Rhue, R.D., Pennell, K.D., Rao, P.S.C., and Reve, W.H. (1989) "Competitive adsorption of alkylbenzene and water vapors on predominantly mineral surfaces," *Chemosphere*, 18(9/10):1971-1986.

Schnitzer, M. (1978) "Humic substances: Chemistry and reactions," In: *Soil Organic Matter*, (M. Schnitzer and S.U. Khan, Editors), Elsevier Scientific Publishing Company, Amsterdam, pp. 1-64.

Schwille, F. (1981) "Groundwater pollution in porous media by fluids immiscible with water," *The Science for the Total Environment*, 21:173-185.

Scribner, S.L., Benzing, T.R., Sun, S., and Boyd, S.A. (1992) "Desorption and bioavailability of aged simazine residues in soil from a continuous corn field," *Journal of Environmental Quality*, 21(1):115-120.

Seagren, E.A., Rittmann, B.E., and Valocchi, A.J. (1993) "Quantitative evaluation of flushing and biodegradation for enhancing in situ dissolution of nonaqueous-phase liquids," *Journal of Contaminant Hydrology*, 12(1/2):103-132.

Sleep, B.E., and Sykes, J.F. (1989) "Modeling the transport of volatile organics in variably saturated media," *Water Resources Research*, 25(1):81-92.

Stumm, W., and Morgan, J.J. (1981) *Aquatic Chemistry*, 2nd Ed., J. Wiley and Sons, Inc., New York, 780p.

Vadas, G.G., MacIntyre, W.G., and Burris, D.R. (1991) "Aqueous solubility of liquid hydrocarbon mixtures containing dissolved solid components," *Environmental Toxicology and Chemistry*, 10(5):633-639.

Van der Waarden, M., Bridie, A.L.A.M., and Groenewoud, W.M. (1971) "Transport of mineral oil components to groundwater, I. Model experiments on the transfer of hydrocarbons from a residual oil zone to trickling water," *Water Research*, 5(2):213-226.

van Genuchten, M. Th. (1981) *Non-Equilibrium Transport Parameters from Miscible Displacement Experiments*, U.S. Department of Agriculture, U.S. Salinity Laboratory, Riverside, CA, Research Report No. 119, 88p.

Wan, J., and Wilson, J.L. (1994) "Visualization of the role of the gas-water interface on the fate and transport of colloids in porous media," *Water Resources Research*, 30(1):11-23.

Weber, W.J., Jr., McGinley, P.M., and Katz, L.E. (1991) "Review paper: Sorption phenomena in subsurface systems: Concepts, models and effects on contaminant fate and transport," *Water Research*, 25(5):499-528.

Wilke, C.R., and Chang, P.(1955) "Correlation of diffusion coefficients in dilute solutions," *AIChE Journal*, 1(2):264-270.

Wood, A.L., Bouchard, D.C., Brusseau, M.L., and Rao, P.S.C. (1990) "Cosolvent effects on sorption and mobility of organic contaminants in soils," *Chemosphere*, 21(4/5):575-587.

BIOGRAPHICAL SKETCH

Edward Heyse was born on 11 June 1959 in Sumter, South Carolina. He was raised in northern Tanzania, where his father taught high school math and science for the Lutheran Church. Following high school graduation, he returned to the United States where he earned the degrees of Bachelor of Science in Civil Engineering from Michigan Technological University in 1980 and Master of Science in Civil and Environmental Engineering from Utah State University in 1982. He received a direct commission in the United States Air Force, Biomedical Sciences Corps, in 1983. He has held positions in environmental research at Tyndall AFB, Florida, and environmental management at Hill AFB, Utah. His work has focused on characterization and remediation of Air Force hazardous waste sites. In 1991, he was selected by the Air Force Institute of Technology to attend the University of Florida in pursuit of a Ph.D. in environmental engineering sciences. In January 1995, Major Heyse will start a new position as assistant professor at the Air Force Institute of Technology, Wright-Patterson AFB, Ohio.

Edward Heyse had the good fortune to marry Jeanna Hill of Panama City, Florida, in 1987. They are blessed with two beautiful and gifted children: a daughter, Sarah, born in 1990, and a son, Lucas, born in 1993.

I certify that I have read this study and that in my opinion it conforms to acceptable standards of scholarly presentation and is fully adequate, in scope and quality, as a dissertation for the degree of Doctor of Philosophy.
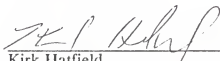
Joseph J. Delfino, Chairman
Professor of Environmental Engineering
Sciences

I certify that I have read this study and that in my opinion it conforms to acceptable standards of scholarly presentation and is fully adequate, in scope and quality, as a dissertation for the degree of Doctor of Philosophy.

P. S. C. Rao, Cochairman
Graduate Research Professor of Soil and
Water Science

I certify that I have read this study and that in my opinion it conforms to acceptable standards of scholarly presentation and is fully adequate, in scope and quality, as a dissertation for the degree of Doctor of Philosophy.
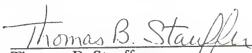
Paul A. Chadik
Assistant Professor of Environmental
Engineering Sciences

I certify that I have read this study and that in my opinion it conforms to acceptable standards of scholarly presentation and is fully adequate, in scope and quality, as a dissertation for the degree of Doctor of Philosophy.

Kirk Hatfield
Associate Professor of Civil Engineering

I certify that I have read this study and that in my opinion it conforms to acceptable standards of scholarly presentation and is fully adequate, in scope and quality, as a dissertation for the degree of Doctor of Philosophy.

Thomas B. Stauffer
Associate Professor of Civil Engineering

This dissertation was submitted to the Graduate Faculty of the College of Engineering and to the Graduate School and was accepted as partial fulfillment of the requirements for the degree of Doctor of Philosophy.

December 1994

Winfred M. Phillips
Dean, College of Engineering

Karen A. Holbrook
Dean, Graduate School